

DISSERTATION

submitted to the
Combined Faculty of Natural Sciences and Mathematics
of the Ruperto Carola University Heidelberg, Germany
for the degree of
DOCTOR OF NATURAL SCIENCES

Presented by

THERESA KORDAß

M.Sc., HEIDELBERG UNIVERSITY, 2016

B.Sc., HEIDELBERG UNIVERSITY, 2013

Born in: Güstrow, Germany

Oral Examination: 21.06.2021

Controlling the immune suppressors:

miRNAs regulating
NT5E, ENTPD1 and CD274

UNDER SUPERVISION OF
PROF. DR. VIKTOR UMANSKY
AND PROF. DR. STEFAN EICHMÜLLER

Abstract

How miRNAs affect the expression of immune checkpoint molecules

Cancer is one of the most common causes of death in the modern world and almost every second person will experience a cancer disease during their lifetime. In general, cancer cells exhibit a degenerated regulation of their gene- and protein expression, which enables them to grow and proliferate unrestrainedly. Furthermore, cancer cells gain the ability to avoid normal control mechanisms like apoptosis or elimination by immune cells. In this study the aim was to analyze the miRNA mediated regulation of immune checkpoint molecules in cancer cells. Expression of immune checkpoint molecules by cancer cells can counter-act tumor reactive immune responses, for example by reducing the susceptibility of tumor cells to cytotoxic T cell (CTL) mediated cytolysis, thereby promoting tumor immune evasion. miRNAs are small non-coding RNAs involved in post-transcriptional regulation. Thus, binding of miRNAs to the 3'-UTR of target mRNAs can block translation or lead to degradation of the targeted mRNAs. Cancer cells often exhibit aberrant miRNA expression profiles, thus tumor derived miRNAs can be utilized as biomarkers for early tumor detection. Within this study a FACS-based human miRNA library screen was conducted and miRNAs affecting surface expression of the immune checkpoint molecules NT5E (CD73), ENTPD1 (CD39) and PD-L1 (CD274) on the human tumor cell lines SK-Mel-28 (melanoma) and MDA-MB-231 (breast cancer) were determined. A set of potential tumor-suppressor miRNAs that decreased expression of the immune checkpoints molecules in these cell lines, as well as a group of potential oncomiRs that induced increased immune checkpoint molecule expression was identified. The results of the high-throughput screen for NT5E were verified in a validation process including up to 12 distinct cancer cell lines. Thus, miR-1285-5p, miR-3134, miR-22-3p and miR-193a-3p were determined as potent inhibitors of NT5E expression. Luciferase-based reporter assays proved that these NT5E inhibitory miRNAs act through direct binding to the NT5E 3'-UTR. Using functional malachite-green assays the net effect of reduced NT5E expression on adenosine production caused by miR-1285-5p and miR-3134 was assessed. As adenosine is known to inhibit effector function of cytotoxic T cells, miRNA mediated alterations in NT5E expression might affect the susceptibility of cancer cells to T cell mediated cytolysis. Moreover, miR-134-3p, miR-6859-3p and miR-224-3p were revealed as miRNAs that could enhance NT5E expression most effectively. Notably, the observed increase of NT5E was very consistent across a panel of melanoma and breast cancer cell lines. Different from the NT5E inhibiting miRNAs above, indirect mechanisms for the miRNA-mediated enhancement of NT5E expression were suspected. In summary, microarray expression profiling was performed on miRNA transfected tumor cells to unravel the mechanisms responsible for the up-regulated NT5E expression observed. By applying different bioinformatic analyses several promising candidates for the "missing link" like ARNT2 or SOX9 could be identified. Future experiments will have to clarify, whether these transcription factors really inhibit NT5E expression. As a next step the measurement of the direct impact of novel identified miRNAs on killing of human cancer cells by T cells is planned. Furthermore, it is planned to review whether these miRNAs might be suitable biomarkers or could be even used for therapeutical intervention.

Zusammenfassung

Wie miRNAs die Expression von Immuncheckpoint-Molekülen beeinflussen

Krebs gehört mit zu den häufigsten Todesursachen in der heutigen Zeit und fast jeder zweite Mensch wird im Laufe seines Lebens an Krebs erkranken. Krebszellen weisen eine aberrierende Regulation ihrer Gen- und Proteinexpression auf. Dies ermöglicht ihnen ein abnormales Wachstum, Proliferation und Resistenz gegenüber Kontrollmechanismen wie Apoptose oder Erkennung und Eliminierung durch Immunzellen. In dieser Arbeit sollte genauer untersucht werden, wie miRNAs sogenannte Immuncheckpoint-Moleküle in Krebszellen regulieren. Die Expression von Immuncheckpoint-Molekülen im Tumor dämpft die Immunantwort, was dazu führen kann, dass Krebszellen nicht mehr von cytotoxischen T-Zellen eliminiert werden. Dieser Prozess wird auch als Immunevasion bezeichnet. miRNAs sind kleine RNA-Moleküle, die in der post-transkriptionellen Regulation eine wichtige Rolle spielen. Indem sie in den 3'-UTR Bereich von bestimmten mRNAs binden, verhindern sie die Translation der mRNA oder können auch zur Degradation der mRNA führen. Sehr häufig weisen Krebszellen ein gestörtes miRNA-Expressionsprofil auf und miRNAs können beispielsweise als Biomarker zur Krebsfrüherkennung dienen. Mittels eines umfassenden auf FACS-Messungen basierenden miRNA-Library-Screenings konnten zahlreiche miRNAs identifiziert werden, die die Expression der Immuncheckpoints NT5E, ENTPD1 und CD274 beeinflussen. Der Screen wurde mit der Melanomlinie SK-Mel-28 als auch mit der Brustkrebslinie MDA-MB-231 durchgeführt. Da direkt die Veränderungen der Oberflächenexpression gemessen wurde, konnten nicht nur potenzielle tumor-supprimierende miRNAs gefunden werden, die die Expression inhibiert haben, sondern auch potenzielle onkogene miRNAs identifiziert werden, die die Expression der Immuncheckpoint-Moleküle verstärkten. Die Ergebnisse des Hochdurchsatz-Screenings für NT5E wurden in bis zu 12 verschiedenen Krebszelllinien validiert. Fast alle Screening-Ergebnisse konnten bestätigt werden und es wurden miR-1285-5p, miR-3134, miR-22-3p und miR-193a-3p als sehr potente NT5E Inhibitoren gefunden. Mit Hilfe von Luziferase-Reporter-Assays konnte die direkte Regulation von NT5E durch diese miRNAs gezeigt werden. Mittels des Malachit-Grün-Assays konnte auch die verminderte Adenosinproduktion nach Transfektion mit miR-1285-5p bzw. miR-3134 nachgewiesen werden. Adenosin vermindert nachweislich die Effektorfunktion u.a. von zytotoxischen T-Zellen. Veränderung der NT5E-Expression führt also auch zur Veränderung der Anfälligkeit von Krebszellen gegenüber immunzellen-induzierter Eliminierung. Zu den stärksten NT5E-aktivierenden miRNAs gehörten miR-134-3p, miR-6859-3p und miR-224-3p. Erstaunlicherweise war die miRNA induzierte Hochregulation von NT5E sehr konsistent über ein breites Spektrum an verschiedenen Melanom- und Brustkrebslinien. Im Gegensatz zu den direkten Effekten der NT5E-inhibierenden miRNAs, wurden indirekte Effekte vermutet, die zu der beobachteten Hochregulation geführt haben. Um die Mechanismen der Hochregulation von NT5E zu verstehen, wurden Microarray-Expression-Profiling nach miRNA-Transfektion durchgeführt. Durch bioinformatische Analysen konnten einige Kandidaten wie ARNT2 oder SOX9 für das fehlende Puzzelstück zwischen den miRNAs und NT5E ausfindig gemacht werden. Zukünftige Experimente werden zeigen, ob diese Transkriptionsfaktoren wirklich NT5E regulieren können. Als nächsten Schritt ist geplant den direkten Effekt der neu gefundenen miRNAs auf das Töten von humanen Tumorzellen durch T-Zellen zu messen und zu überprüfen, ob sich diese miRNAs als Biomarker eignen oder sogar für therapeutische Intervention genutzt werden könnten.

CONTENTS

LIST OF FIGURES	10
LIST OF TABLES	18
LIST OF ABBREVIATIONS	20
CHAPTER 1. INTRODUCTION	27
1.1. Cancer	28
1.1.1 Melanoma	29
1.1.2 Breast cancer	32
1.1.3 Cancer immunosurveillance	35
1.1.4 The immunological synapse	36
1.1.5 Immune checkpoint molecules	37
1.1.6 Immunotherapy	41
1.2. miRNAs	43
1.2.1 Biogenesis	43
1.2.2 Function	44
1.2.3 miRNAs and cancer	45
1.3. Regulation of NT5E/CD73	49
1.3.1 Transcriptional regulation of NT5E	49
1.3.2 Post-transcriptional regulation by miRNAs	50
1.4. Aim of this study	52
CHAPTER 2. MATERIALS	53
2.1. Cell lines	53
2.2. Antibodies	54
2.3. Primers	55
2.4. miRNAs	57
2.5. siRNAs	58
2.6. General instrumentation	59
2.7. General consumables	60
2.8. General chemicals and reagents	61
2.9. Kits	63
2.10. Plasmids	64
2.11. Bacteria	64
2.12. Software	64

CHAPTER 3. METHODS	65
3.1. Bioinformatic analysis	65
3.1.1 miRNA target prediction	65
3.1.2 Prediction of NT5E transcription factors	65
3.2. miRNA screen	67
3.2.1 Preparation of miRNA library	67
3.2.2 Transfection of miRNA library	67
3.2.3 Immunofluorescence staining and measurement	68
3.2.4 Data Analysis	68
3.3. 3'-UTR reporter assay	68
3.4. miRNA/siRNA transfection	69
3.5. Plasmid transformation and purification	69
3.6. XTT assay	69
3.7. RNA isolation and cDNA generation	70
3.8. qPCR	70
3.9. Quick change mutagenesis	71
3.10. Western Blot analysis	72
3.11. Measurement of NT5E/CD73 enzymatic activity by Malachite Green assay . . .	72
3.12. RNA-Seq analysis	73
3.13. Microarray analysis	73
CHAPTER 4. RESULTS	74
4.1. <i>in silico</i> predictions identified large number of miRNAs targeting immune check- point molecules	75
4.1.1 <i>in silico</i> prediction identified 44 miRNAs with strong evidence to target NT5E/CD73	75
4.1.2 <i>in silico</i> prediction identified three miRNAs with strong evidence to target ENTPD1/CD39	77
4.1.3 <i>in silico</i> prediction identified 39 miRNAs with strong evidence to target CD274/PD-L1	79
4.1.4 <i>in silico</i> prediction identified 33 miRNAs with strong evidence to target CTLA4/CD152	80
4.1.5 Several miRNAs are predicted to target multiple immune checkpoint molecules	80
4.2. Gene expression modelling revealed ATF1, GFI1, SMAD4 and TCF7 as most important NT5E transcription factors	82
4.3. NT5E and CD274 are frequently expressed in human cancer cell lines whereas ENTPD1 and CTLA4 are rarely expressed	83
4.4. Lipofectamine RNAiMAX reagent achieved best transfection efficacy	91
4.5. miRNA transfection is also effective at low concentrations	92

4.6.	Finding optimal time point for miRNA library screen	93
4.6.1	A half-life of 4 hours was estimated for NT5E mRNA	93
4.6.2	A half-life of 14 hours was estimated for NT5E surface levels	94
4.6.3	miRNA transfection mediated strongest changes 72 h post transfection on NT5E surface expression	94
4.7.	The immune checkpoint molecules NT5E, ENTPD1 and CD274 were selected for the miRNA library screen	95
4.8.	miRNA library screen	97
4.8.1	Control samples confirmed successful implementation of miRNA library screen	97
4.8.2	Several miRNAs impacting NT5E surface expression were newly-discovered	100
4.8.3	Several miRNAs impacting ENTPD1 surface expression were newly- discovered	111
4.8.4	Several miRNAs affecting CD274 surface expression were newly-discovered	112
4.8.5	27 miRNAs affected both NT5E and CD274 surface expression	116
4.8.6	12 miRNAs affected both ENTPD1 and CD274 surface expression	118
4.8.7	18 miRNAs affected NT5E as well as ENTPD1 surface expression	119
4.8.8	miR-134-3p and miR-6804-3p increased the expression of all three in- vestigated immune checkpoint molecules	122
4.9.	Validation of miRNA hits	123
4.9.1	Individual miRNA transfections could confirm majority of the hits dis- covered by the library screen	124
4.10.	Investigating mode of action of miRNA-mediated changes of NT5E expression	132
4.10.1	Validating direct interactions	132
4.10.2	Investigating indirect mechanisms	140
4.11.	From human to mouse	152
4.11.1	Several miRNAs regulating NT5E are conserved between man and mouse	152
4.11.2	Compared to NT5E less miRNAs regulating CD274 are conserved be- tween man and mouse	154
4.11.3	Effect of miRNAs on NT5E could not be recapitulated in mouse cell line EO771-OVA-Luc ⁺	156
4.11.4	Effect of miRNAs on CTL lysis	159
4.12.	miR-1285-5p and miR-3134 decreased AMP turn-over	164
CHAPTER 5. DISCUSSION		167
CHAPTER 6. CONCLUSION		180
APPENDIX		183
OWN PUBLICATION LIST		186

THANKS TO

Conducting my PhD was a very exiting but also stressful time and I would like to thank all people that accompanied me during this stage of life. First of all, I would like to express my sincere gratitude to my supervisors Prof. Stefan Eichmüller, Prof. Rainer König and Prof. Viktor Umansky, for always encouraging me, giving valuable feedback for my Thesis and also for supporting me during my maternal leave. I also want to thank Prof. Benedikt Brors and Prof. Stefan Wiemann for participating in my Defence committee. Furthermore, I would like to especially thank the Christiane Nüsslein-Volhard-Foundation for supporting me with a stipend designated for young female scientist with children. Especially during the COVID-19 caused lock-downs, this stipend was extremely helpful. A special thanks to all my friends always having an open ear for my problems and always supporting me. Especially I would like to thank Patrick Jersch and I am still convinced we are twins who were separated at birth. Furthermore, I also want to thank Lukas Feilen, Benjamin Spendrin, Leslie and Fabian Simon for always cheering me up and being such credible nice persons. Furthermore, I would like to thank Krishna Das, who was a former lab-member and taught me so many scientific things as well as how to cook super delicious Indian dishes. During our shared time in the Eichmüller group we became very close friends and even if you are far away in Innsbruck you are always in my heart. The same holds true for Julia Neubert. I am so grateful for the time we shared a desk in the office. I would like to thank you for the fun-times in the lab as well as in our spare time. Thanks to David Eisel, Miriam Melake, Edurne Murgaza and Antonino Pane for all the fun times we had on conferences and in the lab. A special thank you is dedicated for Laura Hartmann and Elke Dickes. Our very regular coffee "meetings" were always the bright side of the day and you both were very valuable colleagues during the whole time-span of my thesis. A big extra thank you goes to Elke and Marie, Jana and Paula, always assisting me with my work and especially helping me during the COVID-19 situation to run experiments when I was stuck at home due to closed kindergarten. Also I want to thank my master student Tsu-Yang Chao (Spencer) who was helping me a lot to search for the "missing link". Also I want to thank Claudia Sterzik-Lutsch; it was always nice sharing an office with you and to get a fresh hair cut once in a while. Also a big thank you to Wolfram Osen, who always gave good advices and who proofread this Thesis. Additional thanks to Luisa Marques, Tim Wagner, Wolfgang Müller, Rainer Schell, Dr. Adriane Himmertgen, who always gave good advices on CD73 topic, Andrea Breuer and Mario Koch. I also want to warmly thank my mum Christine Schacht and my dad Jörg Schacht for always supporting me and for bearing my daily calls early in the morning. Also I want to thank my son Ephraim for teaching me time-management skills and how to stay alive with a minimal amount of sleep over a very long period of time. He is one of my biggest achievements during my PhD thesis, and definitely the cutest one.

LIST OF FIGURES

1.1	Hallmarks of cancer. Figure is taken from [96].	28
1.2	Four stages of melanoma. Stage 0 melanoma is very thin and located only in the epidermal region. Treatment is surgical resection with almost complete cure rate. Also stage I and II melanoma exhibit a high cure rate by surgical removal. Stage 0-II mainly differ in their Breslow thickness. Stage III melanoma is defined by spread to lymph nodes. Standard procedure is removal of primary melanoma and adjacent lymph nodes. Stage IV melanoma is defined by spread to other organs and treatment is often surgery of removable sections combined with chemotherapy, targeted therapy, immunotherapy or a combination of previously mentioned options. Figure is adapted from [6]. . .	29
1.3	Four stages of Breast cancer. Different stages of breast cancer and their characteristic Tumor size, location, spreading and survival rate are depicted. Figure is taken from [3].	32
1.4	Breast cancer treating algorithm. Based on breast cancer stage, the molecular subtype and patient decisions different treatments for primary breast cancer are used in the clinics. Figure is taken from [37].	34
1.5	The immunological synapse (IS). The IS is the interface between a T cell and a APC like cancer cell. The IS consists of different SMAC patterns: central cSMAC, peripheral pSMAD and the distal dSMAC. Figure is taken from [232].	36
1.6	Structure and function of NT5E/CD73. The membrane bound ecto-5'-nucleotidase NT5E hydrolyzes extracellular adenosine monophosphate (AMP) into adenosine and inorganic phosphate (P). Upstream of NT5E, adenosine triphosphate (ATP) is hydrolyzed via two reaction steps into AMP by the enzyme ectonucleoside triphosphate diphosphohydrolase-1 (ENTPD1) (CD39). Adenosine thus produced exerts anti-inflammatory effects by binding to the adenosine A2A receptor (ADORA2A) expressed by T cells, natural killer (NK) cells, and dendritic cells (DCs) resulting in cAMP mediated blocking of their effector functions. To some extent, the A2B receptor (ADORA2B) is also expressed on DCs and macrophages which are suppressed by adenosine. Thus, cancer cells can evade the immune system by up-regulating NT5E protein levels. Furthermore, adenosine binds to the A2B receptor expressed by cancer cells leading to Tumor cell survival and proliferation. Cancer cells also express the adenosine A1 receptor (ADORA1) and A3 receptor (ADORA3) and binding of adenosine to these receptors leads to Tumor cell migration and proliferation via signalling through Gi proteins. Adenosine is also involved in the adaption to hypoxia and shows pro-angiogenic potential. All adenosine receptors are depicted as stylized green transmembrane proteins. Adenosine is symbolized as yellow circles marked with "A". Picture is taken from [128]. . .	40

1.7	miRNA biogenesis and function. miRNA genes are mainly transcribed by RNA polymerase II and the resulting pri-miRNA is processed by Drosha/DGCR8 complex into hairpin-structured pre-miRNA. The pre-miRNA is subsequently exported into cytosol by EXPORTIN5 where it is cleaved by Dicer into mature miRNA. The mature miRNA binds together with Ago proteins to target mRNA's 3'-UTR regions thereby blocking translation or even causing degradation of mRNA.	44
1.8	Regulation of NT5E. Network of transcription factors and microRNAs (miRNAs) regulating NT5E expression. This network summarizes the current knowledge on regulation of NT5E on transcriptional (TFs) and post-transcriptional level by TFs and miRNAs, respectively. Transcriptional activators are depicted in blue and transcriptional repressors are highlighted in magenta. miRNAs targeting NT5E directly are shown, as well as miRNAs with indirect impact on NT5E expression through targeting of transcriptional regulators. Picture taken from [128].	51
3.1	Network of genes and their regulative transcription factors. Genes and transcription factors are connected via the edge strength es_{tj}	66
4.1	General work-flow of this study. This study can be divided in three main parts. Firstly, <i>in silico</i> analysis was carried out. Using different prediction algorithms potential miRNAs regulating immune check point molecules were retrieved. Also different expression data sets were analysed and based on this suitable cell lines for the following experiments were selected. The second phase was the miRNA library screen, to experimentally identify miRNAs, that are capable of changing the surface expression of selected immune evasion relevant proteins. This phase generated the largest share of data of this study and was the base for the last phase. The final step was the validation phase, to confirm the screening hits and to investigate their mode of action.	74
4.2	Venn diagram of NT5E targeting miRNAs. The overlap of miRNAs targeting NT5E predicted by the five data bases MicroCosm, microRNA (conserved), miRDB, PITA (all entries) and PACCMIT is shown. Only miR-422a was predicted by all resources.	76
4.3	NT5E mRNA levels among cell lines of different tumor entities (NCI-60 panel). BR: breast cancer; CNS: tumor of central nervous system; CO: colon cancer; LE: leukaemia; ME: melanoma; LC: non-small-cell lung carcinoma; OV: ovarian cancer; RE: renal carcinoma.	83
4.4	ENTPD1 mRNA levels among cell lines of different tumor entities (NCI-60 panel). BR: breast cancer; CNS: tumor of central nervous system; CO: colon cancer; LE: leukaemia; ME: melanoma; LC: non-small-cell lung carcinoma; OV: ovarian cancer; RE: renal carcinoma.	84
4.5	CD274 mRNA levels among cell lines of different tumor entities (NCI-60 panel). BR: breast cancer; CNS: tumor of central nervous system; CO: colon cancer; LE: leukaemia; ME: melanoma; LC: non-small-cell lung carcinoma; OV: ovarian cancer; RE: renal carcinoma.	85

4.6	CTLA4 mRNA levels among cell lines of different tumor entities (NCI-60 panel). BR: breast cancer; CNS: tumor of central nervous system; CO: colon cancer; LE: leukaemia; ME: melanoma; LC: non-small-cell lung carcinoma; OV: ovarian cancer; RE: renal carcinoma.	85
4.7	Expression of immune checkpoint molecules within MaMel panel. Comparison of NT5E, ENTPD1, CD274 and CTLA4 mRNA levels across a panel of human melanoma cell lines.	86
4.8	Ranked NT5E mRNA expression across the MaMel-panel. Expression data was z-score normalized.	87
4.9	Ranked ENTPD1 mRNA expression across the MaMel-panel. Expression data was z-score normalized.	87
4.10	Correlation of NT5E and ENTPD1 expression across the MaMel panel. Across the analysed melanoma cell lines, NT5E showed a significantly negative correlation with ENTPD1 mRNA expression.	88
4.11	FACS analysis of surface NT5E (A) and ENTPD1 (B) expression in selected melanoma cell lines. Only SK-Mel-28 cell line exhibited high levels of both NT5E and ENTPD1 surface expression.	88
4.12	Percentage of NT5E and ENTPD1 positive cells. FACS analysis of surface NT5E and ENTPD1 expression in selected melanoma cell lines.	89
4.13	Ranked CD274 mRNA expression across the MaMel-panel. Expression data was z-score normalized.	90
4.14	Ranked CTLA4 mRNA expression across the MaMel-panel. Expression data was z-score normalized.	90
4.15	Correlation of NT5E and CTLA4 expression across the MaMel panel. Across the analysed melanoma cell lines NT5E was significantly negative correlated with CTLA4 mRNA expression.	91
4.16	Effect of different miRNA concentrations on NT5E surface levels. Three different miRNA/siRNA concentrations were tested. Changes in NT5E surface expression were measured by FACS two days post transfection.	92
4.17	Estimation of the NT5E mRNA half-life. SK-Mel-28 cells were treated with 10 µg/mL Actinomycin D and NT5E mRNA levels were measured by qPCR after different time points of treatment.	93
4.18	Estimating NT5E surface protein half-life. SK-Mel-28 cells were treated with 200 µg cycloheximide and surface NT5E levels were measured by FACS after different time points of treatment.	94
4.19	Time course of change in NT5E surface levels. SK-Mel-28 cells were transfected with 25 nM miRNA/siRNA and changes in NT5E surface levels were measured by FACS 24, 48 and 72 h post transfection. Values were normalized to siRNA control conditions.	95
4.20	Expression of selected genes related to tumor cell killing by cytotoxic T cells in the human melanoma cell line SK-Mel-28. Expression levels were obtained from NCI-60 data.	96

4.21	Expression of selected genes related to tumor cell killing by cytotoxic T cells in the human breast cancer cell line MDA-MB-231. Expression levels were obtained from NCI-60 data.	96
4.22	Work-flow of miRNA library screen.	97
4.23	SK-Mel-28 NT5E controls. From all screening plates the effect of the control samples on NT5E surface expression was plotted.	98
4.24	SK-Mel-28 ENTPD1 controls. From all screening plates the effect of the control samples on ENTPD1 surface expression was plotted.	98
4.25	MDA-MB-231 NT5E controls. From all screening plates the effect of the control samples on NT5E surface expression was plotted.	99
4.26	MDA-MB-231 CD274 controls. From all screening plates the effect of the control samples on CD274 surface expression was plotted.	99
4.27	Waterfall plot of NT5E enhancing miRNAs in SK-Mel-28 cells.	102
4.28	Waterfall plot of miRNAs significantly decreasing NT5E surface levels in SK-Mel-28 cells.	103
4.29	Venn diagram of miRNAs affecting NT5E surface expression. Overlap of miRNAs with significant effect on NT5E surface levels for two screened cell lines SK-Mel-28 (SK28) and MDA-MB-231 (MB231).	106
4.30	Waterfall plot of miRNAs significantly increasing NT5E surface levels in MDA-MB-231 cells.	107
4.31	Waterfall plot of NT5E decreasing miRNAs in MDA-MB-231 cells.	108
4.32	Venn diagram of miRNAs affecting NT5E and CD274 surface expression. Overlap of miRNAs with significant effect on NT5E or CD274 surface levels in MDA-MB-231 (MB231) is depicted.	116
4.33	Venn diagram of miRNAs affecting surface expression of NT5E and CD274. Overlap of miRNAs with significant effect on NT5E in SK-Mel-28 (SK28) or CD274 surface levels in MDA-MB-231 (MB231) is depicted.	117
4.34	Venn diagram of miRNAs affecting surface expression of ENTPD1 and CD274. Overlap of miRNAs with significant effect on ENTPD1 in SK-Mel-28 (SK28) or CD274 surface levels in MDA-MB-231 (MB231) is depicted.	118
4.35	Venn diagram of miRNAs affecting surface expression of NT5E and ENTPD1. The overlap of miRNAs with an significant effect on NT5E and ENTPD1 in SK-Mel-28 cells is depicted.	119
4.36	Validation of NT5E down-regulating miRNAs by FACS. Each dot represents an independent experiment. Cell lines were transfected with 50 nM miRNA. Three days post transfection cells were harvested and stained for FACS analysis. Cells were gated on live cells and isotype control staining was used to set the NT5E positive gate. Median fluorescence intensity of NT5E was determined for every condition. Fold changes were calculated compared to mimic control-1 samples. Significance was assessed by one-sample T-test. *: $p < 0.05$; **: $p < 0.01$; ***: $p < 0.001$; ****: $p < 0.0001$	125

- 4.37 **Validation of miR-1233-3p by FACS.** Each dot represents an independent experiment. Fold changes were calculated compared to mimic control-1 samples. Significance was assessed by one-sample T-test. *: $p < 0.05$; **: $p < 0.01$; ***: $p < 0.001$; ****: $p < 0.0001$ 126
- 4.38 **Validation of NT5E up-regulating miRNAs by FACS.** Each dot represents an independent experiment. Cell lines were transfected with 50 nM miRNA. Three days post transfection cells were harvested and stained for FACS analysis. Cells were gated on live cells and isotype control staining was used to set the NT5E positive gate. Median fluorescence intensity of NT5E was determined for every condition. Fold changes were calculated compared to mimic control-1 samples. Significance was assessed by one-sample T-test. *: $p < 0.05$; **: $p < 0.01$; ***: $p < 0.001$; ****: $p < 0.0001$ 128
- 4.39 **Validation of NT5E down-regulating miRNAs by qPCR.** Each dot represents an independent experiment. Cell lines were transfected with 50 nM miRNA and two days post transfection cells were harvested and RNA was isolated. NT5E mRNA level were determined by qPCR. Fold changes were calculated compared to mimic control-1 samples. RPL19 was used as housekeeping gene. Significance was assessed by one-sample T-test. *: $p < 0.05$; **: $p < 0.01$ 129
- 4.40 **Validation of NT5E up-regulating miRNAs by qPCR.** Each dot represents an independent experiment. Cell lines were transfected with 50 nM miRNA and two days post transfection cells were harvested and RNA was isolated. NT5E mRNA level were determined by qPCR. Fold changes were calculated compared to mimic control-1 samples. RPL19 was used as housekeeping gene. Significance was assessed by one-sample T-test. *: $p < 0.05$; **: $p < 0.01$; ***: $p < 0.001$; ****: $p < 0.0001$ 130
- 4.41 **Effect of miRNA transfection on cellular NT5E protein expression in MaMel-53a cells.** MaMel-53a cells were transfected with 50 nM miRNA/siRNA and 48 h post transfection cells were harvested and protein was isolated subsequently. Total NT5E protein levels were determined by Western Blot. 35 μ g protein were loaded per lane on a 12 % SDS-PAGE gel. Actin was used as normalization control. 131
- 4.42 **NT5E 3'-UTR reporter assay.** Cells were transfected with 100 ng pLS-NT5E plasmid and 50 nM miRNA. Luciferase signal was measured 24 h post transfection. Four cell lines were tested: HEK293, HeLa, SK-Mel-28 and MDA-MB-231. Significance was assessed by one-way ANOVA using Dunnett's multiple comparison test. All samples were compared to mimic control-1. At least four replicates were performed per miRNA. *: $p < 0.05$, **: $p < 0.01$, ***: $p < 0.001$, ****: $p < 0.0001$ 133
- 4.43 **NT5E 3'-UTR assay in SK-Mel-28 cells.** Cells were transfected with 100 ng pLS-NT5E plasmid and 50 nM miRNA. Luciferase signal was measured 24 h post transfection. One-way ANOVA was performed to calculate p-values always comparing to the corresponding pLS-vector only. *: $p < 0.05$, **: $p < 0.01$, ***: $p < 0.001$, ****: $p < 0.0001$ 136

4.44	Mutated NT5E 3'-UTR assay in SK-Mel-28 cells. Cells were transfected with 100 ng pLS-NT5E plasmid and 50 nM miRNA. Luciferase signal was measured 24 h post transfection. One-way ANOVA was performed to calculate p-values for transfections with WT plasmid comparing to mimic control-1 *: $p < 0.05$, **: $p < 0.01$. For the deletions significance was assessed with two-sided T-test.	137
4.45	Mutated NT5E 3'-UTR assay in SK-Mel-28 cells. Cells were transfected with 100 ng pLS-NT5E plasmid and 50 nM miRNA. Luciferase signal was measured 24 h post transfection. Significance was assessed with two-sided T-test. *: $p < 0.05$	138
4.46	NT5E 3'-UTR assay in A375 cells. Cells were transfected with 100 ng pLS-NT5E plasmid and 50 nM miRNA. Luciferase signal was measured 24 h post transfection. One-way ANOVA was performed to calculate p-values always comparing to mimic control-1. *: $p < 0.05$, **: $p < 0.01$, ***: $p < 0.001$.	139
4.47	NT5E 3'-UTR assay in MDA-MB-231 cells. Cells were transfected with 100 ng pLS-NT5E plasmid and 50 nM miRNA. Luciferase signal was measured 24 h post transfection. One-way ANOVA was performed to calculate p-values always comparing to mimic control-1. *: $p < 0.05$	139
4.48	Venn diagram of down-regulated genes in MaMel-02. Overlap of down-regulated genes (fold change < 0.5) between different miRNAs are depicted. .	144
4.49	Venn diagram of down-regulated genes in MDA-MB-231. Overlap of down-regulated genes (fold change < 0.5) between different miRNAs are depicted.	146
4.50	Expression of selected genes in MaMel-02 cells. Expression data from microarray experiment are shown for candidates genes that might drive the observed NT5E up-regulation upon miRNA transfection. One-way ANOVA was performed to calculate p-values always comparing to mimic control-1. *: $p < 0.05$, **: $p < 0.01$, ***: $p < 0.001$, ****: $p < 0.0001$	148
4.51	Expression of selected genes in MDA-MB-231 cells. Expression data from microarray experiment are shown for candidates genes that might drive the observed NT5E up-regulation upon miRNA transfection. One-way ANOVA was performed to calculate p-values always comparing to mimic control-1. *: $p < 0.05$, **: $p < 0.01$, ***: $p < 0.001$, ****: $p < 0.0001$	150
4.52	Binding motifs within human NT5E promoter. ConTraV3 tool was used to assess potential binding sites of transcriptional regulators suspected to inhibit NT5E expression. The NM002526 RefSeq data was used as the input sequence for NT5E and it was searched for binding sites within the promoter region (500-bp upstream). The stringency parameters were set to core = 0.95 and similarity matrix = 0.85.	151
4.53	Change in Nt5e and Cd274 mRNA levels in transfected EO771-OVA-Luc⁺ cells. 48 h post transfection with 50 nM miRNA or siRNA cells were harvested and expression levels were measured by qPCR using Ubc and Actb as housekeeping genes. Fold changes were calculated to mimic control-1 condition.	157

4.54	Change in Nt5e and Cd274 surface levels in transfected EO771-OVA-Luc⁺ cells. Three days post transfection Nt5e and Cd274 surface expression was measured by FACS	158
4.55	Effect of AMP on CTL mediated killing of EO771-OVA-Luc⁺ cancer cells. 10.000 EO771-OVA-Luc ⁺ cells were co-cultured with 6000 OVA-specific CTLs per well in 96-well plate without AMP or with addition of different concentrations of AMP. After 24 h, the luciferase signal intensity was measured to estimate the amount of viable cancer cells. Significance was assessed by one-way ANOVA using Dunnett's multiple comparison test. Samples with AMP addition were compared to 0 nM AMP. Four replicates were performed per condition. *: p < 0.05; **: p < 0.01; ***: p < 0.001; ****: p < 0.0001	159
4.56	Effect of miRNAs on viability of transfected EO771-OVA-Luc⁺ cancer cells 48 h post transfection. All samples were compared to mimic control-1. Four replicates were performed per miRNA. *: p < 0.05; **: p < 0.01.	160
4.57	Effect of miRNAs on the susceptibility of miRNA transfected EO771-OVA-Luc⁺ cells to CTL lysis. 48 h after miRNA transfection, EO771-OVA-Luc ⁺ cells were co-cultured with OVA-specific CTLs and luciferase dependent signal intensity was measured 24 later. All samples were compared to mimic control-1. Four replicates were performed per miRNA. *: p < 0.05; **: p < 0.01; ***: p < 0.001; ****: p < 0.0001.	161
4.58	Difference of Fractional Killing (FK) in transfected EO771-OVA-Luc⁺ cells co-cultured with 1000 CTLs/well.	162
4.59	Effect of miRNAs on killing of transfected EO771-OVA-Luc⁺ cancer cells by CTLs 48 h post transfection. Cancer cells and CTLs were co-cultured for 24 h until luciferase signal was measured. All samples were compared to mimic control-1. Four replicates were performed per miRNA. *: p < 0.05; **: p < 0.01; ***: p < 0.001; ****: p < 0.0001.	163
4.60	Malachite green assay in transfected MaMel-53a cells. Cancer cells were transfected with 50 nM miRNA/siRNA and cultured for 48 h. Then, 400 μM AMP was added in phosphate-free buffer and supernatants were collected after 30 min incubation and the amount of produced free phosphate was measured. All samples were compared to mimic control-1. At least six replicates were performed per condition in malachite assay. Pink: NT5E decreasing miRNAs. Turquoise: NT5E enhancing miRNAs. *: p < 0.05; **: p < 0.01; ***: p < 0.001; ****: p < 0.0001.	164
4.61	Effect of miRNAs on AMP turn-over mediated by NT5E. Cancer cells were transfected with 50 nM miRNA/siRNA and cultured for 48 h. Then, 400 μM AMP was added in phosphate-free buffer and supernatants were collected after 30 min incubation and the amount of produced free phosphate was measured. Fold changes were calculated to mimic control-1 condition of the respective experiment. Each dot represents an independent experiment. *: p < 0.05; **: p < 0.01.	165

6.1	Graphical summary of this Thesis. The most important findings of this work were summarized in this figure. miRNAs that enhanced the expression of a immune checkpoint molecule are marked in green. miRNAs that inhibited the expression of an immune checkpoint molecule are marked in red. miRNAs that had mixed effects are shown in orange. Observations only based on the miRNA library screen are shown with dashed lines. Observations validated with independent experiments are shown with continuous lines.	181
6.2	Vector map of pLS-3'-UTR plasmids used in this study. LightSwitch reporter vectors were used to assess binding of miRNAs to NT5E 3'-UTR in this study. Human NT5E 3'-UTR sequence was fused with gene encoding for Renilla firefly luciferase. Vectors contain Ampicillin cassette for selection. . .	183
6.3	Effect of siRNAs on NT5E surface expression. SK-Mel-28 cells were transfected with 25 nM siRNA and 72 h post transfection changes in surface expression was assessed. Measured conditions were part of the miRNA library screen and NT5E MFI values were z-score normalized. NT5E siRNA pool clearly decreased NT5E expression. Also HIF1A siRNA significantly lowered the surface level of NT5E. Significance was assessed by one-sample t-test. *: $p < 0.05$; ***: $p < 0.001$	184
6.4	Kaplan-Meier curve based on NT5E expression in breast cancer. High NT5E expression is significantly associated with worse prognosis for breast cancer patients. Kaplan-Meier plots were generated with Kaplan-Meier Plotter [90].	184
6.5	Kaplan-Meier curve based on HIF1A expression in breast cancer. High NT5E expression is significantly associated with worse prognosis for breast cancer patients. Kaplan-Meier plots were generated with Kaplan-Meier Plotter [90].	185
6.6	Kaplan-Meier curve based on ARNT2 expression in breast cancer. High NT5E expression is significantly associated with a better prognosis for breast cancer patients. Kaplan-Meier plots were generated with Kaplan-Meier Plotter [90].	185

LIST OF TABLES

2.1	Cell lines used in this study.	53
2.2	Antibodies used in this study. CN = Catalogue number.	54
2.3	Primers used in this study.	55
2.4	Primers used in this study for QuickChange mutagenesis of pLS-NT5E vector. In red the nucleotide is marked for which the deletion primer were designed. .	56
2.5	miRNA used in this study.	57
2.6	siRNAs used in this study.	58
2.7	Devices used for this study.	59
2.8	General consumables used in this study.	60
2.9	Chemicals used in this study.	61
2.10	Reagents used in this study.	62
2.11	Kits used in this study.	63
2.12	Plasmids used in this study.	64
2.13	Bacteria strains used in this study.	64
2.14	Software used in this study.	64
3.1	Thermal conditions of reverse transcription.	70
3.2	Composition of one qPCR reaction.	71
3.3	Thermal conditions of qPCR.	71
3.4	Blocking and washing buffers used in this study.	72
3.5	Phosphate-free-buffer.	73
4.1	miRNAs predicted by at least 3 different data bases to regulate NT5E.	76
4.2	miRNAs predicted by at least 2 different data bases to regulate ENTPD1. . .	78
4.3	miRNAs predicted by at least 3 different data bases to regulate CD274. . . .	79
4.4	miRNAs predicted by at least 3 different data bases to regulate CTLA4. . . .	80
4.5	miRNAs predicted to regulate NT5E, ENTPD1, CD274 and CTLA4. For each target gene the number of data bases that containede miRNA-target interaction is given.	81
4.6	Bottom-Up Approach: Prediction of NT5E gene expression in NCI-60 data set using MIP models to restrict number of TFs. Prediction performance (PP) was calculated with LOO-CV.	82
4.7	Testing transfection efficacy using Lipofectamine RNAiMAX reagent.	91
4.8	Testing transfection efficacy using Dharmafect 1 reagent.	92
4.9	miRNAs up-regulating NT5E in SK-Mel-28.	100

4.10	miRNAs down-regulating NT5E in SK-Mel-28.	101
4.11	miRNAs up-regulating NT5E in MDA-MB-231.	104
4.12	miRNAs down-regulating NT5E in MDA-MB-231.	105
4.13	Shared targets of miRNAs down-regulating NT5E in MDA-MB-231 as well as SK-Mel-28 cells. For each gene it was tested whether its expression is beneficial for patient survival in breast cancer using Kaplan Meier Plotter tool (KM breast cancer).	109
4.14	Shared targets of miRNAs up-regulating NT5E in MDA-MB-231 as well as SK-Mel-28 cells.	110
4.15	GSEA analysis of target genes from NT5E enhancing miRNAs. Also the number of miRNAs with a binding site is given from the nine selected NT5E enhancing miRNAs for validation.	110
4.16	miRNAs up-regulating ENTPD1 in SK-Mel-28.	111
4.17	miRNAs down-regulating ENTPD1 in SK-Mel-28.	112
4.18	miRNAs up-regulating CD274 in MDA-MB-231 part I.	113
4.19	miRNAs up-regulating CD274 in MDA-MB-231 part II.	114
4.20	miRNAs down-regulating CD274 in MDA-MB-231 part I.	114
4.21	miRNAs down-regulating CD274 in MDA-MB-231 part II.	115
4.22	Shared targets of miRNAs upregulating NT5E and ENTPD1 part I.	120
4.23	Shared targets of miRNAs upregulating NT5E and ENTPD1 part II.	121
4.24	GSEA analysis of target genes from NT5E enhancing miRNAs. Also the number of miRNAs with a binding site is given from the six NT5E and ENTPD1 enhancing miRNAs.	122
4.25	Top miRNA hits from library screen affecting NT5E surface expression in both MDA-MB-231 (MDA) and SK-Mel-28 (SK28). miRNAs marked with * were only significant in one cell line.	123
4.26	Compilation of miRNA mediated effects on luciferase signal in NT5E 3'-UTR reporter assays.	134
4.27	List of deletions created in NT5E 3'-UTR for reporter assays to verify direct miRNA interaction. The seed sequence is highlighted in yellow. The deleted nucleotide is marked in red.	135
4.28	Enrichment analysis with TransmiR v2.0. For the enriched TFs correlation with NT5E expression in two data sets was performed: NCI-60 data and expression data from ten melanoma and five NHEM samples (MM).	140
4.29	Correlation analysis with NT5E expression. NCI-60 data was used to assess the correlation of selected transcriptional regulators with NT5E. Also expression levels (z-score) for MDA-MB-231 and SK-Mel-28 are given. Significant correlations are marked in red or blue.	141
4.30	Correlation analysis with NT5E expression. RNAseq data was used to find genes with strongest negative correlation to NT5E mRNA level across ten melanoma cell lines and five NHEM specimens. Top ten genes with highest negative Pearsons correlation coefficient (PCC) are shown. Also the number of NT5E enhancing miRNAs with potential binding sites (BS) are given. . . .	142

4.31	Correlation analysis with NT5E expression. RNAseq data was used to find genes with strongest negative correlation to NT5E mRNA level across ten melanoma cell lines and five NHEM specimens. Top ten gene with highest number of predicted miRNAs are given.	143
4.32	Number of genes with a fold change < 0.5 compared to mimic control-1 samples.	144
4.33	Top shared genes with a fold change < 0.5 compared to mimic control-1 samples for transfected MaMel-02. All genes, that were down-regulated by at least four miRNAs are shown.	145
4.34	Top shared genes with a fold change < 0.5 compared to mimic control-1 samples for transfected MDA-MB-231. All genes, that were down-regulated for by least five miRNAs are shown.	147
4.35	Top ten genes with highest negative correlation to NT5E mRNA levels. Pearson's correlation coefficient (PCC) were calculated for all 27 MDA-MB-231 (MDA231) and all 27 MaMel-02 (MM02) samples, respectively. Potential binding sites for NT5E enhancing miRNAs were obtained with miRmap.	147
4.36	Binding sites of conserved miRNAs in Nt5e 3'-UTR.	152
4.37	Sequence comparison of miRNAs regulating NT5E in humans.	153
4.38	Binding sites of conserved miRNAs in Cd274/Pdl1 3'-UTR.	154
4.39	Sequence comparison of miRNAs regulating CD274 in humans. Differences in sequences are marked in red.	155

LIST OF ABBREVIATIONS

- ABCA1** ATP-binding cassette transporter 1
- ACS** American cancer society
- ADO** Adenosine
- ADORA1/3** Adenosine A1/3 receptor
- ADORA2A** A2A adenosine receptor
- ADORA2B** A2B adenosine receptor
- ADP** Adenosine diphosphate
- AMP** Adenosine monophosphate
- ATCC** American type culture collection
- ATP** Adenosine triphosphate
- AGO** Argonaute protein
- APC** Adenomatous polyposis coli protein
- APCs** Antigen presenting cells
- ARNT2** Aryl hydrocarbon receptor nuclear translocator 2
- BAX** BCL2 associated X, apoptosis regulator
- BCL2** BCL2 apoptosis regulator
- BCS** Breast-conserving surgery
- BMI-1** BMI1 proto-oncogene, polycomb ring finger
- BRAF** V-raf murine sarcoma viral oncogene homolog B1
- BRCA1/2** Breast cancer type 1/2 susceptibility protein
- BSA** Bovine serum albumin
- cAMP** Cyclic adenosine monophosphate
- CAR T-cell** Chimeric antigen receptor T-cell
- Cas9** CRISPR-associated protein 9
- CCND1** Cyclin D1

CD274/PD-L1 Programmed death-ligand 1

CDKN2A Cyclin-dependent kinase inhibitor 2A

CIMP CpG island methylator phenotype

CO2 Carbon dioxide

COMMD4 COMM domain containing 4

CRC Colorectal cancer

CRISPR Clustered regularly interspaced short palindromic repeats

CTLA4 Cytotoxic T lymphocyte associated protein 4

CTLs Cytotoxic T lymphocytes

DCs Dendritic cells

DHA DNA hypomethylating agents

DGCR8 Drosha-DiGeorge syndrome critical region gene 8

DNA Deoxyribonucleic acid

DMSO Dimethyl sulfoxide

ECM Extracellular matrix components

EMT Epithelial-to-mesenchymal transition

ENTPD1/CD39 Ectonucleoside triphosphate diphosphohydrolase-1

ER Estrogen receptor

EV Extracellular vesicles

FACS Fluorescence-activated cell sorter

FC Fold change

FCS/FBS Fetal calf serum

FOXP2/3 Forkhead box transcription factor

GBC Gall bladder carcinoma

GAPDH Glyceraldehyde-3-phosphate dehydrogenase

GFI1 Growth factor independent 1 transcriptional repressor

GM-CSF Granulocyte-macrophage colony stimulating factor

GSEA Gene set enrichment analysis

h Hours

HER-2 Human epidermal growth factor receptor 2

HDL High-density lipoproteins

HIF-1 Hypoxia-inducible factor-1

HK House keeping gene

HNSCC head and neck squamous cell carcinoma

HPLC High performance liquid chromatography

HRP Horseradish peroxidase

HSE-1 Herpes simplex-1 virus

hTERC Telomerase RNA template

hTERT Transcriptase telomerase protein

IgG Immunoglobulin

IS Immunological synapse

ITIM Immunoreceptor tyrosine-based inhibitory motif

ITSM Immunoreceptor tyrosine-based switch motif

kDa Kilo Dalton

MAGE-A3 Melanoma-associated antigen A3

MAPK Mitogen-activated protein kinase

MAZ MYC associated zinc finger protein

MCL1 Induced myeloid leukemia cell differentiation protein

MHC Major histocompatibility complex

MFI Median fluorescence intensity

MICA MHC class I polypeptide-related sequence A

MITF Microphthalmia-associated transcription factor

min Minutes

MIP Mixed-integer programming

miRISC miRNA-induced silencing complex

miRNA microRNA

mRNA messenger RNA

MYBL2 MYB proto-oncogene like 2

NaCl Sodium chloride

NCI National cancer institute

NK Natural killer cell

NKG2D/KLRK1 Killer cell lectin like receptor K1

nt Nucleotides

NT5E 5'-Nucleotidase ecto

NY-ESO-1 New York oesophageal squamous cell carcinoma 1

oncomiR Oncogenic miRNA

ORF Open reading frame

OVA Ovalbumin

PAGE Polyacrylamide gel electrophoresis

PBS Phosphate buffered saline

PCR Polymerase chain reaction

PDCD1 Programmed cell death 1

PMSF Phenylmethylsulfonylfluorid

PR Progesterone receptor

pre-miRNA Precursor miRNA

pri-miRNA Primary miRNA

p.t. Post transfection

PTEN Phosphatase and tensin homolog

qPCR Quantitative real-time PCR

RNA Ribonucleic acid

RNU6B Small nuclear RNA U6

RISC RNA-induced silencing complex

RPL19 Ribosomal protein L19

RPMI Roswell park memorial institute

RT Room temperature

SDS Sodium dodecyl sulfate

sec Seconds

sfm Serum-free medium

siRNA Small interfering RNA

SMAC Supramolecular activation cluster

SMAD SMAD family member

SNAI2 Snail family transcriptional repressor 2

SOX9 SRY-box transcription factor 9

SR-B1 Scavenger receptor class B type 1

STAT Signal transducer and activator of transcription

TAA Tumor-associated antigens

TAMs Tumor-associated macrophages

TBP TATA-box binding protein

TBS Tris-buffered saline

TBS-T TBS with 0.05% Tween-20

TCF-1 T cell factor 1

TCGA The cancer genome atlas

TCR T-cell receptors

TRF1 Telomeric repeat binding factor 1

TF Transcription factor

TILs Tumor infiltrating lymphocytes

Tm Melting temperature

TNBC Triple negative breast cancer

TNF Tumor necrosis factor

TP73 Tumor protein P73

TPTE Trans-membrane phosphatase with tensin homology

TRBP Transactivation response RNA binding protein

tsmiR Tumor-suppressive miRNA

Treg Regulatory T cell

TYR Tyrosinase

ULP2 UL16 binding protein 2

UTR Untranslated region

UVA Long wave ultraviolet

UVB Medium wave ultraviolet

UVR Ultraviolet radiation

WB Western Blot

XPO5 RAnGTP-dependent nuclear transport reporter exportin 5

CHAPTER 1.

INTRODUCTION

Deoxyribonucleic acid (DNA) contains all the information needed to build up a whole organism like a human body. Every single cell contains the same DNA information, but yet our bodies consist of numerous diverse cell types from astrocytes to zygotes, all exerting different functions. The orchestrated interplay between these different cell types and structures is the basis for the development of a mature organism originating from just one fertilized ovum. But if every cell contains the same DNA content, how is their diversity achieved? The DNA just contains the information, which has to be read and translated into functional proteins. Every cell type has a different set of translated molecules and proteins. This process from DNA, to functional proteins is heavily controlled on different levels. It begins with modifications of the DNA like methylation or acetylation of DNA binding histone proteins. The first prevents that the information of the DNA is transcribed, the later facilitates DNA transcription. Transcription factors can activate or inhibit DNA transcription, which is the process of converting the DNA information to messenger RNA (mRNA) by RNA polymerases in the cell nucleus. The mRNA is then exported into the cytosol where it can bind to ribosomes and the mRNA will be subsequently translated into a protein. This process is called translation and the RNA information is converted to a sequence of amino acids, which are the basic modules of proteins. Also this process is regulated by different mechanisms. For example modifications of the mRNA, binding of proteins or small RNA molecules called miRNAs to the end region of the mRNA, which is called 3'-untranslated region (3'-UTR), can impact the mRNA translation. After that the next level of regulation is the modifications of proteins themselves e.g. by phosphorylation, acetylation or methylation, which can alter the protein function, stability and activity.

The focus of this thesis was to study the aberrant regulation of gene and protein expression of particular molecules involved in immune evasion by miRNAs in the context of cancer. In cancer cells the tightly regulated mechanisms of gene and protein expression are degenerated, which leads to uncontrolled cell proliferation, resistance to cell death, genome instability and failures in DNA repair machinery as well as evasion from the immune system. For instance, cancer cells can gain the expression of molecules, that inhibit their killing by immune cells, which can normally eliminate degenerated cells. These proteins are classified as immune checkpoint molecules.

1.1. Cancer

In general, cancer can be defined as malignant transformation of normal cells in a multi-step process. This transformation can be caused by genetic risk factors and external carcinogens, which can be classified into three groups: biological carcinogens like viral or bacterial infections, physical carcinogens like ionizing or ultraviolet radiation and chemical carcinogens like tobacco smoke or asbestos. The different cancer types are mainly defined by the cell type from which the Tumor originated e.g. carcinomas are derived from epithelial cells or sarcomas descended from connective tissue [2, 1, 95].

Four out of ten persons will be diagnosed with cancer within their lifetime [2] and cancer is the second leading cause of death worldwide. 2018 almost ten million people died because of a cancer disease with lung and breast cancer having the highest incidence with 2.09 million caused deaths, respectively. With increasing lifespan the incidence for cancer drastically increases [1].

Although different cancer types can be quite dissimilar, in general for all cancer diseases one rule applies: the earlier the cancer is detected, the better are prospect of treatment and chance for complete cure of the patient. The main portion of cancer-related deaths are caused by metastasised cancers. Within the progression of cancer individual Tumor cells can spread into distant organs from the primary Tumor site. Besides early detection, also cancer prevention is one of the most powerful tools to reduce cancer-related deaths. For example reducing exposure to ultraviolet radiation or avoiding tobacco smoke can drastically lower the risk for skin or lung cancer, respectively. Another prevention strategy is vaccination against viruses like hepatitis B or HPV, which can cause for example liver or cervical cancer [2, 1, 95, 96]. In the following sections the two cancer types malignant melanoma and breast cancer will be introduced more precisely. The general characteristics of cancer cells are illustrated in figure 1.1.

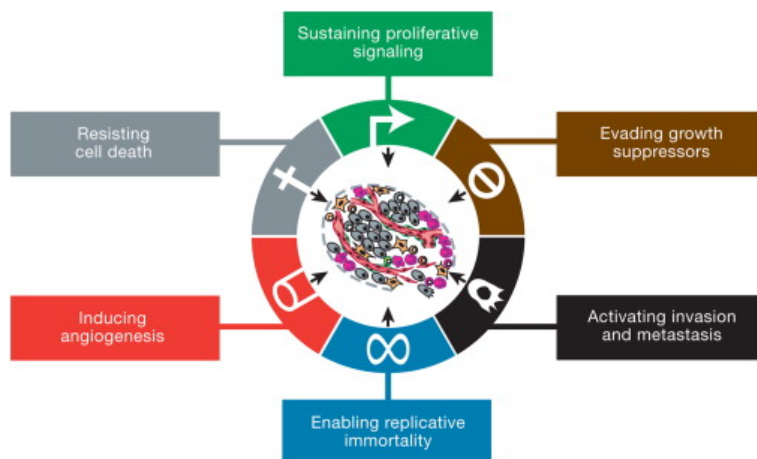


Figure 1.1: Hallmarks of cancer. Figure is taken from [96].

1.1.1 Melanoma

Malignant melanoma is the deadliest form of skin cancer although malignant melanoma only accounts for two percent of all skin cancer cases [217]. Based on the Krebsdaten report 2015/16, malignant melanoma is the fourth frequent cancer type for women in Germany with a rate of 4.8 %. For men its the fifth most common cancer type with a similar frequency of 4.7 % [195]. Early detected melanomas have a quite high cure rate, since primary melanoma can be easily treated by surgical resection. But for progressed melanoma the cure rate drastically declines for advanced stages, because malignant melanoma is very resistant to standard cancer treatments like chemo- or radiotherapy. This is also reflected in the overall survival of different melanoma stages. Stage I melanoma has a 10-year survival rate of > 90 % whereas the 10-year survival rate for stage IV (metastatic melanoma) drops to only 10-15 % [7]. An overview of the different melanoma stages and their treatment is illustrated in figure 1.2. To detect melanoma betimes, regular check-ups of existing moles and benign nevi are very important. Early characteristics of melanoma are summarized by the mnemonic "ABCD^{EF}": **A**symmetry, **B**orders (irregular), **C**olour (multicoloured), **D**iameter (greater than 6 mm), **E**volving over time and **F**unny looking [53].

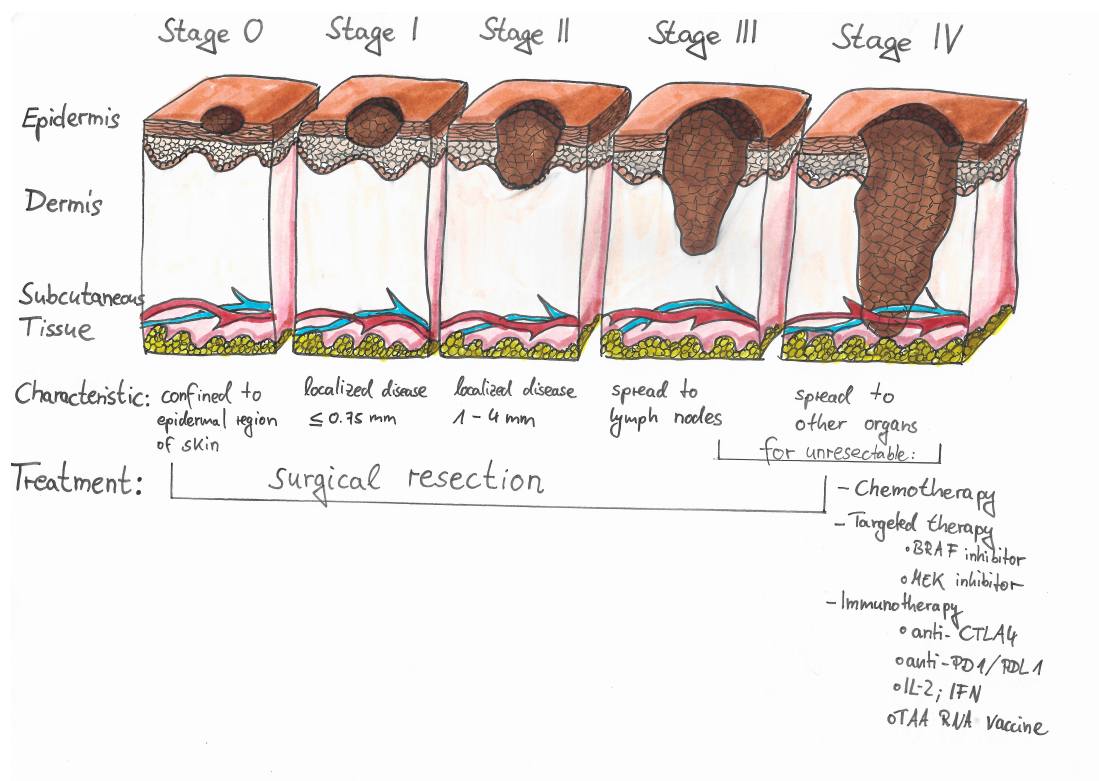


Figure 1.2: Four stages of melanoma. Stage 0 melanoma is very thin and located only in the epidermal region. Treatment is surgical resection with almost complete cure rate. Also stage I and II melanoma exhibit a high cure rate by surgical removal. Stage 0-II mainly differ in their Breslow thickness. Stage III melanoma is defined by spread to lymph nodes. Standard procedure is removal of primary melanoma and adjacent lymph nodes. Stage IV melanoma is defined by spread to other organs and treatment is often surgery of removable sections combined with chemotherapy, targeted therapy, immunotherapy or a combination of previously mentioned options. Figure is adapted from [6].

Melanoma originates from malignantly transformed neural crest-derived melanocytes [156]. Melanoma is a good example for cancers caused by physically carcinogens, since the main risk factor for melanoma development is exposure to sun light. But also genetic mutations can increase the risk for melanoma formation. For example, germ line mutation within cyclin-dependent kinase inhibitor 2A (CDKN2A) can be a predisposition for melanoma accrument. One characteristic of melanoma is the high mutation rate compared to other cancer types. These mutations are mainly caused by exposure to long wave ultraviolet (UVA) and medium wave ultraviolet (UVB) light. One of the most frequent mutations in melanoma is related to v-Raf murine sarcoma viral oncogene homolog B (BRAF). Around 43 % of all melanoma patients exhibit transition of valin into glutamic acid at position 600 in BRAF (BRAF^{V600E}) protein [209]. BRAF belongs to Ras/Raf/MEK/ERK signalling pathway, which is hyper-activated in almost 90 % of melanoma cases and is a key regulator of melanocyte and melanoma cell proliferation. Thus metastatic melanoma, which can not be completely resected, is often treated with small molecule inhibitors targeting this pathway. In general, kinases are very potent targets to inhibit their catalytic sites with small molecules [88]. Thus, several drugs that target BRAF like vemurafenib or dabrafenib or MEK inhibitors like trametinib are used in clinics to treat progressed melanoma. These drugs often show good therapeutic response in the beginning of the treatment. But most patients will experience a relapse, since after six to eight months melanoma cells get resistant to the treatment. One strategy to overcome this resistance mechanisms, is the usage of immunotherapy in combination with targeted therapies [174]. The different approaches of immunotherapy will be further explained in subsequent chapter.

Since metastatic melanoma is very resistant to treatments, it is fundamental to understand the drivers behind melanoma progression and to find potential biomarkers reflecting the different disease stages. Also studying the resistance mechanisms of melanoma cells to therapies might help to further improve treatment by combination of multiple approaches to prevent the often observed relapses of melanoma disease. For example the usage of targeted therapy against BRAF mutated melanoma with vemurafenib was shown to increase the release of extracellular vesicles (EV). Researchers found an increase of miR-211-5p in EVs in melanoma cells upon treatment with BRAF inhibitors. Blocking miR-211-5p could reverse the vemurafenib resistance of melanoma cells and reduced cancer cell proliferation. This example highlights the role of intercellular communication by EVs in melanoma progression and acquisition of resistance to targeted therapies [152]. Also epigenetic modifications are involved in melanoma development and progression. For instance, hypermethylation and thereby silencing of certain Tumor suppressor genes involved in apoptosis or cell cycle regulation like phosphatase and tensin homolog (PTEN) or CDKN2A are common events in melanoma progression [207]. A small subset of melanomas is characterized by a CpG island methylator phenotype (CIMP) especially in patients with genetic mutations in NRAS, IDH1 and ARID2 genes. For IDH1 and ARID2 it is known that they are involved in chromatin remodelling suggesting a direct link between epigenetic alterations and somatic mutations. Since hypermethylation is associated with melanoma progression, DNA hypomethylating agents (DHA) could be a therapeutic option to enhance the effect other treatments like immunotherapy. Melanoma belongs to the group of highly immunogenic cancers and immunotherapy seems to be a very attractive tool to treat metastatic melanoma [156]. But with a broad range of possible treatments, suitable biomarkers will be essential to predict and choose the op-

timal treatment combination. Thus, several studies are focusing on the search for suitable biomarkers. For example circulating EVs originated from immune cells were shown to reflect the state of immune cells within the Tumor microenvironment and could help to select the most appropriate immune-checkpoint inhibitors in order to reactivate the immune cells [235].

Over the last decades also miRNAs became more attractive as biomarkers. One advantage in contrast to mRNA is the high stability of miRNAs in paraffin-embedded tissues. So already collected melanoma material can be re-analysed and correlated with treatment efficacy. For example, miR-21 expression was shown to be a prognostic marker for melanoma. Also miR-659-3p expression was found to predict the outcome of carboplatin/paclitaxel chemotherapy of metastatic melanoma [231]. In melanoma patients bearing the BRAF mutation and treated with small-molecule inhibitors, miR-579-3p expression was found to correlate with development of resistance to the targeted therapy. High miR-579-3p expression is associated with a better survival rate. Not only does miR-579-3p expression correlates with melanoma stages being highly expressed in benign nevi and depressed in stage III/IV melanoma. But interestingly, miR-579-3p was also found at much lower levels in patients that developed resistance to targeted therapy [73].

1.1.2 Breast cancer

Breast cancer is one of the most common malignant diseases for women [93]. Based on the Krebsdaten report 2015/16, breast cancer is the most frequent cancer type for women in Germany with an incidence rate of 29.5 %. Mainly women are developing breast cancer, but also 0.3 % of men were diagnosed with breast cancer in Germany. Furthermore, breast cancer is the deadliest cancer type for women causing 17.6 % of all cancer-related deaths in Germany 2016 [195]. The breast cancer stages are depicted in figure 1.3. The earlier breast cancer is detected the higher is the survival rate. Once breast cancer metastasised the survival rate drastically decreases. Thus, early diagnosis of breast cancer is very important and regularly medical check-ups could decrease breast-cancer related death in last decades [69].

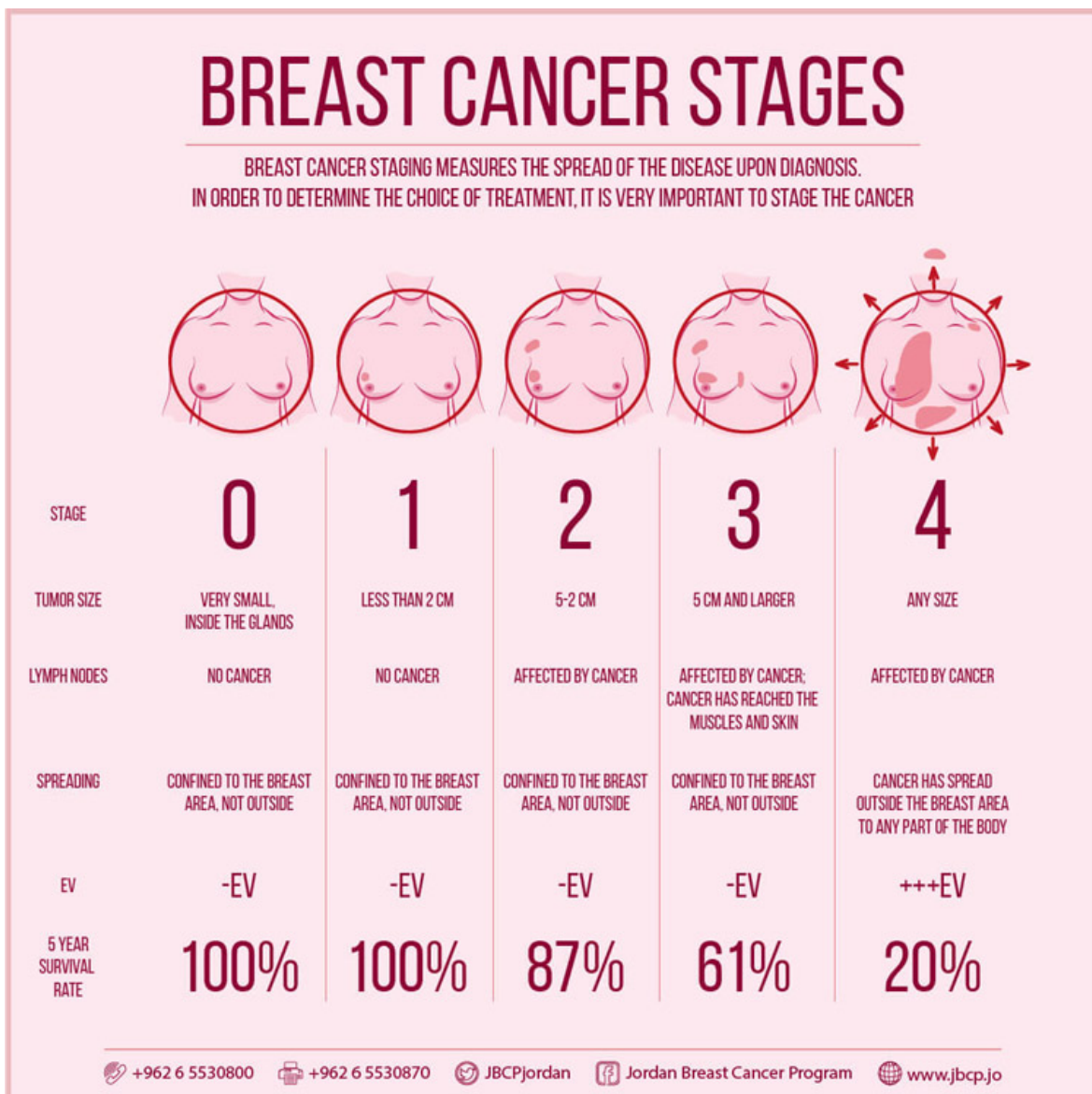


Figure 1.3: Four stages of Breast cancer. Different stages of breast cancer and their characteristic Tumor size, location, spreading and survival rate are depicted. Figure is taken from [3].

In general, breast cancer originates from epithelial cells of the breast. Commonly breast cancer starts from cells of milk-producing ducts and is therefore classified as invasive ductal carcinoma. If breast cancer originates from glandular tissue, also referred to as lobules, it is classified as invasive lobular carcinoma [253]. Breast cancer is a very heterogeneous disease and is categorized into three major subtypes. The subtypes differ in their expression of certain markers, which can be measured by immune-histochemistry or by gene-expression profiling. Knowing the subtype gives prognostic information and helps to predict the most responsive and effective treatment.

The luminal breast cancer subtype is characterized by the expression of estrogen receptor (ER) with or without the expression of progesterone receptor (PR). The luminal subtype is further distinguished into luminal A and luminal B. Overall, the luminal subtype is the most common with 70- 80 % of diagnosed breast cancers falling into this category. The next subtype is breast cancer expressing the human epidermal growth factor receptor 2 (HER-2⁺). Approximately 10 % of all diagnosed breast cancers belong to HER-2⁺ subtype. The most diverse breast cancer subtype is the triple negative breast cancer (TNBC) lacking expression of ER, PR and HER-2. Around 10 - 20 % of all diagnosed breast cancers are TNBCs [218, 17].

The different subtypes differ in their clinical characteristics. Luminal A subtype has the best prognosis from all subtypes. It is less aggressive, slow-growing and the recurrence rate is low. In contrast, luminal B subtype is more aggressive and has far higher proliferation rate. But this subtype is not so prevalent as luminal A with 10-20% of all breast cancer cases [17]. Based on different expression of these receptors, the subtypes can be treated according to their expression profile. For instance the luminal ER⁺ breast cancer subtypes respond to endocrine therapy. The ER⁺ breast cancer cells rely for their growth on the ER receptor. By blocking the estrogen signalling by drugs, the Tumor growth can be inhibited. For example luminal subtype can be treated by tamoxifen, which is a selective estrogen receptor modulator [122]. Compared to luminal subtype, HER-2⁺ and TNBC have a poorer clinical prognosis. HER-2⁺ breast cancer cells grow fast and have a higher chance to metastasise. There are specific targeted therapies for this subtype. For example pertuzumab and trastuzumab are approved agents for treating HER-2⁺ breast cancer. These are monoclonal antibodies blocking HER-2. The standard care is combination of chemotherapy with trastuzumab [177]. TNBC have the highest rate of recurrence and the age at diagnosis is lower compared to the other breast cancer subtypes. There are no targeted therapies for TNBC due to the lack of expression of hormone receptors [157]. The treatment algorithm for early breast cancer is shown in figure 1.4. Finding the optimal treatment for breast cancer can be quite complex. There are local therapy options like surgery and radiotherapy, systemic treatments like chemotherapy, molecular targeted therapies and endocrine therapy. Classifying into the molecular subtypes, the overall Tumor-burden and location of the Tumor helps to define the optimal treatment strategy. Standard treatment for all subtypes is systemic chemotherapy. Depending on the subtype chemotherapy is combined with for example anti-HER2 or endocrine therapy. Breast-conserving surgery (BCS) is the first surgical choice for treating breast cancer. Mastectomy is only performed for very aggressive breast cancer or if the cancer did not respond to chemotherapy prior the surgery [37].

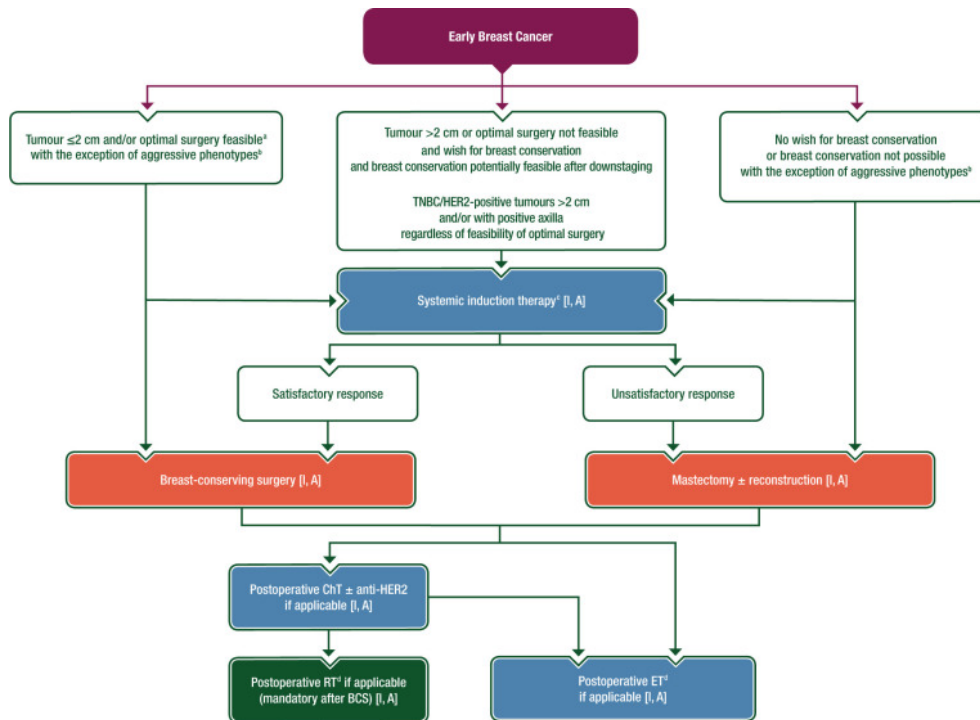


Figure 1.4: Breast cancer treating algorithm. Based on breast cancer stage, the molecular subtype and patient decisions different treatments for primary breast cancer are used in the clinics. Figure is taken from [37].

There are several risk factors for breast cancer. For example being female and advanced age increases the risk for developing breast cancer. But also genetic predispositions can augment the risk for breast cancer. The most common genetic risk factors are mutations within the Breast cancer type 1/2 susceptibility protein (BRCA1 and BRCA2). These two genes are normally expressed in cells of the breast and are involved in DNA damage repair mechanisms. If the function of these proteins are disturbed by genetic mutations, DNA damages can not be correctly repaired and the risk for abnormal cell growth and development of cancer increases. Thus, BRCA1 and 2 can be also classified as Tumor suppressors [78]. For BRCA1 or BRCA2 mutated breast cancer there are special targeted therapies using PARP inhibitors such as talazoparib or olaparib. Since BRCA mutated cancer cells are already deficient in their DNA repair machinery, additional blocking of PPAR proteins, that are also involved in DNA repair, leads to death of cancer cells [72].

The so far mentioned risk factors are fixed risk factors meaning that they can not be circumvented. In contrast to modifiable risk factors. These are for example obesity, exposure to radiation or alcohol consumption. Interestingly, pregnancy and breast-feeding lowers the risk for breast cancer development [124].

1.1.3 Cancer immunosurveillance

The changes in cell cycle, signalling pathways and metabolism in cancer cells are very well studied. But over the last decades it became more obvious that the cancer surrounding environment is also very important in order to understand cancer progression. Indeed, the proportion of cancer cells is often only one third of the whole Tumor. The rest is comprised of stromal cells and Tumor infiltrating immune cells. It has been shown, that very often cancer cells need the surrounding non-cancerous cells to survive and grow [91]. Thus, studying the Tumor microenvironment may also help to gain more insights in cancer progression and to find new strategies for cancer treatment. In this section the role of CD8⁺ and CD4⁺ T cells in cancer microenvironment will be discussed. T cells are very important elements of the adaptive immune system. Within the cancer microenvironment T cells are also often referred to as Tumor infiltrating lymphocytes (TILs) [91].

T cells are a subset of lymphocytes belonging to the group of white blood cells, also called leukocytes [11]. CD8⁺ T cells, also called cytotoxic T lymphocytes (CTLs), recognize foreign antigens presented on major histocompatibility complex (MHC) class I molecules. Cytotoxic T cells express on their cell surface specific T-cell receptors (TCRs) that can recognize a certain antigen presented on MHC I. Upon binding, the cytotoxic T cell can then destroy the antigen presenting target cell [29]. Besides the TCR, also the CD8 transmembrane glycoproteins bind to the MHC I molecules to stabilize the interaction of the TCR with the MHC I. Therefore, CTLs are also called CD8⁺ T cells. The killing is mediated by the release of cytotoxins as granzymes, perforin or granulysin. Interestingly, the CTLs are resistant to their released cytotoxins due to a special composition of their plasma membrane [201].

CD4⁺ T cells, also called T helper cells, express the CD4 surface glycoprotein. In contrast to CD8⁺ T cells, CD4⁺ T cells bind with their TCR and CD4 as co-stimulator to antigens presented on MHC II molecules. MHC II is expressed by specialized antigen presenting cells (APCs) like dendritic cells. The main effector function of T helper cells is the secretion of immuno-stimulatory cytokines such as IFN γ or IL2, which promotes CD8⁺ T cell proliferation and activation. Overall, CD4⁺ T cells have a higher plasticity compared to CD8⁺ T cells. Based on the cytokine milieu they can differentiate into Th1, Th2, Th17 Tfh and iTreg cells. Thus, CD4⁺ T cells can be either pro-immunogenic or anti-immunogenic. For example iTregs, which are mainly characterized by FOXP3 expression, inhibit immune cell effector function amongst other things by producing adenosine via NT5E/CD73 [150, 29].

The "Three ES of cancer immunoediting" suggested by Robert Schreiber summarizes the different stages of the interplay between cancer and immune cells. Due to their high mutational load, cancer cells often express a variety of cancer specific antigens, that can be recognized by CTLs. And indeed, the first ES is the immune-elimination of cancer cells by CTLs accompanied by pro-immunogenic CD4⁺ T cells. The second phase is an equilibrium between cancer and immune cells. And finally the last ES is the immune escape of the cancer cells from the immune cells. In many Tumors TILs can be found and high numbers of T cells are associated as a positive prognostic marker for example in primary melanoma. There are very often cancer-specific T cells within the Tumor microenvironment, but their effector function

is blocked by an overall immunosuppressive milieu. This offers potential treatment options e.g. by reversing the suppressive mechanisms and to re-activate the TILs *inter alia* by using immune checkpoint inhibitors [91, 64].

1.1.4 The immunological synapse

The interface between a T cell and an antigen-presenting cell (APC) is called immunological synapse. The APC can be another immune cell like dendritic cell or a target cell like a cancer cell. This cell-cell interaction is characterized by concentric supra-molecular activation clusters (SMACs). Each of these SMAC clusters has a specialized function and contains distinct types of proteins [25]. Different types of receptors are important for the immunological synapse like receptors that recognize antigens like TCRs, receptors involved in adhesion and mediating cell-cell contacts and co-stimulatory as well as inhibitory molecules [65]. Within the central cSMAC the antigen receptors are located as well as co-stimulatory receptors like CD80/CD86 or immune checkpoint molecules like CTLA4, PD-1/PD-L1. The cSMAC is surrounded by the peripheral pSMAC which exhibits a high content of adhesion molecules like $\alpha_L\beta_2$ integrin Lymphocyte function-associated antigen 1 (LFA-1). The pSMAC also contains Connexin43 (Cx43) molecules which forms hemichannels between the T cell and the APC. The outermost SMAC is the distal dSMAC which forms a dense ring of filamentous actin (F-actin) and is also sometimes referred to as fSMAC [25, 232]. Dis-regulation of the immunological synapse can cause auto-immunity or lead to cancer cell immune evasion. Thus, several treatments have been developed that target the immunological synapse to treat e.g. cancer. Especially immunotherapy targeting immune checkpoint molecules improved cancer treatment [65]. In the following chapter the individual immune checkpoint molecules are introduced and their clinical impact is explained.

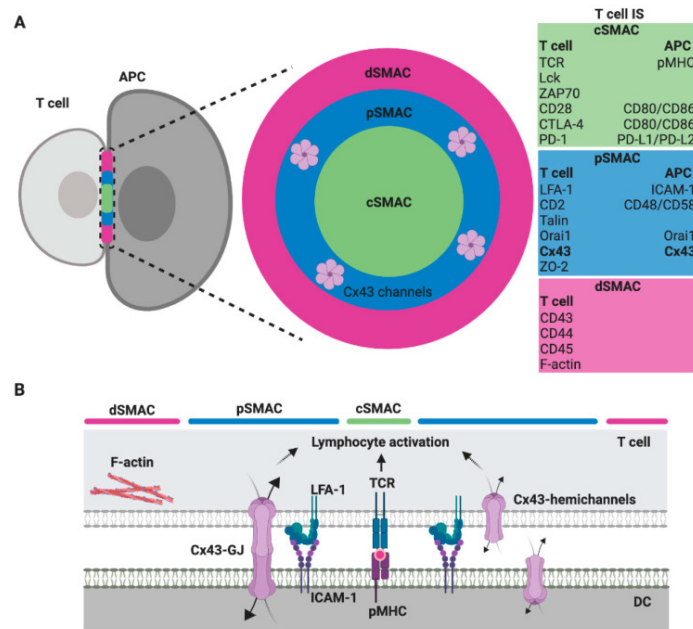


Figure 1.5: The immunological synapse (IS). The IS is the interface between a T cell and a APC like cancer cell. The IS consists of different SMAC patterns: central cSMAC, peripheral pSMAD and the distal dSMAC. Figure is taken from [232].

1.1.5 Immune checkpoint molecules

In this chapter immune checkpoint molecules will be considered in more detail. Their normal function as well as their implication in cancer will be specified. Finally, the usage of agents and in particular antibodies targeting these immune checkpoint molecules for treating cancer will be explained.

PD-1/PDCD1

Programmed cell death protein 1 (PD-1), also referred to as CD279 or PDCD1, which is the official gene name, is expressed on the cell surface of e.g. antigen-specific T cells. Under normal conditions, PD-1 protects from autoimmunity by dampening immune responses. But within Tumor microenvironment, PD-1 expression manifests an immunosuppressive milieu. PD-1 belongs to the immunoglobulin (Ig) superfamily and consists of 288 amino acids with a N-terminal IgG-V domain, a transmembrane domain and a cytosolic domain that contains immunoreceptor tyrosine-based switch motif (ITSM) and an immunoreceptor tyrosine-based inhibitory motif (ITIM). PD-1 is not able to form homodimers and can be only found in monomeric state on cell surface. Upon bidirectional interactions with its ligands PD-L1 or PD-L2, PD-1 transmits its inhibitory signals on T cell activation. Besides inhibiting function of antigen-specific T cells, PD-1 signalling was also shown to induce regulatory T cells (Tregs), which is an additional mechanism of controlling and dampening T cell activation in order to prevent autoimmunity [77, 227].

PD-L1/CD274

Programmed death-ligand 1 (PD-L1) or CD274, which is the official gene name, is one of the two ligands of PD-1 besides PD-L2. Whereas PD-L2 is predominantly expressed on dendritic cells (DCs), mast cells and macrophages, PD-L1 expression can be found on a broader panel of hematopoietic and non-hematopoietic cell types. For example PD-L1 is expressed on T cells, B cells, DCs, mast cells, macrophages, but also on healthy tissue cells like keratinocytes, vascular endothelial cells or astrocytes. But also cancer cells and cancer-associated stromal cells can gain expression of both PD-L1 and PD-L2 [227].

Like PD-1, PD-L1 belongs to the immunoglobulin (Ig) superfamily. It is a type 1 transmembrane protein with a size of 40 kDa. It exerts its function by binding to its receptor PD-1, which is expressed for example by activated B and T cells. PD-L1 has two extracellular Ig domains, one N-terminal Ig-V and one C-terminal Ig-C-like domain. Furthermore, PD-L1 consists of a transmembrane domain and short cytoplasmic tail without any signalling motifs [227, 143]. Upon binding of PD-L1's extracellular domains with PD-1, the conformation of PD-1 is changed which in turn enables Src family kinases to phosphorylate the immunoreceptor tyrosine-based switch motif (ITSM) and the cytoplasmic immunoreceptor tyrosine-based inhibitory motif (ITIM). The phosphorylated tyrosine motifs leads to recruitment of SHP-1 and SHP-2 protein tyrosine phosphatases. SHP-1 and SHP-2 dampens T-cell activation by dephosphorylating the co-stimulatory receptor CD28. Summing up, binding of PD-L1 to PD-1 inhibits T cell survival, production of cytokines and proliferation [84, 270, 111]. Thus, up-regulation of PD-L1 by cancer cells helps them to evade from the immune system. Inter-

estingly, PD-L1 alone on cancer cells also seems to have a protective function without the binding to PD-1. It was shown that the susceptibility to killing by CTLs mediated by type I and type II interferons is lowered by PD-L1 [83].

CTLA4

Cytotoxic T-lymphocyte-associated protein 4 (CTLA4), also previously known as CD152, is also a member of immunoglobulin-related receptors that is also involved in inhibiting T cell function. CTLA4 is normally expressed by CD8⁺ and CD4⁺ T cells, especially in Tregs [200]. But its expression was also found to be up-regulated in melanoma cells upon IFN γ signalling [167]. In contrast to PD-L1, CTLA4 forms homodimers at the cell surface by disulfid bond between cysteins at position 122 [54].

CTLA4 binds to receptors CD80 and CD86 expressed by antigen-presenting cells (APCs), such as macrophages, dendritic cells or B cells, thereby acting as an antagonist of CD28, which can also bind to these co-stimulatory receptors in order to activate T cell function. CTLA4 has a higher avidity and affinity for CD80 and CD86 than CD28 thereby reducing the immunostimulatory function of APCs via CD28 signalling. Normally, CTLA4 signalling is important to maintain self-tolerance, but in setting of cancer diseases CTLA4 expression hinders immune responses against Tumor cells [200].

NT5E/CD73

NT5E, also known as CD73, is an ecto-5'-nucleotidase expressed on the cell surface of various cell types. This membrane-bound enzyme catalyses the hydrolysis of extracellular adenosine monophosphate (AMP) into adenosine (ADO) and inorganic phosphate [196]. As shown in figure 1.6, NT5E consists of a homodimer, which is anchored to the cell membrane by glycosylphosphatidylinositol anchors. Besides AMP, also nucleosidase activity for nicotinamide adenine dinucleotide and nicotinamide mononucleotide was observed for NT5E [127, 226]. NT5E functions together with ENTPD1, also referred to as CD39. As depicted in figure 1.6, ENTPD1 catalyses the hydrolysis from extracellular adenosine triphosphate (ATP) into AMP through two reversible reaction steps. Interestingly, the final reaction step from AMP to adenosine mediated by NT5E is irreversible [19].

There are two conformations of NT5E molecular structure: an open and a closed conformation. NT5E transits through this two stages during substrate cleavage. These conformational changes are enabled by the flexible α -helix which connects the C-terminal domain with the N-terminal domains. The N-terminal domains bind the co-factors Zn²⁺ and Ca²⁺. NT5E is post-transcriptionally modified at four distinct asparagine residues either by mannose saccharide chains or by a mixture of complex glycans and high mannose [127]. The full-length NT5E molecule consists of 574 amino acids (NT5E-201). In different human tissues also a shorter NT5E splice variant (NT5E-203) missing exon 7 with a length of 525 amino acids was detected. To note, this splice variant was found to be intracellularly over-expressed in human hepatocellular carcinoma cell lines [220]. Exon 7 encodes amino acids 404–453, which are crucial for the homodimerization. Thus the shorter splice variant of NT5E is not located

at cell surface and exhibits impaired substrate binding and abrogated 5'-nucleotidase activity. Interestingly, it was found that the shorter splice variants cause proteasome-mediated degradation of the intracellular normal NT5E variant whereas the level of the extracellular native NT5E homodimers is not effected.

Under normal circumstances NT5E is expressed in cardiac myocytes, epithelial cells of the respiratory tract, smooth muscle cells and certain immune cells like regulatory T cells (Tregs) or myeloid-derived suppressor cells (MDSCs) [45, 225]. NT5E is involved in epithelial ion transport thereby preserving mucosal hydration [225]. Furthermore, NT5E acts as a gate keeper on endothelial cells since free adenosine is involved in "resealing" gaps between vascular endothelial cells caused by transmigrating neutrophils [137]. One of the most important functions of NT5E is its regulatory role in inflammatory immune responses. Normally, Tregs express NT5E on their cell surface [123]. The produced adenosine from Tregs is exerting anti-inflammatory functions by binding to adenosine receptors on various immune cells like effector T cells, dendritic cells, macrophages, MDSCs or natural killer cells. This mechanism helps to dampen immune response and is also important to prevent autoimmune diseases and to maintain tolerance to self-antigens [28]. Accumulation of immunosuppressive adenosine produced by NT5E, leads to activation of cAMP signalling cascade in immune cells expressing A2A adenosine receptors (ADORA2A) on their cell surface. The activation of cAMP signalling leads to inhibition of immune cells effector functions [268, 128, 12]. Besides blocking effector functions, adenosine was also found to inhibit proliferation, activation and chemotaxis of T cells [219, 15].

Normally expressed on Tregs, NT5E has been found to be expressed also by many different Tumor entities such as colorectal cancer [146], triple-negative breast cancer [15, 36], melanoma [204, 205, 245] or non-small cell lung cancer [113]. In light with the immunosuppressive effect of adenosine and its expression by various cancer types, NT5E can be considered as an immune-inhibitory checkpoint molecule suitable as a target for cancer immunotherapy. How NT5E-directed immunotherapy can be used to treat cancer patients will be highlighted in the next chapter.

Besides its enzymatic activity, NT5E was also found to function as a receptor molecule mediating cell-cell adhesion between endothelial cells and lymphocytes [10]. Also the interplay of the extracellular matrix components (ECM) with NT5E was shown by several authors [15, 18, 203]. It was proven, that this interaction is independent from NT5E's enzymatic activity since blocking of its ectonucleotidase activity by concanavalin had no impact on the interaction of NT5E with collagen 1, fibronectin or tenascin C. The interaction of NT5E and tenascin C was found to be the mediator of cell adhesion and migration [128]. How NT5E is regulated on the transcriptional and posttranscriptional level is elucidated in a later chapter.

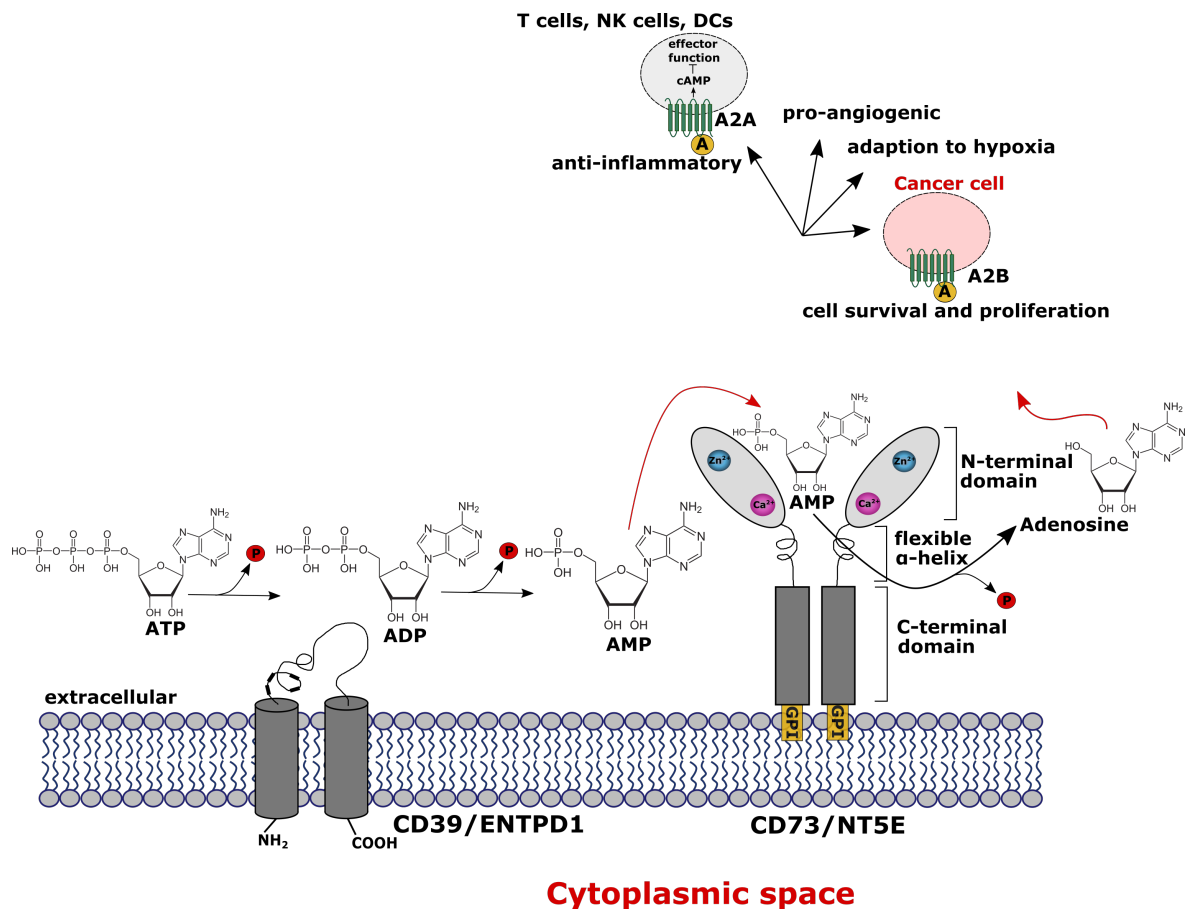


Figure 1.6: Structure and function of NT5E/CD73. The membrane bound ecto-5'-nucleotidase NT5E hydrolyzes extracellular adenosine monophosphate (AMP) into adenosine and inorganic phosphate (P). Upstream of NT5E, adenosine triphosphate (ATP) is hydrolyzed via two reaction steps into AMP by the enzyme ectonucleoside triphosphate diphosphohydrolase-1 (ENTPD1) (CD39). Adenosine thus produced exerts anti-inflammatory effects by binding to the adenosine A2A receptor (ADORA2A) expressed by T cells, natural killer (NK) cells, and dendritic cells (DCs) resulting in cAMP mediated blocking of their effector functions. To some extent, the A2B receptor (ADORA2B) is also expressed on DCs and macrophages which are suppressed by adenosine. Thus, cancer cells can evade the immune system by up-regulating NT5E protein levels. Furthermore, adenosine binds to the A2B receptor expressed by cancer cells leading to Tumor cell survival and proliferation. Cancer cells also express the adenosine A1 receptor (ADORA1) and A3 receptor (ADORA3) and binding of adenosine to these receptors leads to Tumor cell migration and proliferation via signalling through G_i proteins. Adenosine is also involved in the adaption to hypoxia and shows pro-angiogenic potential. All adenosine receptors are depicted as stylized green transmembrane proteins. Adenosine is symbolized as yellow circles marked with "A". Picture is taken from [128].

1.1.6 Immunotherapy

Besides the classical cancer treatments like surgical removal of Tumor, chemo- and radiotherapy, also immunotherapy became more important especially for treating advanced metastasised cancers that showed none or only weak responses to other standard treatments. In general, the principle of immunotherapy is to boost the natural immune defence of the body against cancer cells or to block the inhibitory mechanisms that cancer cells gained to evade from the immune system. There are different types of immunotherapies to treat cancer like cancer vaccines, oncolytic viruses, T-cell based therapies or monoclonal antibodies directed against immune checkpoint molecules.

Monoclonal antibodies

Antibodies binding to immune checkpoint molecules and thereby blocking their immunosuppressive function are widely used in the clinics to treat advanced cancers. First data using PD-1 blocking antibodies were collected 2010 for melanoma, renal cell carcinoma and colorectal cancer. To date, antibodies blocking the PD-1/PD-L1 axis showed good responses for several cancer types e.g. melanoma and are now approved for clinical usage. But for other cancer types like breast cancer, anti-PD-1/PD-L1 monotherapy only have modest antiTumoral effects. Examples for approved antibodies targeting PD-1 in melanoma are: nivolumab and pembrolizumab. Examples for PD-L1 blocking antibodies are atezolizumab and durvalumab [227]. Nivolumab for example had almost 25 % overall response rate (ORR) in phase II trial for metastatic melanoma [175]. Monoclonal antibodies directed against CTLA4 are for example ipilimumab and tremelimumab. To note, ipilimumab was the first approved monoclonal antibody for metastatic melanoma treatment in 2011 with an overall response rate (ORR) of 11 % in a phase III trial. Although the monotherapies showed good clinical responses, the major challenge is resistance to therapy. Therefore, combinations of different antibodies as well as with other treatments are tested and it is checked whether these combinations can have clinical benefit [174]. For example combination of anti-CTLA4 and anti-PD-1 could enhance progression-free survival in melanoma in comparison to the anti-PD-1 monotherapy [227].

Also antibodies blocking CD73 and CD39 are considered for immune checkpoint therapy. The idea hereby is to abrogate the adenosine mediated inhibition of effector immune cell function [178]. There are different possible ways to target adenosine signalling within the Tumor microenvironment. For example small molecule antagonists directed against the adenosine receptors A2A and A2B, small molecules inhibiting CD73 function and monoclonal antibody targeting CD73 and CD39 are used to abrogate adenosine mediated immunosuppression. mAB against CD39 are currently in phase I clinical trial. Preclinical data showed that mAB-CD39 monotherapy reduced cancer metastasis and delayed Tumor growth. Furthermore, synergistic effects of mAB-CD39 and anti-PD-1 or anti-CTLA4 were observed [16]. Also mAB-CD73 treatment reduced cancer metastasis formation, reduced Tumor growth and revoked adenosine-mediated immunosuppression in preclinical studies [14]. There are several clinical phase II trials ongoing with the CD73 blocking monoclonal antibody oleclumab for treatment of triple negative breast cancer, colorectal cancer, pancreatic cancer and other Tumor entities. In many studies oleclumab is combined with PD-L1 targeting durvalumab

monoclonal antibody [161].

Cancer vaccines

The high rate of genomic mutations leads to expression of many new Tumor-associated antigens (TAA). These TAAs are presented at cancer cell surface by major histocompatibility complex (MHC), which can lead to recognition by Tumor-specific T cells. But often cancer cells can evade from this mechanism and avoid being killed e.g. by down-regulating the number of expressed MHC molecules or increasing the expression of immune checkpoint molecules [179]. The TAAs are attractive targets for cancer vaccines to boost the bodies immune response against cancer cells.

One example vaccine currently in clinical phase I trial is the liposomal RNA vaccine (RNA-LPX) FixVac from BioNTech. To note, the principle of RNA vaccine was initially developed for treating especially melanoma diseases. But the concept was also adopted for generating in a fast-track procedure a very potent vaccine against COVID-19 virus, which caused a world-wide pandemic 2020/21. The specific feature of FixVac is that it targets four non-mutated TAAs prevalent for melanoma. Most cancer vaccines are based on mutated TAAs. FixVac contains RNA encoding for the following TAAs, which are known to have a high immunogenicity: trans-membrane phosphatase with tensin homology (TPTE), tyrosinase (TYR), melanoma-associated antigen A3 (MAGE-A3) and New York oesophageal squamous cell carcinoma 1 (NY-ESO-1). Patients expressing at least one of these TAAs are suitable for the vaccination with a prime/repeat boost protocol. FixVac alone or in combination with anti-PD-1 treatment led to durable objective responses in advanced melanoma patients, that previously already underwent checkpoint-inhibitor treatment [206].

Oncolytic viruses

In 2015 the oncolytic viral therapy T-VEC based on herpes simplex-1 virus (HSE-1) was approved for melanoma treatment. In general, viruses used for cancer treatment are modified such as they lack virulence against normal cells and only "infect" cancer cells which results in cancer specific cell-lysis. Cancer cells are more susceptible to oncolytic viruses, since they often lost the normal cellular anti-viral defence mechanisms to gain higher proliferation rate. T-VEC is also modified to express GM-CSF, which leads to an increase in immune cell proliferation and stimulation. T-VEC is injected directly into the Tumor [179]. But there are also oncolytic viruses, that can be administered intravenously which is beneficial for treatment of metastasised cancer diseases. Furthermore, oncolytic viruses can be also modified to encode for TAAs to enhance their anti-Tumor activity [34].

T-cell therapy

Another approach of assisting the bodies immune system to fight cancer are adoptive T cell therapies. There are different approaches like Tumor-infiltrating T cells (TILs) or chimeric antigen receptor T-cell (CAR T-cell) therapy. TILs therapy is based on already existing immunity against cancer cells. Basically, Tumor-specific T-cells are isolated from the patient

and expanded *in vitro* until they get re-infused into the patient alongside with immunostimulatory cytokines [63, 86]. For CAR T-cell therapy, the T cells are additionally genetically engineered *in vitro* often using CRISPR/Cas9 system [179]. The CAR receptors are designed to recognize a specific TAA and to activate cytolytic T cell function. The CARs are not only containing the extracellular TAA-binding domain, but also co-stimulatory intracellular signalling domains like CD28, CD3 and OX40. First, CAR therapies were approved for haematologic cancers like leukaemia, but current clinical trials also focus on solid Tumors [168]. One limitation of CARs compared to TCRs of native T cells is the exclusive recognition of antigens expressed on the Tumor cell surface. Internal antigens presented by Tumor cells MHC can not be recognized by CARs [60].

1.2. miRNAs

As mentioned beforehand, miRNAs are one component of post-transcriptional regulation of gene expression. miRNAs are defined as small non-coding single-stranded RNAs consisting of 19 to 25 nucleotides [30]. Since the last decades these small molecules became more into the focus of researchers trying to unravel their biogenesis, function and impact for diseases such as cancer. Back in 1993, less than 30 years ago, the first miRNA was described by Lee, Feinbaum and Ambros. They discovered the first miRNA lin-4 in *Caenorhabditis elegans*, which regulates the expression of LIN14 protein by binding to 3'-UTR of lin14 mRNA thereby controlling post-embryonic development in *C. elegans* [134]. miRNAs have been found to be highly evolutionary conserved and are important regulators for e.g. cell proliferation, development, metabolic processes, apoptosis and differentiation in many different species [133, 147]. To date, there are 2654 known mature miRNA sequences for *homo sapiens* and 1978 for *mus musculus* according to miRBase data base (release 22.1, October 2018) [129].

1.2.1 Biogenesis

The biogenesis of miRNAs is illustrated in figure 1.7. As for mRNAs, miRNA biogenesis starts with transcription in the cell nucleus. There are two sorts of miRNAs: intragenic and intergenic. Intergenic miRNA genes are similar to normal protein coding genes. They have their own promoter and terminator units. But more than half of miRNA genes are located within genomic region of protein coding genes. These intragenic miRNAs are either intronic or extronic depending on their location within the host gene. Intragenic miRNAs are not transcribed independently since they share the transcriptional units like promoter with their respective host gene [169, 103].

The majority of miRNAs in mammals is transcribed by RNA polymerase II resulting in so-called primary miRNA (pri-miRNA). pri-miRNAs are several kilobases long, contain a stem-loop like structures, have a 7-methyl guanosine cap at their 5'-end and a poly-A tail [135, 210]. To note, a small portion of miRNAs, which contain retrotransposal *Alu* elements, are transcribed by RNA polymerase III [32]. As depicted in figure 1.7 the pri-miRNAs are further processed inside the cell nucleus by a complex of Drosha-DiGeorge syndrome critical region gene 8 (DGCR8) and the RNase III-type endonuclease Drosha. This complex binds and cuts the pri-miRNA into precursor miRNA (pre-miRNA), with a size of around 70 nucleotides

in length and a hairpin structure [94, 199]. For further processing the pre-miRNA is exported to the cytosol by RAnGTP-dependent nuclear transport reporter exportin 5 (XPO5) [266]. In the cytosol the pre-miRNA is bound by the transactivation response RNA binding protein (TRBP) and cleaved by the RNase III enzyme Dicer into approximately 20 nucleotide long mature miRNA/miRNA* duplex, which is bound by Argonaute proteins (Ago) forming the so-called RNA-induced silencing complex (RISC). RNA helicases unwind the miRNA duplex and the passenger strand (miRNA*) is normally degraded, whereas the guide strand (mature miRNA) remains in the RISC complex, which is sometimes also referred to as the miRISC [191].

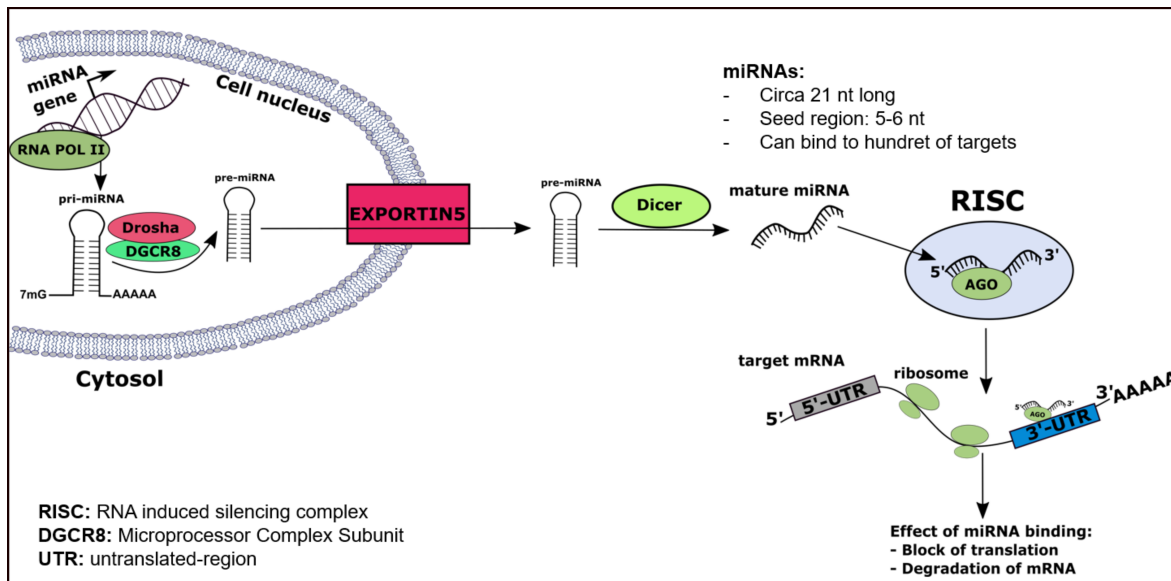


Figure 1.7: miRNA biogenesis and function. miRNA genes are mainly transcribed by RNA polymerase II and the resulting pri-miRNA is processed by Drosha/DGCR8 complex into hairpin-structured pre-miRNA. The pre-miRNA is subsequently exported into cytosol by EXPORTIN5 where it is cleaved by Dicer into mature miRNA. The mature miRNA binds together with Ago proteins to target mRNA's 3'-UTR regions thereby blocking translation or even causing degradation of mRNA.

1.2.2 Function

The miRISC, consisting of mature miRNA and Ago proteins, can bind to target mRNAs and affect their translation and stability. Most miRNAs bind with their 5-6 nucleotide long seed sequence to the 3'-UTR of target mRNAs. In rare cases, miRNAs can also bind to the 5'-UTR or open reading frame (ORF) of target mRNA [180]. It is also described, that a subset of miRNAs can potentially activate gene expression by binding to the promoter region of target genes [278]. Depending on the degree of complementary base pairing, the target mRNA is either degraded or its translation is hindered. If the miRNA sequence shows perfect complementarity to the target mRNA, the mRNA is degraded. But often, the miRNA only binds partially to the mRNA. In this case protein translation is blocked, but the mRNA remains stable [79].

Since the seed sequence of a miRNA only comprises around six nucleotides, one miRNA can target multiple mRNAs and thereby regulate a variety of networks and pathways. But also one target mRNA is regulated by several miRNAs. This makes miRNA mediated regulation a quite complex mechanism that always affects multiple regulators and targets [24, 162]. Approximately more than 33 % of all protein-coding genes are thought to be regulated by miRNAs [154]. Thus, the deeper understanding of miRNA mediated regulation is quite important to further understand diseases like cancer, in which the normal gene regulation is disturbed.

Besides their intracellular functions, miRNAs are also important factors for intercellular communication. miRNAs can be also exported into extracellular space via different mechanisms. For example protein transporters export miRNAs bound to argonaute proteins (AGO) or high-density lipoproteins (HDL) [81]. Thus, the ATP-binding cassette transporter 1 (ABCA1) exports miRNA-HDL complexes. These complexes are then taken up by target cells via scavenger receptor class B type 1 (SR-B1) [87].

Another miRNA export mechanism works via extracellular vesicles (EV). There are various forms of EV basically differing in their size and origin. The encapsulation of miRNAs by EVs protects them from degradation by RNases. miRNAs can be exported via ectosomes, which have a diameter of 50-2000 nm [188]. The smallest EVs are called exosomes with a diameter of 30-180 nm that originate from intracellular endosomes [164]. Exosomes carry a variety of bioactive molecules like miRNAs but also mRNAs, long non-coding RNAs (lncRNAs), lipids and proteins. Interestingly, exosomes have been found to be an useful tool for predicting cancer development and progression [235]. It was found that exosomes contribute to melanoma progression. Via exosomes melanoma cells can transfer miRNAs between each other, but also to other surrounding cell types like endothelial cells or fibroblasts [235, 256]. Furthermore, miRNAs can be also transported by ectosomes, melanosomes, which are specific for melanocytes and melanoma cells, or oncosomes [81]. Oncosomes are quite big EVs with a size of 1-10 μm , which are released by cancer cells and their amount has been related to cancer progression [56]. Ectosomes have a diameter of 50-2000 nm and are formed by outward budding of cell membrane [188].

1.2.3 miRNAs and cancer

Within the last years miRNAs became more important for the understanding of cancer development and progression. Studying miRNA expression profiles among different cancer types and the comparison with healthy counterpart tissues helped to gain more insights in the molecular mechanisms and regulatory networks that drive carcinogenesis. Not only are miRNA expression patterns degenerated in cancer cells, but they play also an important role in all hallmarks of cancer. Within this chapter exemplary miRNAs will be specified for each hallmark of cancer defined by the famous paper of Hanahan and Weinberg [95]. The main focus will be thereby on the two cancer entities melanoma and breast cancer since within this thesis cancer cell lines from those two cancer types are predominantly investigated.

There are two important types of miRNAs with regard to cancer: oncogenic and Tumor

suppressive miRNAs. Oncogenic miRNAs, also referred to as oncomiRs, are expressed at high levels in cancer cells and promote Tumor development or progression e.g. by inhibiting the expression of Tumor suppressor genes. On the contrary, Tumor suppressor miRNAs, also referred to as tsmiRs, are expressed at lower levels in cancer cells compared to healthy tissues. Their loss of expression can also lead to Tumor development and progression since tsmiRs often inhibit the expression of oncogenes.

Sustaining proliferative signals

Under normal conditions cells can only divide for a limited number of cell cycle transitions and will finally arrest in the G0 phase in order to remain a healthy cell density within a tissue. But for cancer cells this adaptive cell cycle arrest mainly caused by inhibitory signalling from surrounding environment is disrupted. Cancer cells can evade this growth suppression and gain an abnormal high proliferation rate [147, 171].

miR-1207-5p was found as an oncomiR in breast cancer. Elevated miR-1207-5p levels increased the proportion of cells at G2 phase of the cell cycle and enhanced cancer cell proliferation. miR-1207-5p was found to directly inhibit the regulator STAT6. STAT6 normally activates transcription of cell cycle-dependent kinase inhibitors CDKN1A and CDKN1B. Thus, the activation of miR-1207-5p leads to decreased CDKN1A and CDKN1B levels, which results in an aberrant high proliferation [260]. An example for a Tumor suppressive miRNA (tsmiR) involved in cancer cell proliferation is miR-193b, which has been found to be significantly down-regulated in melanoma compared to benign nevi resulting in higher cancer cell proliferation. Normally, miR-193b targets cyclin D1 (CCND1), which is an important regulator of cell cycle transition and low levels of CCND1 inhibits cell proliferation [43].

Deregulation of cellular energetics

Cancer cells often exhibit changes in metabolic program known as the Warburg effect characterized by an enhanced uptake and usage of glucose [116]. In breast cancer cells miR-122 was found as an oncomiR highly secreted by cancer cells. The secreted miR-122 is taken up by non-Tumor cells and inhibits their glucose uptake. This supports the high glucose need of the cancer cells. miR-122 inhibits the expression of citrate synthase and pyruvate kinase in non-Tumor cells. Both are important metabolic enzymes and pyruvate kinase is involved in the last step glycolysis. Interestingly, the systemic treatment *in vivo* with antagomiRs directed against miR-122 improved glucose uptake of distant organs and led to lower number of breast cancer metastasis [76].

Resisting apoptosis

Normally apoptosis, also called programmed cell death, is a safety mechanism for the organism if cells exhibit a disrupted genetic or chromosomal content like cancer cells. But cancer cells can get resistant to apoptosis preventing their cell death. miR-21 is an oncomiR involved in apoptotic processes in breast cancer [147] as well as in melanoma [231]. Furthermore, miR-21 expression is significantly higher in metastatic and primary melanoma compared to melanocytes or benign nevi. High miR-21 is associated with shorter survival time of

melanoma patients. Treatment of melanoma cells with antagomiRs targeting miR-21 induces apoptosis, reduces proliferation and enhances the sensitivity to chemo- and radiotherapy [231, 118]. Also in breast cancer, miR-21 expression inhibits apoptosis by imbalancing the ratio of pro-apoptotic BAX protein and anti-apoptotic BCL-2 protein [139]. Interestingly, miR-21 does not act via inhibition of the pro-apoptotic BAX, but it directly up-regulates the anti-apoptotic BCL-2. This is one of the rather rare cases, where binding of miRNA in 3'-UTR of target genes leads to an up-regulation of the target's expression [59].

Genome instability and mutations

miRNAs are also involved in the regulation of proteins of the DNA repair pathways. For example, the ATM serine/threonine kinase is inhibited by miR-630 or miR-421 [132]. ATM serine/threonine kinase is an important enzyme, which is activated and recruited upon DNA double-strand breaks. It subsequently phosphorylates and thereby activates several other factors involved in DNA repair, cell cycle arrest and apoptosis. Many of the regulators activated by ATM serine/threonine kinase are Tumor suppressors [173]. But also miRNA expression patterns itself can be deregulated by genomic instability. In melanoma, the expression of the Tumor suppressive miRNA miR-34b is silenced by increased methylation of a CpG island upstream of the miR-34b gene [159]. Or on the contrary, the expression of the oncogenic miR-182 is activated by hyper-methylation of CpG-islands upstream of mature miR-182 in melanoma cells [159].

Induction of angiogenesis

miR-203 levels were found to be down-regulated in metastatic melanoma compared to primary melanoma due to hypermethylation of miR-203 promoter. Expression of miR-203 was found to have Tumor-suppressive potential by inhibiting angiogenesis and melanoma cell migration *in vitro*. Furthermore, miR-203 expression can limit primary Tumor growth and reduced the incidence of melanoma metastasis in lymph nodes and lungs. miR-203 can directly bind to the 3'-UTR of Snail family transcriptional repressor 2 (SNAI2) and melanoma cells express higher SNAI2 levels compared to benign nevi. It was found that knock-down of SNAI2 could mimic the effects of miR-203 and the re-expression of SNAI2 reversed the effects mediated by miR-203. Furthermore, miR-203 can also reduce the expression of IL-8, which promotes angiogenesis and neovascularization [215, 148]. miR-199a and miR-1908 have been identified as oncomiRs promoting angiogenesis in melanoma by recruiting more endothelial cells [187].

Activating invasion and metastasis

In advance of cancer progression single cancer cells from the primary lesions gain the ability to metastasise to distant organs. Cancers, that already metastasised are more difficult to treat and add up to drastically lower survival rate for patients. Several miRNAs have been linked to metastatic and invasive capacity of cancer cells. The miR-200c/141 cluster was found to be up-regulated in breast cancer resulting in greater metastatic potential by enhancing expression of SerpinB2. The expression of SerpinB2 is associated with higher metastasis risk and could serve as a prognostic marker for triple negative breast cancer patients [120]. In concordance, plasma levels of miR-200c/141 are higher in metastatic breast cancer patients

compared to primary breast cancer lesions [275]. Interestingly, in melanoma miR-200c seems to be a more Tumor suppressive miRNA than an oncomiR. The ZEB1-miR-200c-feedback loop was found to be important for the epithelial-to-mesenchymal transition (EMT) of cancer cells. It was found that miR-200c targets polycomb complex protein BMI-1 (BMI-1) [254], which enhances the expression of E-cadherin thereby inhibiting melanoma cell invasion [198]. Thus, the loss of miR-200c in melanoma activates cell invasion. A comprehensive miRNA screen performed by Weber and co-workers identified several miRNAs with the capacity to enhance or reduce melanoma cell invasion. Based on this screen miR-339-3p was identified as a Tumor suppressor in melanoma by directly targeting MCL1 [251].

Tumor promoting inflammation

Cancer cells also modulate their surrounding microenvironment including immune cells. Melanoma is a very highly immunogenic cancer type [184]. Cancer cells utilize inflammatory mechanisms to sustain their survival and proliferation [95]. For example miR-145 levels are decreased in various cancer types amongst breast cancer. miR-145 expression together with TNF α induces cell death and apoptosis. TNF α is a cytokine secreted by various cell types in the Tumor microenvironment such as T cells, macrophages, fibroblasts and monocytes and can be pro- and anti-Tumoral. With the loss of miR-145 expression, breast cancer cells can avoid the TNF α induced apoptosis [39].

Enabling replicative immortality

At the terminus of each chromosome a specific sequence is present consisting of TTAGGG tandem repeats called telomere. Telomeres protect the chromosome from DNA damage. With every cell division the length of telomeres is shortened until telomere dysfunction is reached which initiates cellular senescence and apoptosis. Cancer cells gain immortality due to aberrant telomerase activity [114]. The activity of telomerase, which maintains the telomeric DNA repeats at the end of chromosomes, is essentially dependent on reverse transcriptase telomerase protein (hTERT) and telomerase RNA template (hTERC) [151]. A group of miRNAs, that directly targets hTERT, have been shown to be down-regulated in breast cancer cells. These Tumor suppressive miRNAs are miR-296-5p and miR-512-5p, which are expressed at low levels in breast cancer. Low expression of these miRNAs and resulting high expression of hTERT is associated with poor survival of breast cancer patients [57]. The oncogenic miR-155 is up-regulated in breast cancer and targets telomeric repeat factor 1 (TRF1) at telomeres [58]. TRF1 is a compartment of shelterin, also referred to as telosome, which protects the telomere [106]. Enhanced expression of miR-155 leads to genomic instability and telomere fragility.

Immune evasion

The immune system normally detects and destroys degenerated cells. But cancer cells can gain mechanisms to hijack physiological immune checkpoint control, which is an important mechanism of the immune system to avoid overshooting immune responses and maintain self-tolerance [95]. miRNAs are also involved in immune evasion of cancer cells e.g. by dysregulating the expression of immune checkpoint molecules like CD274, NT5E, PD-1, B7-H3

or CTLA4. A comprehensive overview of immune modulatory miRNAs was given by Eichmüller *et al.* in 2017 summarizing the already known miRNAs involved in Tumor immune escape [67]. miRNAs targeting NT5E will be mentioned in the following section and can be also considered as miRNAs with potential role in immune evasion.

miR-195 and miR-497 are potential tsmiRs in breast cancer, since they can directly inhibit the expression of CD274 [263]. An example oncomiR involved in immune evasion is miR-519a-3p. Its expression decreased the ability of natural killer cells to kill breast cancer cells by down-regulating ligands for the NK cell-activating receptor NKG2D. miR-519a-3p can directly inhibit the expression of the ligands MICA and ULBP2 on Tumor cell surface allowing cancer cells to evade from NK cell mediated killing. High expression of miR-519a-3p was observed in advanced breast cancer with mutated p53 and its expression is correlated with worse clinical outcome [35]. In melanoma the miR-34 family has been identified to modulate innate immunity with a similar mechanism like miR-519a-3p. Also miR-34a/c can inhibit ULBP2 expression, which is as mentioned above a ligand for NKG2D. Thus, over-expression of miR-34a/c protected melanoma cells from cytotoxic activity of NK cells [101]. A melanoma cell specific mechanism of immune evasion is the regulation of MITF-M. miR-155 up-regulation leads to novel mechanism of melanoma immune evasion. IL-1 β , a cytokine released in Tumor microenvironment, was found to enhance miR-155 expression in melanoma cells. Thus, miR-155 directly targets MITF-M and inhibits its expression. Lower MITF-M levels in turn result in a lower expression of potential cytotoxic T cell target antigens [21]. Besides miRNA affecting immune relevant genes within cancer cells, also miRNAs changing expression pattern in immune cells are important for immune evasion. For example, several miRNAs have been identified to shift macrophages from inflammatory phenotype (M1-like) towards immunosuppressive state (M2-like), like miR-125b-5p secreted by melanoma cells through EVs. miR-125-5p is taken up by Tumor-associated macrophages (TAMs) and causes differentiation into a more Tumor-promoting phenotype [85].

1.3. Regulation of NT5E/CD73

Since the main focus of this thesis was the miRNA-mediated regulation of NT5E, this chapter will summarize the already known regulators of NT5E at the transcriptional and post-transcriptional level.

1.3.1 Transcriptional regulation of NT5E

Figure 1.8 summarizes the already known transcriptional regulators of NT5E. Furthermore, miRNAs are depicted that are known to directly regulate NT5E, or indirectly by binding to one of NT5E's transcriptional regulators 3'-UTR.

The NT5E promoter region possesses binding sites for the following transcriptional regulators: SMAD proteins, SP1 and AP-2. Furthermore, the NT5E promoter contains a cAMP-responsive element. Fausther and co-workers could show via chromatin immunoprecipitation that SP1 as well as SMAD2, SMAD3, SMAD4 and SMAD5 bind to the rat NT5E promoter with the strongest binding observed for SP1 and SMAD5 [99, 74]. The human and the rat

NT5E promoter share a sequence identity of 89 %. Thus, it seems very likely, that also the human NT5E could be regulated by SMAD transcription factor family. Synnestvedt *et al.* found that also the hypoxia-inducible factor-1 (HIF-1) can directly bind to NT5E promoter thereby activating NT5E expression [228]. This is in accordance with the described role of NT5E in adaptation to hypoxic conditions [51]. Hypoxic conditions often arise from uncontrolled proliferation of cancer cells [66], which can induce HIF-1 expression that in turn might lead to up-regulation of NT5E levels in Tumor cells.

Also the β -catenin-dependent Wnt signalling pathway is often degenerated in cancer cells [273]. T cell factor 1 (TCF-1) is one component of the Wnt/ β -catenin signalling pathway and the promoter core sequence of NT5E is flanked upstream by a regulatory region containing consensus motifs for TCF-1. In the presence of TCF-1, β -catenin can strongly increase NT5E expression, and adenomatous polyposis coli protein (APC), an antagonist of β -catenin, can inhibit NT5E expression [222]. Besides β -catenin, also NF κ B/TNF α were identified as positive transcriptional regulators and PPAR γ as a negative regulator of NT5E expression [182].

In murine Th17 cells, which were differentiated *in vitro* with TGF- β and IL-6, it was found that Stat3 activates Entpd1 and Nt5e expression whereas Gfi-1 repressed expression of both exonucleotidases via binding to the respective promoter [40]. Another study based on a genome-wide analysis in murine mature Treg cells identified Nt5e as one target gene of the forkhead box transcription factor (Foxp3) [284]. Foxp3 is a transcription factor specifically expressed in murine and also human Treg cells as well as in recently activated human T cells [149]. The regulation of NT5E by FOXP3 is very likely to be cell-type specific mechanism restricted to a subset of T cells, especially Treg cells, and might not be related to NT5E regulation in cancer cells. Noteworthy, it was found that high FOXP3 expression correlated with poor patient survival in ovarian cancer [255].

1.3.2 Post-transcriptional regulation by miRNAs

The human 3'-UTR has an average size of 800 nucleotides [163]. In fact, the NT5E 3'-UTR consists of 1774 nucleotides (NM_001204813.1) [55] and is more than two times bigger than the average human 3'-UTR. Thus, it appears that regulation of NT5E by miRNAs might play an essential role in the modulation of NT5E expression. Despite the long 3'-UTR region of NT5E, only a few miRNAs are known to directly regulate NT5E to date. Among those miRNAs is miR-422a. Bonnin and co-workers observed a significant negative correlation between NT5E mRNA expression and miR-422a level in neck squamous cell carcinoma (HNSCC) patients. Blocking of endogenously expressed miR-422a by specific antagomiRs enhanced NT5E protein expression. It was found, that lower miR-422a levels correlated with shorter relapse free survival times in HNSCC eventually due to over-expression of NT5E [31].

In colorectal cancer (CRC), the regulation of NT5E by miR-30a was identified. Transfection experiments with miR-30a mimics decreased NT5E mRNA as well as protein expression. Direct targeting of miR-30a was proven by 3'-UTR reporter assays [258]. The regulation of NT5E by miR-30a was also described for non-small cell lung cancer. Over-expression of

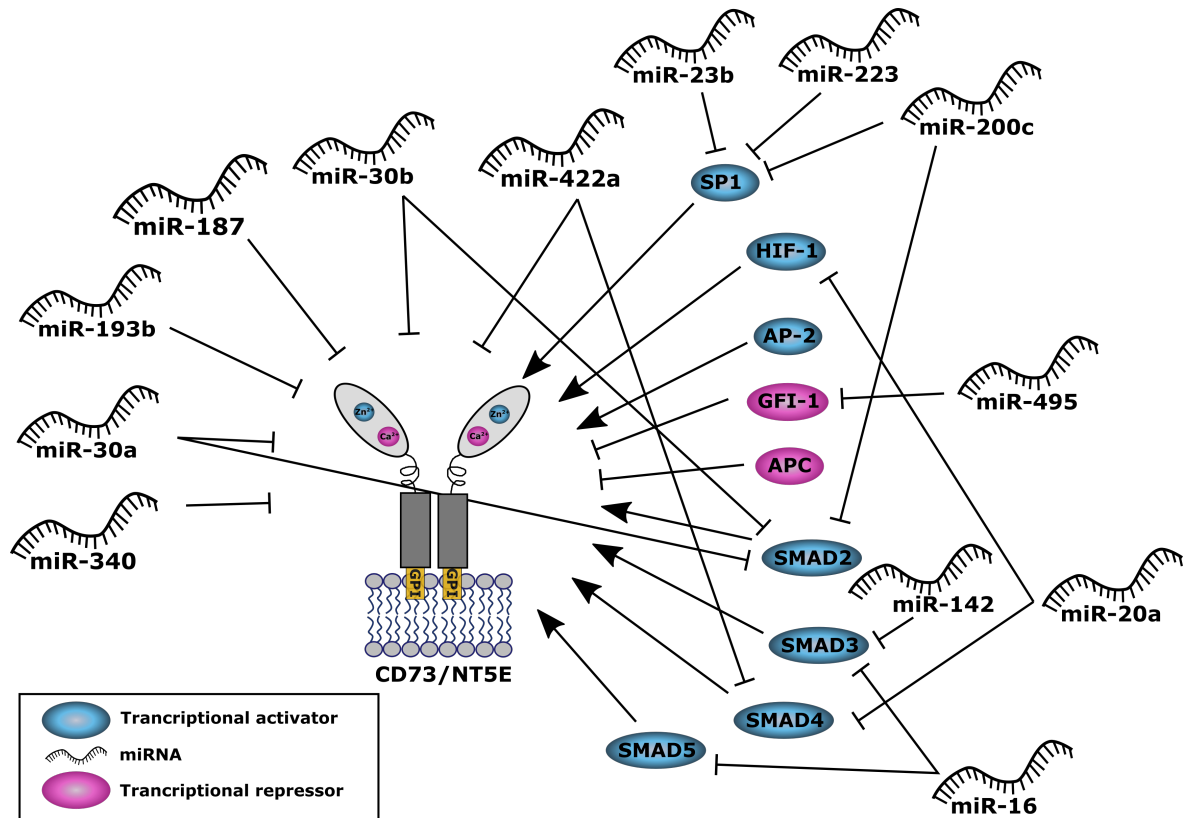


Figure 1.8: Regulation of NT5E. Network of transcription factors and microRNAs (miRNAs) regulating NT5E expression. This network summarizes the current knowledge on regulation of NT5E on transcriptional (TFs) and post-transcriptional level by TFs and miRNAs, respectively. Transcriptional activators are depicted in blue and transcriptional repressors are highlighted in magenta. miRNAs targeting NT5E directly are shown, as well as miRNAs with indirect impact on NT5E expression through targeting of transcriptional regulators. Picture taken from [128].

miR-30a reduced NT5E mRNA and protein levels. Interestingly, over-expression of miR-30a significantly inhibited cell proliferation, migration and survival, which could be also mimicked by silencing NT5E with specific shRNAs [286]. To note, the miR-30 family shares the same seed sequence [89]. Thus, it is very likely, that also other miR-30 family members regulate NT5E expression. For example it was shown, that also miR-30b regulated NT5E in gall bladder carcinoma (GBC). Wang *et al.* demonstrated, that miR-30b as well as miR-340 over-expression reduced NT5E expression and direct interactions were verified by 3'-UTR reporter assays. To note, transfection with miR-30b or miR-340 reduced cell proliferation, migration and invasion of GBC cells [247].

miR-187 expression is strongly decreased in CRC compared to adjacent normal tissue and can be used as a prognostic marker for CRC patients. miR-187 transfection reduced cell proliferation and migration *in vitro* and could slow down Tumor outgrowth of CRC cell lines *in vivo*. A direct targeting of NT5E by miR-187 could be shown in CRC lines [274].

Furthermore, miR-193b was identified as direct regulator of NT5E in a study analysing miRNAs involved in the MAPK pathway in human pancreatic cancer cell lines. Over-expression

of miR-193b decreased NT5E mRNA and protein levels. However, in this study the direct binding to the NT5E 3'-UTR was not verified by mutation of the respective binding site [112].

Besides direct targeting through miRNAs, NT5E expression can be also modulated by indirect circuits e.g. by miRNAs targeting transcription factors of NT5E. Some of these miRNAs are also shown in figure 1.8. For example, miR-23b was identified as direct repressor of the transcription factor SP1 in multiple myeloma cells [80]. In gastric cancer a direct regulation of SP1 by miR-223 was reported [108]. Furthermore, miR-200b and miR-200c were described to target SP1 in gastric cancer [229]. To note, whether the effect the miRNAs on SP1 also had downstream effects on NT5E, was not tested in these studies.

Besides its ability to directly repress NT5E, the miR-30 family can also indirectly modulate NT5E expression by targeting the regulator SMAD2, which activates NT5E transcription. The regulation of SMAD2 by miR-30 and miR-200c was found in a study focused on identification of miRNAs changing the invasive potential of anaplastic thyroid carcinoma [33]. Another example for indirect down-regulation of NT5E could be miR-16, which was shown to inhibit the expression of SMAD3, and to a lesser extend also SMAD5 in human osteosarcoma cell lines [121]. SMAD3 was also found to be regulated by miR-142-5p in human lung, colon and breast cancer cell lines [153, 41].

miR-20a-5p targets two transcriptional activators of NT5E: SMAD4 and HIF-1A [49, 189]. As mentioned before, miR-422a directly regulates NT5E by binding to its 3'-UTR. However, miR-422a targets SMAD4 directly [186] implying that miR-422a has the capacity to inhibit NT5E expression both direct and indirectly. Besides indirect down-regulation, indirect up-regulation of NT5E expression by miRNAs is possible as well e.g. by miRNA-mediated inhibition of transcriptional repressors. For example, miR-495 inhibits the expression of the transcriptional repressor GFI1 in medulloblastoma cells [243]. Hypothetically, miR-495 could lead to an increase in NT5E expression by decreasing GFI1 levels.

1.4. Aim of this study

The rationale of this thesis was the identification and characterization of miRNAs, whose expression could explain the aberrant immune checkpoint molecule expression in Tumor cells and the related immune evasion properties, with particular focus on the immune checkpoint molecule NT5E/CD73. New oncomiRs that drive up-regulation of NT5E/CD73 might give further insight into the mechanisms of cancer progression and immune escape. Thus, tumor-suppressive miRNAs inhibiting NT5E/CD73 might provide new therapeutic targeting options.

CHAPTER 2.

MATERIALS

All materials, instruments and software used in this study are listed in the following tables 2.1-2.14.

2.1. Cell lines

All cell lines used in this study are listed in table 2.1. Cell lines were cultured in medium supplemented with 10% FBS, without antibiotics at 37 °C and 5 % CO₂. Only EO771-OVA-Luc⁺ cells were cultured with the following antibiotics: 1 µg/mL puromycin and 0.2 mg/mL G418. On a regular basis cell lines were checked for mycoplasma contamination by collecting supernatant of cultured cells. The supernatants were boiled at 95 °C for 5 min and 4 µl were used as input for PCR to detect mycoplasma. For human cell lines DNA fingerprints were performed to confirm their authentication at least once a year. For new purchased cell lines an initial fingerprint was performed directly after arrival of the cell line. To note, DNA fingerprint identified, that MaMel-02 was wrongly labelled as MaMel-20. EO771 cells expressing luciferase and OVA antigen were generated by David Eisel [68].

Table 2.1: Cell lines used in this study.

Cell line	Species	Cell type	Entity	Provider	Medium
4T1	Mus mucus	Epithelial cell	Breast cancer	DKFZ, S. Wiemann	RPMI1640
A375	Human	Melanocyte	Melanoma	ATCC	RPMI1640
CCD-18Co	Human	Colon fibroblast	Healthy	ATCC	DMEM
CT26	Mus mucus	Colon fibroblast	Colon cancer	ATCC	RPMI1640
HCT-116	Human	Epithelial cell	Colon cancer	ATCC	McCoy's 5A
HEK293	Human	Epithelial cell	Healthy	DKFZ	RPMI1640
HeLa	Human	Epithelial cell	Adenocarcinoma	DKFZ	RPMI1640
HT29	Human	Epithelial cell	Colon cancer	ATCC	McCoy's 5A
EO771	Mus mucus	Epithelial cell	Breast Cancer	Tebu-bio	RPMI1640
EO771-OVA-Luc ⁺	Mus mucus	Epithelial cell	Breast Cancer	DKFZ, David Eisel	RPMI1640*
MaMel-103b	Human	Melanocyte	Melanoma	D. Schadendorf [236]	RPMI1640
MaMel-02	Human	Melanocyte	Melanoma	D. Schadendorf [236]	RPMI1640
MaMel-26a	Human	Melanocyte	Melanoma	D. Schadendorf [236]	RPMI1640
MaMel-42	Human	Melanocyte	Melanoma	D. Schadendorf [236]	RPMI1640
MaMel-05	Human	Melanocyte	Melanoma	D. Schadendorf [236]	RPMI1640
MaMel-53a	Human	Melanocyte	Melanoma	D. Schadendorf [236]	RPMI1640
MaMel-57	Human	Melanocyte	Melanoma	D. Schadendorf [236]	RPMI1640
MaMel-61a	Human	Melanocyte	Melanoma	D. Schadendorf [236]	RPMI1640
MaMel-68	Human	Melanocyte	Melanoma	D. Schadendorf [236]	RPMI1640
MaMel-73a	Human	Melanocyte	Melanoma	D. Schadendorf [236]	RPMI1640
MaMel-79b	Human	Melanocyte	Melanoma	D. Schadendorf [236]	RPMI1640
MaMel-86b	Human	Melanocyte	Melanoma	D. Schadendorf [236]	RPMI1640
MCF7	Human	Epithelial cell	Breast cancer	ATCC	DMEM
MDA-MB-231	Human	Epithelial cell	Breast cancer	ATCC	RPMI1640
MDA-MB-435	Human	Melanocyte	Melanoma	ATCC	RPMI1640
MRC5	Human	Lung fibroblast	Healthy	ATCC	MEM
SK-Mel-28	Human	Melanocyte	Melanoma	ATCC	RPMI1640
SW480	Human	Epithelial cell	Colon cancer	ATCC	McCoy's 5A
T47D	Human	Epithelial cell	Breast cancer	ATCC	RPMI1640

*: + Puromycin + G418

2.2. Antibodies

All antibodies used in this study for Western Blot (WB) or Fluorescent Activated Cell Sorting (FACS) are listed in table 2.2. For FACS staining antibodies were always used at a 1:100 dilution. Only for the miRNA library screen CD73-PE antibody was used at 1:400 dilution.

Table 2.2: Antibodies used in this study. CN = Catalogue number.

Antibody	Type	CN	Application	Manufacturer
PE anti-human CD73	IgG1, κ	344003	FACS	Biologend, San Diego, USA
BB515 anti-human CD39	IgG2b, κ	565469	FACS	Becton Dickinson, Franklin Lakes, USA
PE-Cy7 anti-human CD274	IgG1, κ	25-5983-41	FACS	Invitrogen, Carlsbad, USA
PE isotype control	IgG2a, κ	12-4714-81	FACS	ebioscience, San Diego, USA
PE-Cy7 isotype control	IgG1, κ	400125	FACS	ebioscience, San Diego, USA
BB515 isotype control	IgG2, κ	564510	FACS	Becton Dickinson, Franklin Lakes, USA
Anti-Actin clone C4 human	Mouse mAB	691001	WB	MP Biomedical, Illkirch, France
Anti-CD73 mAB	Rabbit mAB	ab133582	WB	Abcam, Cambridge, United Kingdom
Donkey anti-goat	IgG-HRP	sc2020	WB	Santa Cruz Biotechnology, Heidelberg, Germany
Goat anti-mouse	IgG-HRP	sc2005	WB	Santa Cruz Biotechnology, Heidelberg, Germany
Goat anti-rabbit	IgG-HRP	sc2004	WB	Santa Cruz Biotechnology, Heidelberg, Germany

2.3. Primers

All primers used in this study are listed in table 2.3. Primers were purchased from Sigma-Aldrich and were all HPLC purified.

Table 2.3: Primers used in this study.

Primer	Amplicon	Source	Sequence
B_Actin_TK_fwd	184 bp	PrimerBank	AGAGCTACGAGCTGCCTGAC
B_Actin_TK_rev	184 bp	PrimerBank	AGCACTGTGTTGGCGTACAG
CD274_fwd	120 bp	PrimerBank	TGGCATTGCTGAACGCATTT
CD274_rev	120 bp	PrimerBank	TGCAGCCAGGTCTAATTGTTTT
CD39_fwd	200 bp	Feng et al. 2016	AGCAGCTGAAATATGCTGGC
CD39_rev	200 bp	Feng et al. 2016	GAGACAGTATCTGCCGAAGTCC
CD73_fwd	198 bp	Bonnin 2016	TTATTCGACTGGGACATTCTG
CD73_rev	198 bp	Bonnin 2016	AGGCCTGGACTACAGGAACC
CD73_Iso2_fwd	185 bp	Bonnin 2016	TGATGAACGCAACAATGGAAT
CD73_Iso2_rev	185 bp	Bonnin 2016	TCTGGAACCCATCTCCACCA
CD73_Pagnotta_fwd	123 bp	Pagnotta 2013	ATTGCAAAGTGGTTCAAAGTCA
CD73_Pagnotta_rev	123 bp	Pagnotta 2013	ACACTTGGCCAGTAAAAATAGGG
CD73_PBI_fwd	196 bp	PrimerBank	GCCTGGGAGCTTACGATTTTTG
CD73_PBI_rev	196 bp	PrimerBank	TAGTGCCCTGGTACTGGTCTG
CD73_PBI_rev	136 bp	PrimerBank	CCAGTACCAGGGCACTATCTG
CD73_PBI_rev	136 bp	PrimerBank	TGGCTCGATCAGTCCTTCCA
CD73_TK_fwd	191 bp	PrimerBlast	CAAACCTTCCTGGCCAATGGTG
CD73_TK_rev	191 bp	PrimerBlast	AGCAAAGCAGGAGGGAGTCA
GAPDH_fwd	238 bp	Bonnin 2016	GAGTCAACGGATTTGGTCTG
GAPDH_rev	238 bp	Bonnin 2016	TTGATTTTTGGAGGGATCTCG
HMBS_fwd	125 bp	PrimerBank	ATGTCTGGTAACGGCAATGC
HMBS_rev	125 bp	PrimerBank	CCTGTGGTGGACATAGCAATGA
HPRT_fwd	128 bp	PrimerBank	ATTGTTTTCTCCTTCCAGCACC
HPRT_rev	128 bp	PrimerBank	ACAAGAAGTGTACCCTAGCC
RPL19_fwd	198 bp	Bonnin 2016	GGCACATGGGCATAGGTAAG
RPL19	198 bp	Bonnin 2016	CCATGAGAATCCGCTTGTTT
SOX9_fwd	85 bp	PrimerBank	AGCGAACGCACATCAAGAC
SOX9_rev	85 bp	PrimerBank	CTGTAGGGCATCTGTTGGGG
TBP_fwd	214 bp	Bonnin 2016	TATAATCCCAAGCGGTTTGC
TBP_rev	214 bp	Bonnin 2016	CACAGCTCCCCACCATATTC
TK01_fwd	82 bp	Own design	TTGACGAGTGTGAAGCTTCCTT
TK01_rev	82 bp	Own design	CCGAAGTCCTTGAGGCAA
TK02_fwd	86 bp	Own design	TGAAGATGGAAGTCTACATGG
TK02_rev	86 bp	Own design	GACAGCCAAATACATCCTTCAA
TK03_fwd	87 bp	Own design	TTGTACTCTTTAAGAACCCCTTCTC
TK03_rev	87 bp	Own design	TGTGTGTCTGCCTTCTCCAA
UBC_fwd	123 bp	PrimerBank	CGGTGAACGCCGATGATTAT
UBC_rev	123 bp	PrimerBank	ATCTGCATTGTCAAGTGACGA

Primers used to mutate the NT5E 3'-UTR binding site of miRNAs to prove direct interaction are listed in table 2.4. These primers were constructed with the online software tool QuickChange Primer Design provided by Agilent (<https://www.genomics.agilent.com/primerDesignProgram.jsp>).

Table 2.4: Primers used in this study for QuickChange mutagenesis of pLS-NT5E vector. In red the nucleotide is marked for which the deletion primer were designed.

Primer	miRNA	Mutation	Sequence
del1670_fwd	miR-193a/b	GG E CAGU	ATTTAGGGTTTATTTTTTTACACTTGGCAGTAAAATAGGGTAAATCCTATTAG
del1670_rev	miR-193a/b	GG E CAGU	CTAATAGGATTTACCCTATTTTACTGCCAAGTGTAATAAATAAACCTAAAT
del1671_fwd	miR-193a/b	GG C EAGU	TTAGGGTTTATTTTTTTACACTTGGCAGTAAAATAGGGTAAATCCTATTAG
del1671_rev	miR-193a/b	GG C EAGU	CTAATAGGATTTACCCTATTTTACTGCCAAGTGTAATAAATAAACCTAA
del1672_fwd	miR-193a/b	GG C A GU	GGGTTTATTTTTTTACACTTGGCCGTAAAATAGGGTAAATCCTATTATA
del1672_rev	miR-193a/b	GG C A GU	TAATAGGATTTACCCTATTTTACGGCCAAGTGTAATAAATAAACCC
del1442_fwd	miR-22-3p	GG E AGCU	CTTAAAAACAGTGTGCAAATGGAGCTAGAGGTTTTGATAGGAAG
del1442_rev	miR-22-3p	GG E AGCU	CTTCCTATCAAACCTCTAGCTCCATTTGCACACTGTTTTTAAG
del1443_fwd	miR-22-3p	GG C A GCU	AAACAGTGTGCAAATGGCGCTAGAGGTTTTGATAGG
del1443_rev	miR-22-3p	GG C A GCU	CCTATCAAACCTCTAGCGCCATTTGCACACTGTTT
del1444_fwd	miR-22-3p	GG C A GCU	AAAACAGTGTGCAAATGGCACTAGAGGTTTTGATAGGAAG
del1444_rev	miR-22-3p	GG C A GCU	CTTCCTATCAAACCTCTAGTGCCATTTGCACACTGTTTT
del984_fwd	miR-1285-5p	UG A GAU	AGGCAGAGCTGATGGAATCCATAAAAATAACAGCTAATGC
del984_rev	miR-1285-5p	UG A GAU	GCATTAGCTGTTATTTTTATGGATTCCATCAGCTCTGCCT
del985_fwd	miR-1285-5p	UG A GAU	GGCAGAGCTGATGGAATTCATAAAAATAACAGCTAATGCC
del985_rev	miR-1285-5p	UG A GAU	GGCATTAGCTGTTATTTTTATGAATTCATCAGCTCTGCC
del986_fwd	miR-1285-5p	UG A GAU	GAGGCAGAGCTGATGGAATTCATAAAAATAACAGCTAATGC
del986_rev	miR-1285-5p	UG A GAU	GCATTAGCTGTTATTTTTATGAGTTCCATCAGCTCTGCCTC
del88_fwd	miR-1285-5p	GU E AGAU	CTAAAAGGCAGATTTGAATCTACTTGAAAAAATGCAGTTTCACACATTA
del88_rev	miR-1285-5p	GU E AGAU	TAATGTGTGAAACTGCATTTTTTCAAGTAGATTCAAATCTGCCTTTTTAG
del89_fwd	miR-1285-5p	GUG A GAU	GTCCATAAAGGCAGATTTGAATCCACTTGAAAAAATGCAGTTTCAC
del89_rev	miR-1285-5p	GUG A GAU	GTGAAACTGCATTTTTTCAAGTGGATTCAAATCTGCCTTTTTAGGAC
del90_fwd	miR-1285-5p	GUG A GAU	TGAAACTGCATTTTTTCAAGTGAATTCAAATCTGCCTTTTTAGGACC
del90_rev	miR-1285-5p	GUG A GAU	GGTCCTAAAAGGCAGATTTGAATTCACTTGAAAAAATGCAGTTTCA
del1107_fwd	miR-148b-3p	CCUG E AC	GAGTAGAATGAATTCATGCTAGCCTCTTGCTGGAGAG
del1107_rev	miR-148b-3p	CCUG E AC	CTCTCCAGCAAGAGGCTAGCATGAATTCATTCTACTC
del1106_fwd	miR-148b-3p	CCU E CAC	TGAGTAGAATGAATTCAGGCTAGCCTCTTGCTGGA
del1106_rev	miR-148b-3p	CCU E CAC	TCCAGCAAGAGGCTAGCCTGAATTCATTCTACTCA
del1105_fwd	miR-148b-3p	CC U GCAC	GAGTAGAATGAATTCAGTCTAGCCTCTTGCTGGAGA
del1105_rev	miR-148b-3p	CC U GCAC	TCTCCAGCAAGAGGCTAGACTGAATTCATTCTACTC
del352_fwd	miR-3134	U E CAUC	CATATTTTTCTTTCATATCCATTTCTAATCATCAAACAGCTTATGTTTTACATAAAAATTT
del352_rev	miR-3134	U E CAUC	AAATTTTTATGTAAACATAAGCTGTTTGATGATTAGAAATGGATATGAAGAAGAAAAATATG
del353_fwd	miR-3134	U C EACU	CATATTTTTCTTCTTCATATCCATTTCTAATCATCAAACAGCTTATGTTTTACATAAAAATTTTAT
del353_rev	miR-3134	U C EACU	ATAAAAATTTTTATGTAAACATAAGCTGTTTGATGATTAGAAATGGATATGAAGAAGAAAAATATG
del354_fwd	miR-3134	U C A UC	TTTTTCTTCTTCATATCCATTTCTAATCCTCAAACAGCTTATGTTTACATAAAAATTTT
del354_rev	miR-3134	U C A UC	AAAATTTTTATGTAAACATAAGCTGTTTGAGGATTAGAAATGGATATGAAGAAGAAAAA
del989_fwd	miR-3134	U E CAUC	GAGGCAGAGCTGATGAATTCATAAAAATAACAGCTAATGCCG
del989_rev	miR-3134	U E CAUC	CGGCATTAGCTGTTATTTTTATGAGATTCATCAGCTCTGCCTC
del990_fwd	miR-3134	U C EACU	GGACAGAGGCAGAGCTGATGAATTCATAAAAATAACAGCT
del990_rev	miR-3134	U C EACU	AGCTGTTATTTTTATGAGATTCATCAGCTCTGCCTCTGTCC
del991_fwd	miR-3134	U C A UC	GTTATTTTTATGAGATTCCTCAGCTCTGCCTCTGTCC
del991_rev	miR-3134	U C A UC	GGACAGAGGCAGAGCTGAGGAATTCATAAAAATAAC

2.4. miRNAs

All miRNAs used in this study are listed in table 2.5 with their respective mature sequence. All miRNAs were purchased from Sigma-Aldrich except for hsa-miR-422a which was bought from Active Motif. Besides individual miRNAs, the MISSION Human miRNA mimics library V21 from Sigma-Aldrich was purchased to perform the miRNA library screen. This library contained 2754 individual miRNAs allotted in 36 96-well plates.

Table 2.5: miRNA used in this study.

miRNA	Sequence
hsa-miR-101	UACAGUACUGUGAUAACUGAA
hsa-miR-127-5p	CUGAAGCUCAGAGGGCUCUGAU
hsa-miR-1233-3p	UGAGCCCUGUCCUCCCGCAG
hsa-miR-1293	UGGGUGGUCUGGAGAUUUGUGC
hsa-miR-1298-3p	CAUCUGGGCAACUGACUGAAC
hsa-miR-134-3p	CCUGUGGGCCACCUAGUCACCAA
hsa-miR-143-5p	GGUGCAGUGCUGCAUCUCUGGU
hsa-miR-148b-3p	UCAGUGCAUCACAGAACUUUGU
hsa-miR-17	CAAAGUGCUUACAGUGCAGGUAG
hsa-miR-182	UUUGGCAAUGGUAGAACUCACACU
hsa-miR-192	CUGACCUAUGAAUUGACAGCC
hsa-miR-193a-3p	UGGGUCUUUGCGGGCGAGAUGA
hsa-miR-193b-3p	AACUGGCCCUCAAAGUCCCGCU
hsa-miR-200c	UAAUACUGCCGGGUAUGAUGGA
hsa-miR-22-3p	AAGCUGCCAGUUGAAGAACUGU
hsa-miR-224-3p	AAA AUGGUGCCCUAGUGACUACA
hsa-miR-30b	UGUAAACAUCCUACACUCAGCU
hsa-miR-30c-1*	CUGGGAGAGGGUUGUUUACUCC
hsa-miR-30d	UGUAAACAUCCCGACUGGAAG
hsa-miR-30e	UGUAAACAUCCUUGACUGGAAG
hsa-miR-3116	UGCCUGGAACAUAGUAGGGACU
hsa-miR-3118	UGUGACUGCAUUAUGAAAAUUCU
hsa-miR-3126-5p	UGAGGGACAGAUGCCAGAAGCA
hsa-miR-3134	UGAUGGAUAAAAGACUACAUUU
hsa-miR-3190-5p	UCUGGCCAGCUACGUCCCCA
hsa-miR-422a	ACUGGACUUAGGGUCAGAAGGC
hsa-miR-4480	AGCCAAGUGGAAGUUACUUUA
hsa-miR-4672	UUACACAGCUGGACAGAGGCA
hsa-miR-4692	UCAGGCAGUGUGGGUAUCAGAU
hsa-miR-518a	CUGCAAAGGGAAGCCCUUC
hsa-miR-548l	AAAAGUAUUUGCGGGUUUUGUC
hsa-miR-507	UUUUGCACCUUUUGGAGUGAA
hsa-miR-557	GUUUGCACGGGUGGGCCUUGUCU
hsa-miR-6514-3p	CUGCCUGUUCUCCACUCCAG
hsa-miR-6859-3p	UGACCCCAUGUCGCCUCUGUAG

2.5. siRNAs

All siRNAs used in this study are listed in table 2.6.

Table 2.6: siRNAs used in this study.

siRNA	Composition	Manufacturer
MISSION® esiRNA HFI1A	heterogeneous mixture of siRNAs	Sigma-Aldrich
SMARTpool non-targeting control	4 individual siRNAs	Dharmacon
SMARTpool ENTPD1	4 individual siRNAs	Dharmacon
SMARTpool NT5E	4 individual siRNAs	Dharmacon
SMARTpool Nt5e	4 individual siRNAs	Dharmacon
SMARTpool SOX9	4 individual siRNAs	Dharmacon
SMARTpool TP73	4 individual siRNAs	Dharmacon

2.6. General instrumentation

All instruments used in this study are listed in table 2.7.

Table 2.7: Devices used for this study.

Machine	Manufacturer
ABI 7300 Real-time PCR System	Applied Biosystems, Foster City, USA
Accu-jet pro Pipette Controller	VWR International, Radnor, USA
Biofuge Fresco Centrifuge	Heraeus, Hanau, Germany
Biological Safety Cabinet	Heraeus, Hanau, Germany
BioPhotometer	Eppendorf, Hamburg, Germany
BioRad Mini-gel apparatus	Bio-Rad, Richmond, USA
CASY Cell counter	Schaerfe System, Reutlingen, Germany
CB 150 Incubator	Binder, Tuttlingen, Germany
Centrifuge 5415 D	Eppendorf, Hamburg, Germany
Centrifuge 5424	Eppendorf, Hamburg, Germany
Centrifuge 5424 R	Eppendorf, Hamburg, Germany
Centrifuge 5810 R	Eppendorf, Hamburg, Germany
ClarioStar Plus	BMG LABTECH, Ortenberg, Germany
FACS Canto II Flow Cytometer	Becton Dickinson, Franklin Lakes, USA
Fluoroskan Ascent Microplate Fluorometer	Thermo Scientific, Dreieich, Germany
Gel Documentation System	Bio-Rad Laboratories, Hercules, USA
Gel iX Imager System	Intas Science Imaging Instruments, Göttingen, Germany
Innova 4230 Incubator Shaker	New Brunswick Scientific, Edison, USA
Leica DM1L Microscope	Leica, Wetzlar, Germany
LSR II Flow Cytometer	Becton Dickinson, Franklin Lakes, USA
Megafuge 2.0R	Heraeus, Hanau, Germany
Micro-centrifuge 2 CMG-060	neoLab Migge, Heidelberg, Germany
Microwave intellowave	LG, Seoul, South Korea
Mini Laboratory Centrifuge	neoLab Migge, Heidelberg, Germany
Mithras LB940	Berthold Technologies, Bad Wildbad, Germany
MP220 pH Meter	Mettler Toledo, Columbus, USA
MR 3002 S Magnetic stirring hot plate	Heidolph Instruments, Schwabach, Germany
Multipipette E3x	Eppendorf, Hamburg, Germany
Multifuge x3 FR centrifuge	Heraeus, Hanau, Germany
Pipetboy	Brand, Wertheim, Germany
Pipette (P2, P10, P100, P200, P1000)	Gilson, Bad Camberg, Germany
Power PAC 300 power supplier	Bio-Rad, Richmond, Germany
QuantStudio 3 Real-Time-PCR-Systeme	Thermo Fisher Scientific, Waltham, USA
Qubit fluorometer	Thermo Fisher Scientific, Waltham, USA
Refrigerator	Liebherr, Ochsenhausen, Germany
Spectrophotometer NanoDrop 2000	Thermo Fisher Scientific, Waltham, USA
Sorvall RT7 Centrifuge	Sorvall, Newton, USA
Thermomixer	Eppendorf, Hamburg, Germany
Trans-Blot Turbo Transfer System	Bio-Rad Laboratories, Hercules, USA
Verti 96-Well Thermal Cycler	Applied Biosystems, Foster City, USA
Vortex-Genie 2	Scientific Industries, New York, USA
Water bath	GFL, Burgwedel, Germany

2.7. General consumables

General consumables used in this study are listed in table 2.8.

Table 2.8: General consumables used in this study.

Material	Manufacturer
14 mL Round Bottom High Clarity PP Test Tube	Corning, New York, USA
5 mL Polystyrene round bottom tube with cell strainer cap	Corning, New York, USA
Cap for PCR microcentrifuge tubes	nerbe plus, Winsen, Germany
CASY ton	OMNI Life Science, Bremen, Germany
CASY cups	OMNI Life Science, Bremen, Germany
Cell culture flask 50 mL	Greiner Bio-One, Kremsmünster, Austria
Centrifuge Tube pp with screw cap PE (15, 50 mL)	nerbe plus, Winsen, Germany
Corning® 96 well Solid Polystyrene Microplate	Sigma-Aldrich, St. Louis, USA
Combitips advanced (0.1, 1, 2.5, 5, 25 mL)	Eppendorf, Hamburg, Germany
Cryotubes	Greiner, Frickenhausen, Germany
Disposable serological pipette (5, 10, 25, 50 mL)	Corning, New York, USA
Einmal-Drigalskispatel Dreiecksform	neoLab Migge, Heidelberg, Germany
Eppendorf Micro Test Tube 3810X 1.5 mL	Eppendorf, Hamburg, Germany
Eppendorf Safe-Lock Microtubes, PCR clean 2.0 mL	Eppendorf, Hamburg, Germany
Eppendorf Tube 3810X 1.5 mL	Eppendorf, Hamburg, Germany
Eppendorf Tubes 5.0 mL	Eppendorf, Hamburg, Germany
Falcon tubes 15 mL, 50 mL	Greiner, Frickenhausen, Germany
LumaPlate 96	PerkinElmer, Waltham, USA
MicroAmp Optical 96-well pate	Applied Biosystems, Foster City, USA
MicroAmp Optical adhesive film	Applied Biosystems, Foster City, USA
Mini-PROTEAN® Combs, 15-well, 1.5 mm, 40 µL	Bio-Rad Laboratories, Hercules, USA
Mini-PROTEAN® Short Plates 1.5 mm	Bio-Rad Laboratories, Hercules, USA
Mini-PROTEAN® tetra hadncast Systems, 1.5 mm, 40 µL	Bio-Rad Laboratories, Hercules, USA
MultiScreen-MESH Filter Plate 40 µM	Merck KGaA, Darmstadt, Germany
Nitrocellulose membrane	Whatmann, Dassel, Germany
Parafilm M	Pechiney Plastic Packaging, Chicago, USA
PCR microcentrifuge tube PP, 0-2 mL, without cap	nerbe plus, Winsen, Germany
Pipette filter tips (10, 20, 100, 200, 1000 µL)	Starlab, Milton Keynes, United Kingdom
Pipette tips (10, 20, 100, 200, 1000 µL)	Greiner, Frickenhausen, Germany
Plastic serium pipette	Greiner Bio-One, Kremsmünster, Austria
Premium Aluminium Foil	VWR International, Radnor, USA
Qubit Assay Tubes	Thermo Fisher Scientific, Waltham, USA
Reagent Reservoir	Corning, New York, USA
Round and Flat bottom 96-well plates	TPP, Trasadingen, Switzerland
Safe-Lock tubes (0.5, 1.5, 2 mL)	Eppendorf, Hamburg, Germany
Sealing Tape	Thermo Fisher Scientific, Waltham, USA
Sterile serological pipettes (5, 10, 25, 50 mL)	Greiner, Frickenhausen, Germany
Tissue culture flasks (25, 75, 150 cm ²)	TPP, Trasadingen, Switzerland
Tissue culture plates (6, 12, 24, 96 wells)	TPP, Trasadingen, Switzerland

2.8. General chemicals and reagents

Chemicals used in this study are listed in table 2.9.

Table 2.9: Chemicals used in this study.

Chemical	Manufacturer
Actinomycin D	MP Biomedical, Illkirch, France
Adenosine	Sigma-Aldrich, St. Louis, USA
Adenosine 5-(α,β -methylene)diphosphate	Sigma-Aldrich, St. Louis, USA
Adenosine-5'-Monophosphat Dinatriumsalz	VWR International, Radnor, USA
Ampicillin sodium salt	Sigma-Aldrich, St. Louis, USA
Agar-Agar	Carl Roth, Karlsruhe, Germany
Agarose	Sigma-Aldrich, St. Louis, USA
Ammonium Persulfate (APS)	Sigma-Aldrich, St. Louis, USA
β -Mercaptoethanol	Sigma-Aldrich, St. Louis, USA
Bromphenol blue	Sigma-Aldrich, St. Louis, USA
Bovine Serum Albumin (BSA)	Sigma-Aldrich,, Saint Louis, USA
Dimethyl sulfoxide (DMSO)	AppliChem, Darmstadt, Germany
Ethanol	Sigma-Aldrich,, St. Louis, USA
Glucose	Carl Roth GmbH, Karlsruhe, Germany
Glycine	GERBU Biotechnik, Gaiberg, Germany
HEPES	Carl Roth GmbH, Karlsruhe, Germany
Magnesium chloride	Sigma-Aldrich,, St. Louis, USA
Methanol	Sigma-Aldrich,, St. Louis, USA
Non-fat milk powder	Carl Roth GmbH, Karlsruhe, Germany
Phenylmethanesulfonyl fluoide	Sigma-Aldrich, St. Louis, USA
Phosphate Buffered Saline (PBS)	Gibco, Carlsbad, USA
Potassium chloride	Sigma-Aldrich, St. Louis, USA
Sodium Chloride (NaCl)	Sigma-Aldrich, St. Louis, USA
Sodium dodecyl sulfate (SDS)	Sigma-Aldrich, St. Louis, USA
Tetramethylethyldiamine (TMED)	Sigma-Aldrich, St. Louis, USA
Tris Base	Sigma-Aldrich, St. Louis, USA
0.25 % Trypsin/EDTA	Gibco, Carlsbad, USA
Tyrptone	Sigma-Aldrich, St. Louis, USA
Tween20	GERBU Biotechnik, Gaiberg, Germany
Yeast Extract	Sigma-Aldrich, St. Louis, USA

All reagents used in this study are listed in table 2.10.

Table 2.10: Reagents used in this study.

Reagent	Manufacturer
10 % SDS	Lonza Group, Basel, Switzerland
30 % Acrylamide/Bis Solution, 37.5:1	Bio-Rad Laboratories, Hercules, USA
6x Orange Loading Dye	Fermantas, St. Leon-Rot, Germany
Amersham ECL Prime Western Blotting Detection Reagent	GE Healthcare Life Sciences, Chalfont St Giles, USA
BD Matrigel Basement Membrane Matrix	BD Biosciences, Bedford, USA
Bio-Rad Protein Assay Reagent	Bio-Rad, Richmond, USA
Cell Dissociation Reagent	Trevigen, Gaithersburg, USA
Cell Lysis Buffer	Cell Signaling Technology, Beverly, USA
CellTiter Glo Reagent	Promega, Mannheim, Germany
Cycloheximide	New England Biolabs, Frankfurt am Main, Germany
DharmaFect 1 Reagent	GE Dharmacon, Lafayette, USA
DharmaFect 4 Reagent	GE Dharmacon, Lafayette, USA
DharmaFect Duo Reagent	GE Dharmacon, Lafayette, USA
DMEM	Gibco, Carlsbad, USA
DPBS, no calcium, no magnesium	Thermo Fisher Scientific, Waltham, USA
Fetal Calf Serum (FCS)	PAA Laboratories, Pasching, Austria
FCS superior	Biochrom, Berlin, Germany
Gene Ruler 100bp DNA Ladder	Fermantas, St. Leon-Rot, Germany
Lipofectamine RNAiMAX Transfection Reagent	Thermo Fisher Scientific, Waltham, USA
McCoy's 5A	Gibco, Carlsbad, USA
MEM	Gibco, Carlsbad, USA
O'Gene Ruler 1kb DNA Ladder	Fermantas, St. Leon-Rot, Germany
Protein Marker IV (Prestained)	VWR International, Radnor, USA
Precision Plus Protein Standard	Bio-Rad, Richmond, USA
Qubit RNA BR Assay Kit 500 reactons	Thermo Fisher Scientific, Waltham, USA
Restriction enzymes	Fermantas, St. Leon-Rot, Germany
RPMI 1640	Gibco, Carlsbad, USA
S.O.C. medium	Thermo Fisher Scientific, Waltham, USA

2.9. Kits

Kits used in this study are listed in table 2.11.

Table 2.11: Kits used in this study.

Name	Manufacturer
12% Mini-PROTEAN TGX Stain-Free Protein	Bio-Rad, Richmond, USA
CellTiter Glo Luminescent Cell Viability Assay	Promega, Mannheim, Germany
Colorimetric Cell Viability Kit III (XTT)	PromoKine, Heidelberg, Germany
ECL Plus Western blotting Detection System	GE Healthcare, Buckinghamshire, UK
LightSwitch™ Luciferase Assay Kit	Active Motif, La Hulpe, Belgium
LIVE/DEAD® Fixable Yellow Dead Cell Stain Kit	Life Technologies, Carlsbad, USA
Malachite Green PO4 Detect Kit	R& D Systems, Minneapolis, USA
miRNeasy Mini kit	Qiagen, Hilden, Germany
Pierce BCA Protein Assay Kit	Thermo Scientific, Boston, USA
Pierce Renilla Luciferase Glow Assay Kit	Thermo Scientific, Boston, USA
QIAGEN Plasmid Maxi Kit	Qiagen, Hilden, Germany
RNAeasy Mini Kit	Qiagen, Hilden, Germany
SYBR green Master Mix	Thermo Fisher Scientific, Waltham, USA
TaqMan™ Gene Expression Assays	Applied Biosystems, Foster City, USA
TaqMan™ miRNA Assays	Applied Biosystems, Foster City, CA, USA
TaqMan™ MicroRNA Reverse Transcription Kit	Applied Biosystems, Foster City, USA
TaqMan™ Gene Expression Assays	Applied Biosystems, Foster City, USA
TaqMan™ Universal PCR Master Mixture	Applied Biosystems, Foster City, USA
TGX Stain-Free™ FastCast™ Acrylamide Kit, 12%	Bio-Rad, Richmond, USA
Transcriptor First Strand cDNA Synthesis	Roche, Applied Science, Mannheim, Germany
Trans-Blot Turbo Transfer Pack, nitrocellulose	Bio-Rad, Richmond, USA
Trans-Blot Turbo Transfer Pack, pvdf	Bio-Rad, Richmond, USA
QuickChangeMutagenesis II	Agilent, Santa Clara, USA

2.10. Plasmids

Plasmids used in this study are listed in table 2.12 and plasmid cards are shown in the Appendix figure 6.2.

Table 2.12: Plasmids used in this study.

Plasmid	Manufacturer
pLight Switch 3'UTR NT5E	Active Motif, La Hulpe, Belgium
pLight Switch empty control vector	Active Motif, La Hulpe, Belgium

2.11. Bacteria

Bacteria strains used in this study are listed in table 2.13.

Table 2.13: Bacteria strains used in this study.

Strain	Manufacturer
TOP10 <i>E.coli</i> competent cells	Invitrogen, Carlsbad, USA
XL1 Blue <i>E.coli</i> competent cells	Agilent, Santa Clara, USA

2.12. Software

Software used in this study to analyse data and to generate figures are listed in table 2.14.

Table 2.14: Software used in this study.

Name	Source
Ascent Software	Thermo Scientific, Dreieich, Germany
Excel version 14.0	Microsoft Cooperation, Redmond, USA
FlowJo version 9.6.4	Becton Dickinson, Heidelberg, Germany
GraphPad Prism 7	GraphPad Software, San Diego, USA
Image Lab Software	Bio-Rad, Richmond, USA
Inkscape	https://inkscape.org/
R 3.0.1	http://www.r-project.org/

CHAPTER 3.

METHODS

3.1. Bioinformatic analysis

3.1.1 miRNA target prediction

The *in silico* analysis to find potential miRNAs regulating the immune checkpoint molecules NT5E, ENTPD1, CTLA4 and CD274 was based on different publicly available data bases. Overall, ten different data bases were used to assess miRNA - target genes connections. All data bases were downloaded at 01-05-2017. The following resources for predicting potential miRNAs were used:

- MircoCosm [170]
- miRanda: microRNA conserved and non conserved [27]
- miRDB V5 [48]
- miRecords [257]
- miRGator [172]
- miRNAMap [107]
- PACCMIT [237]
- PicTar [131]
- PITA Top Score and all predictions [125]
- TargetScan [8]

3.1.2 Prediction of NT5E transcription factors

Concept of Transcription factor activity

To predict gene expression the concept of transcription factor activity was used as described previously [208]. Briefly, the activity of a transcription factor is defined as the cumulative effect on its target genes normalized by the overall number of its target genes instead of just using e.g. the expression value of the transcription factor itself.

$$\text{act}_{tj} = \frac{\sum_{i=1}^n e_{st,i} \cdot g_{ij}}{\sum_{i=1}^n e_{st,i}} \quad (3.1.1)$$

where j indicates the cell line, i the gene and t the transcription factor.

Linear programming and mixed-integer linear programming

Using a linear programming approach and a mixed-integer linear programming model the gene expression of NT5E for several cancer samples was predicted in order to find the most important transcription factors that can explain the different NT5E expression levels across samples. To solve these optimization problems the Gurobi Optimizer 5.5 was utilised [5]. The basic idea of the model was to minimize the differences between the real gene expression values g_{ij} for genes i expressed in cell lines j and the predicted gene expression values \tilde{g}_{ij} , which equals minimizing the sum of error terms e_{ij} (3.1.3). The absolute value function had to be remodelled into two constraints as shown below because the Gurobi Optimizer is not able to handle absolute values (3.1.4, 3.1.5). The formula for the predicted gene expression values \tilde{g}_{ij} (3.1.6) included β -coefficients for an offset value and for each transcription factor. The set of transcription factors was gained from the databases MetaCore™, ChEA and TBA. Overall a list of 1,053 unique transcription factors were obtained. The transcription factors were connected to the genes through the edge strength es_{ti} , which is exemplary shown in figure 3.1, and to the cell line via the activity act_{tj} . The task of the Gurobi Optimizer was the estimation of β -coefficients within the scope given by the constraints in order to minimize the sum of error terms, which will be referred to as the objective value from now on.

$$\sum_{i=1}^n \sum_{j=1}^l |g_{ij} - \tilde{g}_{ij}| = \sum_{i=1}^n \sum_{j=1}^l e_{ij} \quad (3.1.2)$$

$$\text{optimisation: } \min \sum_{i=1}^n \sum_{j=1}^l |g_{ij} - \tilde{g}_{ij}| = \min \sum_{i=1}^n \sum_{j=1}^l e_{ij} \quad (3.1.3)$$

$$\Rightarrow \text{constraint 1: } g_{ij} - \tilde{g}_{ij} - e_{ij} \leq 0 \quad (3.1.4)$$

$$\Rightarrow \text{constraint 2: } -g_{ij} + \tilde{g}_{ij} - e_{ij} \leq 0 \quad (3.1.5)$$

$$\text{with: } \tilde{g}_{ij} = \beta_0 + \sum_{t=1}^T \beta_t \cdot es_{ti} \cdot act_{tj} \quad (3.1.6)$$

where j indicates the cell line, i the gene and t the transcription factor
 β_0 as an offset value i in cell line j .

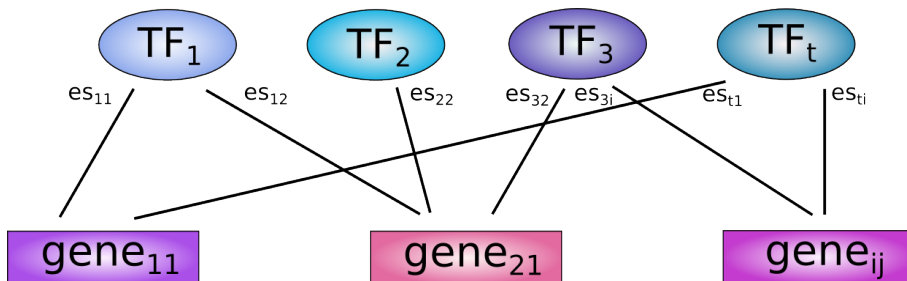


Figure 3.1: Network of genes and their regulative transcription factors. Genes and transcription factors are connected via the edge strength es_{ti} .

The model was based on the 5-Platform gene expression data obtained from the U.S. National Cancer Institute and was downloaded from CellMiner.^[i] The NCI-60 compilation contains 60 cancer cell lines arisen from human tumor samples from nine different types of tissues: breast (BR), central nervous system (CNS), colon (CO), kidney (RE), leukaemia (LE), lung (LC), melanoma (ME), ovary (OV) and prostate (PR) [216, 145]. The 5-Platform data set is based on an integration of the following five microarray platforms: HG-U95, HG-U133, HG-U133 Plus 2.0, GH Exon 1.0 ST from Affymetrix and the WHG from Agilent. An average z-score was ascertained for the respective gene transcript expression value. This data set includes 26,065 genes [194]. All missing values were replaced with the mean of expression values for the particular genes. The cell line CNS.SF_539 was excluded because of a large quantity (10,404) of undefined (NA) entries.

3.2. miRNA screen

3.2.1 Preparation of miRNA library

To find miRNAs regulating immune checkpoint molecules a FACS-based screen was conducted. Therefore, the human microRNA Mimic Version 21 library was used. The library contained 2754 miRNAs allotted in 36 96-well plates. Each plate contained the negative control 1 (ath-miR-416) and negative control 2 (cel-miR-243), which have no homologies to human genes. Each well of the library plates contained 0.25 nmol of lyophilized powder and plates were stored at -20 °C. Before transfection, the library plates were centrifuged and stock solution of 20 µM was prepared by adding 12 µL RNase free water to each well and mixing was ensured by pipetting up and down. In a new 96-well plate a 2 µM working solution was prepared for each library plate shortly before the transfection. Therefore, 2 µL of stock solution was pipetted in the new plate. Next, 18 µL RNase free water was added to each well.

3.2.2 Transfection of miRNA library

For the screen two human cancer cell lines were used: the breast cancer line MDA-MB-231 and the melanoma line SK-Mel-28. The RNAi Lipofectamine Max reagent was used for transfection and a final miRNA concentration of 25 nM per well. $2.5 \cdot 10^4$ cells were seeded one day before transfection in 96-well culture plates. On the day of transfection medium was exchanged with 90 µL fresh medium. In a RNase free Eppendorf the transfection reagent was prepared. For two cell lines and one library plate 60 µL RNAi Max was mixed with 1740 µL serum-free medium (sfm). From the 2 µM library plate, 2.5 µL miRNA was transferred in a new 96-well plate and 15.5 µL sfm was added to each well. Next, 18 µL of the RNAi Max mix was added to each well. After five minute incubation at RT, 10 µL of the miRNA-reagent mix was pipetted onto the cell lines, respectively. One day after transfection 100 µL fresh medium was added to each well. Two days after transfection the medium was exchanged with 200 µL fresh medium. On day three, 72 h after transfection, cells were harvested and prepared for FACS measurement.

^[i](<http://discover.nci.nih.gov/cellminer/>)

3.2.3 Immunofluorescence staining and measurement

Both cell lines were stained for Live/Dead using Pacific orange and NT5E (CD73) expression using a PE conjugated antibody. SK-Mel-28 was also stained for ENTPD1 (CD39) expression using a BB515 conjugated antibody and MDA-MB-231 was stained for CD274 (PD-L1) using a PE-Cy7 conjugated antibody. For the staining cells were always centrifuged for 2 min at 2000 rpm. Before the staining, the cells were washed three times with FACS buffer (PBS + 3% FBS). Then, cells were stained with the respective antibody-mix diluted in FACS buffer. Pacific orange was used at 1:1000 dilution. ENTPD1-BB515 and CD274-PE-Cy7 were used at 1:100 dilution. NT5E-PE was used at 1:400 dilution. Per well 100 μ L staining mixture was used and cells were stained for 1 h at 4 °C protected from light. After incubation, cells were centrifuged, washed three times and finally resuspended in 100 μ L FACS buffer and passed through a mesh of MultiScreen-MESH Filter 96-well plates. Plates were subsequently read out on BD LSRFortessa™ Flow Cytometer with HTS system.

Analysis of FACS data was performed with FlowJo version 10. Cells were gated on single cells and live cells. Using respective isotype controls (see table 2.2), gates were set for NT5E, ENTPD1 and CD274 channel. On each plate NT5E siRNA and ENTPD1 siRNA controls were performed to monitor transfection efficacy.

3.2.4 Data Analysis

From all plates the median fluorescence (MFI) values for each miRNA were exported from FlowJo and the subsequent data analysis was performed using R and RStudio Version 3.5.1. First z-score calculation was performed for each plate and channel using the `scale()` function. The `scale` function sets the mean value of each plate to zero and the standard deviation to one. Before z-score calculation untreated, unstained, isotype controls and empty wells were excluded. The z-scores from all plates were then ranked to find the miRNAs with the strongest effect on either NT5E, ENTPD1 or CD274. miRNAs were considered to exert a significant effect, when their z-score was higher 1.645 or below -1.645.

3.3. 3'-UTR reporter assay

Cells were seeded in flat-bottom 96-well culture plates to achieve a confluency of 60 - 70 % at day of transfection. After 24 h, 50 nM miRNA and 100 ng/ μ L plasmid (pLS-NT5E-3'UTR or mutated versions) were transfected with DharmaFect Duo reagent. 48 h post transfection cells were lysed with 50-100 μ L Luciferase Cell Lysis Buffer per well and plated were shaken for 20 min at 300 rpm until at RT complete lysis was achieved. Working solution was prepared by adding 50 μ L 100X coelenterazine to 5 ml Renilla Glow Assay Buffer (Thermo Scientific, Boston, MA, USA) and 50 μ L working solution was added per well. Immediately, luciferase activity was quantified with a luminescence reader. Luciferase ratios were calculated for each miRNA and plasmid construct by dividing the luminescence of non-targeting control according to following the formula:

$$\text{Luminescence} = \frac{\text{miRNA of interest}}{\text{mimic control-1}} \quad (3.3.1)$$

3.4. miRNA/siRNA transfection

All steps during transfection were performed using RNase free filter-tips. Cells were seeded one day prior to transfection in order to achieve a confluency of 60-70 %. For each cell line a transfection test using a fluorophore coupled siRNA (siR-Cy3) was performed to find the optimal transfection reagent achieving highest transfection efficacy. For most cell lines Lipofectamine RNAiMax or DharmaFect 1 was used. Cells were transfected according to the manufacturer's protocol with a final miRNA mimic, miRNA inhibitor or siRNA concentration of 25 nM or 50 nM. After incubation for 24, 48 or 72 h, the medium was aspirated and the cells were washed with Phosphate-Buffered Saline (PBS), subsequently detached with trypsin solution and resuspended in medium supplied with serum. After centrifugation for 5 min at 3400 rpm cell pellets were shock frozen in liquid nitrogen and stored at -80 °C until further usage for protein or RNA isolation. Alternatively, cells were immediately used to perform FACS staining.

3.5. Plasmid transformation and purification

To amplify pLS plasmids, 25 µL competent TOP10 *Escherichia coli* cells were transformed with 20 ng plasmid. After 5 min incubation on ice, cells were heat-shocked for 45 sec at 42 °C and subsequently placed on ice for 2 min followed by addition of 250 µL pre-warmed S.O.C. medium. Transformed cells were plated 1:10 and 1:100 on selective LB-plates containing 100 µg/mL ampicillin and incubated overnight at 37 °C. Colonies were picked and transferred to 4 mL LB-medium with ampicillin and incubated for 8 h at 250 rpm. From the pre-culture, 2 mL were transferred to 1 L Erlenmeyer flask containing 200 mL LB-medium with ampicillin and cultured for 15 h, 37 °C at 250 rpm. Plasmid purification was performed with the Maxi-Prep kit (Qiagen) according to the manufacturer's protocol. Plasmid was eluted in 250 µL sigma water and concentration was measured with a NanoDrop spectrophotometer.

3.6. XTT assay

To measure proliferation of cells e.g. to assess the effect of specific miRNAs on cell proliferation XTT assays were performed. Therefore, the XTT Cell Viability Kit from Cell Signaling was used. This assay is based on the fact that metabolically active cells have the capability to convert the yellow tetrazolium salt XTT to the orange formazan dye. Cells were seeded in 96-well cell culture plates with $1 \cdot 10^4$ cells per well. After 24 h, cells were treated e.g. transfected with miRNA and 24, 48, 72 and 96 h after treatment proliferation was measured by adding 25 µL XTT detection solution directly onto 100 µL culture medium per well. After 60 min incubation time at 37 °C absorbance was measured with a ClarioStar microplate reader at 450 nm and 630 nm as a reference absorbance. After measuring, the plate was washed twice with PBS and 100 µL fresh medium was added to each well. Thus, the same plate was used to measure each time point. Measurements were performed at least in quintuplicates.

3.7. RNA isolation and cDNA generation

Total RNA from frozen cell pellets was isolated using miRNeasy Mini Kit according to the manufacturer’s protocol, which enables analysis of miRNA expression as well as mRNA expression. Cell pellets were lysed using with QIAzol lysis reagent which is based on phenol/guanidine. Subsequently, RNA was purified with silica-membrane spin columns and eluted in 30 μ L nuclease-free water. If only analysis of mRNA expression was relevant, total RNA was isolated using the RNAeasy Kit according to the manufacturer’s protocol. Until further usage for cDNA synthesis, RNA samples were stored at -80 $^{\circ}$ C.

RNA samples were measured using a NanoDrop spectrophotometer or Qubit device using RNA BR Assay kit. For mRNA, 500 ng of total RNA were reverse transcribed in a 20 μ L reaction utilizing oligo(dT)18 primer using the Transcriptor First Strand cDNA Synthesis Kit (Roche Applied Science, Mannheim, Germany). For miRNA, 40 ng of total RNA were reverse transcribed in a 15 μ L reaction using TaqMan $^{\circledR}$ MicroRNA reverse transcription kit (Applied Biosystems, Foster City, CA, USA) according the manufacturer’s protocol and specific stem-loop primers for mature miRNA. All PCRs were run on a Veriti 96 well Thermal Cyclor and the thermal conditions are shown in table 3.1.

Table 3.1: Thermal conditions of reverse transcription.

Total RNA reverse transcription		
Temperature [$^{\circ}$C]	Time [min]	Cycles
65	10	1
immediately on ice	5	1
50	60	1
85	5	1
4	∞	1
miRNA reverse transcription		
Temperature [$^{\circ}$C]	Time [min]	Cycles
16	30	1
42	30	1
85	5	1
4	∞	1

3.8. qPCR

To perform qPCR with cDNA synthesized from mRNA, 2 μ L cDNA diluted 1:5 with PCR-quality water was used in a 20 μ L reaction using the SYBR Green PowerUP PCR Mastermix for qPCR. The components for one qPCR reaction are summarized in table 3.2. Suitable House keeping (HK) genes were used to normalize samples. The HK were selected based on the criteria to have no putative binding site for transfected miRNAs. In general, two different HK genes were used per experiment. For cDNA synthesized from miRNA, 2 μ L were used in a 20 μ L PCR reaction and small nuclear RNA U6 (RNU6B) was used as endogenous control.

Table 3.2: Composition of one qPCR reaction.

2x Master mix	fwd_Primer	rev_Primer	water
one reaction			
10 μL	0.4 μL	0.4 μL	7.2 μL
20 reactions			
200 μL	8 μL	8 μL	144 μL

An Applied Biosystems 7300 Real Time PCR system or QuantStudio 3 Real-Time-PCR-System was utilized to run all qPCRs and the thermal conditions are summarized in table 3.3. For all samples three technical replicates were performed and relative expression was calculated with the $2^{-\Delta\Delta C_t}$ -method as follows:

$$\Delta C_t = C_{t_{\text{GOI}}} - C_{t_{\text{HK}}} \quad (3.8.1)$$

$$\Delta\Delta C_t = C_{t_{\text{miR-XYZ}}} - C_{t_{\text{control}}} \quad (3.8.2)$$

$$\text{Fold change: } FC = 2^{-\Delta\Delta C_t} \quad (3.8.3)$$

$$\log(FC) = \log_2 \left(2^{-\Delta\Delta C_t} \right) \quad (3.8.4)$$

Table 3.3: Thermal conditions of qPCR.

Temperature [$^{\circ}\text{C}$]	Time	Cycles
50	2 min	1
95	2 min	1
95	15 sec	
60	60 sec	40
72	30 sec	

3.9. Quick change mutagenesis

To proof direct binding of miRNAs to NT5E-3'-UTR the respective binding site of miRNAs were mutated using the Quick change II site directed mutagenesis according to the manufactures protocol. Briefly, for every miRNA that showed significant reduction of luciferase signal in 3'-UTR reporter assay, the respective binding site was mutated by deleting one nucleotide within the predicted binding site. Preferably, the nucleotide in the middle of the binding site was deleted. To design the mutation primer the QuickChange Primer Design webtool was used (<https://www.agilent.com/store/primerDesignProgram.jsp>). All used Primers are listed in table 2.4.

3.10. Western Blot analysis

Protein was isolated from frozen cell pellets by dissociation with appropriate amounts of cell lysis buffer supplemented with phenylmethylsulfonylfluorid (PMSF). After 15 min incubation on ice, samples were centrifuged for 30 min at 13,000 rpm, 4 °C. Protein concentrations were measured using the Pierce™ BCA Protein Assay Kit and cell lysates were stored at -20 °C. Protein lysates were heat denatured for 5 min at 95 °C and 10-50 µg protein were mixed with 5x loading dye and loaded on 10 % polyacrylamid gel, subsequently electro-transferred onto a nitrocellulose membrane using the TransTurboBlot system. After transfer, the membrane was blocked for one hour at RT. The blocking buffers for the different investigated proteins can be found in table 3.4. The membrane was then incubated with the respective primary antibody in 5 % blocking solution in TBS-T at 4 °C over night. After extensive washing (1x 10 min, 4-5x 5 min, washing buffer see table 3.4), the membrane was incubated with the respective horseradish peroxidase conjugated secondary antibody for one hour at RT. After washing with TBS-T protein signals were detected with enhanced chemiluminescence (ECL) system using BioRad ChemiDoc XRS machine. Densitometric quantification of protein bands was performed using ImageLab software. Actin was used as loading control and protein of interest levels were normalized by division with actin levels.

Table 3.4: Blocking and washing buffers used in this study.

Protein	Blocking Buffer	Washing buffer
Actin	5 % non-fat milk	TBS-T
CD73	5 % non-fat milk	TBS-T

3.11. Measurement of NT5E/CD73 enzymatic activity by Malachite Green assay

To verify, that the change of NT5E levels mediated by transfected miRNAs also alters the enzymatic activity of NT5E, an assay to infer NT5E activity was established. NT5E catalyses the hydrolysis of AMP to adenosine. Using the Malachite Green assay the released inorganic phosphate of this hydrolysis reaction can be measured. Using a HPLC-UV based method, the amount of AMP and adenosine can be directly quantified. But in the scope of this study only the malachite green assay was deployed.

Based on protocol published by Allard et al. 2019 [13], NT5E/CD73 enzymatic activity was measured using Malachite green assay. This colorimetric assay measures the amount of inorganic phosphate in solution which reacts with Malachite green molybdate under acidic conditions. The amount of the formed complex can be measured with a spectrophotometer at 620 nm. The amount of inorganic phosphate directly correlates with the NT5E/CD73 enzymatic activity, since in the reaction from AMP to adenosine inorganic phosphate is released.

For this assay cells were seeded in 12 well plates and cultured for 24 h until they were transfected with 50 nM miRNA/siRNA. 48 h post transfection cells were washed twice with phosphate-free buffer. The recipe for the phosphate-free buffer is listed in table 3.5. 500 µL

of phosphate-free buffer were added to each well and cells were incubated for 15 min at 37 °C. 4 µL of freshly prepared 50 mM AMP from 1 M frozen AMP stock were added to each well to achieve a final concentration of 400 µM AMP. Plates were incubated for 30 min, 60 or 90 min at 37 °C. Meanwhile 25 µL 10 mM EDTA diluted in phosphate-free buffer was added to a 96-well reading plate in each well. After defined incubation time, 25 µL supernatant was transferred to the reading plate and mixed with the EDTA. At least quintuplicates were performed per condition. 10 µL Malachite Green Reagent A were added to each well and reading plates were incubated for 10 min at RT on a microplate shaker. Then 10 µL Malachite Green Reagent B were added to each well and absorbance at 620 nm was measured after 5 min incubation time.

Table 3.5: Phosphate-free-buffer.

Chemical	Stock	MW	Preparation stock	V for 450 mL	Final conc.
MgCl ₂	2 M	203.30 g/mol	0.82 g in 2 mL	450 µL	2 mM
NaCl	1.25 M	58.44 g/mol	3.65 g in 50 mL	45 mL	125 mM
KCl	1 M	74.56 g/mol	3.70 g in 50 mL	450 µL	1 mM
Glucose	138 mM	198.17 g/mol	1.40 g in 50 mL	32.4 ml	10 mM
HEPES	2 M	238.31 g/mol	2.40 g in 10 mL	4.5 mL	10 mM
ddH ₂ O				367.2 mL	

3.12. RNA-Seq analysis

To assess expression levels of genes of interest and of miRNAs, RNA-Seq was performed for five normal human melanocyte samples (NHEM) and ten melanoma cell lines. RNA was isolated from the respective samples using miREasy kit. RNA-Seq and miR-Seq was performed by company GeneWIZ. For Gene expression analysis Illumina® NovaSeq™ was used. For small RNA analysis HiSeq® was used. Trimming, mapping and differential gene expression analysis was performed by GeneWIZ.

3.13. Microarray analysis

To investigate the mechanism of NT5E up-regulating miRNAs, gene expression profiling was performed upon miRNA transfection. MaMel-02 and MDA-MB-231 cells were transfected with 50 nM miRNA and 48 h post transfection RNA was isolated using RNAEasy kit. Each condition was performed in triplicates. Samples were sent to the DKFZ - Genomics and Proteomics Core Facility. The Affymetrix Clariom S human chip was used for all samples. Raw data was processed by the Core facility. Differentially gene expression analysis was performed always by comparison to mimic control-1 samples. Venn diagrams were generated using webtool from Bioinformatics & Evolutionary Genomics department of the Ghent university (<http://bioinformatics.psb.ugent.be/webtools/Venn/>) [4].

RESULTS

The main aim of this thesis was the elucidation of the post-transcriptional regulation of immune checkpoint molecule expression, especially NT5E/CD73, exerted by miRNAs. Furthermore, the aim was to gain more insights in the aberrant regulation of immune checkpoint molecules in cancer cells. The general work-flow of this study is depicted in figure 4.1. The work-flow can be divided into three main tasks. First, *in silico* data analysis and predictions was performed. Second, a miRNA library screen was conducted, to experimentally find miRNAs that are capable of changing surface expression of selected immune checkpoint molecules. The last part was the validation of the screening results including more in-depth analysis of the miRNA-mediated effects as well as functional assays.

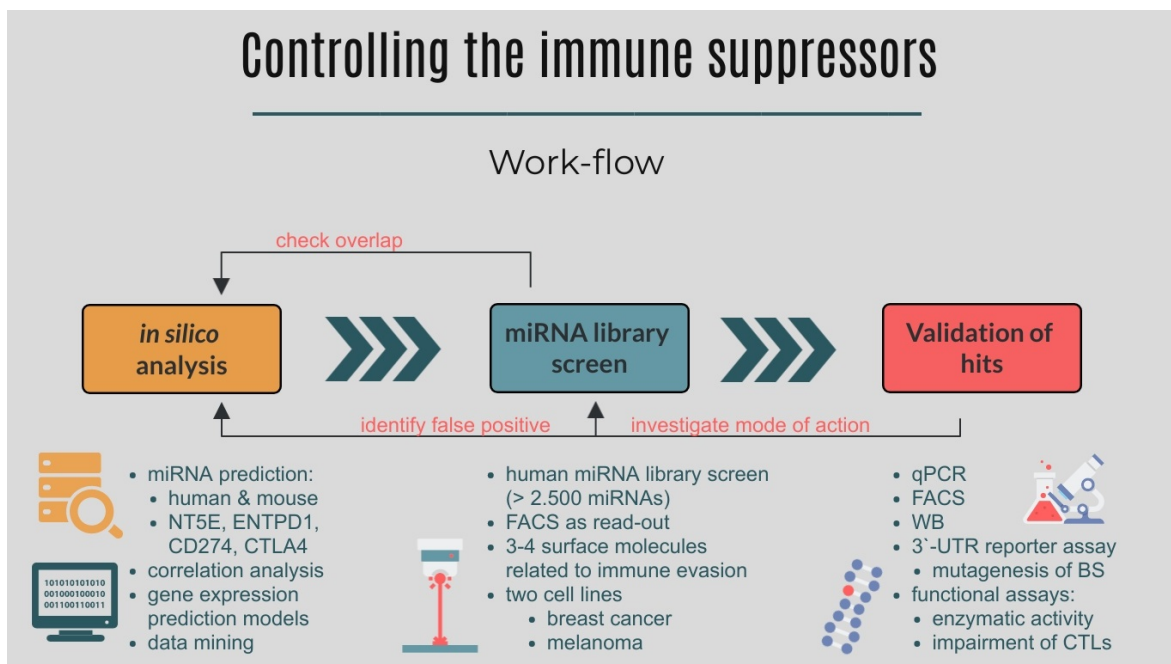


Figure 4.1: General work-flow of this study. This study can be divided in three main parts. Firstly, *in silico* analysis was carried out. Using different prediction algorithms potential miRNAs regulating immune check point molecules were retrieved. Also different expression data sets were analysed and based on this suitable cell lines for the following experiments were selected. The second phase was the miRNA library screen, to experimentally identify miRNAs, that are capable of changing the surface expression of selected immune evasion relevant proteins. This phase generated the largest share of data of this study and was the base for the last phase. The final step was the validation phase, to confirm the screening hits and to investigate their mode of action.

4.1. *in silico* predictions identified large number of miRNAs targeting immune checkpoint molecules

To find potential miRNA candidates regulating immune checkpoint molecules in human, *in silico* prediction algorithms were used. Therefore, different miRNA-target prediction tools were combined. The following resources for predicting potential miRNAs were used: TargetScan Version 6.2, MicroCosm, miRDB Version 5.0, miRecords, miRgator, MicroCosm, microRNA conserved and non-conserved, PITA, PicTar2 and PACCMIT. Since the different databases apply different concepts how a miRNA-target interaction is computed and defined, potential miRNA candidates were selected, which were predicted to regulate the respective immune checkpoint molecule by at least three databases.

4.1.1 *in silico* prediction identified 44 miRNAs with strong evidence to target NT5E/CD73

Ten different data bases were used to find miRNAs that potentially regulate NT5E function and expression in humans. All data bases were downloaded at 01-05-2017. The different data bases are listed below with their respective number of miRNAs, that were connected to NT5E:

- MircoCosm # 30
- microRNA # 64 (conserved) #230 (non conserved)
- miRDB V5 # 84
- miRecords # 4
- miRgator # 4
- miRNAMap # 25
- PACCMIT # 244
- PicTar # 0
- PITA # 4 (Top Score) # 197 (all predictions)
- TargetScan # 8

Adding up all 10 data bases yielded 584 unique miRNAs. The entries of some data bases like miRDB or PACCMIT also appeared frequently in other data bases. But for example the entries of TargetScan were rarely shared with other data bases. This might be due to the fact that TargetScan combined for example the whole hsa-miR-30 family whereas the other data bases listed each family member separately.

The top miRNA candidates from *in silico* prediction for NT5E are listed in table 4.1. hsa-miR-422a was predicted to regulate NT5E by six different data bases. Overall, ten miRNAs were predicted by at least four data bases for example hsa-miR-22. In total, 44 miRNAs were predicted to regulate NT5E by at least three different data bases.

Table 4.1: miRNAs predicted by at least 3 different data bases to regulate NT5E.

miRNA	No. of DBs	miRNA	No. of DBs
hsa-miR-422a	6	hsa-miR-513a-3p	3
hsa-miR-518a-5p	5	hsa-miR-580	3
hsa-miR-548l	5	hsa-miR-587	3
hsa-miR-22	4	hsa-miR-630	3
hsa-miR-507	4	hsa-miR-650	3
hsa-miR-557	4	hsa-miR-662	3
hsa-miR-140-5p	4	hsa-miR-654-3p	3
hsa-miR-590-3p	4	hsa-miR-657	3
hsa-miR-527	4	hsa-miR-1296	3
hsa-miR-1246	4	hsa-miR-1257	3
hsa-miR-448	3	hsa-miR-548n	3
hsa-miR-524-5p	3	hsa-miR-1827	3
hsa-miR-363	3	hsa-miR-378b	3
hsa-miR-30d	3	hsa-miR-3134	3
hsa-miR-30b	3	hsa-miR-3163	3
hsa-miR-153	3	hsa-miR-3185	3
hsa-miR-125a-5p	3	hsa-miR-3201	3
hsa-miR-193a-3p	3	hsa-miR-378c	3
hsa-miR-433	3	hsa-miR-4310	3
hsa-miR-146b-5p	3	hsa-miR-4282	3
hsa-miR-142-5p	3	hsa-miR-30a-5p	3
hsa-miR-520h	3	hsa-miR-30e-5p	3

A Venn diagram showing the overlap of miRNAs targeting NT5E predicted by the five different data bases: MicroCosm, microRNA (conserved), miRDB, PITA (all entries) and PAC-CMIT is given in figure 4.2.

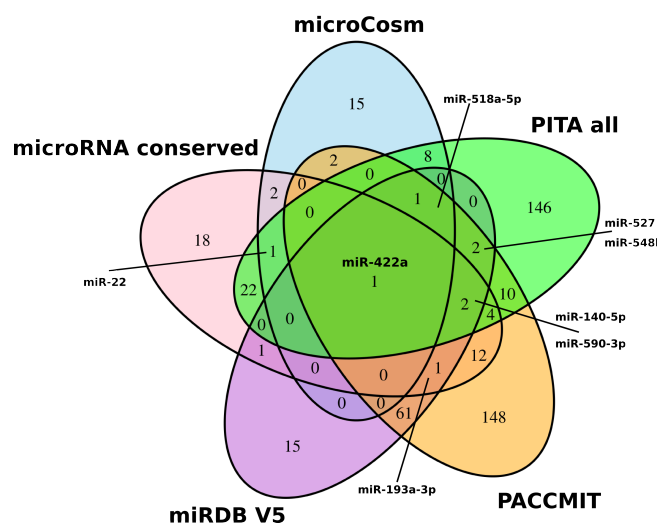


Figure 4.2: Venn diagram of NT5E targeting miRNAs. The overlap of miRNAs targeting NT5E predicted by the five data bases MicroCosm, microRNA (conserved), miRDB, PITA (all entries) and PACCMIT is shown. Only miR-422a was predicted by all resources.

4.1.2 *in silico* prediction identified three miRNAs with strong evidence to target ENTPD1/CD39

Ten different data bases were used to find potential miRNAs that regulate ENTPD1 in humans. All data bases were downloaded at 01-05-2017. The different data bases are listed below with their respective number of miRNAs connected to ENTPD1:

- MircoCosm # 98
- microRNA # 17 (conserved) # 55(non conserved)
- miRDB V5 # 70
- miRecords # 0
- TarBase # 16
- miRNAMap # 0
- PACCMIT # 13
- PicTar # 1
- PITA # 1 (Top Score) # 335 (all predictions)
- TargetScan # 46

Combining all data bases yielded overall 563 unique miRNAs that are predicted to regulate ENTPD1. Compared to NT5E, the overlap of miRNAs between the tools was smaller. Thus, the stringency for selecting potential ENTPD1 regulators was relaxed and all miRNAs were considered which were predicted by at least two different data bases. Those miRNAs are listed in table 4.2. Only the three miRNAs hsa-miR-421, hsa-miR-140-5p and hsa-miR-346 were predicted by three different tools. Overall, 59 miRNAs were contained in at least two data bases.

Table 4.2: miRNAs predicted by at least 2 different data bases to regulate ENTPD1.

miRNA	No. of DBs	miRNA	No. of DBs
hsa-miR-421	3	hsa-miR-30c	2
hsa-miR-140-5p	3	hsa-miR-30b	2
hsa-miR-346	3	hsa-miR-140-3p	2
hsa-miR-300	2	hsa-miR-573	2
hsa-miR-146b-5p	2	hsa-miR-595	2
hsa-miR-381	2	hsa-miR-607	2
hsa-miR-144	2	hsa-miR-649	2
hsa-miR-337-5p	2	hsa-miR-802	2
hsa-miR-520e	2	hsa-miR-1276	2
hsa-miR-193a-3p	2	hsa-miR-3175	2
hsa-miR-338-3p	2	hsa-miR-15a-5p	2
hsa-miR-766	2	hsa-miR-15b-5p	2
hsa-miR-526b	2	hsa-miR-16-5p	2
hsa-miR-936	2	hsa-miR-195-5p	2
hsa-miR-520a-5p	2	hsa-miR-2110	2
hsa-miR-499-5p	2	hsa-miR-424-5p	2
hsa-miR-328	2	hsa-miR-429	2
hsa-let-7e	2	hsa-miR-4428	2
hsa-miR-520b	2	hsa-miR-4742-3p	2
hsa-miR-625	2	hsa-miR-497-5p	2
hsa-miR-545*	2	hsa-miR-548l	2
hsa-miR-23b	2	hsa-miR-641	2
hsa-miR-708	2	hsa-miR-590-3p	2
hsa-miR-16-2*	2	hsa-miR-331-3p	2
hsa-miR-630	2	hsa-miR-330-5p	2
hsa-miR-27b*	2	hsa-miR-136	2
hsa-miR-920	2	hsa-miR-326	2
hsa-miR-493	2	hsa-miR-194	2
hsa-miR-545	2	hsa-miR-205	2
hsa-miR-30b*	2		

4.1.3 *in silico* prediction identified 39 miRNAs with strong evidence to target CD274/PD-L1

39 miRNAs were predicted to regulate CD274 by at least three different sources. These miRNAs are listed in table 4.3. The following three miRNAs were contained in four different data bases: hsa-miR-140-3p, hsa-miR-28-3p and hsa-miR-384. The top *in silico* candidate to regulate NT5E, was also predicted to regulate CD274: hsa-miR-422a.

Table 4.3: miRNAs predicted by at least 3 different data bases to regulate CD274.

miRNA	No. of DBs	miRNA	No. of DBs
hsa-miR-140-3p	4	hsa-miR-1205	3
hsa-miR-28-3p	4	hsa-miR-548e	3
hsa-miR-384	4	hsa-miR-548l	3
hsa-miR-140-5p	3	hsa-miR-1243	3
hsa-miR-429	3	hsa-miR-1270	3
hsa-miR-501-5p	3	hsa-miR-302f	3
hsa-miR-383	3	hsa-miR-513b	3
hsa-miR-422a	3	hsa-miR-1273c	3
hsa-miR-188-3p	3	hsa-miR-378c	3
hsa-miR-219-2-3p	3	hsa-miR-4264	3
hsa-miR-485-3p	3	hsa-miR-4279	3
hsa-miR-520h	3	hsa-miR-17-5p	3
hsa-miR-513a-5p	3	hsa-miR-320a	3
hsa-miR-563	3	hsa-miR-377-3p	3
hsa-miR-576-3p	3	hsa-miR-548a-5p	3
hsa-miR-548a-3p	3	hsa-miR-548b-5p	3
hsa-miR-636	3	hsa-miR-548i	3
hsa-miR-128	3	hsa-miR-559	3
hsa-miR-802	3	hsa-miR-93-5p	3
hsa-miR-1225-3p	3		

4.1.4 *in silico* prediction identified 33 miRNAs with strong evidence to target CTLA4/CD152

The miRNAs predicted to target CTLA4 are listed in table 4.4. Overall, 33 miRNAs were contained in at least three data bases. One miRNA was contained in five data bases: hsa-miR-561a-3p. The following three miRNAs were predicted by four different tools to regulate CTLA4: hsa-miR-656, hsa-miR-429 and hsa-miR-324-5p.

Table 4.4: miRNAs predicted by at least 3 different data bases to regulate CTLA4.

miRNA	No.of DBs	miRNA	No. of DBs
hsa-miR-516a-3p	5	hsa-miR-579	3
hsa-miR-656	4	hsa-miR-581	3
hsa-miR-429	4	hsa-miR-582-3p	3
hsa-miR-324-5p	4	hsa-miR-583	3
hsa-miR-384	3	hsa-miR-548c-3p	3
hsa-miR-380	3	hsa-miR-1200	3
hsa-miR-155	3	hsa-miR-1287	3
hsa-miR-494	3	hsa-miR-1243	3
hsa-miR-496	3	hsa-miR-1248	3
hsa-miR-542-3p	3	hsa-miR-1261	3
hsa-miR-1297	3	hsa-miR-302f	3
hsa-miR-140-3p	3	hsa-miR-548p	3
hsa-miR-127-5p	3	hsa-miR-1279	3
hsa-miR-330-3p	3	hsa-miR-3182	3
hsa-miR-511	3	hsa-miR-4311	3
hsa-miR-502-5p	3	hsa-miR-4282	3
hsa-miR-502-3p	3		

4.1.5 Several miRNAs are predicted to target multiple immune checkpoint molecules

Having performed the *in silico* prediction for the different immune checkpoint molecules, miRNAs regulating all four investigated genes or a subset of them were investigated more closely. In table 4.5 all miRNAs are listed, that were predicted by at least one data base to bind to the 3'-UTR of NT5E, ENTPD1, CD274 and CTLA4. Overall, 49 miRNAs were predicted to regulate all four targets. Among them was miR-422a, which was the miRNA predicted by most data bases to regulate NT5E. Also miR-548l seems to be a promising miRNA involved in regulating genes relevant for immune evasion since it was predicted by five data bases to regulate NT5E and three data bases predicted it to bind to CD274 3'-UTR. And at least two data bases gave evidence of regulation of ENTPD1 by miR-548l and one for the regulation of CTLA4 by this miRNA. Furthermore, there was also evidence that miR-193a and miR-193b target all four immune checkpoint molecules.

Table 4.5: miRNAs predicted to regulate NT5E, ENTPD1, CD274 and CTLA4. For each target gene the number of data bases that containede miRNA-target interaction is given.

miRNA	NT5E	ENTPD1	CD274	CTLA4
hsa-miR-422a	6	1	3	1
hsa-miR-548l	5	2	3	1
hsa-miR-590-3p	4	2	1	2
hsa-miR-1246	4	1	2	1
hsa-miR-662	3	1	2	2
hsa-miR-656	2	1	1	4
hsa-miR-338-5p	1	3	2	2
hsa-miR-548n	3	1	1	2
hsa-miR-28-5p	2	2	2	1
hsa-miR-495	2	3	1	1
hsa-miR-330-3p	2	1	1	3
hsa-miR-511	2	1	1	3
hsa-miR-3148	2	1	2	2
hsa-miR-496	1	1	2	3
hsa-miR-485-3p	1	1	3	2
hsa-miR-641	1	2	2	2
hsa-miR-607	1	2	2	2
hsa-miR-490-5p	2	1	1	2
hsa-miR-410	2	1	1	2
hsa-miR-875-5p	2	1	1	2
hsa-miR-708	2	2	1	1
hsa-miR-491-3p	2	1	2	1
hsa-miR-219-2-3p	1	1	3	1
hsa-miR-155	1	1	1	3
hsa-miR-487a	1	1	2	2
hsa-miR-1248	1	1	1	3
hsa-miR-548a-3p	1	1	3	1
hsa-miR-378	2	1	1	1
hsa-miR-374b	2	1	1	1
hsa-miR-582-5p	2	1	1	1
hsa-miR-584	2	1	1	1
hsa-miR-1208	2	1	1	1
hsa-miR-548m	2	1	1	1
hsa-miR-501-3p	1	1	1	2
hsa-miR-193b	1	1	2	1
hsa-miR-335*	1	2	1	1
hsa-miR-548k	1	1	2	1
hsa-miR-326	1	2	1	1
hsa-miR-142-3p	1	1	2	1
hsa-miR-519d	1	1	1	2
hsa-miR-568	1	1	1	2
hsa-miR-548f	1	1	2	1
hsa-miR-1206	1	1	1	2
hsa-miR-29b-2*	1	1	1	1
hsa-miR-512-3p	1	1	1	1
hsa-miR-340-5p	1	1	1	1
hsa-miR-138	1	1	1	1
hsa-miR-150	1	1	1	1
hsa-miR-193a-5p	1	1	1	1

4.2. Gene expression modelling revealed ATF1, GFI1, SMAD4 and TCF7 as most important NT5E transcription factors

Since also detection of NT5E enhancing or inhibiting miRNAs lacking a binding site for NT5E 3'-UTR is expected when conducting the miRNA library screen, the transcriptional regulation of NT5E was analysed in order to explain miRNA mediated indirect effects. Therefore, an approach that considers the activity of transcription factors was used to explain the change of target genes expression over a panel of different samples. In this study, the NCI-60 cell line expression data set was used [194]. As described in the method section and in previous publication [208], the so called EdgeStrength-Matrix (ES) was employed to obtain a list of potential NT5E transcription factors. With the used ES-matrix, 11 potential transcriptional regulators of NT5E were obtained which had an ES value greater than 0: **ATF1, ATF2, FOXP3, GFI1, SMAD2, SMAD3, SMAD4, SMAD5, SP1, STAT3 and TCF7.**

To find the most important regulators that explain the change in NT5E expression across the NCI-60 panel, a bottom-up approach was implemented. Using MIP models the number of transcription factors for the model was restricted and the model chose the TFs that could best account for the changes in NT5E expression. The performance of the model was calculated by Leave-One-Out cross validation (LOO-CV). The results are summarized in table 4.6.

Table 4.6: Bottom-Up Approach: Prediction of NT5E gene expression in NCI-60 data set using MIP models to restrict number of TFs. Prediction performance (PP) was calculated with LOO-CV.

Transcription factors	PP
SMAD2	0.37
ATF1, SMAD2	0.51
ATF1,GFI1,SMAD4	0.50
ATF1,GFI1,SMAD4,TCF7	0.53
ATF1,FOXP3,GFI1,SMAD4,TCF7	0.49
ATF1,ATF2,FOXP3,GFI1,SMAD4,TCF7	0.47
ATF1,ATF2,FOXP3,GFI1,SMAD4,SMAD5,TCF7	0.52
ATF1,ATF2,FOXP3,GFI1,SMAD4,SMAD5,SP1,TCF7	0.49
ATF1,ATF2,FOXP3,GFI1,SMAD2,SMAD3,SMAD4,SP1,TCF7	0.46
ATF1,ATF2,FOXP3,GFI1,SMAD2,SMAD3,SMAD4,SMAD5,SP1,TCF7	0.40
ATF1,ATF2,FOXP3,GFI1,SMAD2,SMAD3,SMAD4,SMAD5,SP1,STAT3,TCF7	0.33

SMAD2 was the transcription factor, that alone could best predict NT5E expression. The prediction performance could be further increased by adding a second regulator. The MIP model picked SMAD2 and ATF1 and the performance reached 0.51. This performance could be only slightly increased by adding additional regulators. The best performance was achieved with a model consisting of the following four transcription factors: ATF1, GFI1, SMAD4 and TCF7.

4.3. NT5E and CD274 are frequently expressed in human cancer cell lines whereas ENTPD1 and CTLA4 are rarely expressed

To find NT5E expressing human cancer cell lines suitable for the miRNA library screen and for subsequent experiments, gene expression data sets were used. First, the NCI-60 panel was examined [194], to check in which cancer entities NT5E is predominantly expressed. The expression level across eight different cancer types for NT5E mRNA is shown in figure 4.3.

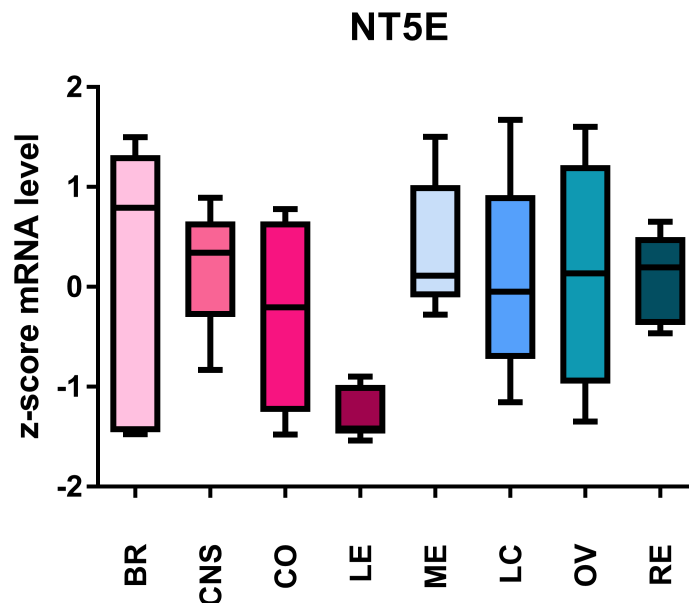


Figure 4.3: NT5E mRNA levels among cell lines of different tumor entities (NCI-60 panel). BR: breast cancer; CNS: tumor of central nervous system; CO: colon cancer; LE: leukaemia; ME: melanoma; LC: non-small-cell lung carcinoma; OV: ovarian cancer; RE: renal carcinoma.

In most cancer types NT5E expression could be found, except for leukaemia cell lines showing the lowest NT5E levels (mean z-score = -1.3). The highest mean expression was found in melanoma (mean z-score = 0.40). To note, one of the cell line with the highest NT5E expression was the melanoma cell line SK-Mel-28 (z-score = 1.5), closely followed by the breast cancer cell line MDA-MB-231 (z-score = 1.49). The expression of NT5E in breast cancer was quite scattered. For example, the breast cancer line T-47D exhibited one of the lowest NT5E values in the panel (z-score = -1.4).

The NCI-60 panel was also screened for expression of ENTPD1. The result is compiled in figure 4.4. ENTPD1 was rarely expressed across the different cancer types. One exception was melanoma exhibiting the highest overall ENTPD1 expression (mean z-score = 1.0). The cell line with the highest ENTPD1 expression within the NCI-60 panel was the melanoma cell line SK-Mel-28 (z-score = 4.5), followed by SK-Mel-5 (z-score = 3.6) and SK-Mel-2 (z-score = 2.4). The lowest ENTPD1 expression was found in colon cancer (mean z-score = -0.4). In breast cancer (mean z-score = 0.0) only the HS 578T cell line showed sustained ENTPD1 levels (z-score = 0.7). Also in ovarian cancer (mean z-score = 0.0), some cell lines showed intermediate ENTPD1 levels: OVCAR-3 (z-score = 0.5) and OVCAR-4 (z-score = 0.4).

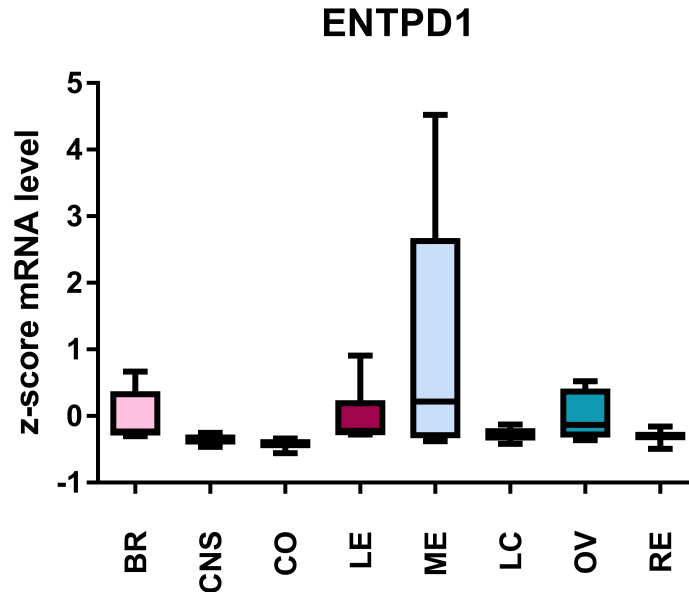


Figure 4.4: ENTPD1 mRNA levels among cell lines of different tumor entities (NCI-60 panel). BR: breast cancer; CNS: tumor of central nervous system; CO: colon cancer; LE: leukaemia; ME: melanoma; LC: non-small-cell lung carcinoma; OV: ovarian cancer; RE: renal carcinoma.

Also for CD274, the expression across the NCI-60 panel was checked and the result is shown in figure 4.5. CD274 expression could be found in most of the cancer types, except for colon cancer (mean z-score = -0.2) and melanoma (mean z-score = -0.4). Only one melanoma cell line, LOX-IMVI, showed high CD274 expression (z-score = 1.9). Overall the highest mean expression was found in CNS cancer (mean z-score = 0.5). The expression of CD274 in breast cancer cell lines was quite varying between the different cell lines (mean z-score = 0.1). For example, MDA-MB-231 was strongly CD274 positive (z-score = 1.5) while T-47D (z-score = -0.8) or MCF7 were CD274 negative (z-score = -0.8). The cell line with the highest CD274 levels was the leukaemia cell line SR (z-score = 3.7).

The expression across the NCI-60 panel for CTLA is shown in figure 4.6. In most cancer types CTLA4 was not expressed or just to small extend e.g. in leukaemia (mean z-score = 0.0). Only in melanoma CTLA4 was expressed at higher levels (mean z-score = 1.2). The three cell lines with the highest CTLA4 expression among the panel were UACC-257 (z-score = 4.9), MALME-3M (z-score = 2.4) and SK-Mel-28 (z-score = 2.0).

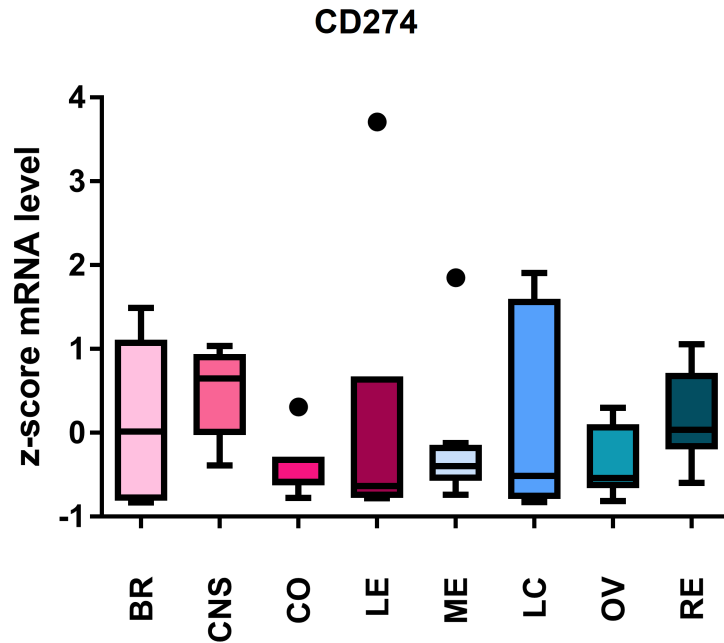


Figure 4.5: CD274 mRNA levels among cell lines of different tumor entities (NCI-60 panel). BR: breast cancer; CNS: tumor of central nervous system; CO: colon cancer; LE: leukaemia; ME: melanoma; LC: non-small-cell lung carcinoma; OV: ovarian cancer; RE: renal carcinoma.

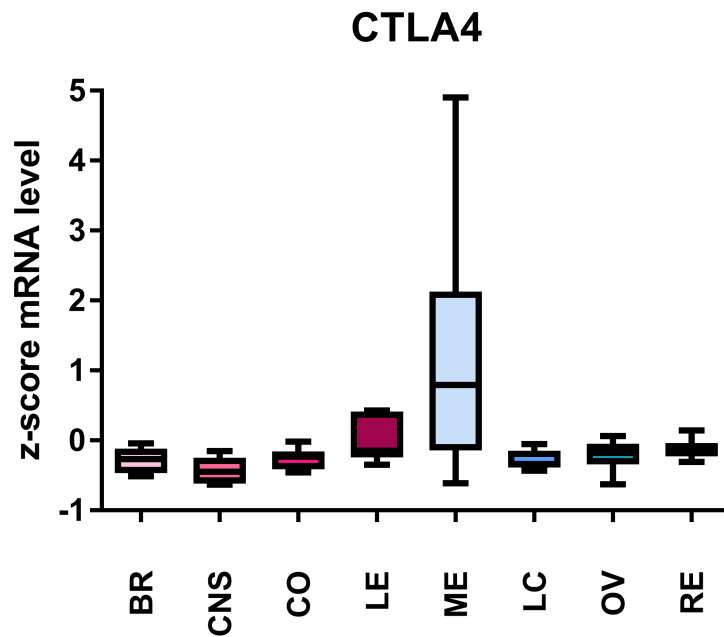


Figure 4.6: CTLA4 mRNA levels among cell lines of different tumor entities (NCI-60 panel). BR: breast cancer; CNS: tumor of central nervous system; CO: colon cancer; LE: leukaemia; ME: melanoma; LC: non-small-cell lung carcinoma; OV: ovarian cancer; RE: renal carcinoma.

One focus in this work was human melanoma. Thus, the expression of the studied checkpoint molecules was also analysed in a panel of human melanoma cell lines. This MaMel panel consists of 34 human melanoma cell lines [236]. The expression of NT5E, ENTPD1, CD274 and CTLA4 across this panel is shown in figure 4.7. Overall, NT5E had the highest mean expression ($\text{mean}_{\text{NT5E}} = 7.3$), followed by CD274 ($\text{mean}_{\text{CD274}} = 6.0$). For most cell lines ENTPD1 was not highly expressed ($\text{mean}_{\text{ENTPD1}} = 4.7$), but few cell lines exhibit high ENTPD1 mRNA levels. The lowest expression was observed for CTLA4 ($\text{mean}_{\text{CTLA4}} = 4.6$).

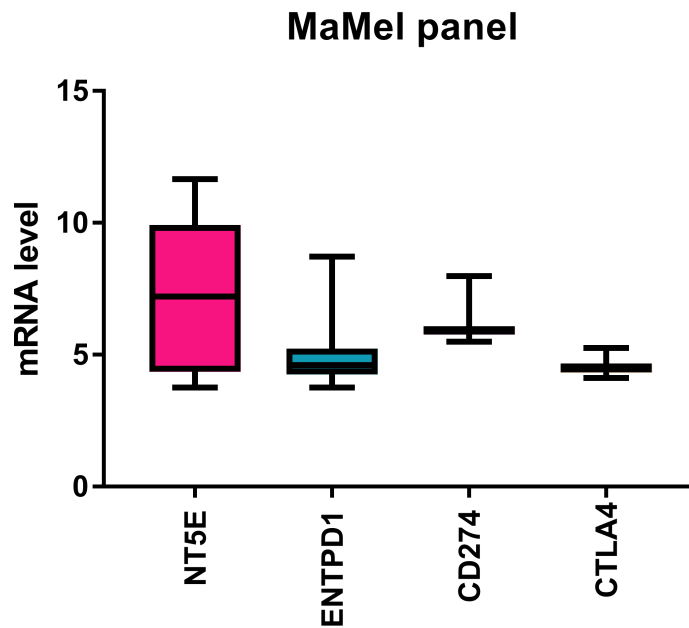


Figure 4.7: Expression of immune checkpoint molecules within MaMel panel. Comparison of NT5E, ENTPD1, CD274 and CTLA4 mRNA levels across a panel of human melanoma cell lines.

To have a closer look on the individual cell lines, the expression data was z-score normalized and expression of the checkpoint molecules was ranked from low to high expression. Figure 4.8 shows the ranked expression of NT5E across the MaMel panel. MaMel-61e exhibited the highest NT5E level ($\text{z-score}_{\text{NT5E}} = 1.66$), followed by MaMel-53a ($\text{z-score}_{\text{NT5E}} = 1.48$) and MM038 ($\text{z-score}_{\text{NT5E}} = 1.30$). NT5E negative were for example the cell lines MaMel-79b ($\text{z-score}_{\text{NT5E}} = -1.33$), MaMel-35 ($\text{z-score}_{\text{NT5E}} = -1.32$) and MaMel-39a ($\text{z-score}_{\text{NT5E}} = -1.31$).

The ranked expression for ENTPD1 across the MaMel panel is shown in figure 4.9. Seven cell lines had pronounced ENTPD1 expression. MaMel-86b was the cell line with the highest ENTPD1 levels ($\text{z-score}_{\text{ENTPD1}} = 2.5$), followed by MaMel-75 ($\text{z-score}_{\text{ENTPD1}} = 2.4$) and MaMel-79b ($\text{z-score}_{\text{ENTPD1}} = 2.4$). MM019 ($\text{z-score}_{\text{ENTPD1}} = -1.0$), MM103 ($\text{z-score}_{\text{ENTPD1}} = -0.9$) and MM8a ($\text{z-score}_{\text{ENTPD1}} = -0.8$) exhibited the lowest ENTPD1 mRNA expression. NT5E/CD73 and ENTPD1/CD39 are enzymes working in a cascade catalysing ATP to adenosine. Interestingly, both enzymes were not co-expressed in the melanoma panel. The mRNA levels of NT5E and ENTPD1 were significantly negatively correlated ($\text{PCC} = -0.42$, $p = 0.013$). The plot of NT5E against ENTPD1 mRNA levels is shown in figure 4.10.

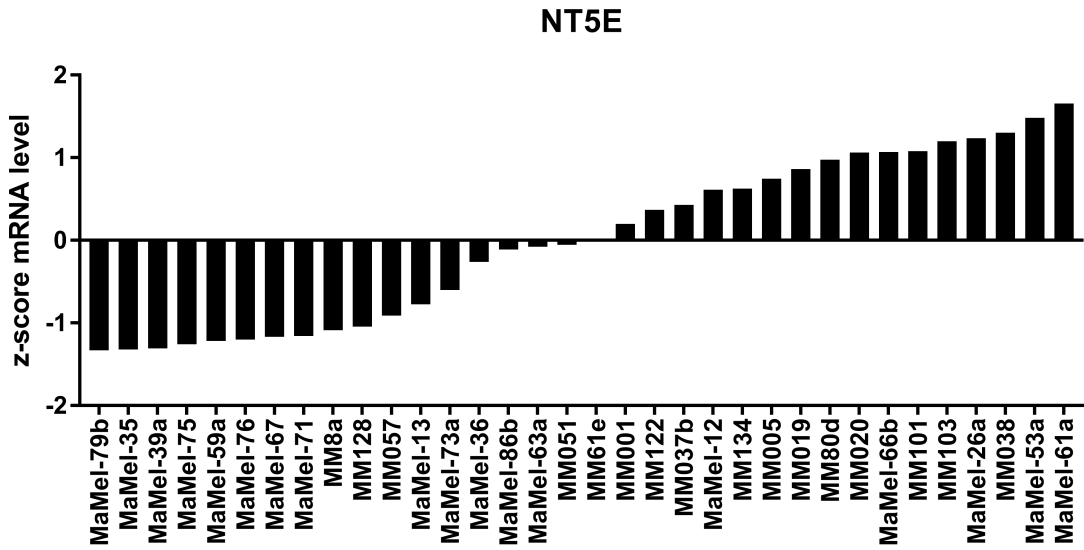


Figure 4.8: Ranked NT5E mRNA expression across the MaMel-panel. Expression data was z-score normalized.

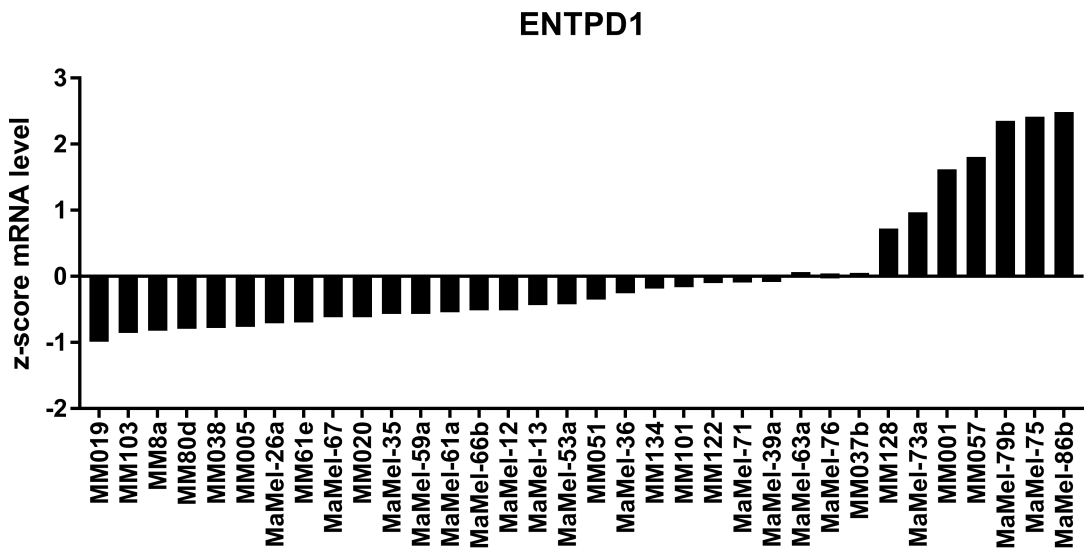


Figure 4.9: Ranked ENTPD1 mRNA expression across the MaMel-panel. Expression data was z-score normalized.

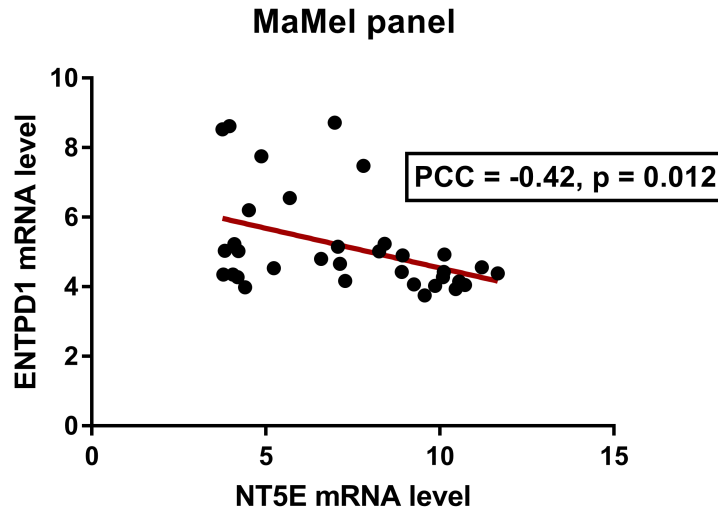


Figure 4.10: Correlation of NT5E and ENTPD1 expression across the MaMel panel. Across the analysed melanoma cell lines, NT5E showed a significantly negative correlation with ENTPD1 mRNA expression.

For five selected cell lines, which showed high ENTPD1 mRNA levels or NT5E levels, also ENTPD1 and NT5E surface expression was measured by FACS to confirm the mRNA data and to eventually find additional cell lines expressing both enzymes. The surface expression of NT5E for those cell lines is given in figure 4.11 A and the surface expression of ENTPD1 is shown in figure 4.11 B.

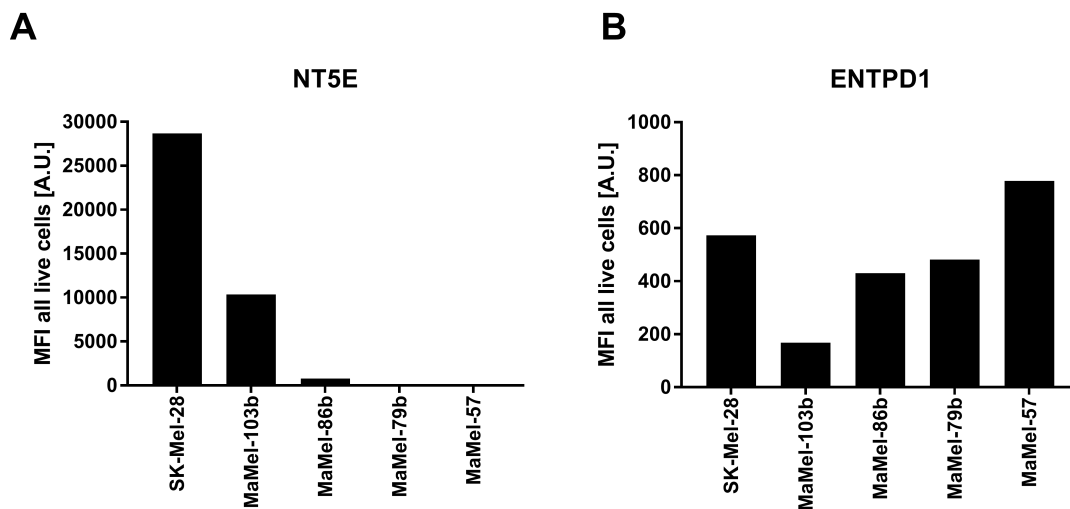


Figure 4.11: FACS analysis of surface NT5E (A) and ENTPD1 (B) expression in selected melanoma cell lines. Only SK-Mel-28 cell line exhibited high levels of both NT5E and ENTPD1 surface expression.

As expected from the NT5E mRNA data, SK-Mel-28 and MaMel-103b showed high NT5E levels. MaMel-86b showed minor surface NT5E expression and MaMel-79b and MaMel-57 were NT5E negative. But those two cell lines exhibited high ENTPD1 surface expression.

Also SK-Mel-28 and MaMel-86b expressed ENTPD1 at the cell surface. Only MaMel-103b exhibited weak ENTPD1 surface levels. Since cell lines expressing both enzymes would have been most suitable for follow-up experiments, the percentage of NT5E and ENTPD1 positive cells was determined and is depicted in figure 4.12. SK-Mel-28 had the highest rate of NT5E⁺ and ENTPD1⁺ cells with 84 %, followed by MaMel-86b with 61%. MaMel-103b only showed 19 % double positive cells. MaMel-57 only exhibited 4 % double positive cells, although it was the cell line with the highest ENTPD1 levels. MaMel-79b was NT5E negative, thus having 0 % double positive cells. For subsequent experiments, the SK-Mel-28 cell line was selected since it showed the highest percentage of double positive cells.

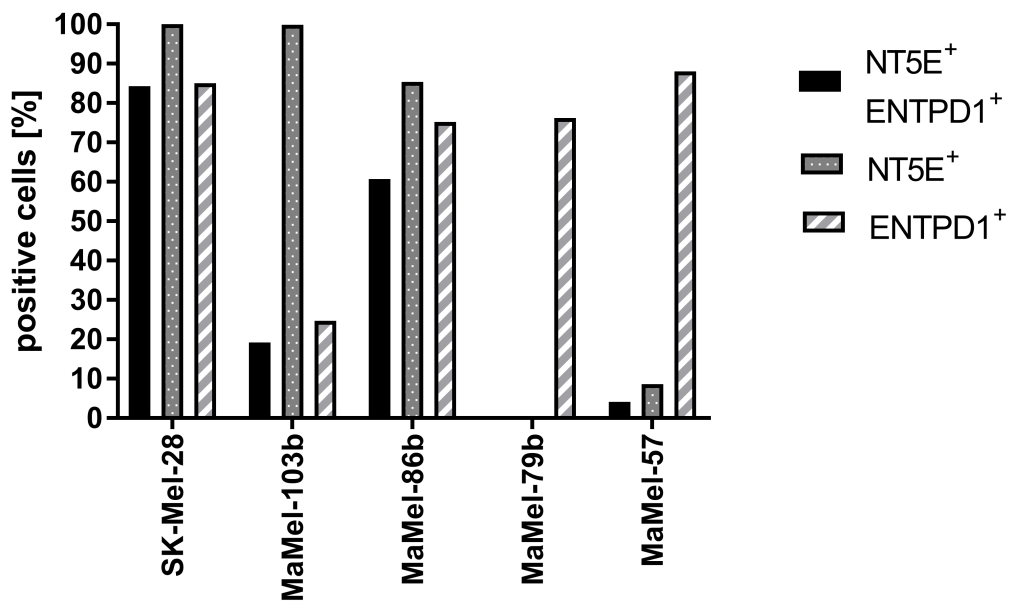


Figure 4.12: Percentage of NT5E and ENTPD1 positive cells. FACS analysis of surface NT5E and ENTPD1 expression in selected melanoma cell lines.

Figure 4.13 depicts the ranked expression of CD274. Most human melanoma cell lines of the panel exhibited a rather low CD274 mRNA level, except for three cell lines with quite high CD274 expression. By far the strongest CD274 expression exhibited MaMel-66b ($z\text{-score}_{\text{CD274}} = 4.6$), followed by MM038 ($z\text{-score}_{\text{CD274}} = 1.9$) and MaMel-26a ($z\text{-score}_{\text{CD274}} = 1.0$). MM103 and MaMel-13 both had the lowest CD274 levels ($z\text{-score}_{\text{CD274}} = -1.1$).

The ranked expression of CTLA4 in the MaMel panel is given in figure 4.14. Five cell lines of the panel showed high CTLA4 expression: MaMel-63a ($z\text{-score}_{\text{CTLA4}} = 2.2$), MaMel-73a ($z\text{-score}_{\text{CTLA4}} = 2.1$), MaMel-67 ($z\text{-score}_{\text{CTLA4}} = 2.0$), MM051 ($z\text{-score}_{\text{CTLA4}} = 1.8$) and MaMel-86b ($z\text{-score}_{\text{CTLA4}} = 1.8$). The lowest expression of the panel had MM61e ($z\text{-score}_{\text{CTLA4}} = -1.4$), followed by MM101 ($z\text{-score}_{\text{CTLA4}} = -1.3$) and MM057 ($z\text{-score}_{\text{CTLA4}} = -1.2$).

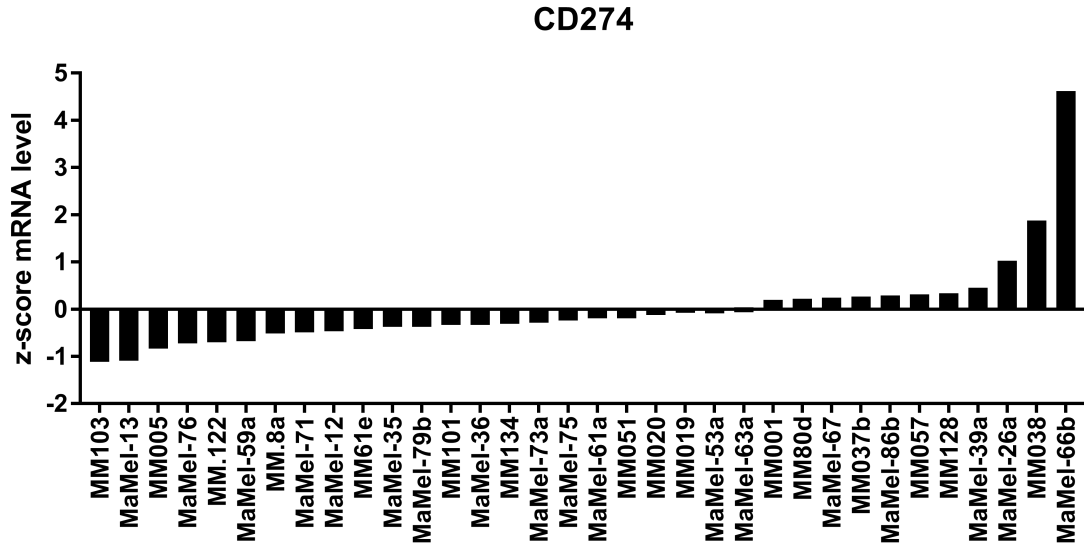


Figure 4.13: Ranked CD274 mRNA expression across the MaMel-panel. Expression data was z-score normalized.

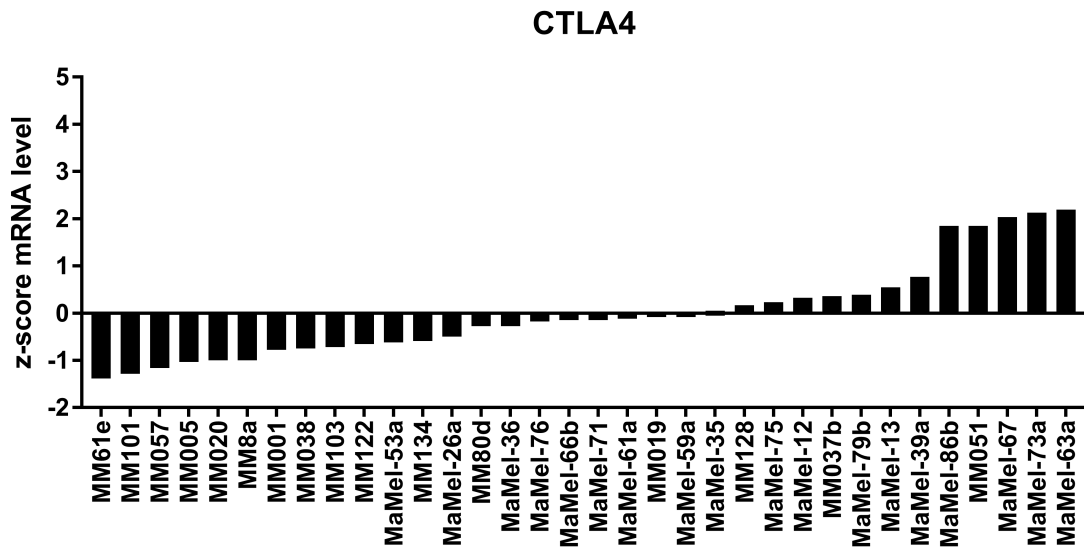


Figure 4.14: Ranked CTLA4 mRNA expression across the MaMel-panel. Expression data was z-score normalized.

To note, the expression of CTLA4 showed a significant negative correlation to the expression of NT5E (PCC = -0.35, p = 0.044) as it is shown in figure 4.15.

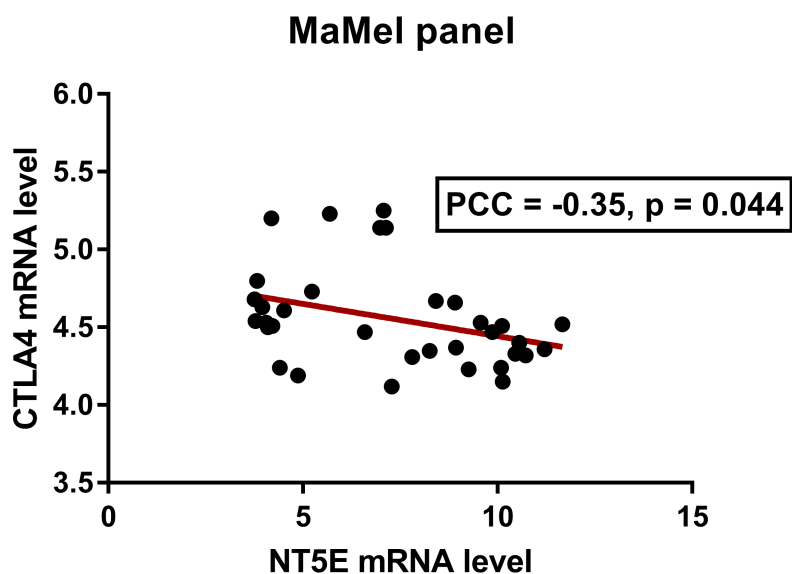


Figure 4.15: Correlation of NT5E and CTLA4 expression across the MaMel panel. Across the analysed melanoma cell lines NT5E was significantly negative correlated with CTLA4 mRNA expression.

4.4. Lipofectamine RNAiMAX reagent achieved best transfection efficacy

To find optimal transfection protocol for the miRNA screen and in general for transfection experiments, different reagents were tested. Using a fluorophore coupled negative control siRNA the transfection efficacy was monitored and also the effect on cell viability was measured by staining with the cell viability dye pacific orange. SK-Mel-28 and MDA-MB-231 cell lines were used for the test. Cells were transfected with siR-Cy3 at different final concentrations: 5, 10, 25 or 50 nM. Lipofectamine RNAiMAX and Dharmafect 1 reagents were tested. Transfection efficacy was measured 48 h post transfection. The results are shown in table 4.7 and 4.8. The Lipofectamine RNAiMAX reagent gave better results for the MDA-MB-231 cell line with almost complete transfection at 10 nM whereas Dharmafect 1 could only transfect less than half of all cells at the same concentration. Due to these advantages and the fact, that the Lipofectamine RNAiMAX protocol was 20 min faster, this reagent was selected for the library screen and subsequent experiments.

Table 4.7: Testing transfection efficacy using Lipofectamine RNAiMAX reagent.

siRNA-Cy3	Transfection efficacy	Dead cells
MDA-MB-231		
mock	0.0 %	0.7 %
5 nM	76.9 %	1.2 %
10 nM	98.9 %	1.0 %
25 nM	100 %	0.8 %
50 nM	100 %	1.2 %

Table 4.8: Testing transfection efficacy using Dharmafect 1 reagent.

siRNA-Cy3	Transfection efficacy	Dead cells
MDA-MB-231		
mock	0.18 %	2.10 %
5 nM	16.10 %	1.91 %
10 nM	41.90%	1.93 %
25 nM	71.40 %	2.53 %
50 nM	89.50 %	2.07 %
SK-Mel-28		
mock	0.42 %	8.24 %
5 nM	86.50 %	7.65 %
10 nM	93.90 %	6.68 %
25 nM	98.50 %	5.16 %
50 nM	96.90 %	6.75 %

4.5. miRNA transfection is also effective at low concentrations

To find a suitable miRNA concentration for the transfection with the human miRNA library, different miRNA concentrations were tested. Therefore, SK-Mel-28 cell line was transfected with NT5E siRNA and with miRNAs known from the bioinformatic analysis to regulate NT5E: miR-22-3p, miR-193a-3p and miR-30b-5p. Also, one miRNA was included, which was not predicted by the *in silico* analysis to regulate NT5E: miR-200c-3p. Two days post transfection the NT5E surface expression was measured. The results are shown in figure 4.16.

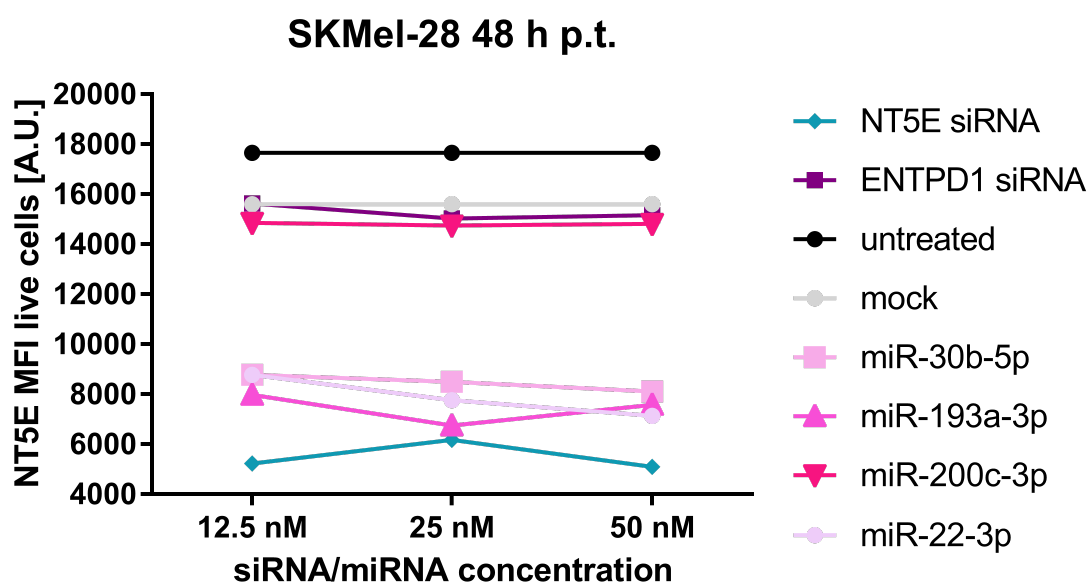


Figure 4.16: Effect of different miRNA concentrations on NT5E surface levels. Three different miRNA/siRNA concentrations were tested. Changes in NT5E surface expression were measured by FACS two days post transfection.

The transfection reagent itself had a modest decreasing effect on NT5E surface levels as it can be seen from the difference of untreated and mock. As expected ENTPD1 siRNA and hsa-miR-200c-3p had no effect on NT5E levels and are similar to mock. NT5E siRNA strongly decreased NT5E levels, also at the lowest concentration of 12.5 nM ($MFI_{NT5E} = 5235$), which was similar to the effect of 50 nM ($MFI_{NT5E} = 5103$). For 25 nM the effect was a little bit weaker, but still NT5E was strongly decreased ($MFI_{NT5E} = 6186$). The down-regulation by miR-30b-5p was quite similar for all three concentrations. For miR-22-3p the effect increased with higher concentrations. But for miR-193a-3p the effect was highest at 25 nM ($MFI_{NT5E} = 6747$). But overall, at all concentrations sufficient effects on NT5E surface levels could be observed. In order to save reagents and avoiding off-target effects, a miRNA/siRNA concentration of 25 nM was chosen for the miRNA library screen.

4.6. Finding optimal time point for miRNA library screen

4.6.1 A half-life of 4 hours was estimated for NT5E mRNA

Treatment with Actinomycin D was used to estimate the half-life of NT5E mRNA and determine the suitable time point for qPCR analysis after miRNA transfection. Therefore, the SK-Mel-28 cells were treated with 10 $\mu\text{g}/\text{mL}$ Actinomycin D. Actinomycin D is an antibiotic that inhibits transcription by blocking the RNA-polymerase thus preventing elongation [71, 26]. After different time points of treatment, cells were harvested and NT5E mRNA levels were determined by qPCR. The results of this assay are shown in figure 4.17. With time, the NT5E mRNA levels was decreasing after Actinomycin D treatment resulting in higher Ct values. From the linear fitted curve a half-life of 4.2 h (250 min) was calculated. For subsequent qPCR analysis after miRNA transfection, time points of 48 h post transfection were used for cell harvest and RNA isolation. This allows the miRNA to enter the cells and due to the estimated half-life, changes in NT5E levels should be measurable.

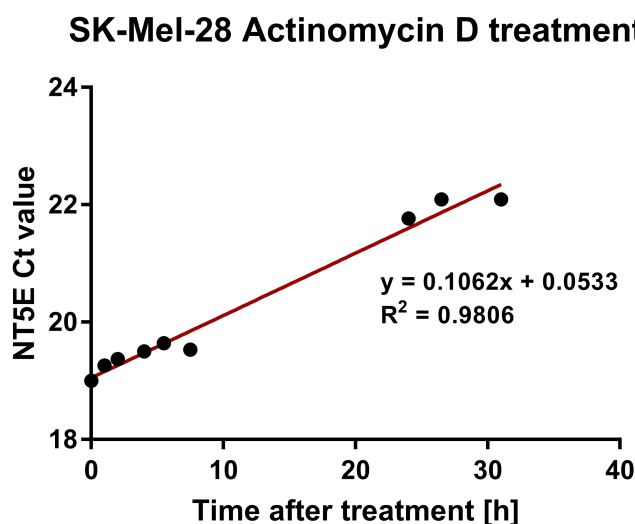


Figure 4.17: Estimation of the NT5E mRNA half-life. SK-Mel-28 cells were treated with 10 $\mu\text{g}/\text{mL}$ Actinomycin D and NT5E mRNA levels were measured by qPCR after different time points of treatment.

4.6.2 A half-life of 14 hours was estimated for NT5E surface levels

To get an impression on the stability of the NT5E protein and its half-life, SK-Mel-28 cells were treated with cycloheximide. Cycloheximide blocks the translation in eukaryotes thereby inhibiting protein synthesis. Adding cycloheximide to the cell culture medium allows the estimation of protein half-life, since no new protein can be produced [211]. SK-Mel-28 cells were treated with 200 μg cycloheximide for 0, 0.5, 1, 1.5, 2, 3, 4 or 24 h. All conditions were measured at the same time and NT5E surface levels were determined by FACS. The median fluorescence intensities (MFIs) were normalized to untreated (0 h) condition. The corresponding plot is shown in figure 4.18. With time, the NT5E surface level was decreasing. From the formula of the linear fit, the half-life of NT5E was calculated. Based on this experiment the half-life of NT5E surface protein was approximately 820 min (~ 14 h).

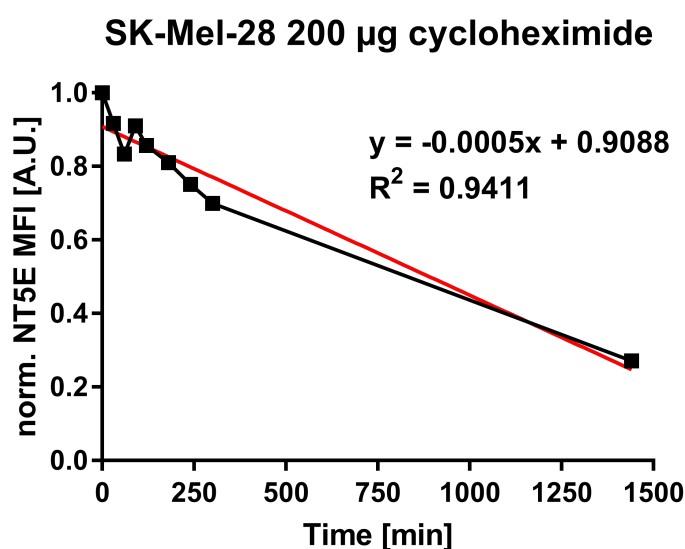


Figure 4.18: Estimating NT5E surface protein half-life. SK-Mel-28 cells were treated with 200 μg cycloheximide and surface NT5E levels were measured by FACS after different time points of treatment.

4.6.3 miRNA transfection mediated strongest changes 72 h post transfection on NT5E surface expression

To choose the optimal time point for measuring changes in NT5E surface expression after transfection with the miRNA library, a time course experiment was carried out. Therefore, SK-Mel-28 cells were transfected with 25 nM miRNA/siRNA and the change of NT5E surface levels was measured by FACS 24 h, 48 h and 72 h post transfection. The result is given in figure 4.19. For all time points the values were normalized to the respective siRNA control sample. For all three time points mock is very similar to siRNA control. The miRNA controls mimic control-1 and mimic control-2 are close to siRNA control and mock values only 24 h and 48 h post transfection. 72 h after transfection mimic control-2 led to increased NT5E level ($\text{norm}_{\text{NT5E}} = 1.3$) while mimic control-1 had a decreasing effect ($\text{norm}_{\text{NT5E}} = 0.8$). The knock-down of NT5E by siRNA was more pronounced over time, from 20 % at 24 h to 80%

knock-down at 72 h. Also the effect of miRNAs was increasing with time and for all three miRNAs the change in NT5E levels was the highest at 72 h post transfection. Thus, for the miRNA library screen the 72 h time point was chosen for analysing the change in NT5E surface levels by FACS after miRNA transfection.

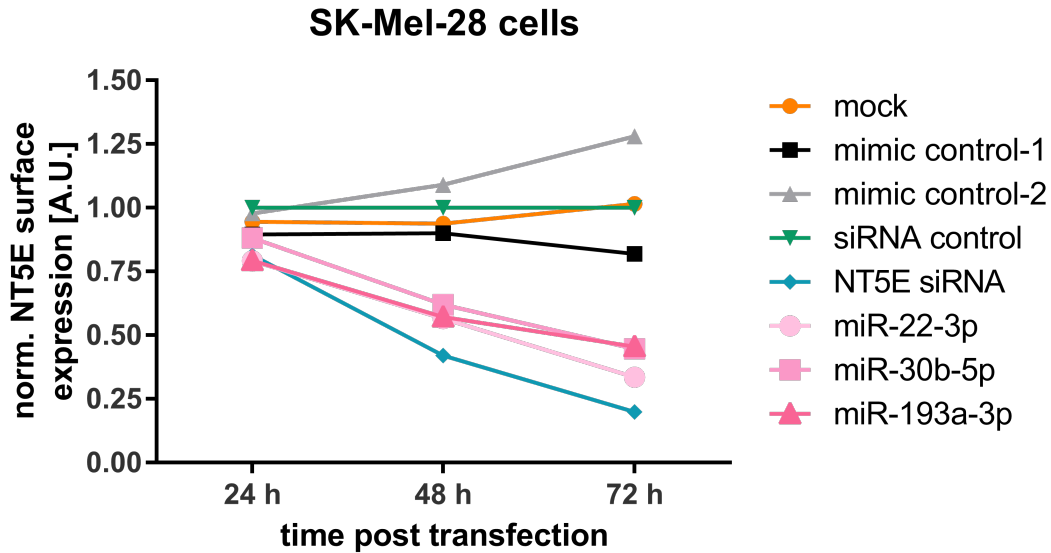


Figure 4.19: Time course of change in NT5E surface levels. SK-Mel-28 cells were transfected with 25 nM miRNA/siRNA and changes in NT5E surface levels were measured by FACS 24, 48 and 72 h post transfection. Values were normalized to siRNA control conditions.

4.7. The immune checkpoint molecules NT5E, ENTPD1 and CD274 were selected for the miRNA library screen

The main focus of this work was the regulation of NT5E/CD73 levels by miRNAs. Therefore, the melanoma cell line SK-Mel-28 and the breast cancer cell line MDA-MB-231 were selected for the miRNA library screen, since both cell lines express NT5E to high extend on their cell surfaces. Since the impact of miRNAs on NT5E expression was planned to be analysed by fluorescence activated cell sorting (FACS), both cell lines were checked for expression of additional molecules known to be involved in tumor cell killing by cytotoxic T cells.

Figure 4.20 shows the mRNA levels of the selected immune evasion genes for SK-Mel-28. Besides NT5E, SK-Mel-28 also expressed ENTPD1. Both enzymes work in a cascade producing adenosine by hydrolyzation of ATP in a multi-step reaction. Adenosine contributes to an immunosuppressive cancer microenvironment and for example blocks effector T cell function. For this reason, both NT5E and ENTPD1 were added to the SK-Mel-28 FACS panel for the miRNA library screen. But none of the adenosine receptors (ADORA1, ADORA2A, ADORA2B and ADORA3) were expressed by this cell line. But SK-Mel-28 exhibited expression of MCAM, MLANA, PMEL and TRYP1, which are all known melanoma antigens, which can be recognised by T cells. Also CTLA4 was expressed by SK-Mel-28. To small extend also TFRC was expressed in this melanoma cell line. IDO1 and CD274 exhibited only low mRNA levels.

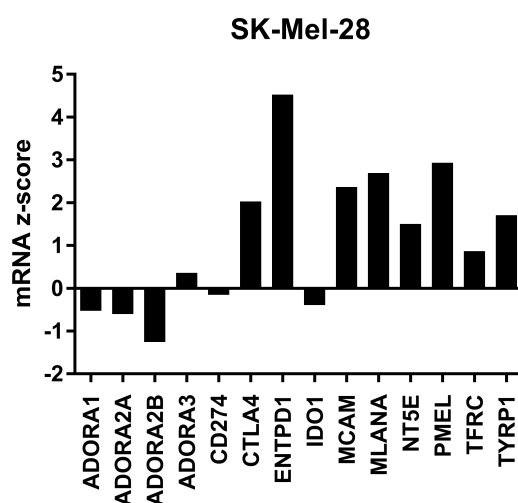


Figure 4.20: Expression of selected genes related to tumor cell killing by cytotoxic T cells in the human melanoma cell line SK-Mel-28. Expression levels were obtained from NCI-60 data.

Figure 4.21 shows the mRNA levels of the selected immune evasion genes for MDA-MB-231. Besides high expression of NT5E, also CD274 was highly expressed in MDA-MB-231. As expected this cell line was negative for the melanoma associated antigens MCAM, MLANA, PMEL and TYRP1. Also CTLA4, ENTPD1, IDO1 and TFRC were not expressed. But one adenosine receptor ADORA2B showed high expression and two additional adenosine receptors were expressed at intermediate level: ADORA2A and ADORA3. Hence, changes in adenosine levels could also have direct effects on MDA-MB-231 cells. Indeed, it was previously shown that adenosine can enhance MDA-MB-231 proliferation via ADORA2B signalling [75]. For the miRNA library screen, CD274 was selected for the FACS panel besides NT5E.

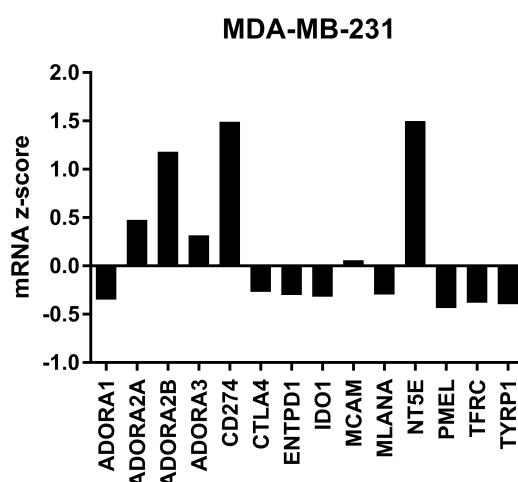


Figure 4.21: Expression of selected genes related to tumor cell killing by cytotoxic T cells in the human breast cancer cell line MDA-MB-231. Expression levels were obtained from NCI-60 data.

4.8. miRNA library screen

To find miRNAs that alter the surface expression of the immune checkpoint molecule NT5E, a miRNA library screen was conducted using FACS as readout. Two cancer cell lines were tested: the human melanoma line SK-Mel-28 and the human breast cancer line MDA-MB-231. The work-flow of the miRNA library screen is illustrated in figure 4.22. Briefly, cells were transfected in 96-well plate format and three days post transfection cells were measured by FACS. For SK-Mel-28, changes in NT5E and ENTPD1 were measured and for MDA-MB-231 changes in NT5E and CD274 were recorded.

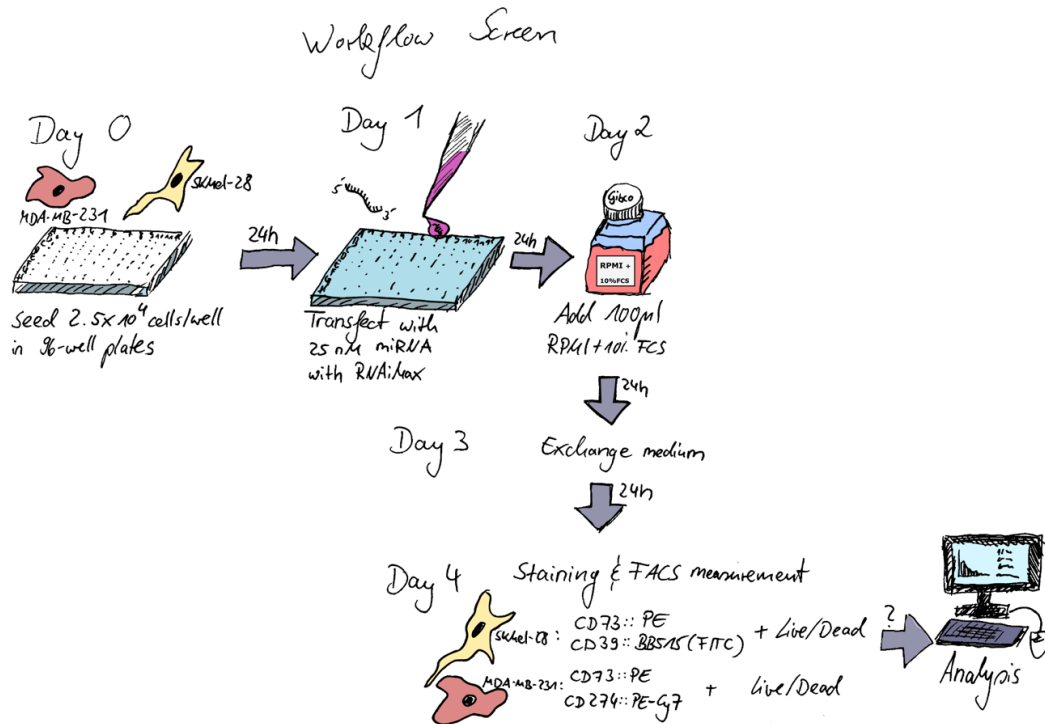


Figure 4.22: Work-flow of miRNA library screen.

In order to compare the data of different screening plates, the median expression values were normalized with z-score normalization method.

4.8.1 Control samples confirmed successful implementation of miRNA library screen

In total, 36 96-well plates were screened for each cell line. On each plate one well was transfected with mimic control-1, mimic control-2 and transfection reagent only (mock), respectively. Furthermore, one each plate two wells were transfected with ENTPD1 siRNA and NT5E siRNA, respectively. The siRNA controls were used to monitor transfection efficacy. In theory, the mimic control-1 and 2 are designed to have no effects in human cell lines.

The effect of the controls on NT5E surface expression levels in SK-Mel-28 is shown in figure 4.23. Mimic control-1 and mock showed no effect on NT5E levels. Mimic control-2 had an increasing effect on NT5E levels, and is therefore not suited as a negative control. ENTPD1

siRNA led to slightly decreased NT5E levels, but overall no significant effect was observed. As expected, NT5E siRNA led to strong and significant decrease in NT5E levels.

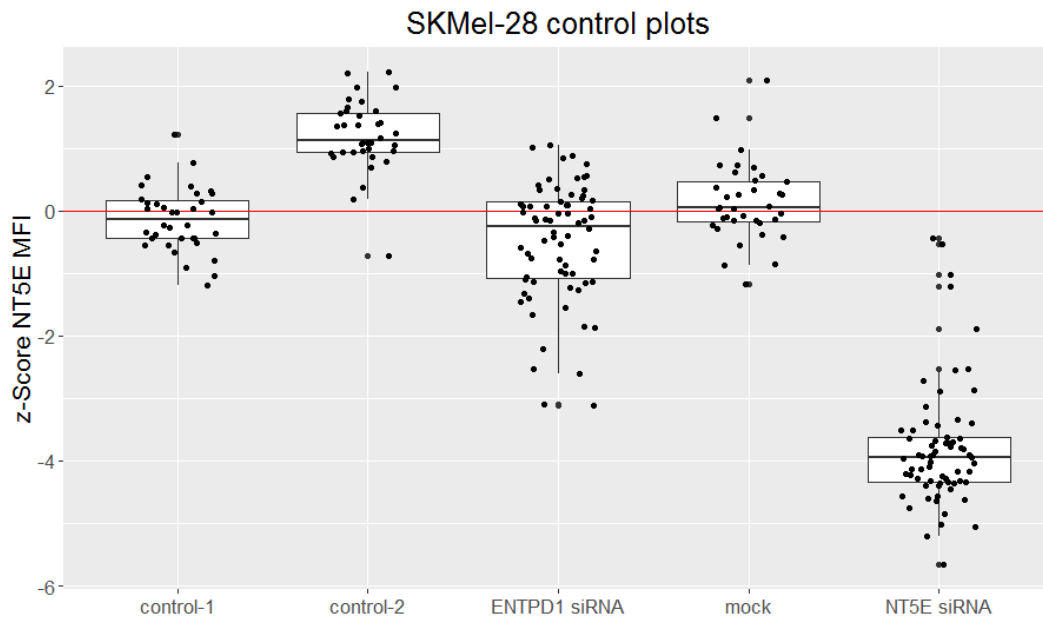


Figure 4.23: SK-Mel-28 NT5E controls. From all screening plates the effect of the control samples on NT5E surface expression was plotted.

The effect of the controls on ENTPD1 surface expression levels in SK-Mel-28 is shown in figure 4.24. All negative controls (mimic control1-1, mimic control-2 and mock) had no effect on ENTPD1 levels. ENTPD1 siRNA led to significantly decreased ENTPD1 levels with only few exceptions. NT5E siRNA had a minor decreasing effect on ENTPD1 levels.

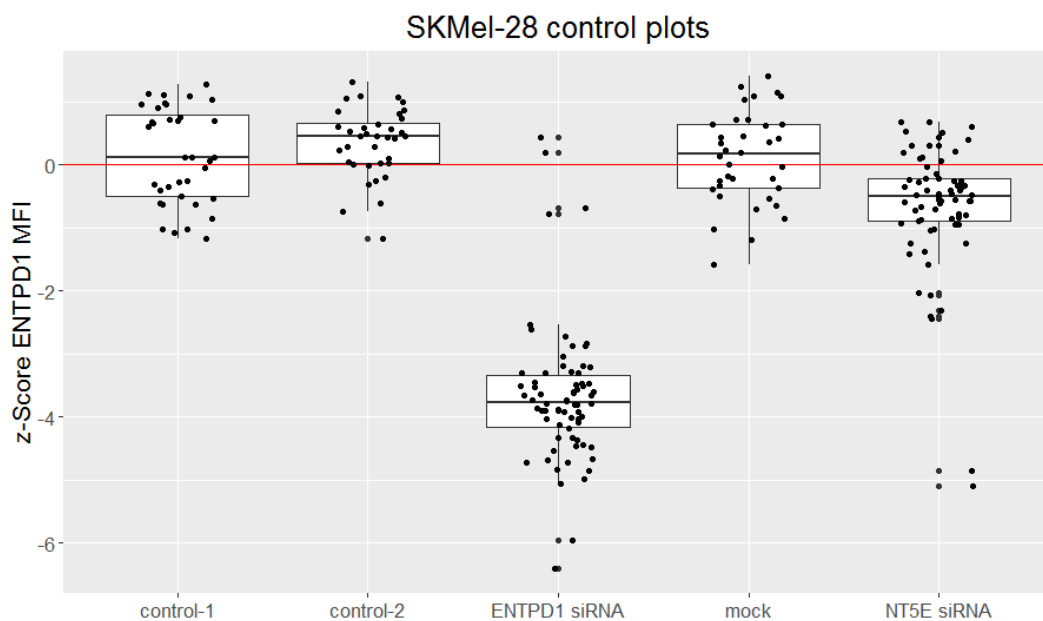


Figure 4.24: SK-Mel-28 ENTPD1 controls. From all screening plates the effect of the control samples on ENTPD1 surface expression was plotted.

The effect of the control in MDA-MB-231 cell line is shown in figure 4.25 for NT5E and in figure 4.26 for CD274. The negative controls mimic control-1 and mock had no effect on NT5E levels. Mimic control-2 showed again an increasing effect similar as observed in SK-Mel-28. ENTPD1 siRNA led to no significant change in NT5E levels. Only NT5E siRNA led to strong decrease of NT5E surface expression with few exceptions.

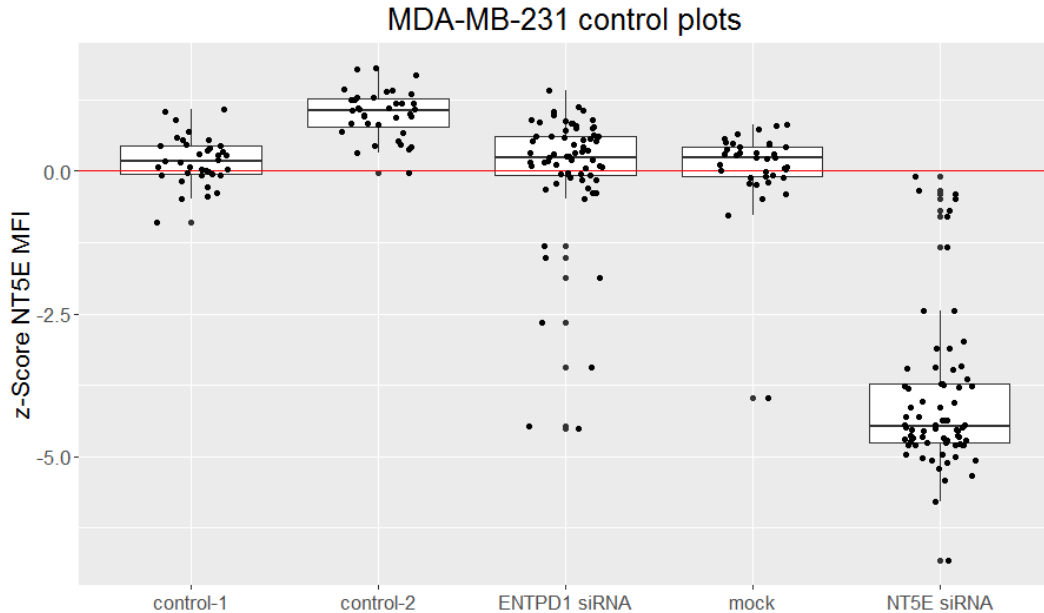


Figure 4.25: MDA-MB-231 NT5E controls. From all screening plates the effect of the control samples on NT5E surface expression was plotted.

None of the controls had a significant effect on CD274 surface levels in MDA-MB-231 cells.

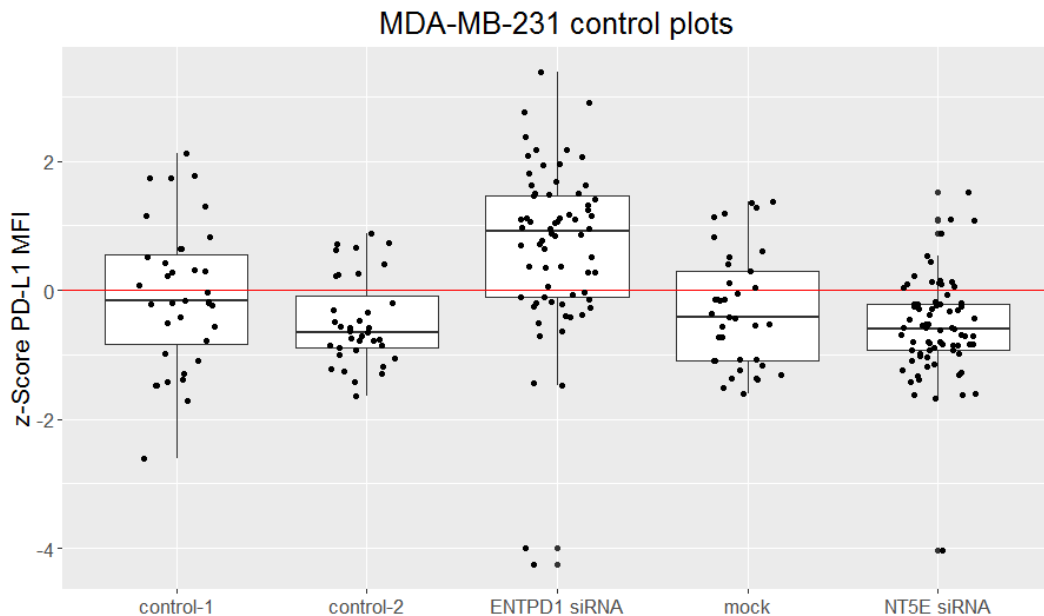


Figure 4.26: MDA-MB-231 CD274 controls. From all screening plates the effect of the control samples on CD274 surface expression was plotted.

4.8.2 Several miRNAs impacting NT5E surface expression were newly-discovered

After evaluating the control samples, the effect of miRNAs on NT5E surface expression was analysed. Therefore, miRNA mediated changes in NT5E MFI values were ranked based on their z-score for the two screened cell lines, respectively. In table 4.9 19 miRNAs are listed that had a strong increasing effect (z-score > 2) on NT5E surface level in SK-Mel-28 cells. miR-134-3p led to the highest NT5E level (z-score = 4.75) followed by miR-8485 (z-score = 3.16). Also miR-34b-5p led to strong increase of NT5E (z-score = 2.01). Interestingly, this miRNA had three predicted binding sites for NT5E.

Table 4.9: miRNAs up-regulating NT5E in SK-Mel-28.

miRNA	z-score	plate	target sites
hsa-miR-134-3p	4.75	plate25	0
hsa-miR-8485	3.16	plate36	2
hsa-miR-7854-3p	3.04	plate35	1
hsa-miR-6514-3p	2.93	plate29	0
hsa-miR-6132	2.82	plate29	0
hsa-miR-3152-5p	2.52	plate20	0
hsa-miR-146b-3p	2.52	plate3	0
hsa-miR-6736-3p	2.47	plate30	0
hsa-miR-3605-5p	2.23	plate16	1
hsa-miR-5697	2.13	plate28	1
hsa-miR-593-5p	2.13	plate11	0
hsa-miR-34b-5p	2.10	plate7	3
hsa-miR-548au-3p	2.10	plate27	0
hsa-miR-6818-5p	2.08	plate32	1
hsa-miR-4692	2.05	plate22	1
hsa-miR-555	2.04	plate10	0
hsa-miR-516b-5p	2.02	plate9	1
hsa-miR-520a-5p	2.02	plate9	0
hsa-miR-34b-3p	2.01	plate7	0

Compared to up-regulating miRNAs, more miRNAs had a strong decreasing effect (z-score < -2) on NT5E surface levels in SK-Mel-28. Those 26 miRNAs are listed in table 4.10. Also miRNA 27 and 28 were included in the table, since miR-193a-3p was extensively analysed in further experiments. miR-6787-3p led to the lowest NT5E levels (z-score = -3.03) followed by miR-22-3p (z-score = -2.80). miR-22-3p had one predicted binding site for NT5E. Also miR-193a-3p (z-score = -1.91) led to significantly reduced NT5E levels and had also one binding site for NT5E 3'-UTR. Eight out of 19 miRNAs up-regulating NT5E in SK-Mel-28 harboured at least one binding site for NT5E. miRNAs down-regulating NT5E levels contained more often a binding site with 20 miRNAs out of 28 (p = 0.0695, two-sided Fishers exact test). Waterfall plots for all miRNAs, that had an significant effect on NT5E surface expression in SK-Mel-28 are shown in figure 4.27 and 4.28.

Table 4.10: miRNAs down-regulating NT5E in SK-Mel-28.

miRNA	z-score	plate	target sites
hsa-miR-6787-3p	-3.03	plate31	0
hsa-miR-22-3p	-2.80	plate5	1
hsa-miR-92b-3p	-2.57	plate12	1
hsa-miR-1285-5p	-2.45	plate25	2
hsa-miR-6795-3p	-2.41	plate31	0
hsa-miR-1233-3p	-2.39	plate1	0
hsa-miR-6888-3p	-2.37	plate34	2
hsa-miR-921	-2.34	plate12	0
hsa-miR-4647	-2.28	plate21	1
hsa-miR-6876-3p	-2.27	plate33	3
hsa-miR-5584-3p	-2.23	plate28	2
hsa-miR-4714-5p	-2.21	plate22	1
hsa-miR-3134	-2.20	plate14	2
hsa-miR-6780a-3p	-2.17	plate31	0
hsa-miR-6759-3p	-2.14	plate30	0
hsa-miR-373-3p	-2.14	plate7	1
hsa-miR-3176	-2.12	plate14	2
hsa-miR-6820-3p	-2.10	plate32	4
hsa-miR-3942-3p	-2.09	plate21	1
hsa-miR-548t-3p	-2.08	plate18	1
hsa-miR-199a-5p	-2.08	plate5	0
hsa-miR-3118	-2.04	plate13	2
hsa-miR-578	-2.03	plate10	1
hsa-miR-885-5p	-2.02	plate12	1
hsa-miR-124-3p	-2.02	plate2	3
hsa-miR-664b-3p	-2.00	plate29	4
hsa-miR-34a-3p	-1.92	plate7	0
hsa-miR-193a-3p	-1.91	plate4	1

miRNAs that had a strong increasing effect on NT5E levels for MDA-MB-231 cells are listed in table 4.11. In total, 29 miRNAs had an increasing effect with z-score > 2 . miR-196a-3p had the strongest up-regulating effect on NT5E (z-score = 3.49). Also miR-134-3p had an increasing effect on NT5E levels (z-score = 1.99) in concordance with the effect in SK-Mel-28 cell line.

SK-Mel-28
upregulating miRNAs

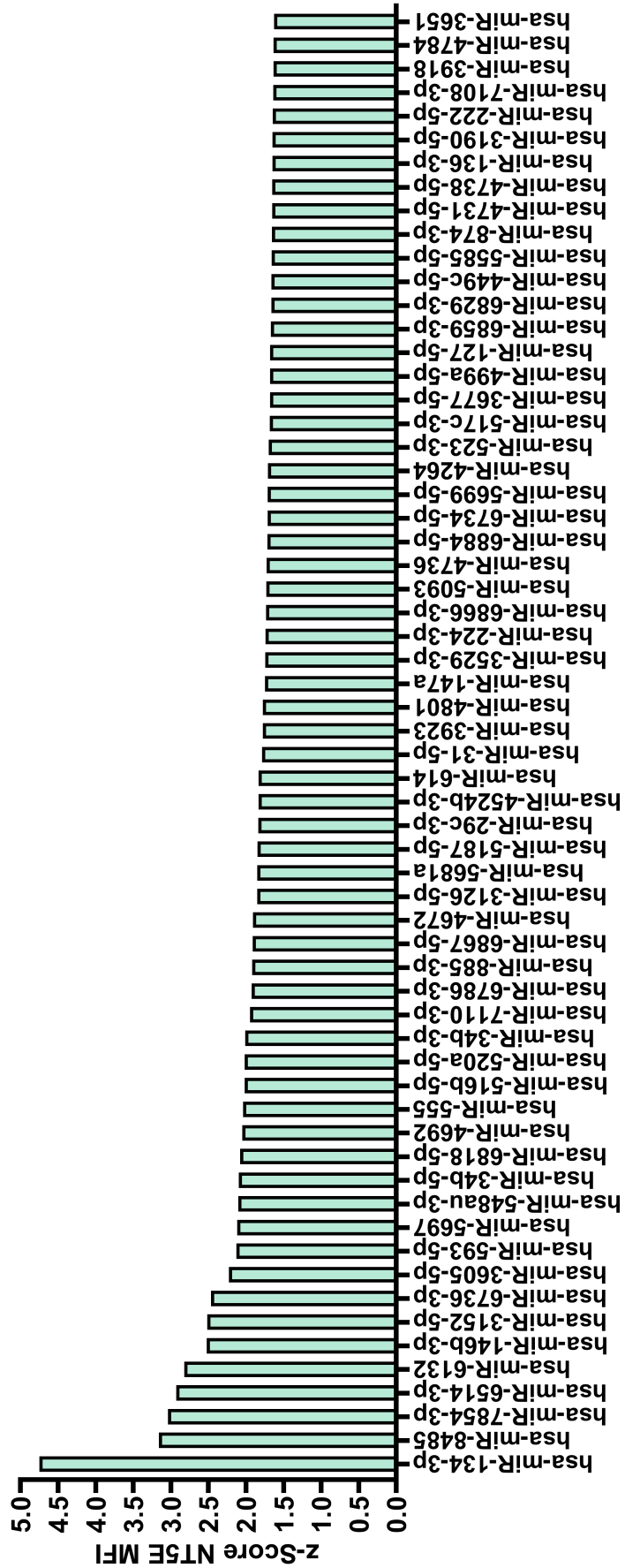


Figure 4.27: Waterfall plot of NT5E enhancing miRNAs in SK-Mel-28 cells.

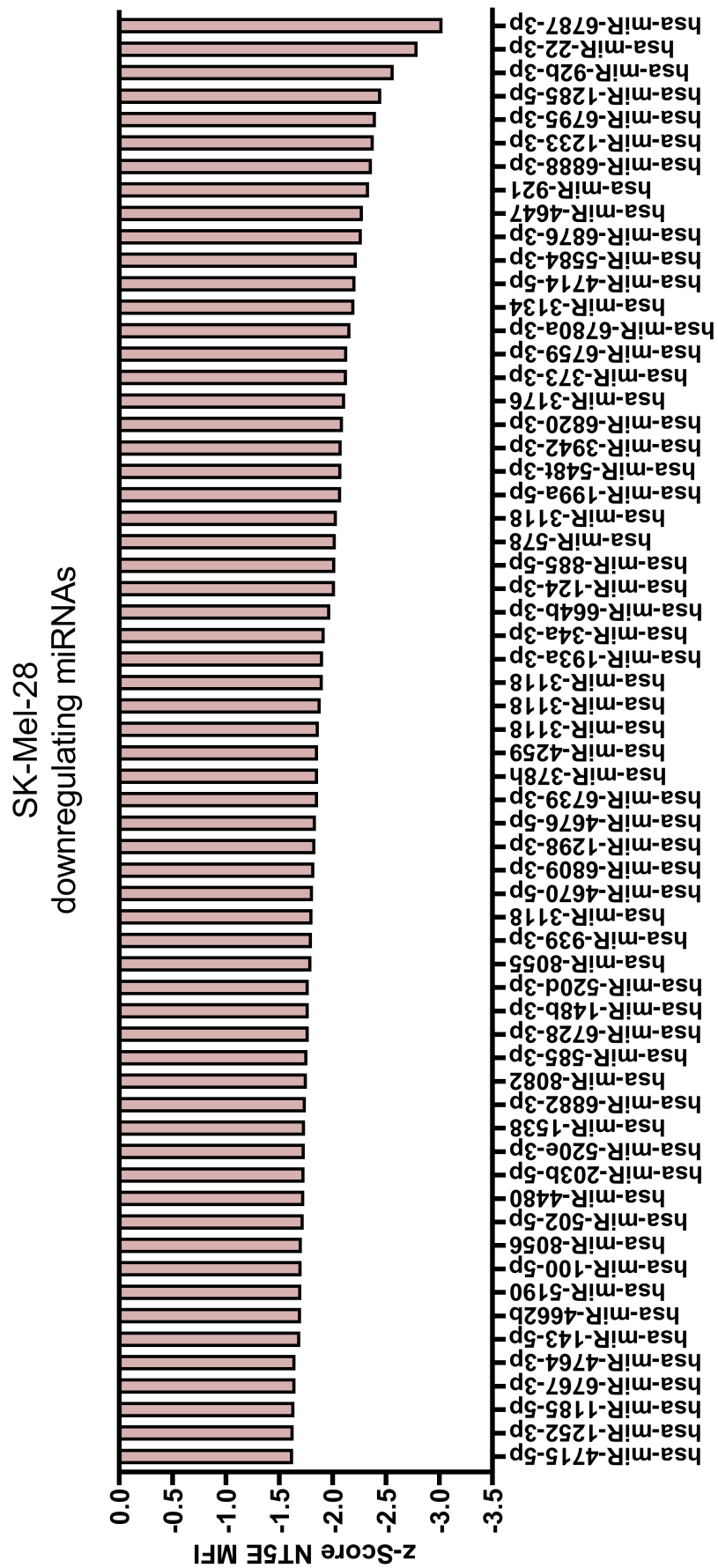


Figure 4.28: Waterfall plot of miRNAs significantly decreasing NT5E surface levels in SK-Mel-28 cells.

Table 4.11: miRNAs up-regulating NT5E in MDA-MB-231.

miRNA	z-score	plate	target sites
hsa-miR-196a-3p	3.49	plate5	0
hsa-miR-5589-3p	2.93	plate28	1
hsa-miR-181d-3p	2.70	plate25	0
hsa-miR-3189-3p	2.70	plate15	0
hsa-miR-4673	2.63	plate22	0
hsa-miR-6514-3p	2.63	plate29	0
hsa-miR-191-5p	2.57	plate4	0
hsa-miR-6859-3p	2.50	plate33	0
hsa-miR-3116	2.50	plate13	0
hsa-miR-5689	2.48	plate28	0
hsa-miR-608	2.44	plate11	0
hsa-miR-1249-5p	2.38	plate36	0
hsa-miR-6819-5p	2.34	plate32	0
hsa-miR-4664-5p	2.34	plate21	0
hsa-miR-4514	2.31	plate20	1
hsa-miR-8073	2.27	plate35	0
hsa-miR-4672	2.26	plate22	1
hsa-miR-4732-5p	2.23	plate23	0
hsa-miR-593-5p	2.21	plate11	0
hsa-miR-92a-1-5p	2.17	plate12	0
hsa-miR-5589-5p	2.17	plate28	0
hsa-miR-6804-3p	2.15	plate32	0
hsa-miR-16-5p	2.10	plate4	0
hsa-miR-3126-5p	2.07	plate14	1
hsa-miR-3616-3p	2.05	plate16	0
hsa-miR-3918	2.05	plate18	0
hsa-miR-4688	2.03	plate22	0
hsa-miR-6515-5p	2.02	plate29	1
hsa-miR-1199-3p	2.02	plate25	0
hsa-miR-134-3p	1.99	plate25	0

In contrast to SK-Mel-28, less miRNAs showed a down-regulating effect on NT5E levels in MDA-MB-231 cells. 20 miRNAs had a strong decreasing effect and are listed in table 4.12. miR-512-3p caused the lowest NT5E levels (z-score = -4.99) and exhibits one binding site for NT5E 3'-UTR. Similar to the SK-Mel-28 cell line, miR-193a-3p also decreased NT5E levels in MDA-MB-231 cells (z-score = -2.48).

Five out of 30 miRNAs up-regulating NT5E in MDA-MB-231 cells exhibited at least one binding site for NT5E. miRNAs down-regulating NT5E levels harboured significantly more often a binding site with 11 miRNAs out of 20 ($p = 0.0063$, two-sided Fishers exact test). This observation was similar to SK-Mel-28 cells. Waterfall plots for all miRNAs, that had an significant effect on NT5E surface expression in MDA-MB-231 cells are shown in figure 4.30 for the NT5E enhancing miRNAs and in figure 4.31 for the NT5E inhibiting miRNAs.

Having analysed the NT5E affecting miRNAs separately for each cell line, it was searched

Table 4.12: miRNAs down-regulating NT5E in MDA-MB-231.

miRNA	z-score	plate	target sites
hsa-miR-512-3p	-4.99	plate8	1
hsa-miR-1225-3p	-4.08	plate1	0
hsa-miR-1233-3p	-4.07	plate1	0
hsa-miR-1206	-4.06	plate1	0
hsa-miR-2467-3p	-2.57	plate24	4
hsa-miR-455-5p	-2.54	plate8	0
hsa-miR-193a-3p	-2.48	plate4	1
hsa-miR-376c-5p	-2.47	plate26	1
hsa-miR-659-3p	-2.38	plate12	0
hsa-miR-203b-3p	-2.29	plate22	0
hsa-miR-376b-5p	-2.28	plate26	1
hsa-miR-550b-2-5p	-2.23	plate27	0
hsa-miR-3134	-2.27	plate14	2
hsa-miR-5190	-2.27	plate27	1
hsa-miR-1285-5p	-2.27	plate25	2
hsa-miR-4480	-2.20	plate19	1
hsa-miR-4703-5p	-2.14	plate22	0
hsa-miR-143-5p	-2.09	plate3	1
hsa-miR-519a-3p	-2.02	plate9	1
hsa-miR-181-2-3p	-2.01	plate36	0

for miRNAs, that had an significant effect on both SK-Mel-28 and MDA-MB-231 cells. The overlap of miRNAs affecting NT5E surface levels in both cell lines is illustrated in figure 4.29. For this figure all miRNAs with a significant effect on NT5E levels were considered (z-score < -1.645 or > 1.645). The following nine miRNAs led to increased NT5E levels in both cell lines:

miR-134-3p, miR-6514-3p, miR-593-5p, miR-4692, miR-4672, miR-3126-5p, miR-224-3p, miR-6859-3p and miR-127-5p.

The following 15 miRNAs led to decreased NT5E levels in both cell lines:

miR-193a-3p, miR-22-3p, miR-143-5p, miR-5190, miR-8056, miR-4480, miR-520d-3p, miR-148b-3p, miR-1298-3p, miR-3118, miR-1285-5p, miR-4676-5p, miR-3134, miR-5584-3p and miR-1233-3p.

Only one miRNA had a contrary effect on NT5E surface levels in both lines: miR-3190-5p. In SK-Mel-28, miR-3190-5p led to enhanced NT5E levels, whereas in MDA-MB-231 cells NT5E expression was decreased. miR-3190-5p had two binding sites for the 3'-UTR of NT5E, which could explain the reduced expression levels in MDA-MB-231 cells. This miRNA also contained two bindings site for the transcriptional repressor ZNF814, one binding site for the transcription factor SOX9 and one binding site for two receptors binding and transmitting TGF β 1 signal (TGFBR1 and TGFBR3), which might explain the increasing effect of miR-3190-5p.

NT5E

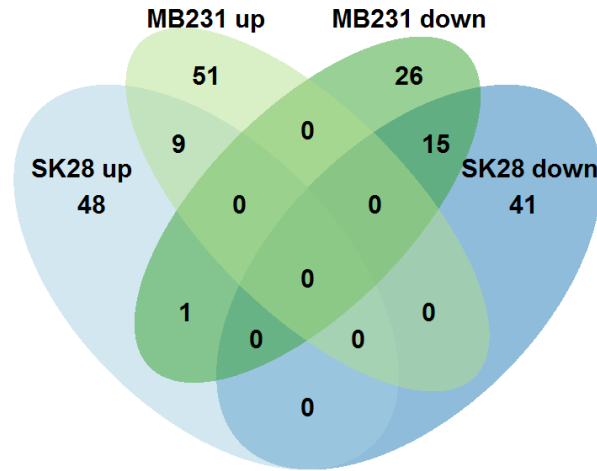


Figure 4.29: Venn diagram of miRNAs affecting NT5E surface expression. Overlap of miRNAs with significant effect on NT5E surface levels for two screened cell lines SK-Mel-28 (SK28) and MDA-MB-231 (MB231).

Common targets of miRNAs that impacted NT5E surface expression

For the 15 miRNAs that caused decrease of NT5E surface levels in both cell lines, target prediction was performed. The list of shared targets is shown in table 4.13. Six of this ten miRNAs exhibit a binding site for NT5E 3'-UTR. But nine miRNAs did not exhibit a binding site. Thus, the observed down-regulation of NT5E levels during the screen was not only caused by direct interactions of miRNA with the 3'-UTR of NT5E, but also through indirect effects e.g. by targeting a positive regulator of NT5E. Table 4.13 lists the target genes with the highest number of miRNAs having a binding site for this particular gene (Hits). A short description of the gene function is given. For each gene it was also tested whether the expression is beneficial for patient survival in breast cancer using Kaplan Meier Plotter (KM breast cancer) [90]. Three genes were targeted by ten out of the fifteen miRNAs: Cyclin Dependent Kinase 14 (CDK14), Cell Adhesion Molecule 2 (CADM2) and EPH Receptor A4 (EPHA4). 25 genes exhibited binding sites for nine out of the fifteen miRNAs. The assumption was, that miRNAs target a positive regulator of NT5E, thereby leading to lower NT5E levels. Thus, especially transcription factors and proteins involved in signalling cascades were of particular interest like PHD Finger Protein 6 (PHF6), Grainyhead Like Transcription Factor 2 (GRHL2) or CDK14. Furthermore, it was assumed, that a high expression of a positive NT5E regulator would also be worse for patient survival in breast cancer. Thus, target genes with low expression beneficial were also of particular interest like WEE1 G2 Checkpoint Kinase (WEE1) or the transcriptional regulators PHF6 and GRHL2. PHF6 was found to be over-expressed in many cancer types e.g. in breast cancer and colorectal cancer [92]. Also high expression of GRHL2 was found in different cancer types and its expression could be used as a biomarker for breast cancer metastasis [264]. For further analysis CDK14, PHF6 and GRHL2 might be the most interesting candidates.

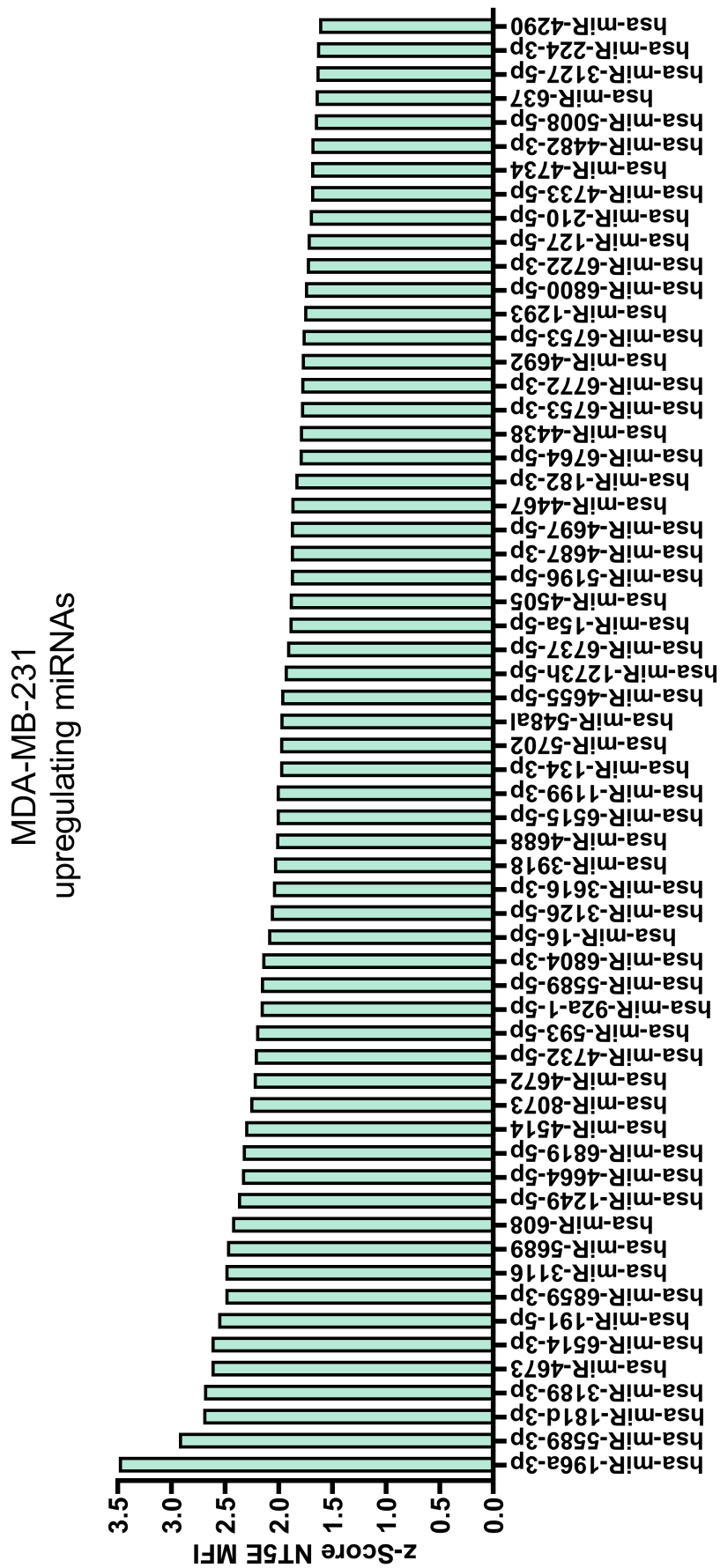


Figure 4.30: Waterfall plot of miRNAs significantly increasing NT5E surface levels in MDA-MB-231 cells.

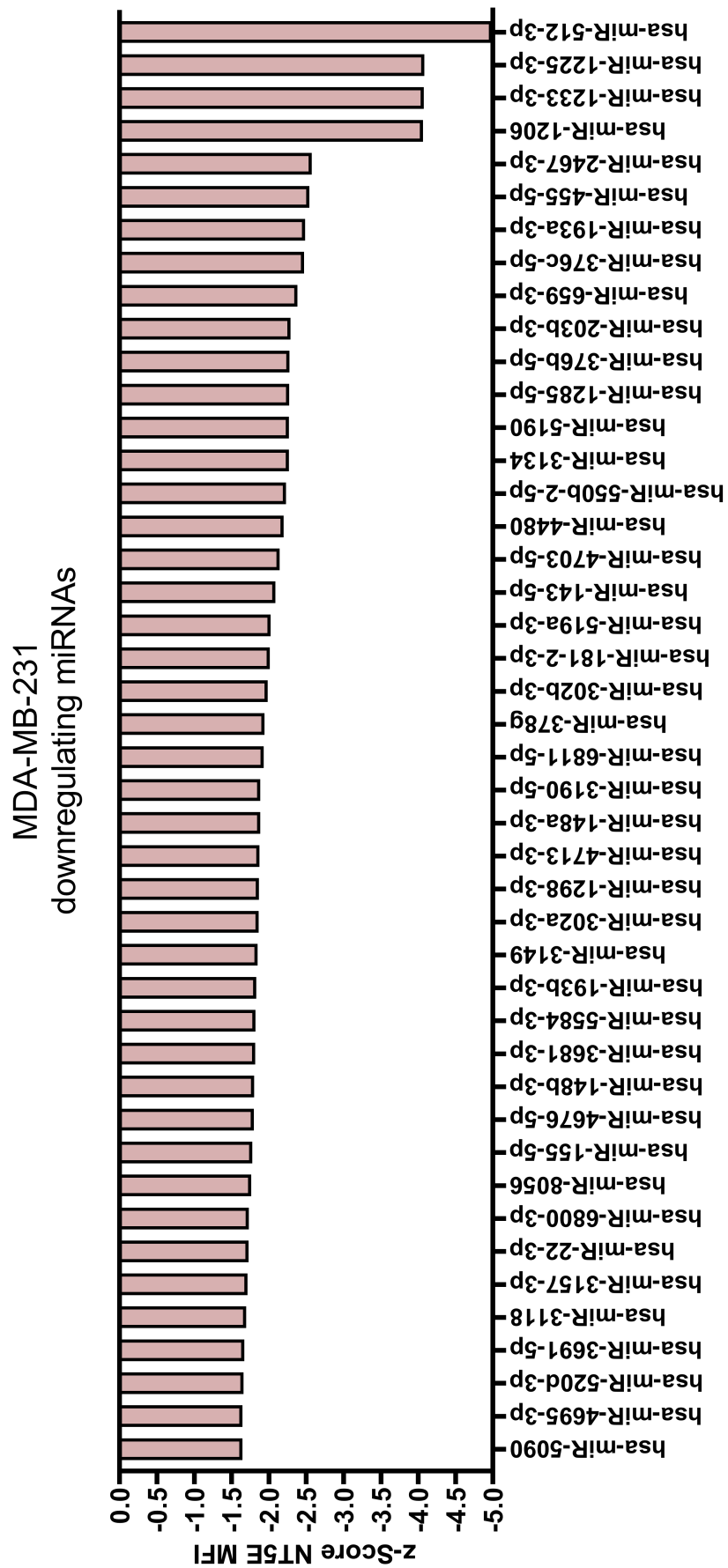


Figure 4.31: Waterfall plot of NT5E decreasing miRNAs in MDA-MB-231 cells.

Table 4.13: Shared targets of miRNAs down-regulating NT5E in MDA-MB-231 as well as SK-Mel-28 cells. For each gene it was tested whether its expression is beneficial for patient survival in breast cancer using Kaplan Meier Plotter tool (KM breast cancer).

Gene	Hits	gene function	KM breast cancer
CDK14	10	PFTK1: regulator of cell proliferation	high expression beneficial
CADM2	10	adhesion molecule	high expression beneficial
EPHA4	10	receptor tyrosine kinase	no effect
PAFAH1B2	9	inactivates PAF	high expression beneficial
CXCL12	9	chemoattractant	high expression beneficial
KCNMA1	9	potassium channel	high expression beneficial
NUP205	9	NPC assembly	low expression beneficial
WEE1	9	negative regulator of mitosis	low expression beneficial
NTRK2	9	receptor tyrosine kinase	high expression beneficial
UNC5D	9	neuronal cell survival	no effect
HAS3	9	hyaluronan synthase	no effect
PHF20L1	9	—	no effect
PCDH9	9	calcium-dependent cell-adhesion protein	high expression beneficial
SLC30A4	9	zinc transport	no effect
BMPR2	9	MP receptor	no effect
PDK1	9	pyruvate dehydrogenase kinase	no effect
MAP3K1	9	serine/threonine kinase	high expression beneficial
CHIC1	9	—	high expression beneficial
STK4	9	pro-apoptotic kinase	high expression beneficial
FAM168B	9	negative regulator of CDC42 and STAT3; positive regulator of STMN2	no effect
GRHL2	9	transcription factor	low expression beneficial
KCTD21	9	inhibits cell growth	high expression beneficial
PHF6	9	transcriptional regulator	low expression beneficial
SVOP	9	—	high expression beneficial
SBF2	9	GEF	high expression beneficial
GPD1L	9	regulates cardiac sodium	high expression beneficial
LNX2	9	—	no effect
RPP30	9	component of ribonuclease P	high expression beneficial

Also for the nine miRNAs, that up-regulated NT5E in both cell lines during the screen, target prediction was performed. The list of targets shared by at least six out of the nine miRNAs is shown in table 4.14. Only one gene was targeted by seven miRNAs. 13 genes were targeted by six miRNAs. Of particular interest was the transcriptional repressor Forkhead Box P2 (FOXP2). Blocking of FOXP2 by binding of miRNAs could explain the observed increase of NT5E levels. Interestingly, high expression of FOXP2 was beneficial for patient survival in breast cancer. It was reported, that FOXP2 has a binding site for NT5E promoter [193]. Thus, FOXP2 was selected for further analysis.

Table 4.14: Shared targets of miRNAs up-regulating NT5E in MDA-MB-231 as well as SK-Mel-28 cells.

Gene	Hits	gene function	KM breast cancer
SLC26A7	7	gastric acid secretion	no effect
SYPL2	6	communication between the T-tubular and junctional sarcoplasmic reticulum (SR) membranes	high expression beneficial
DAGLA	6	diacylglycerol lipase	high expression beneficial
PDGFRB	6	tyrosine-protein kinase	high expression beneficial
ANO6	6	small-conductance calcium-activated non-selective cation (SCAN) channel	high expression beneficial
PEAK1	6	non-receptor tyrosine kinase	high expression beneficial
BBX	6	transcription factor	no effect
DLG2	6	membrane-associated guanylate kinase	high expression beneficial
MBNL1	6	pre-mRNA alternative splicing regulation	no effect
FOXP2	6	transcriptional repressor	high expression beneficial
AGFG1	6	mediate nucleocytoplasmic transport	no effect
LMO7	6	protein-protein interactions	high expression beneficial
SLC41A1	6	magnesium transporter	no effect
WASF3	6	transduce signals that involve changes in cell shape, motility or function	no effect

For the shared targets, that were at least predicted to be regulated by four of the NT5E enhancing miRNAs, GeneSet enrichment analysis (GSEA) was performed using MSigDB. The focus was set on finding common transcription factors for these target genes. The results for the top ten enriched motifs with a known associated transcription factor are listed in table 4.15.

Table 4.15: GSEA analysis of target genes from NT5E enhancing miRNAs. Also the number of miRNAs with a binding site is given from the nine selected NT5E enhancing miRNAs for validation.

Gene Set Name	Gene in overlap	p value	FDR q value	No miR BS
TGAAAA-NFAT-Q4-01	115	7.46E-25	3.57E-22	4
TGACAGNY-MEIS1-01	62	7.84E-18	1.87E-15	5
GCM2-TARGET-GENES	102	9.30E-18	1.87E-15	3
ZNF618-TARGET-GENES	84	9.77E-18	1.87E-15	9
SALL4-TARGET-GENES	94	2.44E-16	3.64E-14	1
CTTTGA-LEF1-Q2	74	3.76E-16	4.50E-14	3
RTAAACA-FREAC2-01	62	8.18E-16	8.71E-14	0
YTATTTNR-MEF2-02	53	1.07E-15	9.29E-14	7
CATTGTYT-SOX9-B1	37	2.27E-15	1.72E-13	6

4.8.3 Several miRNAs impacting ENTPD1 surface expression were newly-discovered

The effect of miRNAs on ENTPD1 expression was only tested in SK-Mel-28 cells, because for MDA-MB-231 cell line no ENTPD1 expression could be detected. miRNAs that caused an strong up-regulation (z-score > 2) of ENTPD1 surface levels on SK-Mel-28 cells are listed in table 4.16. In total, 25 miRNAs showed a strong enhancement of ENTPD1. miR-6733-3p exhibited the strongest increase of ENTPD1 levels (z-score = 3.49), followed by miR-34b-3p (z-score = 3.33).

Table 4.16: miRNAs up-regulating ENTPD1 in SK-Mel-28.

miRNA	z-score	plate	target sites
hsa-miR-6733-3p	3.49	plate30	1
hsa-miR-34b-3p	3.33	plate7	0
hsa-miR-208a-3p	3.13	plate5	0
hsa-miR-499a-5p	2.93	plate8	1
hsa-miR-6778-3p	2.78	plate31	0
hsa-miR-1250-3p	2.71	plate25	0
hsa-miR-6834-3p	2.59	plate32	0
hsa-miR-1269b	2.46	plate20	0
hsa-miR-887-5p	2.41	plate35	0
hsa-miR-1273e	2.37	plate17	0
hsa-miR-30b-5p	2.29	plate6	0
hsa-miR-1295b-5p	2.26	plate25	0
hsa-miR-7978	2.21	plate35	0
hsa-miR-1273h-3p	2.20	plate25	0
hsa-miR-6826-3p	2.18	plate32	0
hsa-miR-203a-3p	2.18	plate5	0
hsa-miR-6514-3p	2.14	plate29	0
hsa-miR-1252-3p	2.13	plate25	0
hsa-miR-193b-3p	2.10	plate4	1
hsa-miR-299-3p	2.09	plate6	0
hsa-miR-491-3p	2.03	plate8	0
hsa-miR-1273-3p	2.03	plate25	NA
hsa-miR-605-3p	2.02	plate28	0
hsa-miR-5589-3p	2.00	plate28	0
hsa-miR-8068	2.00	plate25	0

miRNAs that strongly decreased (z-score < -2) ENTPD1 levels in SK-Mel-28 cells are listed in table 4.17. From this 14 miRNAs, miR-6730-5p led to the lowest ENTPD1 levels (z-score = -3.26), followed by miR-5681a (z-score = -3.22) and miR-585-3p (z-score = -2.85).

Table 4.17: miRNAs down-regulating ENTPD1 in SK-Mel-28.

miRNA	z-score	plate	target sites
hsa-miR-6730-5p	-3.26	plate30	1
hsa-miR-5681a	-3.22	plate28	2
hsa-miR-585-3p	-2.85	plate11	0
hsa-miR-575	-2.69	plate10	1
hsa-miR-203a-5p	-2.61	plate36	0
hsa-miR-181-2-3p	-2.59	plate36	0
hsa-miR-6717-5p	-2.35	plate29	0
hsa-miR-221-3p	-2.21	plate5	0
hsa-miR-6787-3p	-2.20	plate31	0
hsa-miR-921	-2.17	plate12	0
hsa-miR-1538	-2.07	plate4	0
hsa-miR-516b-3p	-2.06	plate9	1
hsa-miR-124-3p	-2.05	plate2	0
hsa-miR-4645-3p	-2.05	plate21	1

4.8.4 Several miRNAs affecting CD274 surface expression were newly-discovered

The effect of miRNAs on CD274 surface expression was only tested in MDA-MB-231 cells, since SK-Mel-28 did not express CD274. miRNAs that caused an strong increase of CD274 surface levels (z-score > 2) are listed in table 4.18 and 4.19. Overall, 75 miRNAs had a strong effect on CD274 levels. miR-3928-5p led to the highest CD274 surface expression (z-score = 5.07), followed by miR-5701 (z-score = 4.48), miR-6513-3p (z-score = 4.22) and miR-5589-5p (z-score = 4.21).

In total, 48 miRNAs led to a strong decrease (z-score < -2) of CD274 surface levels in MDA-MB-231 cells. These miRNAs are listed in table 4.20 and 4.21. miR-1233-3p caused the lowest CD274 surface levels (z-score = -4.69), closely followed by miR-1225-3p (z-score = -4.69) and miR-1206 (z-score = -4.69). miR-1233-3p and miR-1225-3p also exhibited two binding sites for CD274.

35 out of 75 miRNAs that strongly enhanced CD274 surface levels, harboured at least one binding site for CD274. miRNAs strongly decreasing CD274 surface levels exhibited significantly more often at least one binding site for the 3'-UTR of CD274 ($p = 0.0125$, two-sided Fishers exact test). More than 80 % of the inhibiting miRNAs, 40, had at least one binding site.

Table 4.18: miRNAs up-regulating CD274 in MDA-MB-231 part I.

miRNA	z-score	plate	target sites
hsa-miR-3928-5p	5.07	plate26	1
hsa-miR-5701	4.48	plate28	0
hsa-miR-6513-3p	4.22	plate29	0
hsa-miR-5589-5p	4.21	plate28	0
hsa-miR-1539	3.65	plate4	0
hsa-miR-6516-5p	3.61	plate29	0
hsa-miR-6804-3p	3.58	plate32	1
hsa-miR-128-1-5p	3.53	plate25	0
hsa-miR-605-5p	3.45	plate11	2
hsa-miR-4474-5p	3.35	plate21	0
hsa-miR-1237-3p	3.29	plate2	0
hsa-miR-92a-1-5p	3.20	plate12	0
hsa-miR-7855-5p	3.20	plate35	0
hsa-miR-4435	3.13	plate18	1
hsa-miR-4536-5p	2.93	plate20	0
hsa-miR-548az-3p	2.91	plate27	1
hsa-miR-4485-3p	2.88	plate19	0
hsa-miR-3190-5p	2.83	plate36	0
hsa-miR-7157-3p	2.83	plate34	1
hsa-miR-1972	2.78	plate5	0
hsa-miR-548f-3p	2.73	plate10	1
hsa-miR-6736-5p	2.72	plate30	4
hsa-miR-299-3p	2.72	plate6	1
hsa-miR-2114-5p	2.71	plate13	1
hsa-miR-140-3p	2.69	plate3	5
hsa-miR-6737-3p	2.69	plate30	0
hsa-miR-203b-5p	2.67	plate22	1
hsa-miR-629-3p	2.65	plate11	2
hsa-miR-6768-5p	2.62	plate31	3
hsa-miR-3683	2.60	plate17	1
hsa-miR-4300	2.58	plate15	0
hsa-miR-4684-3p	2.56	plate22	0
hsa-miR-29c-3p	2.56	plate6	1
hsa-miR-6781-5p	2.52	plate31	0
hsa-miR-33a-3p	2.51	plate7	0
hsa-miR-451b	2.50	plate23	1
hsa-miR-4660	2.47	plate21	0
hsa-miR-8068	2.47	plate35	1
hsa-miR-6769a-5p	2.44	plate31	2
hsa-miR-3922-3p	2.42	plate18	0
hsa-miR-6893-3p	2.40	plate34	1
hsa-miR-3186-3p	2.38	plate15	0
hsa-miR-203a-3p	2.38	plate5	3
hsa-miR-548b-3p	2.37	plate10	2
hsa-miR-18b-5p	2.37	plate4	1
hsa-miR-3620-3p	2.33	plate16	1
hsa-miR-124-3p	2.31	plate2	3
hsa-miR-4494	2.31	plate19	1
hsa-miR-4703-3p	2.29	plate22	1
hsa-miR-5096	2.27	plate25	0
hsa-miR-541-3p	2.26	plate9	0

Table 4.19: miRNAs up-regulating CD274 in MDA-MB-231 part II.

miRNA	z-score	plate	target sites
hsa-miR-3666	2.26	plate17	1
hsa-miR-197-3p	2.22	plate5	0
hsa-miR-513a-3p	2.20	plate9	2
hsa-miR-3679-3p	2.19	plate17	1
hsa-miR-7156-5p	2.17	plate34	0
hsa-miR-6752-3p	2.15	plate30	1
hsa-miR-6797-3p	2.15	plate31	1
hsa-miR-19b-2-5p	2.14	plate5	0
hsa-miR-595	2.13	plate11	0
hsa-miR-301b-5p	2.11	plate36	1
hsa-miR-6830-3p	2.10	plate32	3
hsa-miR-3177-3p	2.09	plate15	0
hsa-miR-409-3p	2.09	plate7	0
hsa-miR-7151-3p	2.08	plate34	2
hsa-miR-4435	2.06	plate18	1
hsa-miR-4763-3p	2.06	plate24	0
hsa-miR-8075	2.04	plate35	1
hsa-miR-6511a-3p	2.03	plate29	0
hsa-miR-3074-5p	2.03	plate20	0
hsa-miR-3138	2.03	plate14	0
hsa-miR-6856-3p	2.02	plate33	0
hsa-miR-6868-5p	2.00	plate33	3
hsa-miR-548f-3p	2.00	plate10	1
hsa-miR-5580-3p	2.00	plate27	3

Table 4.20: miRNAs down-regulating CD274 in MDA-MB-231 part I.

miRNA	z-score	plate	target sites
hsa-miR-1233-3p	-4.69	plate1	2
hsa-miR-1225-3p	-4.69	plate1	2
hsa-miR-1206	-4.69	plate1	0
hsa-miR-512-3p	-3.93	plate8	1
hsa-miR-1273c	-3.88	plate14	1
hsa-miR-3117-3p	-2.97	plate13	3
hsa-miR-4633-5p	-2.68	plate21	1
hsa-miR-2467-3p	-2.66	plate24	0
hsa-miR-631	-2.65	plate11	0
hsa-miR-769-5p	-2.49	plate12	1
hsa-miR-7114-3p	-2.46	plate34	0
hsa-miR-4754	-2.45	plate23	0
hsa-miR-1299	-2.42	plate3	1
hsa-miR-1293	-2.42	plate3	2
hsa-miR-151a-5p	-2.40	plate3	0
hsa-miR-4522	-2.37	plate20	1
hsa-miR-6821-3p	-2.37	plate32	2

Table 4.21: miRNAs down-regulating CD274 in MDA-MB-231 part II.

miRNA	z-score	plate	target sites
hsa-miR-3116	-2.36	plate13	1
hsa-miR-2467-5p	-2.35	plate24	2
hsa-miR-6733-5p	-2.35	plate30	6
hsa-miR-3188	-2.34	plate15	2
hsa-miR-641	-2.31	plate11	1
hsa-miR-4504	-2.30	plate20	2
hsa-miR-6894-3p	-2.26	plate34	3
hsa-miR-7853-5p	-2.24	plate35	2
hsa-miR-4285	-2.23	plate16	0
hsa-miR-6880-5p	-2.23	plate34	2
hsa-miR-4678	-2.22	plate22	2
hsa-miR-4786-5p	-2.22	plate24	1
hsa-miR-511-5p	-2.21	plate8	3
hsa-miR-3173-3p	-2.21	plate14	2
hsa-miR-1273a	-2.19	plate2	1
hsa-miR-876-3p	-2.19	plate12	2
hsa-miR-214-3p	-2.19	plate5	1
hsa-miR-4475	-2.17	plate19	1
hsa-miR-3921	-2.14	plate18	1
hsa-miR-6744-3p	-2.13	plate30	3
hsa-miR-4662a-5p	-2.13	plate21	0
hsa-miR-5008-5p	-2.13	plate26	0
hsa-miR-3910	-2.13	plate17	3
hsa-miR-4269	-2.10	plate16	1
hsa-miR-3672	-2.10	plate17	2
hsa-miR-6807-5p	-2.09	plate32	1
hsa-miR-3689d	-2.05	plate19	0
hsa-miR-6717-5p	-2.03	plate29	0
hsa-miR-1287-5p	-2.01	plate2	1
hsa-miR-766-5p	-2.00	plate35	2

4.8.5 27 miRNAs affected both NT5E and CD274 surface expression

The overlap of miRNAs affecting NT5E and CD274 surface levels in MDA-MB-231 cells is illustrated in figure 4.32. For this figure all miRNAs with a significant effect on NT5E or CD274 levels were considered. The following five miRNAs led to increased NT5E and CD274 levels:

miR-92a-1-5p, miR-6804-3p, miR-134-3p, miR-4482-3p and miR-5589-5p.

The following seven miRNAs led to decreased NT5E and CD274 surface expression:

miR-6800-3p, miR-2467-3p, miR-1206, miR-1233-3p, miR-1225-3p, miR-5190 and miR-512-3p.

Interestingly, there are miRNAs with opposed effects on NT5E and CD274 in MDA-MB-231 cells. The following four miRNAs caused enhanced NT5E levels but lowered CD274 expression:

miR-3116, miR-4514, miR-5008-3p and miR-1293.

The following six miRNAs caused increased NT5E, but decreased CD274 surface expression:

miR-3190-5p, miR-6811-5p, miR-378g, miR-519a-3p, miR-4480 and miR-203b-3p.

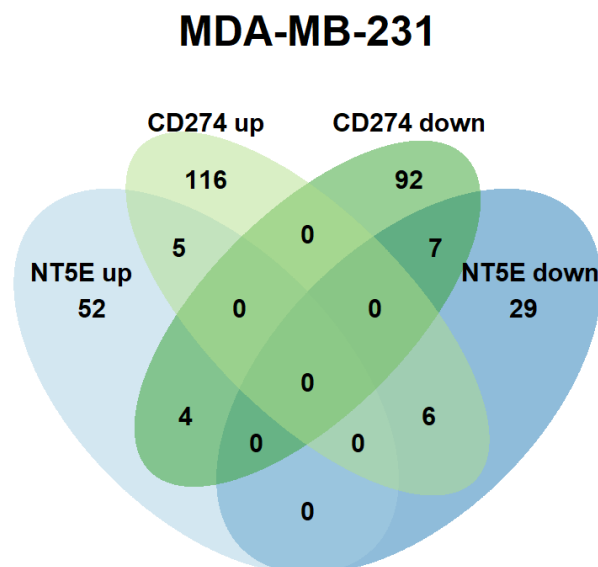


Figure 4.32: Venn diagram of miRNAs affecting NT5E and CD274 surface expression. Overlap of miRNAs with significant effect on NT5E or CD274 surface levels in MDA-MB-231 (MB231) is depicted.

The overlap of miRNAs affecting CD274 in MDA-MB-231 cells and NT5E in SK-Mel-28 cells is shown in figure 4.33. Five miRNAs up-regulated NT5E in SK-Mel-28 as well as CD274 in MDA-MB-231 cells:

miR-134-3p, miR-146b-3p, miR-29c-3p, miR-3190-5p and miR-147a.

Only two miRNAs **miR-1233-3p and miR-5190** caused reduced CD274 levels in MDA-MB-231 as well as reduced NT5E expression in SK-Mel-28 cells.

Overall, there were seven miRNAs with contrary effects. Two miRNAs, **miR-6884-5p and miR-5093**, led to increased NT5E levels in SK-Mel-28, but lower CD274 levels in MDA-MB-231 cells.

Up-regulation of CD274 in MDA-MB-231, but down-regulation of NT5E in SK-Mel-28 cells was caused by the following five miRNAs:

miR-203b-5p, miR-502-5p, miR-4480, miR-124-3p and miR-92b-3p.

But in view of the high number of miRNAs with an significant effect on either NT5E or CD274, the overlap of miRNAs regulating both immune checkpoint molecules was very minor.

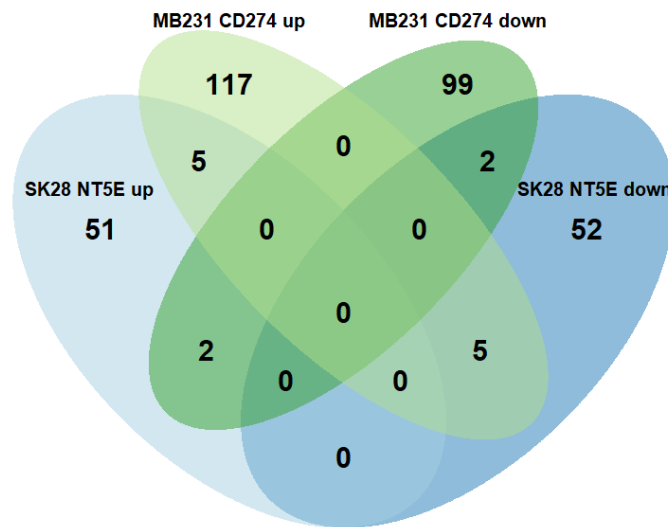


Figure 4.33: Venn diagram of miRNAs affecting surface expression of NT5E and CD274. Overlap of miRNAs with significant effect on NT5E in SK-Mel-28 (SK28) or CD274 surface levels in MDA-MB-231 (MB231) is depicted.

4.8.6 12 miRNAs affected both ENTPD1 and CD274 surface expression

The overlap of miRNAs affecting CD274 in MDA-MB-231 cells and ENTPD1 in SK-Mel-28 cells is shown in figure 4.34. Six miRNAs up-regulated ENTPD1 in SK-Mel-28 as well as CD274 in MDA-MB-231 cells:

miR-134-3p, miR-6778-3p, miR-203a-3p, miR-299-3p, miR-8068 and miR-6804-3p.

Only **miR-6717-5p** caused reduced CD274 levels in MDA-MB-231 and reduced ENTPD1 levels in SK-Mel-28 cells.

Overall, there were five miRNAs with opposed effects on ENTPD1 and CD274. Two miRNAs, **miR-511-5p and miR-219a-2-3p**, led to increased ENTPD1 levels in SK-Mel-28, but lower CD274 levels in MDA-MB-231 cells.

Up-regulation of CD274 in MDA-MB-231, but down-regulation of ENTPD1 in SK-Mel-28 cells was caused by the following three miRNAs:

miR-124-3p, miR-365b-3p and miR-137-3p.

But in general, the overlap of miRNAs regulating both ENTPD1 and CD274 was very low in view of the high number of miRNAs with a significant effect on one of the immune evasion relevant genes alone.

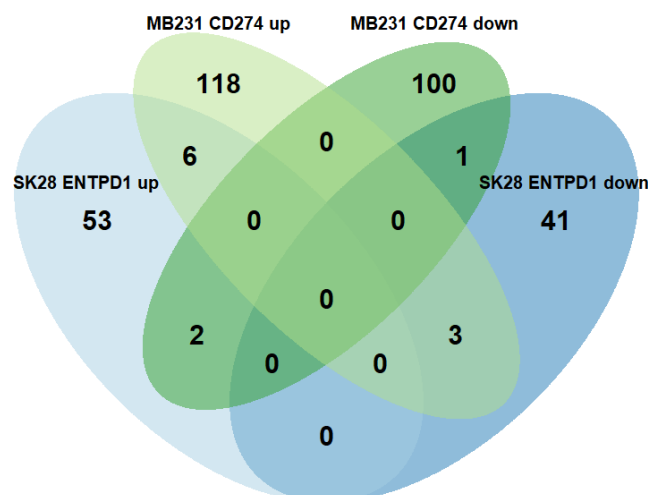


Figure 4.34: Venn diagram of miRNAs affecting surface expression of ENTPD1 and CD274. Overlap of miRNAs with significant effect on ENTPD1 in SK-Mel-28 (SK28) or CD274 surface levels in MDA-MB-231 (MB231) is depicted.

4.8.7 18 miRNAs affected NT5E as well as ENTPD1 surface expression

The overlap of miRNAs regulating ENTPD1 and NT5E in SK-Mel-28 cells is shown in figure 4.35. The following six miRNAs led to enhanced NT5E and ENTPD1 levels:

miR-134-3p, miR-6867-5p, miR-6514-3p, miR-3152-5p, miR-34b-3p and miR-499a-5p.

Ten miRNAs reduced both, NT5E and ENTPD1 surface expression levels in SK-Mel-28 cells:

miR-4662b, miR-585-3p, miR-939-3p, miR-3118, miR-124-3p, miR-1538, -miR-4647, miR-921, miR-6876-3p and miR-6787-3p.

Only two miRNA exhibited opposed effects on NT5E and ENTPD1. **miR-5681a** caused reduced ENTPD1 expression but increased NT5E levels in SK-Mel-28 cells. Whereas **miR-1252-3p** increased ENTPD1 and decreased NT5E surface levels.

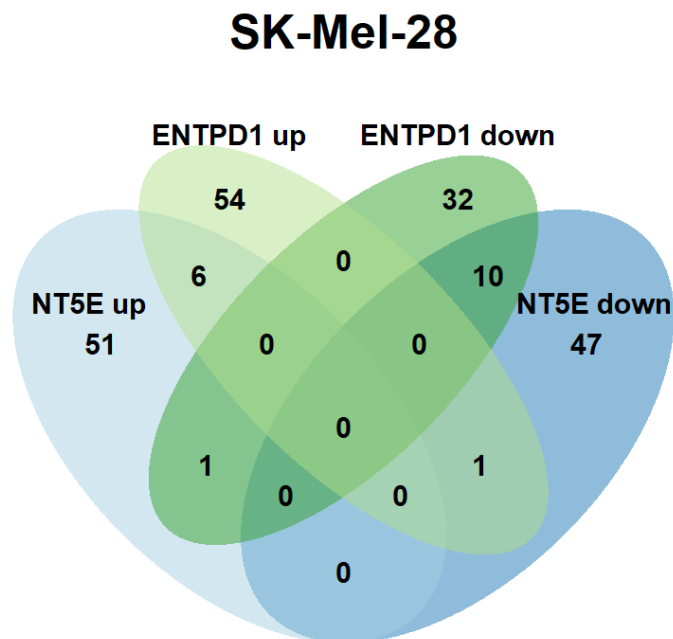


Figure 4.35: Venn diagram of miRNAs affecting surface expression of NT5E and ENTPD1. The overlap of miRNAs with a significant effect on NT5E and ENTPD1 in SK-Mel-28 cells is depicted.

For the six miRNAs that caused increase of NT5E and ENTPD1 surface levels, target prediction was performed to unravel the underlying mechanism of the up-regulation. The list of shared targets is shown in table 4.22 and table 4.23.

Table 4.22: Shared targets of miRNAs upregulating NT5E and ENTPD1 part I.

Gene	Hits	gene function	KM breast cancer
LCOR	5	transcriptional corepressor	high expression beneficial
ZEB2	5	transcriptional inhibitor	high expression beneficial
RIMS1	5	RAB effector involved in exocytosis	high expression beneficial
RTKN2	4	involved in lymphopoiesis	no effect
KIAA1468	4	regulates intracellular cholesterol distribution	high expression beneficial
VAMP4	4	involved in docking of synaptic vesicles	high expression beneficial
FLRT2	4	cell-cell adhesion, cell migration	high expression beneficial
NM000706	4	receptor for arginine vasopressin	
CREBZF	4	transcription factor	high expression beneficial
RC3H1	4	binds CDE in the 3'UTR of mRNAs, leading to mRNA degradation	high expression beneficial
BNC2	4	transcription factor specific for keratinocytes	high expression beneficial
CDK14	4	kinase associated with transcriptional misregulation in cancer	high expression beneficial
EIF3J	4	component of the translation initiation factor	low expression beneficial
ELAVL2	4	binds to 3'UTR of target mRNAs	low expression beneficial
FGF2	4	involved in cell survival, cell differentiation and migration	high expression beneficial
FOXP1	4	transcriptional repressor	high expression beneficial
NRIP1	4	modulates transcriptional activation and inhibition	high expression beneficial
SERTAD2	4	coactivator or corepressor	low expression beneficial
SH3BGRL2	4	—	high expression beneficial
STAU2	4	required for microtubule-dependent transport	no effect
SYT1	4	calcium sensor	high expression beneficial
TGFBR1	4	TFG β receptor, regulation of cellular processes	no effect
TRIM67	4	—	high expression beneficial
XKR4	4	—	high expression beneficial
YY1	4	transcriptional activator and inhibitor	no effect
ZBTB10	4	zinc finger TF	no effect
SSX3	4	modulator of transcription	high expression beneficial
KIF1B	4	transports mitochondria	no effect
ZFP3	4	zinc finger TF	high expression beneficial
PCDH11Y	4	cell-adhesion	high expression beneficial
PLCL1	4	inositol phospholipid-based intracellular signaling	high expression beneficial
MBNL1	4	pre-mRNA alternative splicing regulation	no effect
DMD	4	anchors extracellular matrix to cytoskeleton	no effect
MBL2	4	innate immune defense	high expression beneficial

Table 4.23: Shared targets of miRNAs upregulating NT5E and ENTPD1 part II.

Gene	Hits	gene function	KM breast cancer
NHS	4	actin remodeling	no effect
PHF20L1	4	—	no effect
PIK3R5	4	regulatory subunit of PI3K complex	high expression beneficial
VASH2	4	activator of angiogenesis	no effect
TSN	4	activator of RISC	no effect
RAB6B	4	retrograde membrane traffic	high expression beneficial
RNF144A	4	E3 ubiquitin ligase	no effect
SLITRK3	4	suppresses neurite outgrowth	high expression beneficial
LRAT	4	catalyzes esterification of all-trans-retinol	high expression beneficial
NSF	4	vesicle-mediated transport	no effect
IL1RAP	4	component of the interleukin 1 receptor complex	low expression beneficial
MICAL3	4	monooxygenase	no effect
LYRM7	4	mitochondrial respiratory chain	high expression beneficial
NEK11	4	response to DNA damage	high expression beneficial
LRP2BP	4	regulates LRP2 function	no effect
TRIM2	4	E3 ubiquitin ligase	no effect

To understand the mechanisms of miRNAs up-regulating NT5E and ENTPD1, transcriptional regulators, especially repressors are interesting candidates for further investigations. In total, 50 genes were predicted to be targets of at least four of the NT5E and ENTPD1 enhancing miRNAs. None of these genes was predicted to be targeted by all six relevant miRNAs. Only three genes were targeted by five of the NT5E and ENTPD1 enhancing miRNAs. These were Ligand Dependent Nuclear Receptor Corepressor (LCOR), Zinc Finger E-Box Binding Homeobox 2 (ZEB2) and Regulating Synaptic Membrane Exocytosis 1 (RIMS1). Interestingly, LCOR and ZEB2 are both transcriptional inhibitors. miRNA mediated decrease in their expression, could explain the observed increase in NT5E and ENTPD1 surface expression levels upon miRNA transfection. ZEB2 for example is known to be involved in melanoma progression. High ZEB2 expression promotes melanoma cell proliferation, but inhibits melanoma cell invasion. Whereas ZEB1 drives melanoma cell invasion [239].

Also for the miRNAs that enhanced NT5E and ENTPD1 GSEA analysis was performed to find enriched transcription factor motifs within the target genes of these miRNAs. The list of predicted target genes that were shared by at least three of the six NT5E and ENTPD1 activating miRNAs was used as input for GSEA. In total, 465 genes were used as input and analysis was restricted to transcription factor targets. The results for the top ten enriched motifs with a known associated transcription factor are compiled in table 4.24. Among the significantly enriched motifs were several transcription factors that were also enriched for the NT5E enhancing miRNAs alone. For example SOX9, NFAT, MEIS1 and GCM2 were again amongst the top ten enriched regulators. Additionally, target genes from six miRNAs that enhanced NT5E as well as ENTPD1 were also enriched for motifs of PAX3, NFY, CHX10, NAB2, ZSCAN30 and FREAC2.

Table 4.24: GSEA analysis of target genes from NT5E enhancing miRNAs. Also the number of miRNAs with a binding site is given from the six NT5E and ENTPD1 enhancing miRNAs.

Gene Set Name	Gene in overlap	p value	FDR q value	No miR BS
TGGAAA-NFAT-Q4-01	76	1.04E-20	4.98E-18	3
RTAAACA-FREAC2-01	44	6.33E-15	1.21E-12	1
GATTGGY-NFY-Q6-01	49	1.63E-14	2.23E-12	5
TGACAGNY-MEIS1-01	41	2.23E-14	2.66E-12	3
GCM2-TARGET-GENES	65	4.19E-14	4.46E-12	1
PAX3-TARGET-GENES	61	7.91E-14	7.58E-12	3
TAATTA-CHX10-01	39	1.72E-13	1.49E-11	5
NAB2-TARGET-GENES	54	1.89E-13	1.49E-11	1
ZSCAN30-TARGET-GENES	59	2.02E-13	1.49E-11	3
CATTGTYT-SOX9-B1	26	3.23E-13	2.21E-11	3

4.8.8 miR-134-3p and miR-6804-3p increased the expression of all three investigated immune checkpoint molecules

Since miRNAs that are capable of simultaneously regulate several immune checkpoint molecules would be of greater interest for potential therapeutical intervention it was checked, whether there were miRNAs, that enhanced NT5E, ENTPD1 and CD274 or decreased NT5E, ENTPD1 and CD274 surface levels. Therefore, all miRNAs that had a significant effect in either of the two screened cell lines were analysed and only miRNAs were considered, that led to uniform changes: increasing or decreasing all three investigated immune checkpoint molecules. Interestingly, no miRNA led to significant decrease of all three immune checkpoint molecules. Two miRNAs, **miR-134-3p** and **miR-6804-3p**, could significantly increase NT5E, ENTPD1 as well as CD274 surface levels. To note, only miR-134-3p led to significant increase of NT5E in both SK-Mel-28 (z-score = 4.9) and MDA-MB-231 (z-score = 2.0). miR-6804-3p had only a significant enhancing effect on NT5E levels in MDA-MB-231 cells (z-score = 2.2). In SK-Mel-28 miR-6804-3p even reduced surface expression of NT5E, but not to a significant extend (z-score = -1.2). But the increase of CD274 by miR-6804-3p was very strong and among the top ten CD274 up-regulating miRNAs (z-score = 3.6). For ENTPD1 the up-regulation of miR-6804-3p was not so pronounced as for CD274 but significant (z-score = 1.9). Also miR-134-3p enhanced ENTPD1 to similar extend as miR-6804-3p (z-score = 1.9). The increase of CD274 by miR-134-3p was not amongst the strongest hits, but still a significant enhancement was measured (z-score = 1.8). Especially miR-134-3p was an interesting hit and might be an important miRNA driving cancer cell immune evasion by multiple mechanisms.

4.9. Validation of miRNA hits

Based on the miRNA library screen the most promising miRNAs were selected for further validation. The main focus was set to miRNAs that had a significant effect on NT5E surface expression in both screened cancer cell lines to avoid false positive hits. In total, 24 miRNAs fulfilled this criteria. They are listed in table 4.25 with their respective z-score in the screen for MDA-MB-231 and SK-Mel-28. The miRNAs were ranked by their sum of z-scores. Also the information from miRBase about the respective read number from deep sequencing (Reads) was included to preferentially select confirmed miRNAs. Also the number of predicted binding sites (BS) within the NT5E 3'-UTR for the respective miRNA was included in table 4.25.

Table 4.25: Top miRNA hits from library screen affecting NT5E surface expression in both MDA-MB-231 (MDA) and SK-Mel-28 (SK28). miRNAs marked with * were only significant in one cell line.

NT5E enhancing miRNAs					
miRNA	BS	z-score MDA	z-score SK-28	Sum	Reads
miR-134-3p	0	2.0	4.8	6.8	199
miR-6514-3p	0	2.6	2.9	5.5	786
miR-593-3p	1	2.2	2.1	4.3	10
miR-6859-3p	0	2.5	1.7	4.2	1388
miR-4672	1	2.2	1.9	4.1	44
miR-3126-5p	1	2.1	1.9	4.0	241
miR-4692	1	1.8	2.1	3.9	6
miR-127-5p	1	1.7	1.7	3.4	207374
miR-224-3p	1	1.6	1.7	3.3	5757
miR-34b-3p*	0	1.4	2.0	3.4	3180
miR-1293*	0	1.8	1.4	3.2	173
miR-3116*	0	2.5	1.0	3.5	303
NT5E inhibiting miRNAs					
miRNA	BS	z-score MDA	z-score SK-28	Sum	Reads
miR-1233-3p	0	-4.1	-2.4	-6.5	80
miR-1285-5p	2	-2.3	-2.5	-4.8	17819
miR-3134	2	-2.3	-2.2	-4.5	132
miR-22-3p	1	-1.7	-2.8	-4.5	1254963
miR-193a-3p	1	-2.5	-1.9	-4.4	72316
miR-5584-3p	2	-1.8	-2.2	-4.0	5
miR-5190	1	-2.3	-1.7	-4.0	31
miR-4480	1	-2.2	-1.7	-3.9	5
miR-143-5p	1	-2.1	-1.7	-3.8	458908
miR-3118-3p	2	-1.7	-2.0	-3.7	344
miR-1298-3p	1	-1.9	-1.8	-3.7	487
miR-4676-5p	1	-1.8	-1.8	-3.6	40
miR-148b-3p	1	-1.8	-1.8	-3.6	1313333
miR-8056	2	-1.8	-1.7	-3.5	3
miR-520d-3p	1	-1.7	-1.8	-3.5	58
miR-193b-3p*	1	-1.8	-0.4	-2.2	163980

Also four additional miRNAs were included, that were only significant hits in one of the cell lines, but also showed the same tendency on the second cell line. These miRNAs are marked with * in table 4.25. miR-3116 and miR-1293 were included since they enhanced NT5E and CD274 in MDA-MB-231 cells. miR-34b-3p was included, since it enhanced NT5E and ENTPD1 in SK-Mel-28 cells. miR-193b-3p was included, since it has the same binding site as miR-193a-3p and they belong to the same family of miRNAs. But in the library screen miR-193b-3p only had a significant effect on NT5E surface expression in MDA-MB-231 cells. In SK-Mel-28 the inhibition of NT5E was very minor. Also miR-3190-5p was included for validation experiments since it was the only miRNA that exhibited opposed effects in the two screened cell lines although it only had 16 reads. Interestingly, from the NT5E inhibiting miRNAs almost all had a binding site for the NT5E 3'-UTR. Only one of these miRNAs, miR-1233-3p, did not exhibit a binding site for the NT5E 3'-UTR. There was evidence, that the inhibiting miRNAs mediate the observed effects directly by binding to 3'-UTR of NT5E. But also six of the enhancing miRNAs were predicted to be binders of the NT5E 3'-UTR. Either their binding to NT5E 3'-UTR was not altering the NT5E translation or other indirect effects outweighed their potential NT5E inhibiting activity. Overall, the selected NT5E inhibiting miRNAs had significantly more often a binding site for NT5E 3'-UTR than the selected NT5E up-regulating miRNAs ($p = 0.0228$, Fisher's Exact test).

For the further validation experiments, only miRNAs were selected, that had a read number greater than 40. Hence, seven miRNAs were excluded. For the remaining miRNAs the effects observed in the screen were validated by individual miRNA transfections in a broader panel of cell lines.

4.9.1 Individual miRNA transfections could confirm majority of the hits discovered by the library screen

For most miRNAs their effect on NT5E surface expression could be verified

The selected miRNAs were transfected into various cancer cell lines. Up to twelve different cell lines were tested to assess the consistency of the observed effects, especially for the NT5E enhancing miRNAs. Briefly, the cells were transfected with 50 nM miRNA and 72 h post transfection, changes in NT5E surface levels were monitored by FACS. Using NT5E siRNA, the transfection efficacy was monitored for each individual experiment. Transfection was repeated with different cell passages to collect biological replicates. Fold changes were calculated to the respective mimic control-1 sample. Significance was assessed by one-sample T-tests. In figure 4.36 the compendious results of changes in NT5E surface levels upon transfection with NT5E inhibiting miRNAs are shown. For miR-1233-3p, the results are separately shown in figure 4.37. The two cell lines used for the miRNA library screen were tested, as well as nine additional melanoma cell lines. For some miRNAs, also the colon cancer line HCT-116 was tested once as well as fibroblast cell lines MRC5 and CCD-18Co. To note, MaMel-68, MaMel-73a and MaMel-57 exhibited only a very low basal expression level of NT5E. Thus, in those cell lines a reduction of NT5E levels could not be easily monitored by FACS. Also the NT5E siRNA pool only had modest to no effect on NT5E surface levels in these three cell lines.

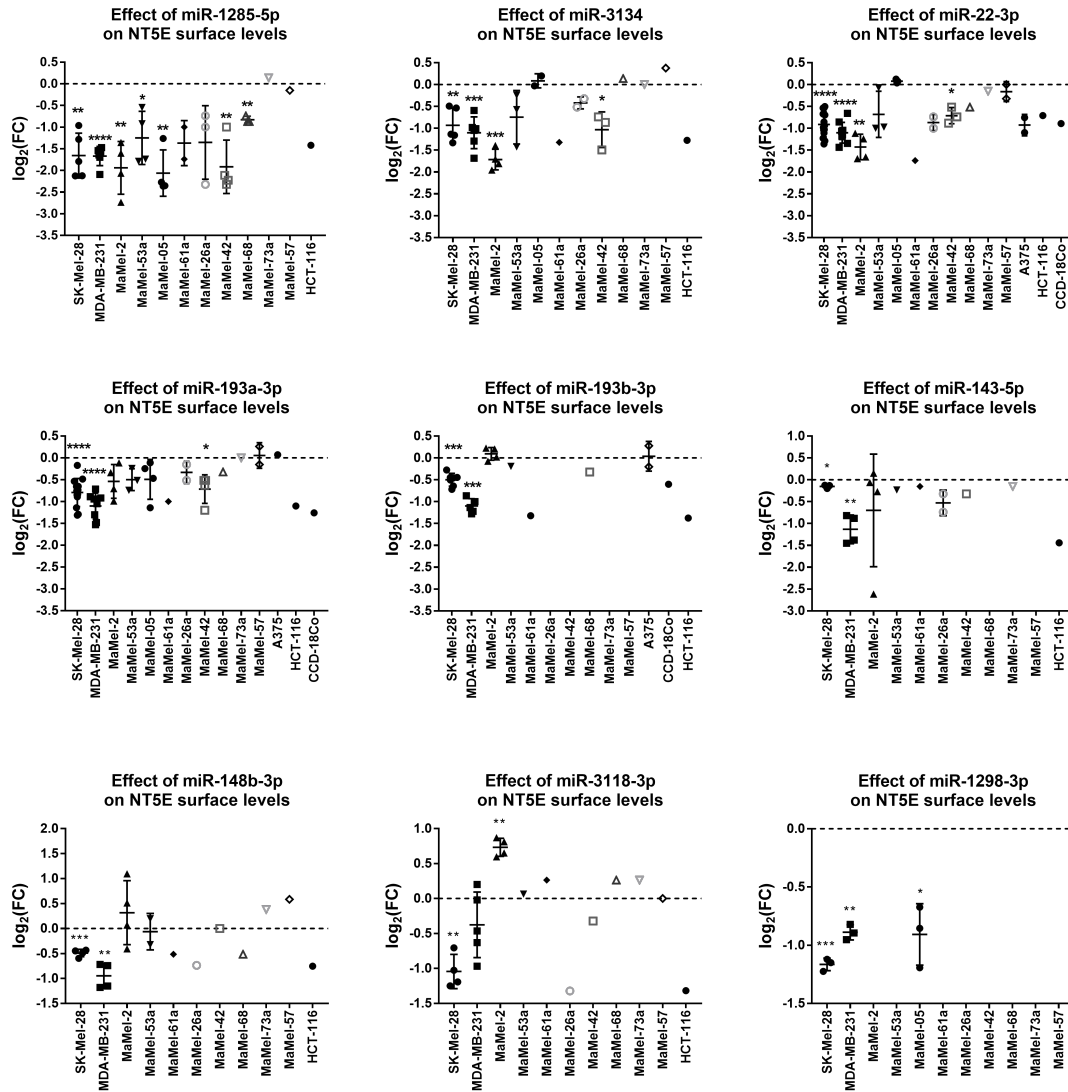


Figure 4.36: Validation of NT5E down-regulating miRNAs by FACS. Each dot represents an independent experiment. Cell lines were transfected with 50 nM miRNA. Three days post transfection cells were harvested and stained for FACS analysis. Cells were gated on live cells and isotype control staining was used to set the NT5E positive gate. Median fluorescence intensity of NT5E was determined for every condition. Fold changes were calculated compared to mimic control-1 samples. Significance was assessed by one-sample T-test. *: $p < 0.05$; **: $p < 0.01$; ***: $p < 0.001$; ****: $p < 0.0001$.

miR-1285-5p led to a decrease of NT5E surface levels in ten out of 12 tested cell lines. In seven cell lines this effect was statistically significant. miR-3134 decreased NT5E surface expression in eight out of 12 tested cell lines with a significant reduction in four cell lines. Also, the effect of miR-22-3p was quite consistent over different cell lines. In 11 out of 14 tested cell lines a reduction of NT5E expression could be measured with a significant effect in four cell lines. The NT5E inhibitory effect of miR-193a-3p could be observed in 11 out of 14 tested cell lines. But overall, the effect of miR-193a-3p and miR-193b-3p was lower compared to miR-1285-5p and only significant for the two cell lines SK-Mel-28 and MDA-MB-231, which were also used for the miRNA library screen. miR-143-5p and miR-148b-3p

only had significant effect on NT5E surface levels in SK-Mel-28 and MDA-MB-231 cells. In SK-Mel-28 the effect was only minor with a mean fold change of -0.12 for miR-143-5p and -0.44 for miR-148b-5p. miR-3118-3p exerted mixed effects on NT5E surface levels in different cell lines. For example, miR-3118-3p significantly reduced NT5E expression in SK-Mel-28, but significantly increased it in MaMel-2. In the scope of this thesis miR-1298 could only be tested in three cell lines and significant reduction of surface NT5E levels was measured for SK-Mel-28, MDA-MB-231 and MaMel-05. miR-1233-3p was the strongest hit from the screen. However, in the validation it was the only miRNA, that showed an opposite effect. Instead of the expected NT5E down-regulation, miR-1233-3p led to significant increase in NT5E surface expression in SK-Mel-28 and MaMel-02 cells as shown in figure 4.37. And also in the other two tested cell lines the tendency was towards up-regulation. For this reason, miR-1233-3p was excluded from further analysis.

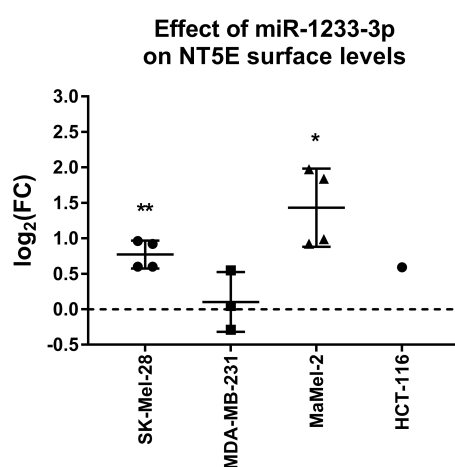


Figure 4.37: Validation of miR-1233-3p by FACS. Each dot represents an independent experiment. Fold changes were calculated compared to mimic control-1 samples. Significance was assessed by one-sample T-test. *: $p < 0.05$; **: $p < 0.01$; ***: $p < 0.001$; ****: $p < 0.0001$.

The changes in NT5E surface levels for the up-regulating miRNAs are shown in figure 4.38. Notably, the up-regulatory effect of these miRNAs was quite consistent across the different cell lines. Especially miR-134-3p increased NT5E surface expression in all 12 tested cell lines and for nine cell lines this effect was even statistically significant. In ten out of 11 cell lines tested, miR-1293 increased NT5E surface levels and in three cell lines SK-Mel-28, MDA-MB-231 and MaMel-02 this effect was significant. miR-6514-3p also enhanced NT5E levels in 10 out of 12 cell lines. But the effect was not as strong as for example for miR-134-3p. The effect on NT5E surface expression upon miR-6514-3p transfection was significant for the cell lines MaMel-68, SK-Mel-28, MDA-MB-231, MaMel-05 and MaMel-02. miR-34b-3p, miR-4672, miR-6859-3p, miR-3116 and miR-3126-5p significantly increased NT5E surface levels in SK-Mel-28, MDA-MB-231 and MaMel-02 cell lines. For miR-4672 and miR-34b-3p the effect was also significant for MaMel-05 and for miR-6859-3p also for MaMel-05 and MaMel-53a cells. miR-224-3p significantly enhanced NT5E levels in MDA-MB-231, MaMel-02, MaMel-05 and MaMel-68 cells. In SK-Mel-28 cells, miR-224-3p showed a tendency towards increasing NT5E levels as well. miR-3190-5p was excluded from further analysis, since the strong opposed ef-

fects as seen in the miRNA library screen could not be recapitulated.

In the scope of this study miR-127-5p could be only tested in four different cell lines. But in all transfected cell lines an increase in NT5E surface expression could be observed with significant effects in SK-Mel-28, MDA-MB-231, MaMel-53a and MaMel-05 cells. To note, the effect in SK-Mel-28 was not very strong with a mean fold change of 0.13. Although it was suspected that the NT5E enhancing miRNAs might act via indirect mechanism, e.g. by targeting a NT5E inhibitor, it was quite astonishing that the up-regulation caused by these miRNAs was so consistent between different cell lines and tumor entities.

Most miRNAs inhibiting NT5E surface expression also decreased NT5E mRNA levels

Having validated the effect of the top screen hits on NT5E surface expression, it was tested whether the selected miRNAs would also change NT5E mRNA levels. Therefore, SK-Mel-28 and MDA-MB-231 cell lines were transfected with 50 nM miRNA and RNA was isolated two days post transfection and NT5E mRNA levels were subsequently measured by qPCR. Samples were normalized to house keeping gene RPL19, since none of the miRNAs was predicted to regulate this gene. Additionally TBP or UBC were used as a second house keeping gene. Biological replicates were performed with individual experiments using different cell passage numbers. For some miRNAs, also the MaMel-42 and MaMel-68 cell lines were tested. The compiled results for the NT5E inhibiting miRNAs are shown in figure 4.39. To note, miRNA binding to the 3'-UTR does not necessarily lead to lower mRNA levels. Depending on the degree of complimentary base pair binding it is also possible, that only the translation is blocked, and the target gene's mRNA is not degraded.

miR-1285-5p not only decreased NT5E surface levels, but also significantly reduced its mRNA levels in transfected SK-Mel-28 and MDA-MB-231 cells. miR-3134 led to a significant reduction in NT5E mRNA expression in these two cell lines, too. Also in MaMel-42 and MaMel-68 cells, the reduction of NT5E by miR-3134 could be observed. Furthermore, miR-22-3p, miR-193a-3p and miR-193b-3p lowered NT5E mRNA levels in the four tested cell lines with significant reduction in SK-Mel-28 and MDA-MB-231 cells. miR-143-5p had no effect in SK-Mel-28 cells, but here only one experiment was performed. In MDA-MB-231 cells, miR-143-5p could significantly reduce NT5E expression. miR-148b-3p only had minor inhibiting effect in the tested cell lines and also miR-3118-3p could not significantly reduce NT5E mRNA levels.

Additionally, the effect of the NT5E enhancing miRNAs was tested by qPCR and the results are compiled in figure 4.40. From the NT5E up-regulating miRNAs only miR-3116 showed significant increase in NT5E levels on both MDA-MB-231 and SK-Mel-28 cells. Furthermore, miR-134-3p and miR-1293 had a significant NT5E mRNA enhancing effect in MDA-MB-231 cell line. But also the other miRNAs at least showed a tendency of increasing NT5E mRNA levels, although the observed effects were not statistically significant. It could be, that the effect of the up-regulating miRNAs takes a little longer to be measurable on NT5E mRNA level, since indirect mechanisms might need more time than the direct inhibition by miRNA binding to NT5E 3'-UTR.

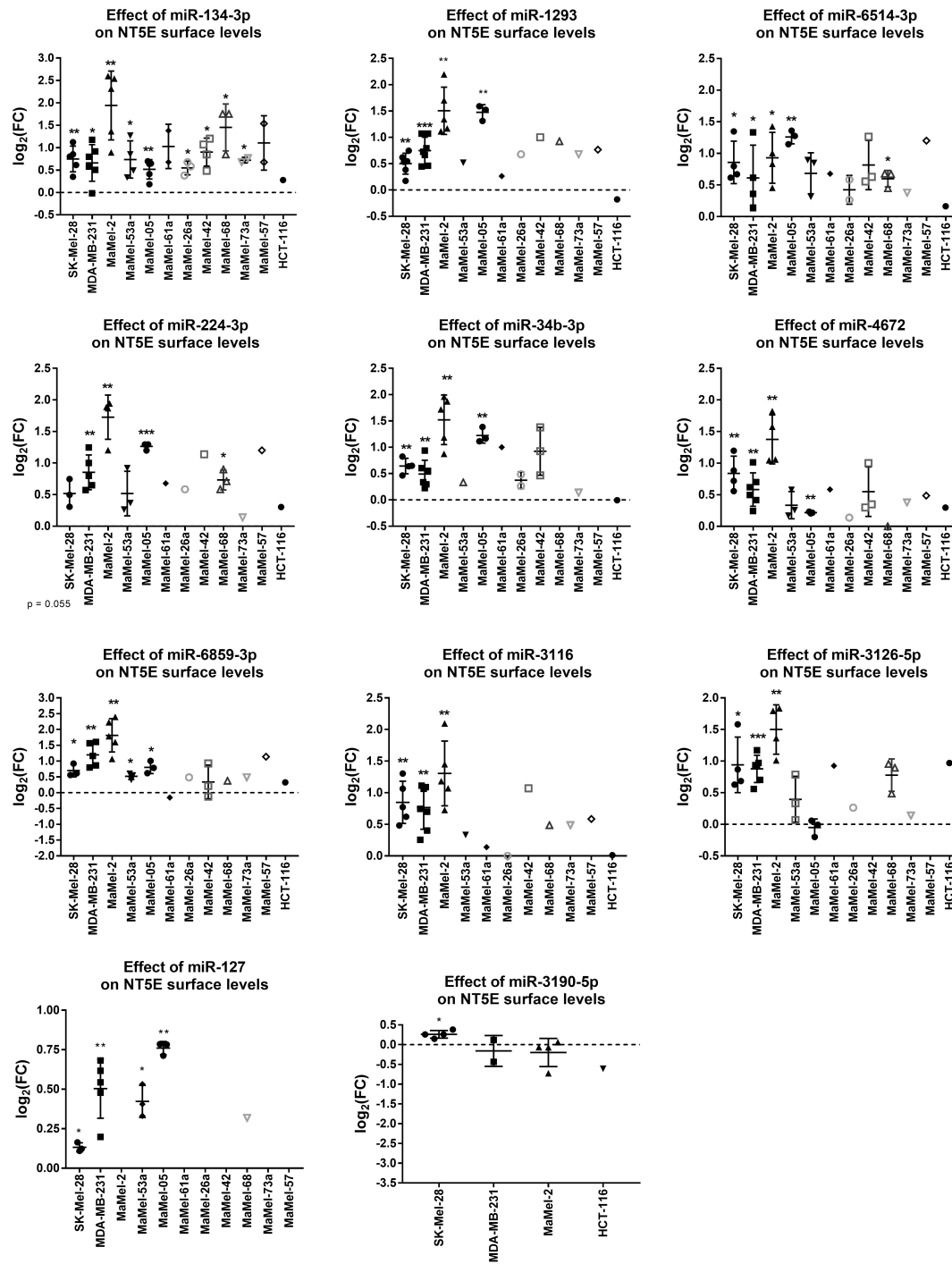


Figure 4.38: Validation of NT5E up-regulating miRNAs by FACS. Each dot represents an independent experiment. Cell lines were transfected with 50 nM miRNA. Three days post transfection cells were harvested and stained for FACS analysis. Cells were gated on live cells and isotype control staining was used to set the NT5E positive gate. Median fluorescence intensity of NT5E was determined for every condition. Fold changes were calculated compared to mimic control-1 samples. Significance was assessed by one-sample T-test. *: p < 0.05; **: p < 0.01; ***: p < 0.001; ****: p < 0.0001.

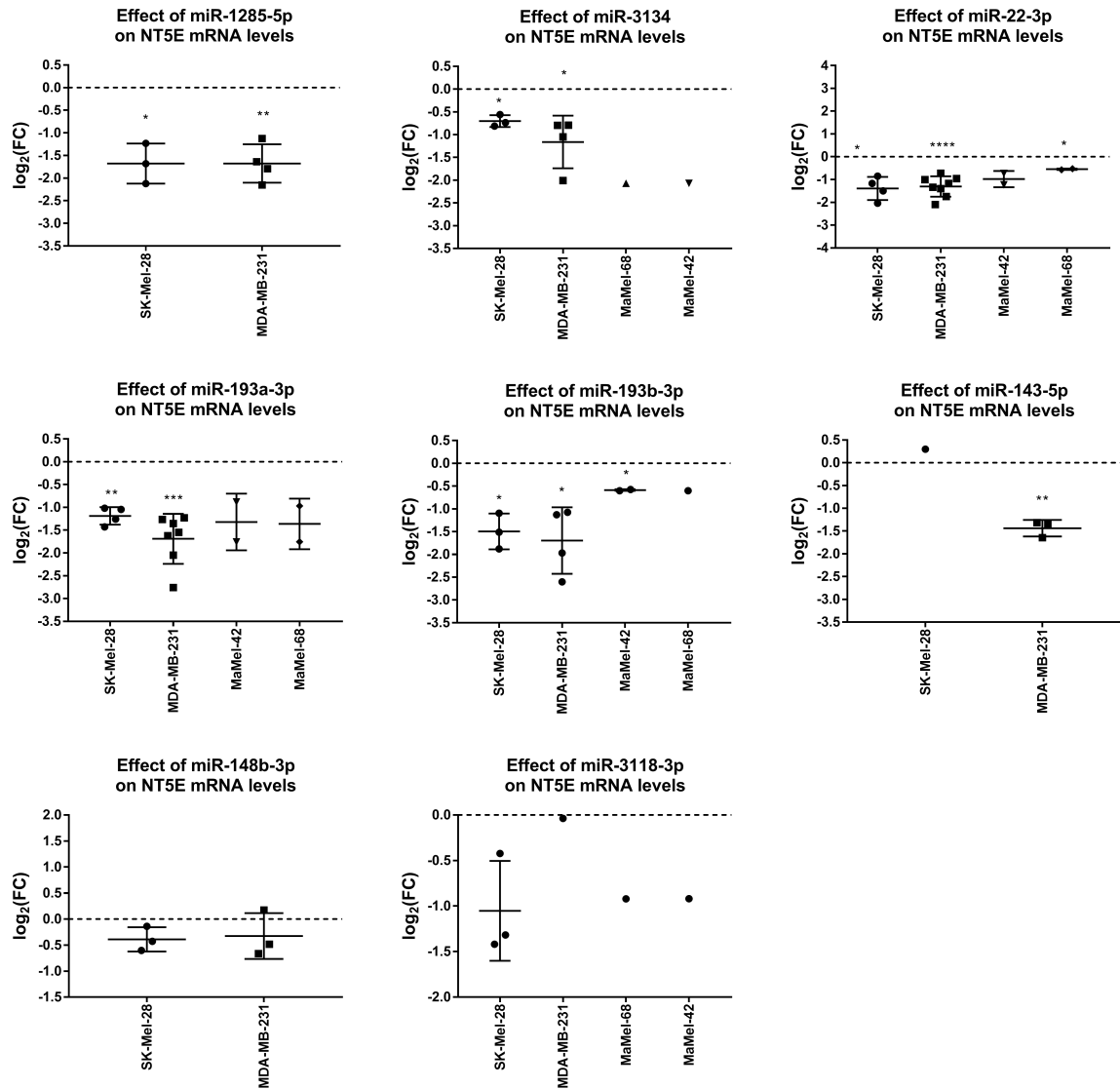


Figure 4.39: Validation of NT5E down-regulating miRNAs by qPCR. Each dot represents an independent experiment. Cell lines were transfected with 50 nM miRNA and two days post transfection cells were harvested and RNA was isolated. NT5E mRNA level were determined by qPCR. Fold changes were calculated compared to mimic control-1 samples. RPL19 was used as housekeeping gene. Significance was assessed by one-sample T-test. *: $p < 0.05$; **: $p < 0.01$.

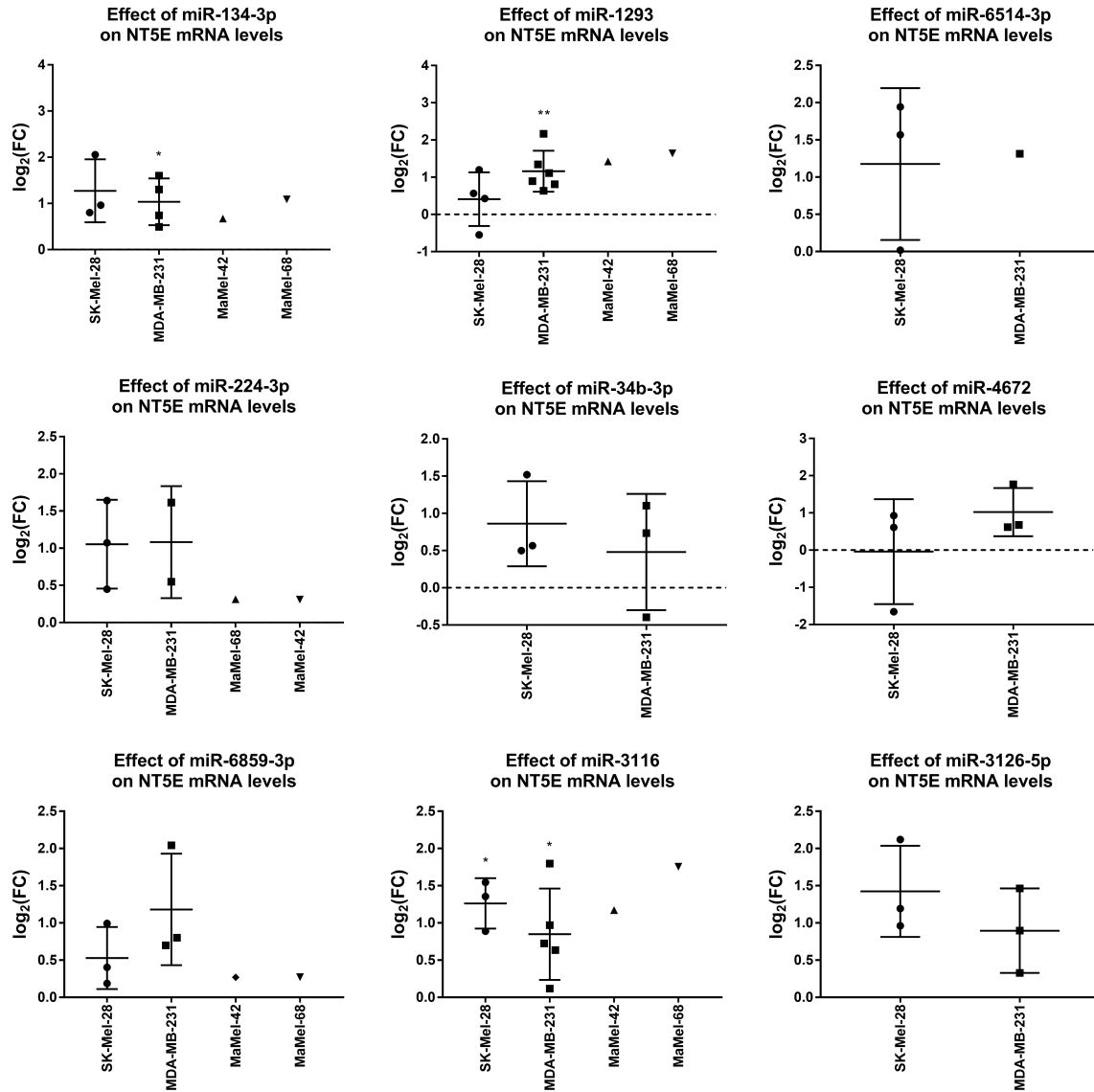


Figure 4.40: Validation of NT5E up-regulating miRNAs by qPCR. Each dot represents an independent experiment. Cell lines were transfected with 50 nM miRNA and two days post transfection cells were harvested and RNA was isolated. NT5E mRNA level were determined by qPCR. Fold changes were calculated compared to mimic control-1 samples. RPL19 was used as housekeeping gene. Significance was assessed by one-sample T-test. *: $p < 0.05$; **: $p < 0.01$; ***: $p < 0.001$; ****: $p < 0.0001$.

miR-1285-5p decreased cellular NT5E protein expression

For six selected miRNAs, their effect on cellular NT5E protein expression was quantified by Western Blot analysis. Therefore, the NT5E high expressing cell line MaMel-53a was transfected with 50 nM miRNA or NT5E siRNA pool. Two days post transfection cells were harvested and protein was isolated and used for Western Blot procedure. 35 µg protein were loaded per lane. Actin was used as reference protein. The result is shown in figure 4.41. A NT5E siRNA pool was used as a positive control and to monitor transfection efficacy. The siRNA strongly decreased the total NT5E protein level. Compared to mimic control-1 condition the NT5E siRNA decreased NT5E level about 73.4 %. Also miR-1285-5p clearly decreased NT5E protein expression by 78.8 % and exhibited an even stronger effect than the NT5E siRNA. Furthermore, miR-193a-3p decreased NT5E protein level by 57.3 %. miR-148b and miR-22-3p only had minor decreasing effect on NT5E total protein levels. miR-148b decreased NT5E about 12.1 % compared to mimic control-1 and miR-22-3p only led to a 2 % decrease. To note, also in validation by FACS miR-22-3p did not clearly reduce NT5E surface expression on the MaMel-53a cell line. miR-4672 and miR-134-3p belong to the NT5E enhancing miRNAs identified by the miRNA library screen. But only miR-134-3p could slightly increase total NT5E protein levels in MaMel-53a about 16.4 % compared to mimic control-1. However, miR-4672 decreased total NT5E protein levels about 52.5 %, although it caused slight up-regulation of NT5E surface expression on MaMel-53a (see figure 4.38). Interestingly, this miRNA has a potential binding site for NT5E 3'-UTR. It might be, that this miRNA is on the one-hand directly inhibiting NT5E translation, but on the other hand by indirect mechanisms enhancing its surface expression levels.

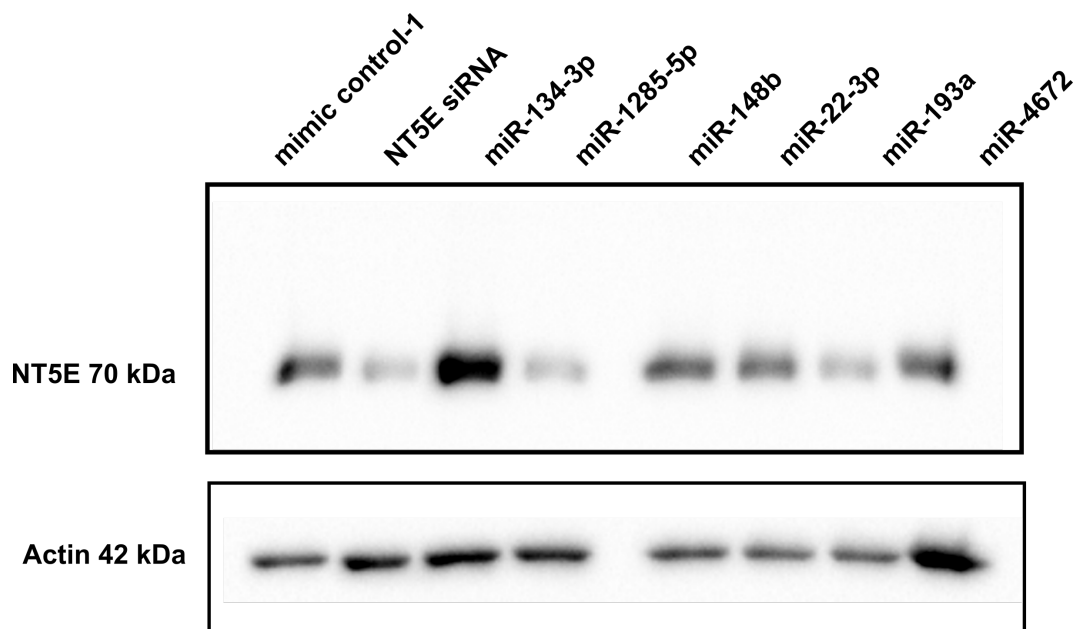


Figure 4.41: Effect of miRNA transfection on cellular NT5E protein expression in MaMel-53a cells. MaMel-53a cells were transfected with 50 nM miRNA/siRNA and 48 h post transfection cells were harvested and protein was isolated subsequently. Total NT5E protein levels were determined by Western Blot. 35 µg protein were loaded per lane on a 12 % SDS-PAGE gel. Actin was used as normalization control.

4.10. Investigating mode of action of miRNA-mediated changes of NT5E expression

Having validated the effect of the top miRNA hits from the library screen on NT5E expression, their mode of action was elucidated. For the validated NT5E inhibiting miRNAs a direct interaction with NT5E 3'-UTR was suspected thereby blocking NT5E protein translation. Thus, luciferase reporter assays were performed to verify this hypothesis.

4.10.1 Validating direct interactions

To verify a direct interaction of miRNAs with their target gene, 3'-UTR reporter assays were performed. Briefly, the 3'-UTR of target gene is linked to a luciferase encoding gene. By measuring the luciferase signal, it can be determined, whether a miRNA can block the target gene translation by binding to its 3'-UTR. If a miRNA can bind, the luciferase signal is decreasing. To verify a direct interaction, the miRNA binding site within the 3'-UTR is mutated e.g. by deleting one nucleotide of the core binding region. Binding of the miRNA to the mutated 3'-UTR should not decrease the luciferase signal.

Binding of miR-22-3p, miR-193a-3p, miR-3134, miR-1285-5p and miR-148b-3p to NT5E 3'-UTR could be proven by reporter assays

Luciferase reporter assays were performed for all miRNAs, that had a predicted binding site for the NT5E 3'-UTR. Also the NT5E enhancing miRNAs that exhibited a binding site were tested. To note, luciferase assays for miR-22-3p and miR-193a/b-3p were performed separately, because these miRNAs were validated before the library screen was finished, since these were promising candidates from the *in silico* predictions. Briefly, reporter assays were performed by co-transfecting a plasmid containing the gene for renilla luciferase fused with NT5E's 3'-UTR. Ideally, miRNAs with a binding site should lower the translation of luciferase enzyme leading to lower luminescence signal. This assay was performed in several cell lines like HeLa, HEK293, SK-Mel-28 and MDA-MB-231 to account for cell line specific effects. The compiled results are shown in figure 4.42.

miR-1285-5p strongly decreased the luciferase signal in all four tested cell lines. This miRNA exhibited two bindings sites within the NT5E 3'-UTR, which could explain the strong consistent inhibition. Besides miR-1285-5p, also miR-3134 had two binding sites for the NT5E 3'-UTR and led to significant decrease in luciferase signal in all studied cell lines. miR-148b-3p also significantly lowered luciferase signal in all cell lines, but only to weaker extend in HeLa cells. This miRNA had only one binding site for NT5E 3'-UTR. miR-3118-3p also significantly reduced the luciferase expression, but to lower extend in HeLa and MDA-MB-231 cells. miR-4480 only exhibited a significant effect in HEK293 cells. Notably, miRNA-143-5p was the only miRNA that showed no effect in any of the cell lines tested. Interestingly, for the miRNAs that up-regulate NT5E expression, also reduction of luciferase activity could be observed. In fact, miR-224-3p and miR-3126-5p had significant effects in HEK293 and MDA-MB-231 cells, but not in the other two cell lines.

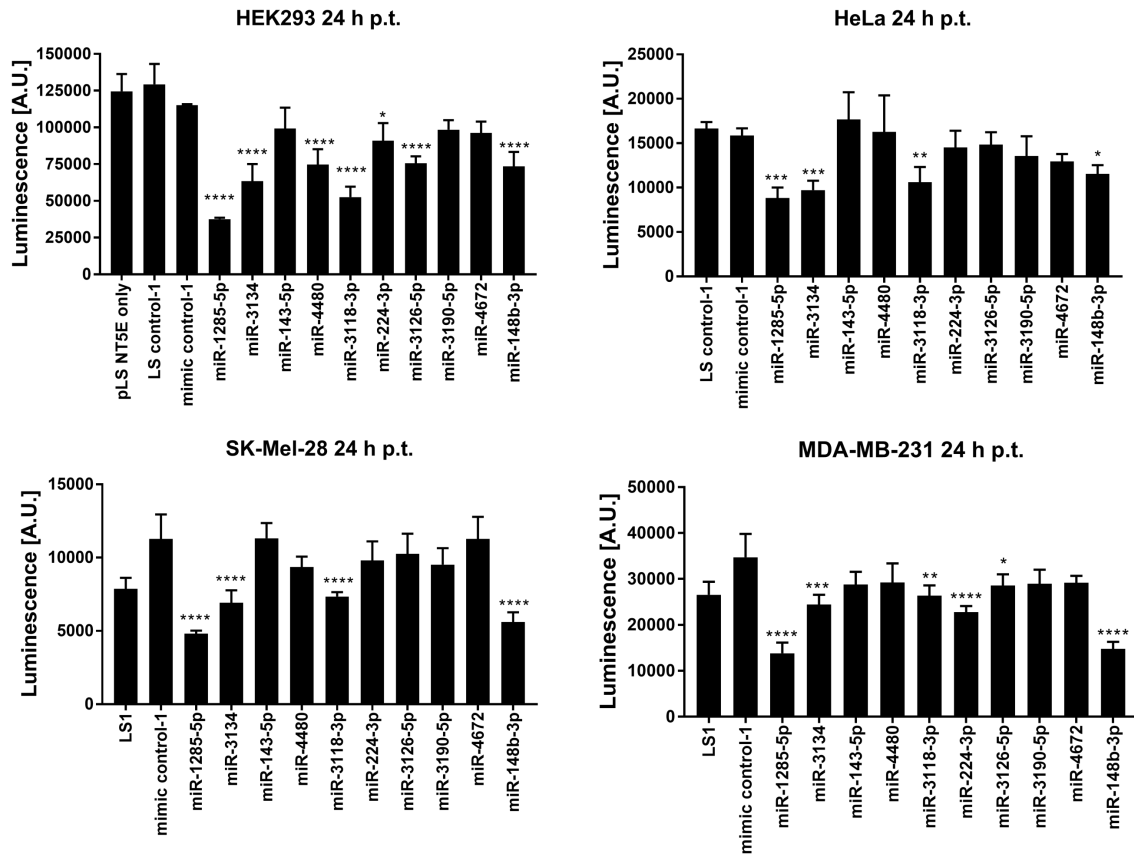


Figure 4.42: NT5E 3'-UTR reporter assay. Cells were transfected with 100 ng pLS-NT5E plasmid and 50 nM miRNA. Luciferase signal was measured 24 h post transfection. Four cell lines were tested: HEK293, HeLa, SK-Mel-28 and MDA-MB-231. Significance was assessed by one-way ANOVA using Dunnett's multiple comparison test. All samples were compared to mimic control-1. At least four replicates were performed per miRNA.

*: $p < 0.05$, **: $p < 0.01$, ***: $p < 0.001$, ****: $p < 0.0001$.

For the cell lines MDA-MB-231 and SK-Mel-28 the luciferase reporter assay was performed three times. The results of all NT5E 3'-UTR reporter assays performed with the wild-type plasmid are compiled in table 4.26. Arrows indicate the effect of the miRNA on the luciferase signal. Strong significant effects ($p < 0.001$) are highlighted yellow. miR-1285-5p and miR-3134 were the two best performing miRNAs with the strongest reduction of luciferase signal in all four tested cell lines. miR-1285-5p reduced luciferase signal in all eight experiments performed and miR-3134 in seven out of eight experiments. Also miR-193a-3p and miR-3118-3p reduced luciferase signal in all four cell lines as well as miR-148b-3p. The effect of miR-22-3p was not as consistent as for the other NT5E inhibiting miRNAs, and the luciferase signal was only reduced in four out of eight experiments. miR-143-5p did not show the expected effect and only slightly reduced the luciferase signal in one assay for MDA-MB-231 cells. Since miR-143-5p had only weak effect in the SK-Mel-28 cell line in FACS validation and almost no effect in the reporter assay, it was decided to exclude this miRNA from subsequent mutagenesis experiments.

Table 4.26: Compilation of miRNA mediated effects on luciferase signal in NT5E 3'-UTR reporter assays.

miRNA	MDA-MB-231	SK-Mel-28	HeLa	Hek293
miR-1285-5p	↓ ↓↓	↓↓↓	↓	↓
miR-3134	- ↓↓	↓ ↓↓	↓	↓
miR-22-3p	- - ↓	↓-↓	-	↓
miR-193a-3p	- ↓ ↓	- ↓↓	↓	↓
miR-148b-3p	- ↓↓	- ↓↓	↓	↓
miR-143-5p	- - ↓	- - -	-	-
miR-3118-3p	- ↓ ↓	- ↓ ↓	↓	↓
miR-4480	- - ↓	↓ - ↓	-	↓
miR-3190-5p ^{mixed}	- - ↓	- - ↓	-	-
miR-224-3p ^{up}	↓ ↓↓	- - -	-	↓
miR-3126-5p ^{up}	- ↓↓	- - ↓	-	↓
miR-4672 ^{up}	- - -	- - ↓	-	-
miR-6859-3p ^{up}	- - ↓	- - ↓	-	-

↓: strong significant effect (at least *** $p < 0.001$).

up: miRNAs that enhanced NT5E surface expression.

mixed: miRNA that had mixed effects on NT5E surface expression in different cell lines.

Although miR-3118-3p performed quite well in the reporter assay, also this miRNA was excluded from further in-depth analysis, since in the validation it showed mixed effects across different cell lines. Also miR-4480 was not further investigated. miR-3190-5p, which showed mixed effect in the miRNA library screen, only slightly reduced luciferase signal in two assays. Since this miRNA only showed very weak to no effects in the validation, this miRNA was not considered for further analysis. The NT5E enhancing miRNAs did not show as strong and consistent effects as most of the NT5E inhibiting miRNAs. miR-4672 and miR-6859-3p had almost no effect on luciferase signal. miR-3126-5p had an effect in four out of eight experiments. miR-224-3p seems to have cell-type specific effects, since it clearly reduced luciferase signal in all experiments performed in MDA-MB-231, but in none performed in SK-Mel-28 or HeLa cells. Since overall the effect of the NT5E activating miRNAs was not so pronounced in the reporter assays, no mutagenesis experiments were performed for these miRNAs. For these miRNAs, an indirect mechanism was suspected, since they clearly enhanced NT5E surface expression as well as mRNA levels. To note, there are a few studies describing activating effects on protein expression mediated by miRNA binding to 3'-UTR, which is contrary to their normal functioning. Whether a miRNA inhibits or activates translation seems to be dependent on proteins binding to miRNA and 3'-UTR like AGO2 and FXR1 [202].

But in this study the focus was set on NT5E inhibiting miRNAs that clearly had a reducing effect on luciferase signal in reporter assays to perform subsequent mutation of their respective binding site to verify direct interaction with the NT5E 3'-UTR.

Mutagenesis of NT5E 3'-UTR verified direct binding of miR-22-3p, miR-193b-3p and miR-193a-3p

In table 4.27 the mutations are listed, which were generated within the NT5E 3'-UTR to verify direct miRNA binding. The seed sequences, consisting of six to seven nucleotides, are marked in yellow and the deleted nucleotide is marked in red. The primers used to insert the deletion are listed in table 2.4 in the materials and method section. For miR-193b-3p and miR-193a-3p the same deletion at position 1670 was used, since both miRNAs share the same seed sequence. Deletions at position 1671 and 1672 could not successfully be generated by quick change mutagenesis during this study. Regarding miR-22-3p, deletions at three different positions could be generated, respectively. For miR-148b-3p, two deletions at position 1106 and 1107 were introduced, respectively. miR-1285-5p and miR-3134 have two distinct binding sites within the NT5E 3'-UTR. For these two miRNAs constructs harbouring a deletion in only one of the two binding sites as well as constructs with a single nucleotide deletion in each of the two binding sites were planned to generate, respectively. Within the scope of this Thesis only the single mutated constructs were generated so far.

Table 4.27: List of deletions created in NT5E 3'-UTR for reporter assays to verify direct miRNA interaction. The seed sequence is highlighted in yellow. The deleted nucleotide is marked in red.

miRNA	position	binding site
miR-193a-3p	del-1670	UACACUU GGQCAGU AAAAUA
miR-193b-3p	del-1670	UACACUU GGQCAGU AAAAUA
miR-22-3p	del-1442	UGCAA AU GGQAGCU AGAGGUUUU
miR-22-3p	del-1443	UGCAA AU GGCAGCU AGAGGUUUU
miR-22-3p	del-1444	UGCAA AU GGCAQCU AGAGGUUUU
miR-1285-5p	del-984	UAUUUUA UGAGAU UCCAUC
miR-1285-5p	del-985	UAUUUUA UGAQGAU UCCAUC
miR-1285-5p	del-986	UAUUUUA UGAGAU UCCAUC
miR-1285-5p	del-88	UUUUC AA GUQAGAU UCAA AUC
miR-1285-5p	del-89	UUUUC AA GUGAGAU UCAA AUC
miR-1285-5p	del-90	UUUUC AA GUGAQAU UCAA AUC
miR-3134	del-989	AUGAGAU UQCAUC AGCUCUGCCUC
miR-3134	del-990	AUGAGAU UCQAUC AGCUCUGCCUC
miR-3134	del-991	AUGAGAU UCCAUC AGCUCUGCCUC
miR-148b-3p	del-1106	CAGCAAGAGGCUA GCACUG AAUUCAUUC
miR-148b-3p	del-1107	CAGCAAGAGGCUA GCAQUG AAUUCAUUC

The first 3'-UTR assay with mutated pLS-NT5E plasmids was performed in SK-Mel-28 cells transfected with 100 ng plasmid containing either the wild type NT5E 3'-UTR or a mutated version with a deleted nucleotide at position 1670. The results are depicted in figure 4.43. This assay was performed prior the miRNA library screen. Here, mimic control-2 was used as control miRNA. But from the screen it was obvious, that this control miRNAs itself had strong effects on NT5E levels *per se*. In the screen it constantly led to up-regulated NT5E surface levels. In this reporter assay mimic control-2 led to a significant strong decrease in luminescence signal ($\text{mean}_{\text{WT:ctrl2}} = 7710$, $p < 0.0001$) compared to the vector only ($\text{mean}_{\text{WT:only}} = 38400$). Also miR-193a-3p ($\text{mean}_{\text{WT:miR-193a}} = 18728$, $p < 0.0001$), miR-193b-3p ($\text{mean}_{\text{WT:miR-193b}} = 19050$, $p < 0.0001$) and miR-22-3p ($\text{mean}_{\text{WT:miR-22}} = 15560$, $p < 0.0001$) led to reduced luciferase expression by binding to the NT5E 3'-UTR. If the vector with mutation at position 1670 is co-transfected with miR-193a-3p ($\text{mean}_{\text{del1670:miR-193a}} = 48504$, $p = 0.0002$) or miR-193b-3p ($\text{mean}_{\text{del1670:miR-193b}} = 39914$, $p = 0.0143$), the luminescence signal is restored and even significantly higher than the pLS-NT5E-del1670 vector only ($\text{mean}_{\text{del1670:only}} = 27623$). Interestingly, mimic control-2 co-transfected with the mutated 3'-UTR led to no significant change compared to the vector only ($\text{mean}_{\text{del1670:ctrl2}} = 22360$).

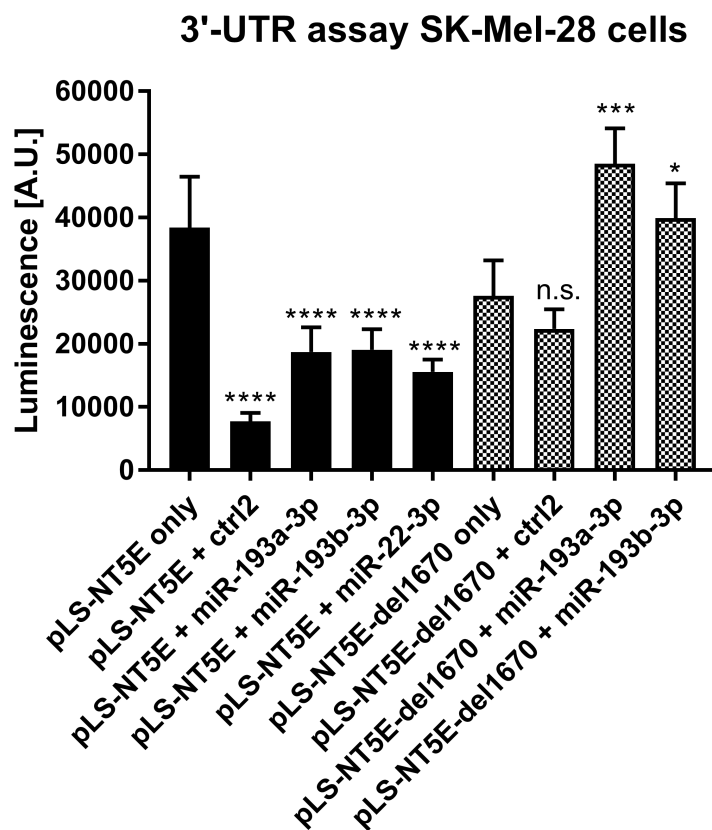


Figure 4.43: NT5E 3'-UTR assay in SK-Mel-28 cells. Cells were transfected with 100 ng pLS-NT5E plasmid and 50 nM miRNA. Luciferase signal was measured 24 h post transfection. One-way ANOVA was performed to calculate p-values always comparing to the corresponding pLS-vector only. *: $p < 0.05$, **: $p < 0.01$, ***: $p < 0.001$, ****: $p < 0.0001$.

For subsequent reporter assays, mimic control-1 was used as reference control. SK-Mel-28

cells were again co-transfected with 50 nM miRNA and 100 ng of plasmid containing either the wild type NT5E 3'-UTR or mutated version. The outcome of this reporter assay in SK-Mel-28 cells is shown in figure 4.44. The luciferase signal was measured 24 h post transfection. Compared to pLS-NT5E WT + mimic control-1 ($\text{mean}_{\text{WT:ctrl1}} = 36820$), miR-22-3p significantly reduced the luciferase signal ($\text{mean}_{\text{WT:miR-22}} = 22122$, $p = 0.0024$). Also miR-193a-3p significantly reduced the luciferase signal ($\text{mean}_{\text{WT:miR-193a}} = 26996$, $p = 0.0297$). The transfection with miR-193a-3p ($\text{mean}_{1670:\text{miR-193a}} = 30548$) and the mutated NT5E 3'-UTR with a deletion at position 1670 did not lead to a change in luciferase signal compared to mimic control-1 ($\text{mean}_{1670:\text{ctrl1}} = 29788$). Also for miR-22-3p ($\text{mean}_{1444:\text{miR-22}} = 52463$) there was no significant change in luciferase signal compared to mimic control-1 ($\text{mean}_{1444:\text{ctrl1}} = 56468$) when the position 1444 was deleted within the NT5E 3'-UTR.

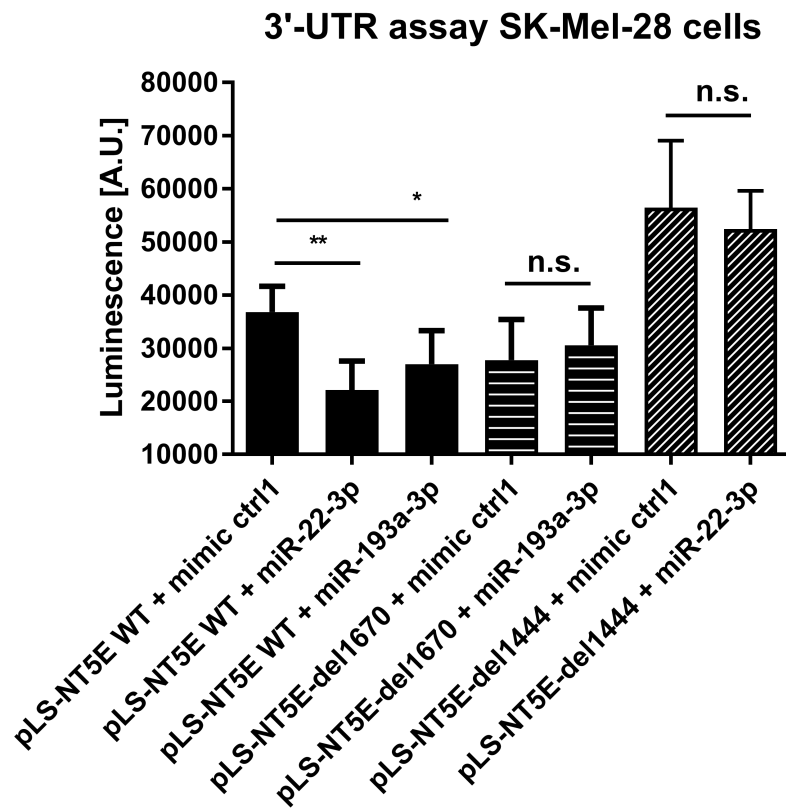


Figure 4.44: Mutated NT5E 3'-UTR assay in SK-Mel-28 cells. Cells were transfected with 100 ng pLS-NT5E plasmid and 50 nM miRNA. Luciferase signal was measured 24 h post transfection. One-way ANOVA was performed to calculate p-values for transfections with WT plasmid comparing to mimic control-1 *: $p < 0.05$, **: $p < 0.01$. For the deletions significance was assessed with two-sided T-test.

For miR-22-3p two additional deletions at position 1442 and 1443 were generated and tested, respectively. The result of the corresponding luciferase reporter assay is shown in figure 4.45. For deletion at position 1442 the luminescence values for the plasmid pLS-NT5E-del1442 only ($\text{mean}_{1442} = 29043$), plasmid with mimic control-1 ($\text{mean}_{1442:\text{ctrl1}} = 36606$) and miR-22-3p ($\text{mean}_{1442:\text{miR-22}} = 30292$) were similar and no significant difference could be observed. For deletion at position 1443 of the NT5E 3'-UTR there was no significant difference between plasmid only ($\text{mean}_{1443} = 45423$) and miR-22-3p ($\text{mean}_{1443:\text{miR-22}} = 47702$). But the

transfection with pLS-NT5E-del1443 and mimic control-1 (mean_{1443:ctrl1} = 33004, p = 0.014) led to significantly lower luciferase activity compared to transfection with miR-22-3p. Overall, all three deletions within the binding site of miR-22-3p in NT5E 3'-UTR rescued the luciferase signal compared to wild type 3'-UTR proofing the direct binding of miR-22-3p to NT5E 3'-UTR.

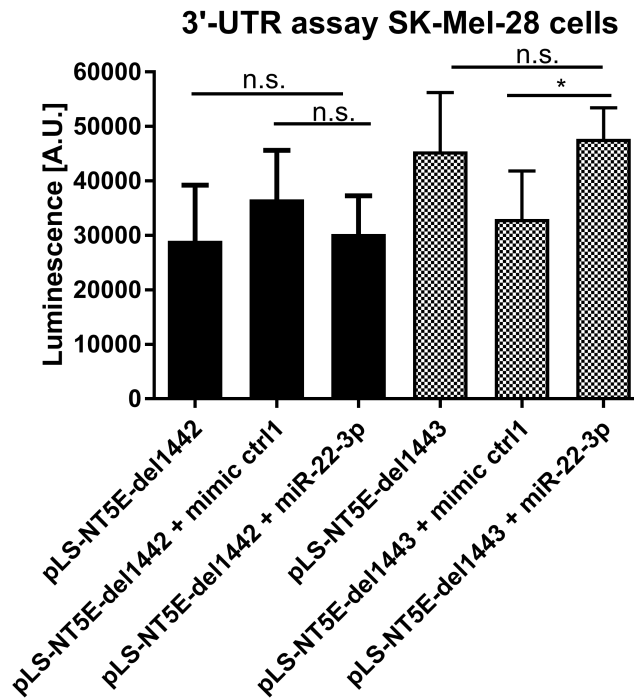


Figure 4.45: Mutated NT5E 3'-UTR assay in SK-Mel-28 cells. Cells were transfected with 100 ng pLS-NT5E plasmid and 50 nM miRNA. Luciferase signal was measured 24 h post transfection. Significance was assessed with two-sided T-test. *: p < 0.05.

Another reporter assay performed in A375 cells for miR-22-3p and miR-193a/b-3p is shown in figure 4.46. Only the wild type NT5E 3'-UTR was co-transfected with miRNAs. As reference mimic control-1 was used. To note, transfection with mimic control-1 compared to pLS-NT5E only led to a significantly higher luminescence signal (mean_{WT:ctrl1} = 10778, p = 0.017, two-sided T-test). But based on the one-way ANOVA analysis this change was not significant. For all transfected miRNAs the luminescence signal was significantly reduced compared to mimic control-1. miR-422a was used as a positive control, since this miRNAs was already published to target NT5E 3'-UTR.

Also in the breast cancer cell line MDA-MB-231 the NT5E 3'-UTR assay with the wild type plasmid was conducted. The results are shown in figure 4.47. In this cell line mimic control-1 led to a significant lower luminescence signal compared to pLS-NT5E only (mean_{WT:ctrl1} = 9224, p = 0.006, two-sided T-test). Compared to mimic control-1, only miR-22-3p (mean_{WT:miR-22} = 8800, p = 0.0376) and miR-193a-3p (mean_{WT:miR-193a} = 8773, p = 0.0365) significantly decreased the luciferase activity.

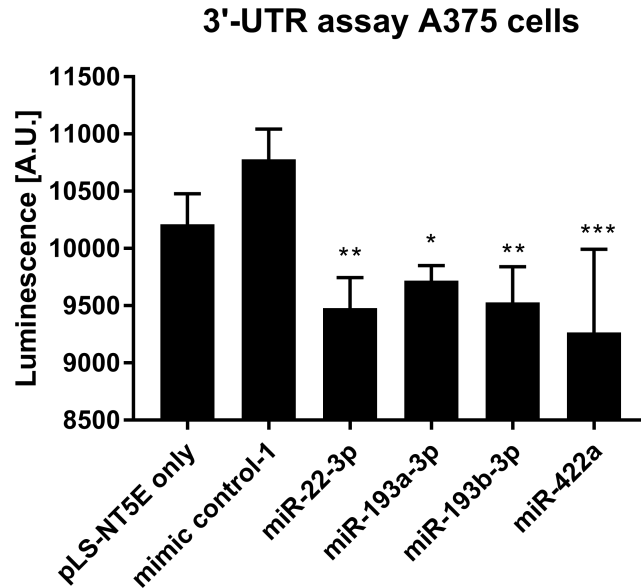


Figure 4.46: NT5E 3'-UTR assay in A375 cells. Cells were transfected with 100 ng pLS-NT5E plasmid and 50 nM miRNA. Luciferase signal was measured 24 h post transfection. One-way ANOVA was performed to calculate p-values always comparing to mimic control-1. *: $p < 0.05$, **: $p < 0.01$, ***: $p < 0.001$.

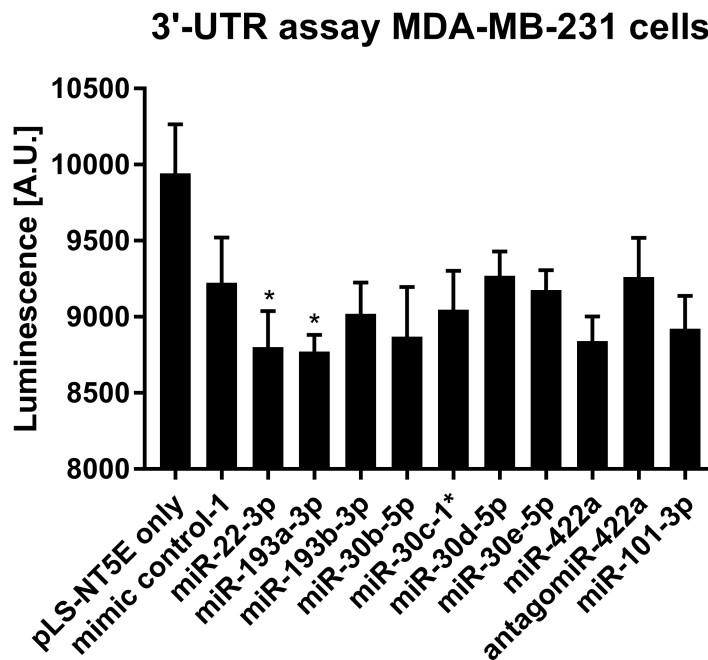


Figure 4.47: NT5E 3'-UTR assay in MDA-MB-231 cells. Cells were transfected with 100 ng pLS-NT5E plasmid and 50 nM miRNA. Luciferase signal was measured 24 h post transfection. One-way ANOVA was performed to calculate p-values always comparing to mimic control-1. *: $p < 0.05$.

4.10.2 Investigating indirect mechanisms

Especially for the NT5E enhancing miRNAs, indirect mechanisms were suspected to drive the observed up-regulation of NT5E surface expression upon miRNA transfection. During the validation of the library screen candidates it was seen, that the up-regulatory effects had a high consistency across different cancer cell lines. It was assumed, that the miRNAs, which drove NT5E surface expression, inhibit regulatory proteins such as transcription factors, that normally would repress NT5E expression. Thus, different strategies were applied to find the missing link between the miRNAs and the up-regulated NT5E levels. First, different *in silico* analyses were used to find promising targets. Then, it was globally screened for genes that are altered upon miRNA transfection by microarray gene expression profiling. Finally, the most promising targets were individually tested by siRNA knock-down experiments.

Bioinformatic predictions yielded several potential candidates explaining miRNA-mediated up-regulation of NT5E levels

Analysis of shared targets of miRNAs, that up-regulated NT5E in both cell lines used for the miRNA library screen, was already performed and is shown in table 4.14. From this analysis FOXP2 came up as a potential candidate, since this is a transcriptional repressor. Thus, FOXP2 was included for subsequent experiments. But based on NCI-60 expression data, we know, that FOXP2 was only weakly expressed in SK-Mel-28 and MDA-MB-231. It might be, that the NT5E enhancing miRNAs are regulating FOXP2, but that FOXP2 is not the effector driving the observed changes in NT5E expression. Next, TransmiR v2.0 database [233] was used to find transcription factors that are connected with the list of NT5E enhancing miRNAs. The enrichment analysis of TransmiR was used and the following miRNAs were entered for analysis: hsa-mir-134, hsa-mir-6514, hsa-mir-6859, hsa-mir-4672, hsa-mir-3126, hsa-mir-224, hsa-mir-34b, hsa-mir-1293 and hsa-mir-3116. The results are summarized in table 4.28. Only transcription factors with significant enrichment are shown. For these transcription factors it was checked, how many of the NT5E enhancing miRNAs exhibit a binding site based on miRmap. Also, the correlation of the transcription factor expression with the NT5E mRNA level was calculated for the NCI-60 data set. Furthermore, ten melanoma samples and five NHEM samples were sent for RNA sequencing and correlation of the selected transcription factors with NT5E levels was checked in this data set.

Table 4.28: Enrichment analysis with TransmiR v2.0. For the enriched TFs correlation with NT5E expression in two data sets was performed: NCI-60 data and expression data from ten melanoma and five NHEM samples (MM).

TF	Count	p-value	miR with BS	PCC NCI-60	PCC MM
KDM4A	3	0.03354925	9/10	-0.04	-0.57
FOXO3	1	0.03560158	8/10	0.09	0.37
MAZ	6	0.04064093	4/10	-0.59	-0.55
FOXA1	7	0.04372247	5/10	-0.27	0.18
TP73	2	0.04666879	8/10	-0.11	-0.11
SNAI1	1	0.05299111	6/10	-0.05	0.04

The transcription factor MYC Associated Zinc Finger Protein (MAZ) was connected to six of the miRNAs and showed strong negative correlation with NT5E expression in both data sets. But only four miRNAs also exhibited a binding site for MAZ. These four miRNAs were miR-134-3p, miR-1293, miR-6859-3p and miR-3126-5p. Lysine Demethylase 4A (KDM4A) exhibited a strong negative correlation with NT5E in the MM data set and nine miRNAs exhibited a potential binding site for the KDM4A 3'-UTR. Only miR-3126-5p had no binding site for KDM4A. TP73 expression was only slightly negatively correlated with NT5E levels but eight miRNAs could bind to TP73 3'-UTR. All transcription factors from table 4.28 were selected for further analysis.

For the revealed 11 transcription factors based on the EdgeStrength-Matrix, their correlation with NT5E expression in the NCI-60 data set was tested to extract the potential transcriptional repressors. The results of the correlation analysis are shown in table 4.29. Significant correlations with NT5E are marked in red or blue. Four transcription factors exhibited a significant correlation with NT5E expression across the NCI-60 panel. SMAD3 and SMAD5 were strongly positively correlated with NT5E and are likely transcriptional activators. But to find the missing link the focus was set on potential NT5E inhibitors. Thus, GFI1 and SP1, which showed significant negative correlation with NT5E, were of most interest. These two regulators are likely to be transcriptional repressors. Indeed, GFI1 is a transcriptional repressor and has been already described in literature to inhibit NT5E in murine cells [40]. SP1 is a transcription factor, that can activate or inhibit target gene expression. For these two potential NT5E inhibitors it was checked, whether the NT5E enhancing miRNAs would exhibit binding sites for their respective 3'-UTR. For SP1 only miR-6859-3p had a binding site. The other nine miRNAs were not predicted to interact with SP1 3'-UTR. Also, the expression level of SP1 in MDA-MB-231 and especially in SK-Mel-28 was really low. Thus, it was unlikely, that SP1 was the missing link. GFI1 was also weakly expressed in the two cell lines, but the levels were not as low as for SP1. And for GFI1, seven out of ten miRNAs exhibited a binding site for the GFI1 3'-UTR. Thus, GFI1 was included for further analysis.

Table 4.29: Correlation analysis with NT5E expression. NCI-60 data was used to assess the correlation of selected transcriptional regulators with NT5E. Also expression levels (z-score) for MDA-MB-231 and SK-Mel-28 are given. Significant correlations are marked in red or blue.

Transcription factor	Correlation	MDA-MB-231	SK-Mel-28
ATF1	-0.31	-0.30	-2.12
ATF2	-0.01	0.37	0.75
FOXP3	-0.17	-0.80	0.58
GFI1	-0.40	-0.20	-0.38
SMAD2	-0.06	-0.31	0.02
SMAD3	0.51	0.57	-0.40
SMAD4	0.12	0.09	-0.45
SMAD5	0.42	0.59	-0.55
SP1	-0.48	-0.45	-1.69
STAT3	-0.02	0.15	-0.99
TCF7	-0.17	-0.49	-0.50

For the RNA-Seq data from ten melanoma cell lines and five NHEM samples generated in this study, it was searched for genes that are significantly negatively associated with NT5E mRNA levels. The top ten genes with the highest negative correlation to NT5E expression are given in table 4.30. Also a short gene information is given as well as the number of NT5E enhancing miRNAs that harboured a potential binding site for the respective gene based on miRmap. There were some genes with a very strong negative association to NT5E levels like C-Terminal Src Kinase (CSK) or COMM Domain Containing 4 (COMMD4). Also the transcriptional repressor TCF25 exhibited a very strong negative correlation with NT5E expression. Nevertheless, none of the relevant miRNAs had a binding site for this transcription factor. Since overall only one gene was associated with more than half of the NT5E enhancing miRNAs, correlation analysis was repeated with a focus on genes, that are predicted to be regulated by a set of NT5E enhancing miRNAs. The results are shown in table 4.30. Only genes with negative correlation ($PCC < -0.4$) were considered. The top ten genes with highest number of predicted miRNAs regulating them are shown. Five genes were predicted to be regulated by seven of ten NT5E enhancing miRNAs. Especially Zinc Finger Protein 346 (ZNF346) appeared as promising, since its function involves binding to specific miRNA hairpins. Also CCR4-NOT Transcription Complex Subunit 6 Like (CNOT6L) was an interesting candidate targeted by six miRNAs. It has a 3'-5' poly(A) exoribonuclease activity and is linked to miRNA-mediated repression, translational repression and mRNA degradation. Since NT5E has a quite big 3'-UTR and is heavily regulated by miRNAs, a knock-down of a gene involved in this miRNA-mediated repression might enhance the overall NT5E levels observed upon transfection of the selected miRNAs. Also Ring Finger Protein 4 (RNF4) could be interesting to further study since it is known to be involved in transcriptional regulation. But the negative correlation in this data set was not significant. CNOT6L and ZNF346 were selected for subsequent experiments.

Table 4.30: Correlation analysis with NT5E expression. RNAseq data was used to find genes with strongest negative correlation to NT5E mRNA level across ten melanoma cell lines and five NHEM specimens. Top ten genes with highest negative Pearson's correlation coefficient (PCC) are shown. Also the number of NT5E enhancing miRNAs with potential binding sites (BS) are given.

Gene	PCC	p-value	Gene info	miR with BS
CSK	-0.91	< 0.0001	Non-receptor tyrosine-protein kinase	1/10
COMMD4	-0.91	< 0.0001	Downregulates NFkB	0/10
NELFA	-0.87	< 0.0001	Negative Elongation Factor Complex Member	4/10
POLR2E	-0.83	0.00013	RNA Polymerase II, I And III Subunit E	0/10
TIMM13	-0.82	0.00021	Mitochondrial intermembrane chaperon	6/10
TCF25	-0.81	0.00024	Acts as a transcriptional repressor	0/10
YBX1P1	-0.80	0.00033	Pseudogene	no data
AC012306.2	-0.80	0.00038	Novel Transcript	no data
AAMP	-0.78	0.00055	Angio Associated Migratory Cell Protein	2/10
TARBP2	-0.78	0.00055	Subunit of RISC Complex	1/10

Table 4.31: Correlation analysis with NT5E expression. RNAseq data was used to find genes with strongest negative correlation to NT5E mRNA level across ten melanoma cell lines and five NHEM specimens. Top ten gene with highest number of predicted miRNAs are given.

Gene	PCC	p-value	Gene info	miR with BS
ACAD9	-0.59	0.01942	acyl-CoA dehydrogenase	7/10
TRIM2	-0.54	0.03964	E3 ubiquitin-protein ligase	7/10
HNRNPA0	-0.51	0.05346	mRNA-binding component of ribonucleosomes	7/10
ZNF346	-0.49	0.06622	may bind to specific miRNA hairpins	7/10
RANBP10	-0.45	0.09251	act as an adapter protein	7/10
DNAJB12	-0.64	0.01042	acts as a co-chaperone	6/10
CNOT6L	-0.57	0.02685	mRNA degradation, miRNA-mediated repression	6/10
DRG2	-0.56	0.02898	GTP-binding protein known to function in the regulation of cell growth and differentiation	6/10
SORT1	-0.54	0.0382	sorting receptor in the Golgi compartment	6/10
RNF4	-0.47	0.07778	acts as a transcription regulator	6/10

Microarray analysis identified ARNT2 and MYBL2 as potential repressors of NT5E expression

To globally assess the changes upon miRNA transfection, microarray gene expression profiling was used. Therefore, MaMel-02 and MDA-MB-231 cells were transfected with NT5E enhancing miRNAs and RNA was isolated two days post transfection and sent for microarray profiling using Affymetrix Clarion S human chip. The transfection of MDA-MB-231 cells was performed by the master student Tsu-Yang Chao in our lab. Each condition was performed in triplicates and fold changes were calculated relative to mimic control-1 samples. There was a special interest in the down-regulated genes upon miRNA transfection. Thus, the analysis was focussed on genes, that were down-regulated compared to mimic control-1 which is reflected by fold change smaller than 0.5. The number of down-regulated genes for each miRNA and cell line are given in table 4.32. Also the overlap between the cell lines is given. To note, miR-1293 and miR-3116 were only tested in MaMel-02. miR-6514-3p and miR-224-3p were only tested in MDA-MB-231 cells. A mock condition (transfection reagent only) was tested and it was found that the difference between mock samples and mimic control-1 transfected samples was marginal. For MaMel-02, only six genes were down-regulated (FC < 0.5) compared to control-1, and in MDA-MB-231 only one gene was differentially lower expressed in mock. The first priority was to find common down-regulated target gene shared by most of transfected miRNAs and ideally also consistent between the different cell lines tested. Thus, it was searched for genes with the highest overlap between conditions. Overall, miR-34b-3p led to the lowest number of strongly decreased genes and seven targets were inhibited in both cell lines. For miR-134-3p, the highest overlap between the cell lines could be observed with 36 shared genes. For miR-4672, 25 genes were down-regulated in both cell lines and 22 genes for miR-6859-3p. For miR-3126-5p, 13 genes overlapped between MaMel-02 and MDA-MB-231.

Table 4.32: Number of genes with a fold change < 0.5 compared to mimic control-1 samples.

Gene	MaMel-02	MDA-MB-231	Overlap
miR-134-3p	99	168	36
miR-34b-3p	20	41	7
miR-3126-5p	87	155	13
miR-4672	125	82	25
miR-6859-3p	73	51	22
miR-6514-3p	NA	288	-
miR-224-3p	NA	98	-
miR-1293	158	NA	-
miR-3116	170	NA	-
mock	6	1	0

The overlap of down-regulated genes for MaMel-02 are depicted in figure 4.48. miR-34b-3p and miR-3116 were not included in this Venn diagram, since five gene lists was the maximum number for generating a Venn diagram with the tool used. But in table 4.33 the top-shared targets for all miRNAs are listed including information about how many miRNAs have a predicted binding site for the respective 3'-UTR. Nine genes were inhibited by at least four miRNAs. TKTL1 was inhibited by six of the seven miRNAs followed by PPTC7, which was decreased by five miRNAs. But both genes encode for enzymes rather related to metabolism and are probably not related to NT5E regulation. More interesting were transcription factors like ARNT2 and MYBL2, which were inhibited by four miRNAs.

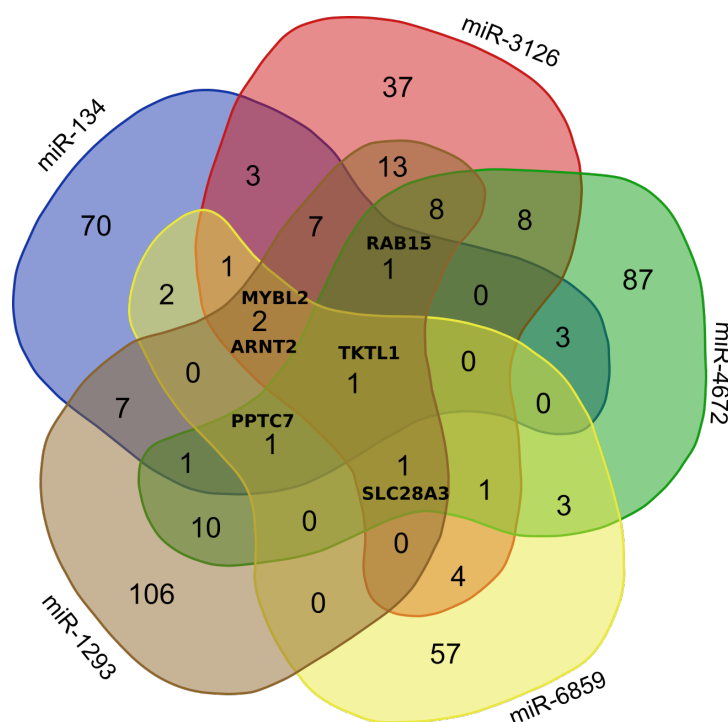


Figure 4.48: Venn diagram of down-regulated genes in MaMel-02. Overlap of down-regulated genes (fold change < 0.5) between different miRNAs are depicted.

Interestingly, the ARNT2 3'-UTR had binding sites for all seven miRNAs and the MYBL2 3'-UTR for five miRNAs, which made them promising candidates for further investigations. Also RAB15 and FURIN might be interesting for further testing. RAB15 is a GTPase involved in autophagy and protein metabolism. FURIN is an endoprotease that is important for activating TGF β 1.

Table 4.33: Top shared genes with a fold change < 0.5 compared to mimic control-1 samples for transfected MaMel-02. All genes, that were down-regulated by at least four miRNAs are shown.

Gene	No down	No BS	Gene info
TKTL1	6	2	Transketolase Like 1; This reaction links the pentose phosphate pathway with the glycolytic pathway; Protein phosphatase which positively regulates biosynthesis of the ubiquinone, coenzyme Q
PPTC7	5	6	Protein Phosphatase Targeting COQ7
RAB15	4	5	Member RAS Oncogene Family; Among its related pathways are Metabolism of proteins and Autophagy Pathway
ARNT2	4	7	Aryl Hydrocarbon Receptor Nuclear Translocator 2; Among its related pathways are Transcriptional misregulation in cancer; Transcription factor
MYBL2	4	5	MYB Proto-Oncogene Like 2, Transcription factor involved in the regulation of cell survival, proliferation, and differentiation. Transactivates the expression of the CLU gene
FURIN	4	6	Ubiquitous endoprotease; Mediates processing of TGF β 1, an essential step in TGF-beta-1 activation
MFSD2A	4	2	Sodium-dependent lysophosphatidylcholine (LPC) symporter
SLC28A3	4	4	Nucleoside transporters, such as SLC28A3, regulate multiple cellular processes, including neurotransmission, vascular tone, adenosine concentration in the vicinity of cell surface receptors
KCNN4	4	1	Forms a voltage-independent potassium channel that is activated by intracellular calcium

The overlap of down-regulated genes for MDA-MB-231 cells is depicted in figure 4.49. miR-34b-3p and miR-224-3p were not included in this Venn diagram. In table 4.34 the top-shared genes with a decreased expression for all miRNAs are listed. Overall, 20 genes were down-regulated compared to mimic control-1 (Fold change < 0.5) for at least five of the seven individually transfected miRNAs. 40 genes were inhibited by at least four miRNAs. Surprisingly, a majority of these genes were histones. But none of the histone genes except HIST2H2AA3 exhibited any binding sites for the investigated miRNAs within their 3'-UTR. Only miR-6514-3p had a predicted binding site for HIST2H2AA3 3'-UTR. Only the two genes Denticleless E3 Ubiquitin Protein Ligase Homolog (DTL) and Aurora Kinase A And Ninein Interacting Protein (AUNIP) exhibited a binding site for four miRNAs. DTL is involved in DNA damage pathways, cell cycle control and also has connection to TGF β signalling.

Also AUNIP is involved in DNA damage mechanisms. A direct link of these genes to NT5E seems unlikely. To uncover further more relevant genes, it was decided to specifically look for genes exhibiting a significant negative correlation with NT5E mRNA levels. Therefore, the Pearson's correlation coefficient was calculated for all genes with NT5E levels across all 27 MaMel-02 samples and all 27 MDA-MB-231 samples, respectively. In total, there were 194 genes with a significant negative correlation ($PCC < -0.38$) in both cell lines. For the ten genes, with the best correlation in both cell lines, it was checked whether these genes have potential binding sites within their 3'-UTR for the ten NT5E enhancing miRNAs. The results are summarized in table 4.35. The strongest negative correlation with NT5E expression was found for Proline Rich Coiled-Coil 2A (PRRC2A). But none of the ten NT5E enhancing miRNAs had a predicted binding site for this gene. The second strongest negative correlation was observed for ARNT2. Excitingly, all ten NT5E enhancing miRNAs had a predicted binding site for ARNT2 3'-UTR. The ARNT2 transcription factor was a very promising candidate for the missing link and will be further investigated. The ARNT and ARNT2 transcription factors belong to the family of basic helix-loop-helix Period/ARNT/Single-minded (bHLH PAS) and form heterodimers with hypoxia-inducible factors 1 and 2 (HIF-1/2) or aryl hydrocarbon receptor (AHR) [97].

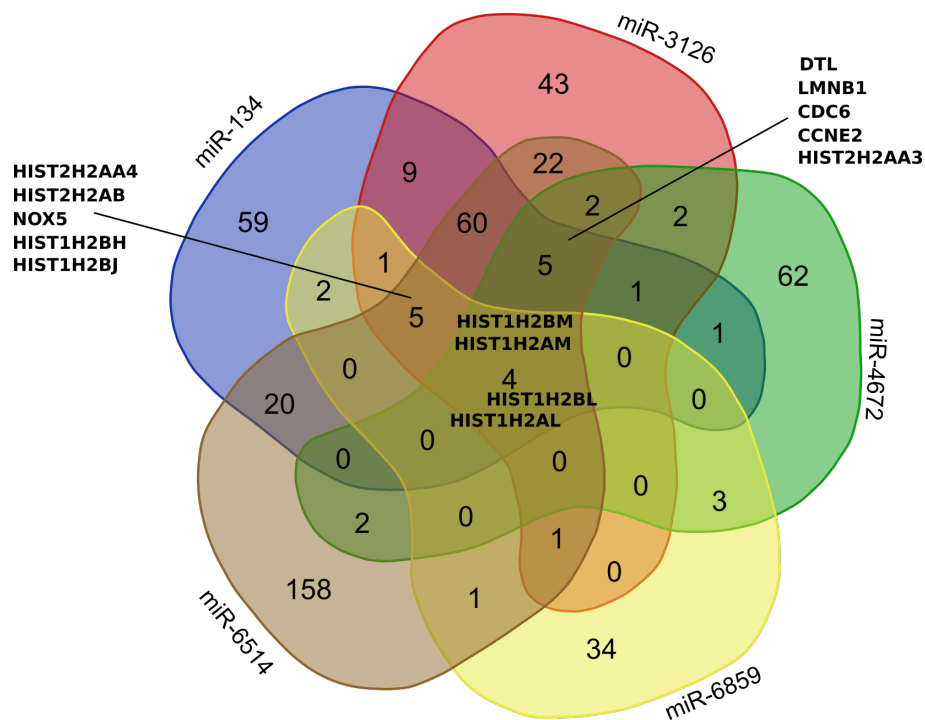


Figure 4.49: Venn diagram of down-regulated genes in MDA-MB-231. Overlap of down-regulated genes (fold change < 0.5) between different miRNAs are depicted.

Table 4.34: Top shared genes with a fold change < 0.5 compared to mimic control-1 samples for transfected MDA-MB-231. All genes, that were down-regulated for by least five miRNAs are shown.

Gene	No down	No BS	Gene info
HIST1H2BM	7	0	Histone, core component of nucleosome
HIST1H2BL	7	0	Histone, core component of nucleosome
HIST1H2AM	7	0	Histone, core component of nucleosome
HIST2H2AA3	6	1	Histone, core component of nucleosome
HIST2H2AA4	6	0	Histone, core component of nucleosome
HIST1H2AL	6	0	Histone, core component of nucleosome
HIST1H2BJ	6	0	Histone, core component of nucleosome
DTL	5	4	Denticleless E3 Ubiquitin Protein Ligase Homolog
AUNIP	5	4	Aurora Kinase A And Ninein Interacting Protein
HIST2H2AB	5	0	Histone, core component of nucleosome
RFC4	5	1	Replication Factor C Subunit 4
CENPU	5	2	Centromere Protein U
HIST1H2BH	5	0	Histone, core component of nucleosome
HIST1H3B	5	0	Histone, core component of nucleosome
CCNE2	5	3	Cyclin E2
FAM111B	5	1	trypsin-like cysteine/serine peptidase
POLE2	5	1	DNA polymerase epsilon, which is involved in DNA repair and replication
NOX5	5	1	NADPH Oxidase 5
CDC6	5	3	Cell Division Cycle 6
KIF15	5	1	Kinesin Family Member 15

Table 4.35: Top ten genes with highest negative correlation to NT5E mRNA levels. Pearson's correlation coefficient (PCC) were calculated for all 27 MDA-MB-231 (MDA231) and all 27 MaMel-02 (MM02) samples, respectively. Potential binding sites for NT5E enhancing miRNAs were obtained with miRmap.

Gene	PCC MDA231	PCC MM02	No BS	Gene info
PRRC2A	-0.884	-0.573	0	may play a role in the regulation of pre-mRNA splicing
ARNT2	-0.537	-0.913	10	transcription factor
WDR82	-0.775	-0.628	6	regulatory component of the SET1 complex implicated in the tethering of this complex to transcriptional start sites of active genes
ACSL1	-0.577	-0.791	5	long-chain fatty-acid-coenzyme A ligase
STXBP1	-0.552	-0.816	8	Syntaxin Binding Protein 1
TMEM214	-0.814	-0.527	4	critical mediator, in cooperation with CASP4, of endoplasmic reticulum-stress induced apoptosis
FBL	-0.761	-0.562	0	S-adenosyl-L-methionine-dependent methyltransferase
WDR5	-0.645	-0.667	3	contributes to histone modification
TM9SF4	-0.761	-0.536	7	associates with proteins harboring glycine-rich transmembrane
ZNHIT3	-0.665	-0.628	4	Zinc Finger HIT-Type Containing 3

To find the missing link between miRNAs and elevated NT5E levels, the following genes were selected for further analysis: **ARNT2**, **CNOT6L**, **COMMD4**, **FOXP2**, **FURIN**, **GFI1**, **MAZ**, **MYBL2**, **PPTC7**, **TP73** and **ZNF346**.

The expression of these genes and changes upon miRNA transfection are shown in figure 4.50 for MaMel-02 and in figure 4.51 for MDA-MB-231. Also the effect on NT5E was included. For both cell lines all transfected miRNAs could significantly increase NT5E expression.

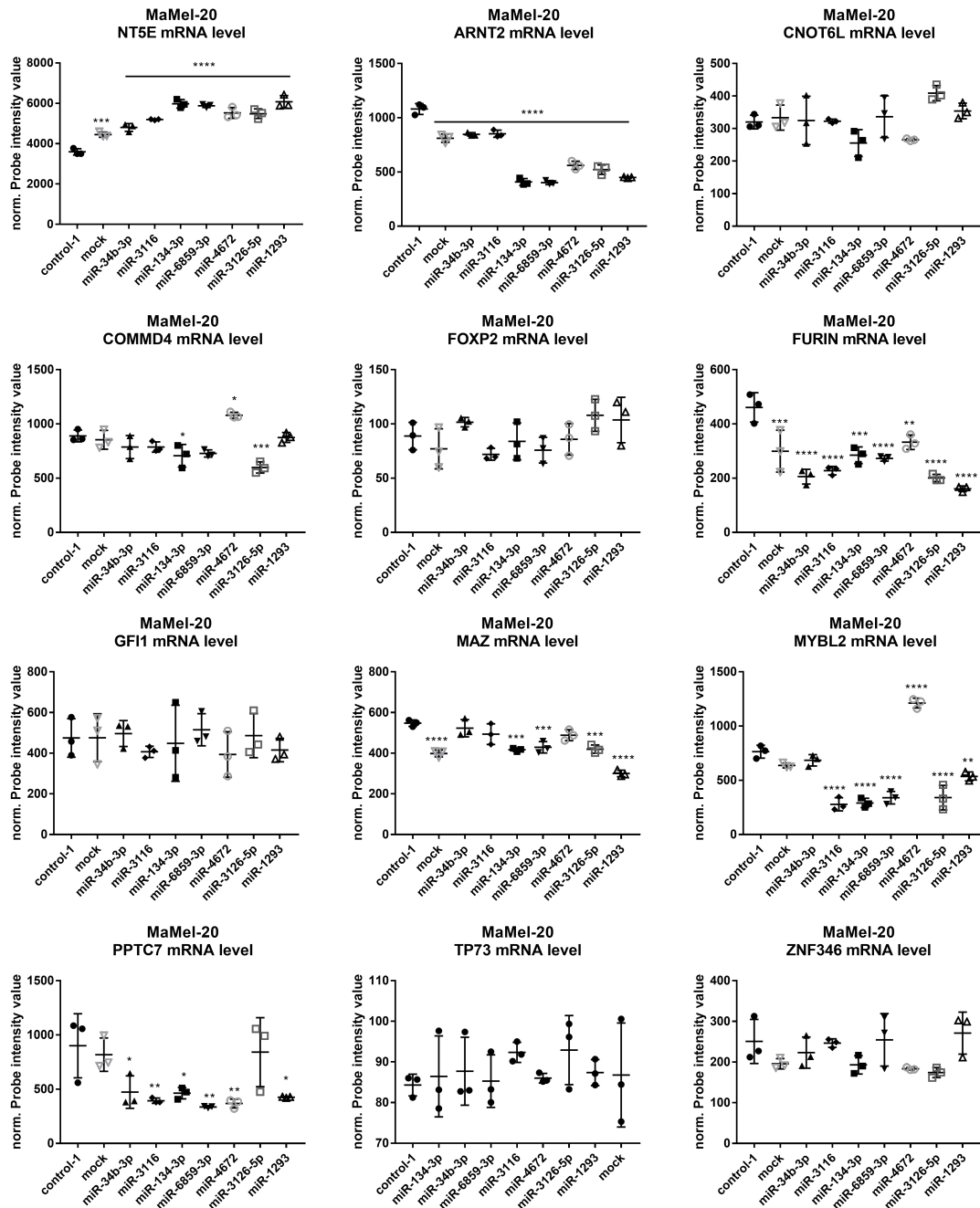


Figure 4.50: Expression of selected genes in MaMel-02 cells. Expression data from microarray experiment are shown for candidates genes that might drive the observed NT5E up-regulation upon miRNA transfection. One-way ANOVA was performed to calculate p-values always comparing to mimic control-1. *: $p < 0.05$, **: $p < 0.01$, ***: $p < 0.001$, ****: $p < 0.0001$.

Strikingly, ARNT2 expression was significantly lower for all transfected miRNAs except miR-6514-3p in both cell lines. Only the decrease mediated by miR-6514-3p in MDA-MB-231 was not significant. For CNOT6L no significant changes in MaMel-02 could be observed. In MDA-MB-231 cells, miR-224-3p, miR-134-3p and miR-4672 led to significant inhibition of CNOT6L.

FOXP2 expression was very low in both cell lines, and no changes upon miRNA transfection could be measured. COMMD4 showed quite sustained expression in both cell lines. In MaMel-02 cells miR-134-3p and miR-3126-5p could lower COMMD4 expression whereas miR-4672 increased COMMD4 levels. For MDA-MB-231 cells five of seven transfected miRNAs significantly reduced COMMD4 mRNA levels. Only miR-4672 and miR-224-3p had no effect. FURIN levels were strongly decreased by all transfected miRNAs for MaMel-02. In MDA-MB-231 cells, only miR-34b-3p and miR-3126-5p could decrease FURIN mRNA levels and miR-224-3p even led to an increase in expression levels. For the already known NT5E inhibitor GF11, no significant alterations could be detected upon miRNA transfection. MAZ mRNA levels could be significantly repressed in MaMel-02 cells by miR-134-3p, miR-6859-3p, miR-3126-5p and miR-1293. In MDA-MB-231 cells also a significant reduction of MAZ levels caused by miR-134-3p, miR-3126-5p and miR-6859-3p were observed. But miR-224-3p and miR-4672 strongly enhanced MAZ expression. MYBL2 levels were lowered by six of the seven transfected miRNAs in MDA-MB-231 cells. Only miR-4672 had no significant effect. In MaMel-02 cells also most miRNAs drastically decreased MYBL2 levels, except for miR-34b-3p and even a strong increase could be measured upon miR-4672 treatment. For TP73, the basal expression levels were quite low and only in MDA-MB-231 cells a significant reduction caused by miR-224-3p and miR-6514-3p could be detected. Regarding the ZNF346 no changes in both cell lines were determined. But PPTC7 levels were significantly altered. In MDA-MB-231 cells, miR-224-3p, miR-6859-3p, miR-4672 and miR-6514-3p reduced PPTC7 levels whereas miR-3126-5p caused an up-regulation. In MaMel-02 cells six miRNAs caused a significant reduction of PPTC7 expression and only miR-3126-5p had no effect compared to mimic control-1.

The next step would be to test by siRNA-mediated knock-down, whether the selected genes really have an impact on NT5E expression levels. Ideally, the siRNA treatment would enhance NT5E expression and mimic the observed effects of the NT5E enhancing miRNAs. Most promising candidates for such knock-down experiments were ARNT2, MAZ, MYBL2 and COMMD4. Furthermore, the miRNA mediated inhibition of those genes should be verified in additional independent experiments and a direct interaction must be proven by luciferase reporter assays.

To get more information on the selected genes and their potential interaction with NT5E, the ConTraV3 tool was used to check for potential binding sites within the NT5E promoter [130]. It was investigated whether the following transcription factors have a binding site within the NT5E promoter: ARNT2, FOXP2, GF11, MAZ, MITF, MYBL2, SOX9 and TP73. SOX9 was included, since this transcription factor was enriched for target genes of NT5E enhancing miRNAs as well as for the miRNAs that activated NT5E and ENTPD1 surface expression. SOX9 might be a relevant regulator of both surface enzymes. FOXP2 was included, since it

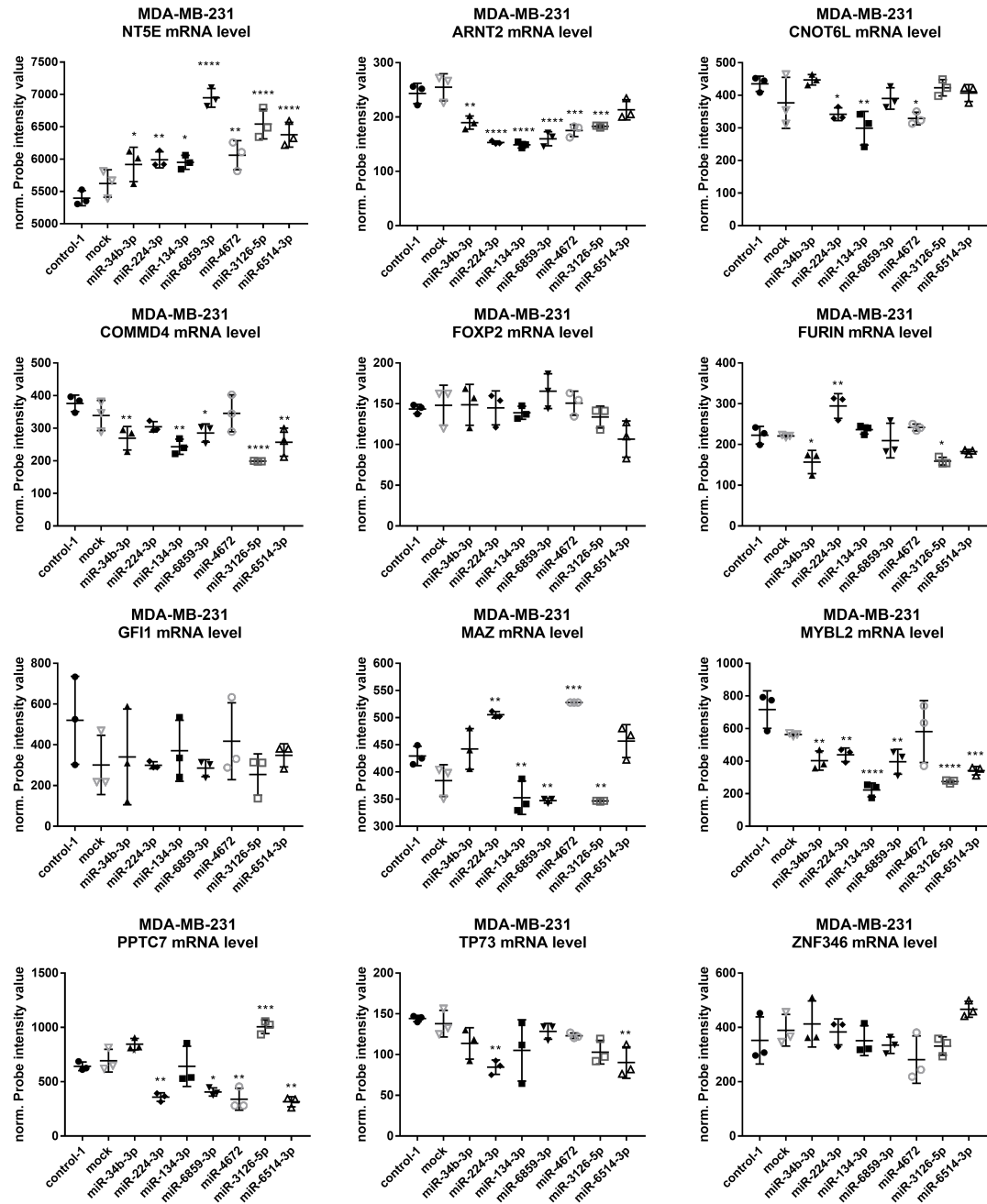


Figure 4.51: Expression of selected genes in MDA-MB-231 cells. Expression data from microarray experiment are shown for candidates genes that might drive the observed NT5E up-regulation upon miRNA transfection. One-way ANOVA was performed to calculate p-values always comparing to mimic control-1. *: $p < 0.05$, **: $p < 0.01$, ***: $p < 0.001$, ****: $p < 0.0001$.

was among the top shared targets of miRNAs up-regulating NT5E in both cell lines used for the library screen. GFI1 was included, since it was one of the few already known transcriptional repressors of NT5E. MITF was also used for this analysis, since this key regulator in melanocytes and melanoma cells was identified by Tsu-Yang Chao in our lab to be amongst the most important regulators of differentially expressed genes caused by miRNA transfection.

tion. The outcome of the ConTraV3 analysis is shown in figure 4.52. For five transcription factors, binding motifs within the NT5E promoter were found. MITF exhibits one binding site within the front part of the promoter. MYBL2 exhibits three distinct binding sites as well as GFI1. For SOX9 also one binding site could be determined. The highest number of potential binding sites was found for FOXP2. In total, the NT5E promoter contained four distinct motifs for potential FOXP2 binding. For ARNT2, MAZ and TP73 no motifs were found within the NT5E promoter. Either these regulators can bind to other regulatory elements e.g. in 5'-UTR or 3'-UTR of NT5E or they might exert their potential negative function indirectly e.g. by targeting other regulators involved in controlling NT5E expression. Interestingly, comparison with the mouse *Nt5e* promoter revealed several binding sites for SOX9 and one binding site for MYBL2 and FOXP2, respectively.

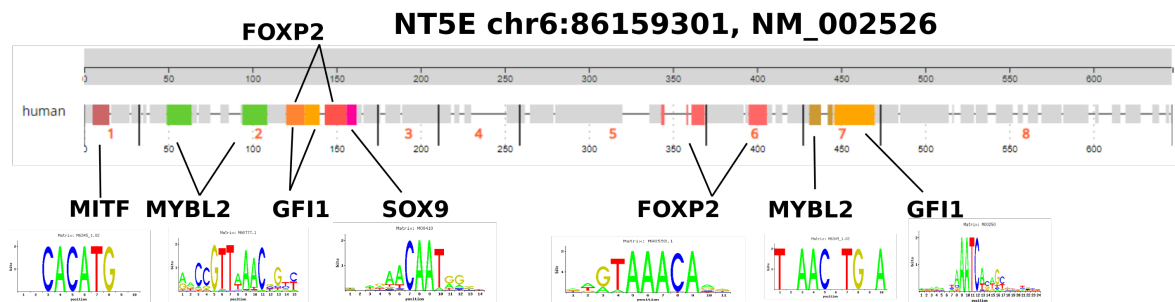


Figure 4.52: Binding motifs within human NT5E promoter. ConTraV3 tool was used to assess potential binding sites of transcriptional regulators suspected to inhibit NT5E expression. The NM002526 RefSeq data was used as the input sequence for NT5E and it was searched for binding sites within the promoter region (500-bp upstream). The stringency parameters were set to core = 0.95 and similarity matrix = 0.85.

4.11. From human to mouse

For the top miRNA candidates regulating immune checkpoint molecules NT5E or CD274 it was checked, whether these miRNAs are conserved between mouse and man and whether these miRNAs also regulate the corresponding target gene in *Mus musculus*.

4.11.1 Several miRNAs regulating NT5E are conserved between man and mouse

Search for orthologous miRNAs was performed for 18 selected miRNAs, that showed a down-regulation of NT5E levels in the miRNA library screen in both tested cell lines. In addition, also the miRNAs showing the strongest effect for each individual cell lines were included. Here, only miRNAs with a predicted binding site within the 3'-UTR of NT5E were considered. In table 4.37 the human miRNAs with their corresponding sequences are compared with the murine miRNA sequence. Non matching nucleotides are marked in red. For ten miRNAs no corresponding mouse miRNA could be found. The following five miRNAs were fully conserved between mouse and man: miR-92b-3p, miR-22-3p, miR-193a-3p, miR-143-5p and miR-148b-3p. miR-1298-3p also had a corresponding mouse orthologous miRNA only differing by one nucleotide at the end of the mmu-miR-1298-3p sequence. Also miR-376c-3p had a mouse orthologous miRNA only differing in one nucleotide compared to the human sequence. For miR-520d-3p also a corresponding mouse miRNA could be found by searching for sequence similarity. The matching mouse miRNA was mmu-miR-294-3p, differing in four nucleotides to hsa-miR-520d-3p. For the eight miRNAs which were conserved in mouse, it was tested whether these miRNAs also exhibited binding sites in the mouse Nt5e 3'-UTR. Using miRmap the number of binding sites was checked and the results are summarized in table 4.38.

Five of the eight conserved miRNAs had one binding site within the mouse Nt5e 3'-UTR. The direct binding of hsa-miR-22-3p and hsa-193a-3p in the human NT5E 3'-UTR was proven by luciferase reporter assay. Also the orthologous miRNAs in *Mus musculus* could bind Nt5e 3'-UTR.

Table 4.36: Binding sites of conserved miRNAs in Nt5e 3'-UTR.

miRNA	Number binding sites
mmu-miR-22-3p	1
mmu-miR-193a-3p	1
mmu-miR-92b-3p	0
mmu-miR-1298-3p	0
mmu-miR-376c-3p	0
mmu-miR-143-5p	1
mmu-miR-148b-3p	1
mmu-miR-294-3p	1

Table 4.37: Sequence comparison of miRNAs regulating NT5E in humans.

miRNA	miRNA sequence
hsa-miR-92b-3p	UAUUGCACUCGUCCCCGGCCUCC
mmu-miR-92b-3p	UAUUGCACUCGUCCCCGGCCUCC
hsa-miR-22-3p	AAGCUGCCAGUUGAAGAACUGU
mmu-miR-22-3p	AAGCUGCCAGUUGAAGAACUGU
hsa-miR-193a-3p	AACUGGCCUACAAAGUCCCAGU
mmu-miR-193a-3p	AACUGGCCUACAAAGUCCCAGU
hsa-miR-8056	CGUGGAUUGUCUGGAUGCAU
not conserved	—
hsa-miR-1298-3p	CAUCUGGGCAACUGACUGAAC
mmu-miR-1298-3p	CAUCUGGGCAACUGAUUGAACU
hsa-miR-3118	UGUGACUGCAUUAUGAAAUUCU
not conserved	—
hsa-miR-1285-5p	GAUCUCACUUUGUUGCCCAGG
not conserved	—
hsa-miR-4647-5p	GAAGAUGGUGCUGUGCUGAGGAA
not conserved	—
hsa-miR-3134	UGAUGGAUAAAAGACUACAUUU
not conserved	—
hsa-miR-5584-3p	UAGUUCUUCCCUUGCCCAAUU
not conserved	—
hsa-miR-1233-3p	UGAGCCCUGUCCUCCCGCAG
not conserved	—
hsa-miR-512-3p	AAGUGCUGUCAUAGCUGAGGUC
not conserved	—
hsa-miR-376c-3p	AACAUAGAGGAAAUUCCACGU
mmu-miR-376c-3p	AACAUAGAGGAAAUUCACGU
hsa-miR-143-5p	GGUGCAGUGCUGCAUCUCUGGU
mmu-miR-143-5p	GGUGCAGUGCUGCAUCUCUGG
hsa-miR-5190	CCAGUGACUGAGCUGGAGCCA
not conserved	—
hsa-miR-4480	AGCCAAGUGGAAGUUACUUUA
not conserved	—
hsa-miR-520d-3p	AAAGUGCUCUCUUCUUUGGUGGGU
mmu-miR-294-3p	AAAGUGCUCUCUUCUUUGUGUGU
hsa-miR-148b-3p	UCAGUGCAUCACAGAACUUUGU
mmu-miR-148b-3p	UCAGUGCAUCACAGAACUUUGU

4.11.2 Compared to NT5E less miRNAs regulating CD274 are conserved between man and mouse

Among the miRNAs which showed the strongest decreasing effect (z-score < -2.0) on CD274 expression in the miRNA library screen, only four miRNAs were conserved in mouse. Thus, all 111 miRNAs with a significant decreasing effect on CD274 levels (z-score < -1.645) were analysed for murine orthologous miRNAs. Only for 15 miRNAs orthologous miRNAs were found. These miRNAs are listed in table 4.39. Six miRNAs including miR-151a-5p, miR-330-3p or miR-214-3p were fully conserved between man and mouse with 100 % sequence similarity. Four miRNAs differed in only one or two nucleotides like miR-222-3p or miR-380-5p. For five miRNAs the sequences between man and mouse were more dissimilar e.g. miR-7-2-3p.

Seven of the fifteen conserved miRNAs exhibited at least one binding site within the mouse Cd274 3'-UTR. The highest amount of distinct binding sites was found for mmu-miR-7a-3p with six binding sites, followed by mmu-miR-146a-5p with four binding sites.

Table 4.38: Binding sites of conserved miRNAs in Cd274/Pd11 3'-UTR.

miRNA	Number binding sites
mmu-miR-222-3p	0
mmu-miR-380-5p	0
mmu-miR-6769b-3p	0
mmu-miR-218-1-3p	2
mmu-miR-330-3p	0
mmu-miR-219a-2-3p	1
mmu-miR-6769b-5p	2
mmu-miR-122b-5p	1
mmu-miR-146a-5p	4
mmu-miR-330-5p	0
mmu-miR-7a-2-3p	6
mmu-miR-214-3p	3
mmu-miR-876-3p	0
mmu-miR-511-5p	0
mmu-miR-151-5p	0

Table 4.39: Sequence comparison of miRNAs regulating CD274 in humans. Differences in sequences are marked in red.

miRNA	miRNA sequence
hsa-miR-222-3p	AGCUACAUCUGGCUACUGGGU
mmu-miR-222-3p	AGCUACAUCUGGCUACUGGGU CU
hsa-miR-380-5p	UGGUUGACCAUAGAACAUGCG C
mmu-miR-380-5p	AUGGUUGACCAUAGAACAUGCG
hsa-miR-6769b-3p	CCUCUC UGUCCCACCCA UAG
mmu-miR-6769b-3p	CAUCUUC CCUGUCCCACCC AG
hsa-miR-218-1-3p	AUGGUUCCGUCAAGCACC AUGG
mmu-miR-218-1-3p	AAACA AUGGUUCCGUCAAGCACC
hsa-miR-330-3p	GCAAAGCACACGGCCUGCAGAGA
mmu-miR-330-3p	GCAAAGCACAGGGCCUGCAGAGA
hsa-miR-219a-2-3p	AGAAUUGUGGCUGGACAUCUGU
mmu-miR-219a-2-3p	AGAAUUGUGGCUGGACAUCUGU
hsa-miR-6769b-5p	UGGUGGGUGGGGAGGAGAAGUGC
mmu-miR-6769b-5p	CCUGGUGGGUGGGGAAGAGC
hsa-miR-122b-5p	UUUAGUGUGAUAAUGGCGUUUG A
mmu-miR-122b-5p	UUUAGUGUGAUAAUGGCGUUUG
hsa-miR-146a-5p	UGAGAACUGAAUCCAUGGGUU
mmu-miR-146a-5p	UGAGAACUGAAUCCAUGGGUU
hsa-miR-330-5p	UCUCUGGGCCUGUGUCUUAGGC
mmu-miR-330-5p	UCUCUGGGCCUGUGUCUUAGGC
hsa-miR-7-2-3p	CAACAAA U CCCAGUCU ACCUAA
mmu-miR-7a-2-3p	CAACAA G UCCCAGUCU GCCACA
hsa-miR-214-3p	ACAGCAGGCACAGACAGGCAGU
mmu-miR-214-3p	ACAGCAGGCACAGACAGGCAGU
hsa-miR-876-3p	UGGUGGUUU ACAAAGUAAUUCA
mmu-miR-876-3p	UAGUGGUUU ACAAAGUAAUUCA
hsa-miR-511-5p	GUGU CUUUUGCUCUGCA G UCA
mmu-miR-511-5p	AUGC CUUUUGCUCUGCA C UCA
hsa-miR-151a-5p	UCGAGGAGCUCACAGUCUAGU
mmu-miR-151-5p	UCGAGGAGCUCACAGUCUAGU

4.11.3 Effect of miRNAs on NT5E could not be recapitulated in mouse cell line EO771-OVA-Luc⁺

Since T cell assays and *in vivo* experiments could be more easily implemented in mouse model, the effect of validated miRNAs was tested also in the murine breast cancer cell line EO771-OVA-Luc⁺, which is known to express Nt5e [212, 224]. After comparing sequence similarities between human and murine miRNAs that could potentially regulate Nt5e and Cd274 in the murine system, the effects of the miRNAs in mouse breast cancer cell line EO771-OVA-Luc⁺ were tested. Also the non-conserved miRNAs were tested. For the following experiments EO771 cell line stably expressing OVA and luciferase was utilized. Since this cell line is a suitable target for killing assays, as there is an established OVA specific CTL line available in our lab. By measuring luciferase signal intensity, the amount of killed cancer cells can be easily monitored.

EO771-OVA-Luc⁺ cells were transfected with 50 nM miRNA or siRNA pool targeting Nt5e. Two days post transfection the effect on Nt5e mRNA levels was assessed by qPCR and three days post transfection the effect on Nt5e surface expression was measured by FACS. Also, the change in Cd274 mRNA and surface levels were measured, since this could also impair the T cell mediated killing. The results are shown in figure 4.53 and figure 4.54. miR-22-3p and miR-193a/b-3p showed strong decreasing effect on NT5E in human cancer cells. But in EO771-OVA-Luc⁺ cells this could not be detected on mRNA levels as well as on surface expression levels. Although these miRNAs are conserved between mouse and human and are also predicted to bind to the murine Nt5e 3'-UTR. miR-4480, miR-1285-5p and miR-3134 showed, similar to human cells, a reduction in Nt5e mRNA levels. Interestingly, none of the up-regulatory miRNAs showed a comparative effect in murine EO771-OVA-Luc⁺ cells. Most of them even led to contrary results and decreased Nt5e mRNA levels upon transfection, like miR-6514-3p and miR-224-3p. To note, miR-4480 and miR-3134 not only strongly decreased Nt5e, but also Cd274 mRNA levels. Regarding cell surface levels miR-6514-3p, miR-4672 and miR-3126-5p enhanced Nt5e expression like in human cancer cells. But miR-134-3p, which was one of the top-enhancing miRNAs, exerts an opposite effect in EO771-OVA-Luc⁺ cells and led to decreased Nt5e levels. Also, the top inhibiting miRNA miR-1285-5p did not show the same effect in murine cells. miR-422a, miR-3118 and miR-3134 could decrease Nt5e surface levels. Also, miR-4480 and miR-193a-3p slightly decreased Nt5e surface expression. But only the siRNA pool could strongly decrease Nt5e expression at cell surface.

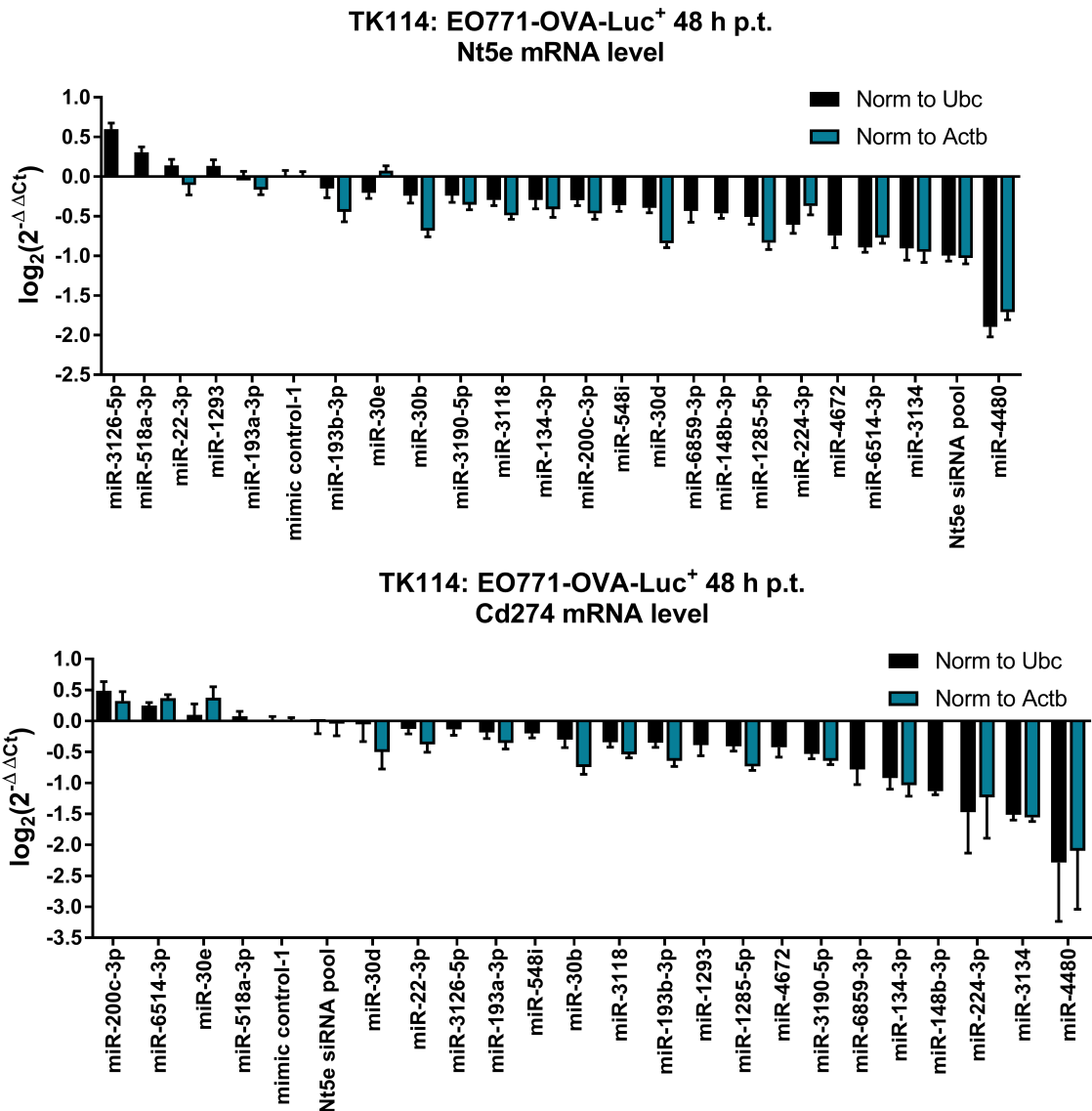
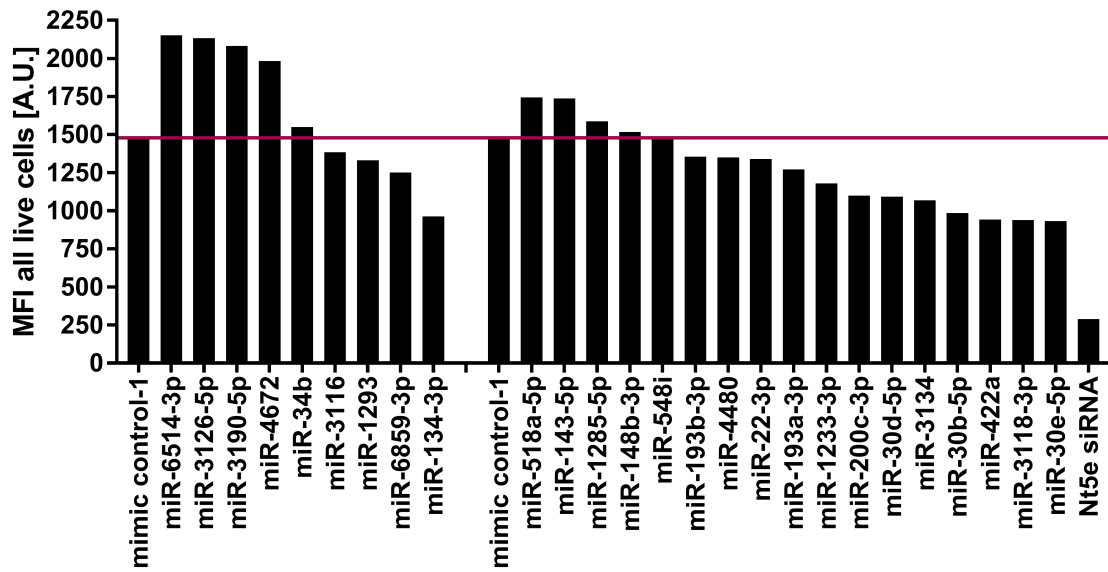


Figure 4.53: Change in Nt5e and Cd274 mRNA levels in transfected EO771-OVA-Luc⁺ cells. 48 h post transfection with 50 nM miRNA or siRNA cells were harvested and expression levels were measured by qPCR using Ubc and Actb as housekeeping genes. Fold changes were calculated to mimic control-1 condition.

TK116: EO771-OVA-Luc⁺ 72 h p.t.
Nt5e surface level



TK116: EO771-OVA-Luc⁺ 72 h p.t.
Cd274 surface level

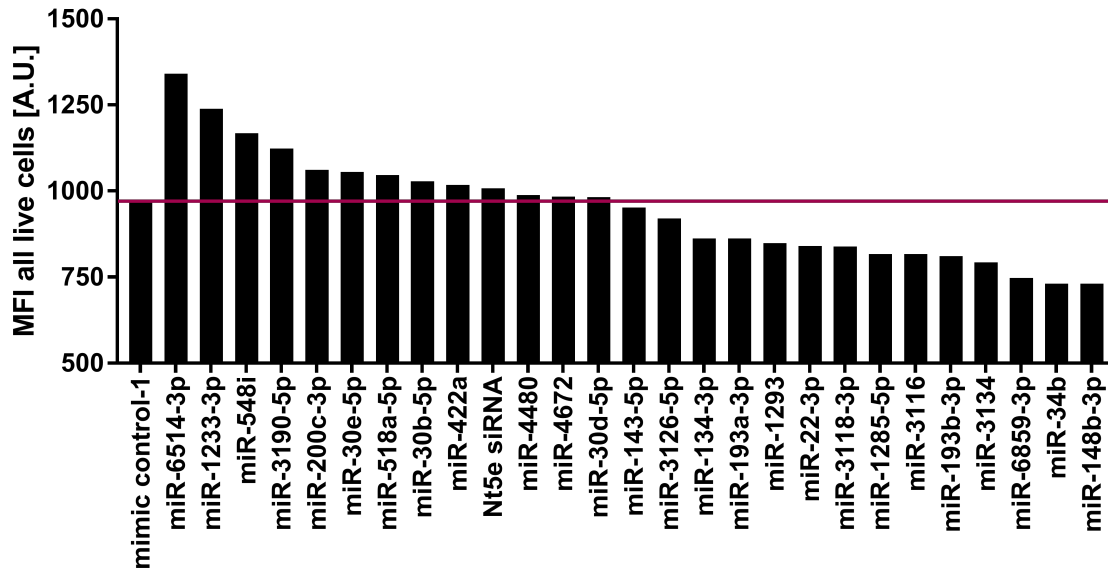


Figure 4.54: Change in Nt5e and Cd274 surface levels in transfected EO771-OVA-Luc⁺ cells. Three days post transfection Nt5e and Cd274 surface expression was measured by FACS

4.11.4 Effect of miRNAs on CTL lysis

First, the effect of AMP addition to the co-culture of the OVA-specific CTL line with EO771-OVA-Luc⁺ cells was tested. 6000 CTLs per well were co-cultured with 10.000 tumor cells for 24 h. The luciferase signal was measured to assess the amount of remaining viable cancer cells. As shown in figure 4.55, the addition of CTLs without addition of AMP killed around 94 % of all cancer cells. With the addition to AMP to the co-culture, significantly less cancer cells were killed compared to 0 mM AMP. For example, upon addition of 1 mM AMP the CTLs killed around 87.5 % of all cancer cells. Compared to 0 mM AMP twice as much cancer cells survived. But still killing was quite strong and in further assays a lower effector to target ratio should be used, so that miRNA-mediated changes in killing can be monitored more easily.

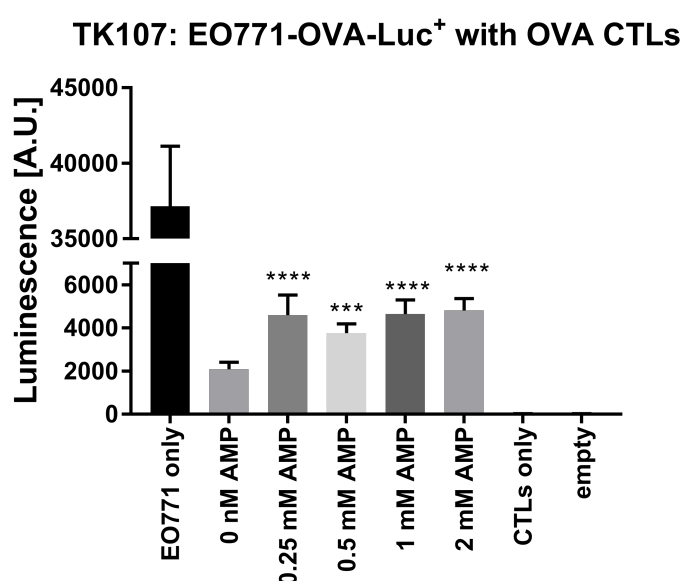


Figure 4.55: Effect of AMP on CTL mediated killing of EO771-OVA-Luc⁺ cancer cells. 10.000 EO771-OVA-Luc⁺ cells were co-cultured with 6000 OVA-specific CTLs per well in 96-well plate without AMP or with addition of different concentrations of AMP. After 24 h, the luciferase signal intensity was measured to estimate the amount of viable cancer cells. Significance was assessed by one-way ANOVA using Dunnett's multiple comparison test. Samples with AMP addition were compared to 0 nM AMP. Four replicates were performed per condition. *: $p < 0.05$; **: $p < 0.01$; ***: $p < 0.001$; ****: $p < 0.0001$

Before testing effect of miRNAs on CTL lysis, their effect on EO771-OVA-Luc⁺ cell viability *per se* was tested since this could interfere with the CTL activity in the functional assays. Therefore, EO771-OVA-Luc⁺ cells were seeded in 96-well plate and transfected with 50 nM miRNA or Nt5e siRNA pool. After two days cell viability was assessed with XTT-Assay. The results are shown in figure 4.56. Some miRNAs had great impact on EO771-OVA-Luc⁺ cell survival like miR-1285-5p, which significantly decreased cell number compared to mimic control-1. Also, miR-22-3p and miR-4672 significantly lowered EO771-OVA-Luc⁺ cell number. Whereas miR-148b-3p and miR-6514-3p showed a tendency of enhancing cell proliferation, but these effects were not significant.

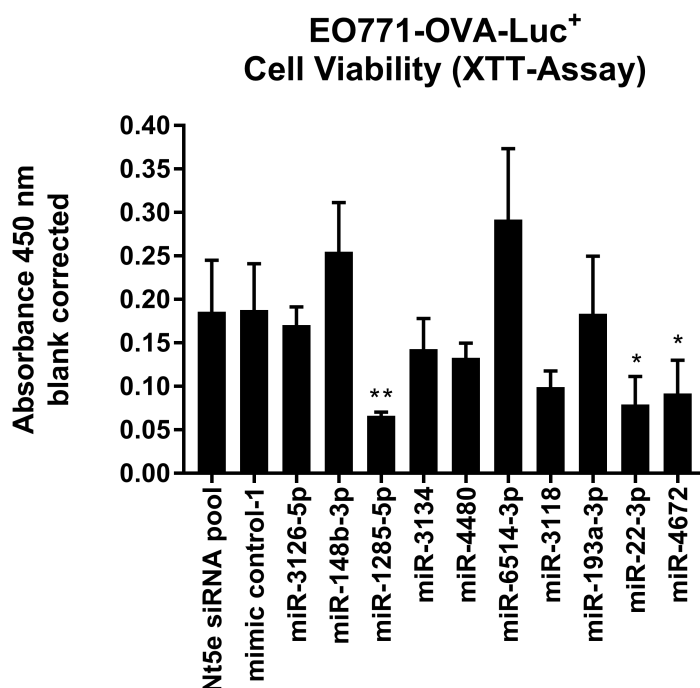


Figure 4.56: Effect of miRNAs on viability of transfected EO771-OVA-Luc⁺ cancer cells 48 h post transfection. All samples were compared to mimic control-1. Four replicates were performed per miRNA. *: $p < 0.05$; **: $p < 0.01$.

To account for potential effect on cell proliferation caused by the transfected miRNAs, the assay was performed with the following conditions: no AMP + no CTLs, no AMP + CTLs, AMP + no CTLs, AMP + CTLs. The results are conducted in figure 4.57 and 4.59.

As observed before, miR-1285-5p had a huge impact on viability of EO771-OVA-Luc⁺ cells *per se*. First, we compared the effect of added AMP to EO771-OVA-Luc⁺ cells alone, without the addition of CTLs. For five out of 12 tested miRNAs we observed significant differences between 0 mM and 1 mM AMP. For miR-4480, miR-6514-3p, miR-3118 and miR-193a-3p the luciferase signal was significantly higher in 1 mM AMP condition reflecting a higher number of EO771-OVA-Luc⁺ cells. For these miRNAs somehow the cell proliferation increased when AMP was added. Only for miR-4672, cell number of EO771-OVA-Luc⁺ was significantly lower in 1 mM AMP treated group. EO771-OVA-Luc⁺ cells have a high expression of Adora2b receptor. Mittal and co-workers showed that knockdown of Adora2b in EO771 cells led to reduced cell viability and proliferation [166]. Interestingly, miR-4672 has two bindings sites for the Adora2b 3'-UTR. Moreover, human miR-4672 is also predicted to bind to ADORA2B 3'-UTR. It could be, that miR-4672 reduces the expression level of the Adora2b receptor, which in turn could lead to lower cell viability. Maybe miR-4480, miR-6514-3p, miR-3118 and miR-193a-3p have an increasing effect on Adora2b expression, which might explain the higher cell viability. To further understand the direct effects of AMP and adenosine on EO771-OVA-Luc⁺ cells, it would be worth checking Adora2b mRNA expression changes after miRNA transfections. Next, we compared the effects of AMP on co-culture of EO771-OVA-Luc⁺ cells and CTLs as depicted on the lower graph of figure 4.57. In six of the 12 tested miRNAs we observed significant differences between 0 mM AMP and 1 mM AMP groups. For miR-1285-

5p, miR-3134, miR-6514-3p, miR-3118 and miR-22-3p a higher proportion of viable target cells was left upon CTL co-culture, if AMP was added. In general, it would be expected, that addition of AMP and subsequent production of adenosine decreases the killing of cancer cells, since the CTL function is inhibited by adenosine. Only for miR-4672 the opposite effect was observed and less EO771-OVA-Luc⁺ cells were alive in 1 mM AMP condition. As mentioned above, this might be due to miR-4672 mediated inhibition of Adora2b receptor on EO771 cells.

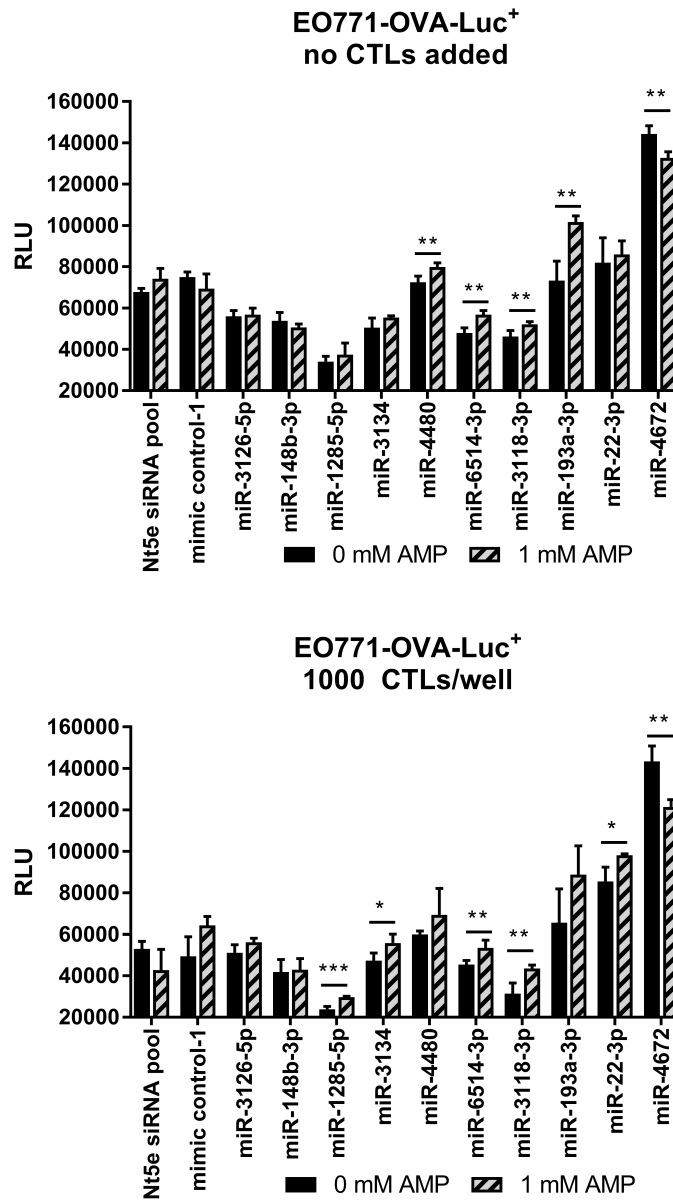


Figure 4.57: Effect of miRNAs on the susceptibility of miRNA transfected EO771-OVA-Luc⁺ cells to CTL lysis. 48 h after miRNA transfection, EO771-OVA-Luc⁺ cells were co-cultured with OVA-specific CTLs and luciferase dependent signal intensity was measured 24 later. All samples were compared to mimic control-1. Four replicates were performed per miRNA. *: p < 0.05; **: p < 0.01; ***: p < 0.001; ****: p < 0.0001.

Figure 4.59 shows the viability of miRNA transfected EO771-OVA-Luc⁺ cells in the presence or absence of OVA-specific CTLs. In the conditions without AMP, for most transfected miRNAs less the number of viable target cells declined when CTLs were added. For example, for mimic control-1 a killing of 34 % was estimated. For Nt5e siRNA, mimic control-1, miR-148b-3p, miR-1285-5p, miR-4480 and miR-3118 a significant killing could be measured. In the lower graph of figure 4.59 the effect of CTLs vs. no CTLs is shown when AMP was added to the cultures. Overall, less killing could be observed, which is in line with the adenosine mediated blocking of CTL functions. For example, no significant difference in mimic control-1 between with or without CTLs could be detected. For Nt5e siRNA, miR-148b-3p, miR-1285-5p, miR-3118 and miR-4672, which are all Nt5e decreasing agents except for miR-4672, still significant killing could be observed despite the addition of AMP. Surprisingly, for miR-22-3p transfected EO771-OVA-Luc⁺ cells a significantly higher number of target cells could be detected in the group of added CTLs. The fractional killing was calculated for with (FK_{AMP}) or without AMP (FK_{noAMP}) added with the following formula, where RLU stands for relative luminescence unit:

$$FK = \frac{RLU_{woCTLs} - RLU_{withCTLs}}{RLU_{woCTLs}} \quad (4.11.1)$$

Figure 4.58 shows the differences in fractional killing for the conditions without and with AMP. The higher this difference, the more target cells were killed in the condition without AMP. For example, in mimic control-1 transfected EO771-OVA-Luc⁺ cells 32 % more cells were killed in setting without AMP addition. In Nt5e transfected cells 21 % more cells were killed with the addition of AMP. Overall, in all conditions compared to mimic control-1 the difference in fractional killing between 0 mM AMP and 1 mM AMP was lower. This makes sense for the agents, that inhibit Nt5e expression like Nt5e siRNA or miR-148b-3p, miR-3118, miR-4480, miR-3134, miR-22-3p and miR-193a-3p. Although miR-3126-5p showed up-regulation of Nt5e in FACS, also for this miRNA the difference in fractional killing was lower.

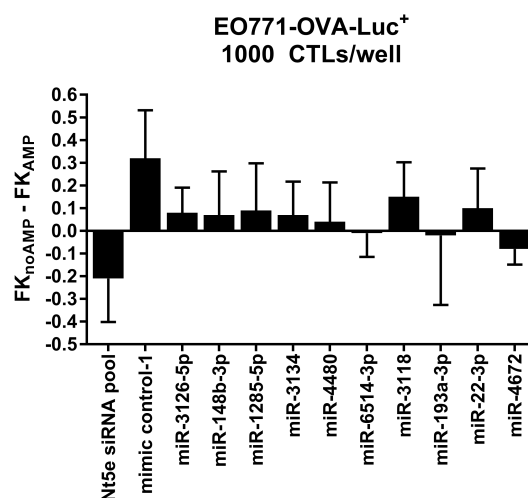


Figure 4.58: Difference of Fractional Killing (FK) in transfected EO771-OVA-Luc⁺ cells co-cultured with 1000 CTLs/well.

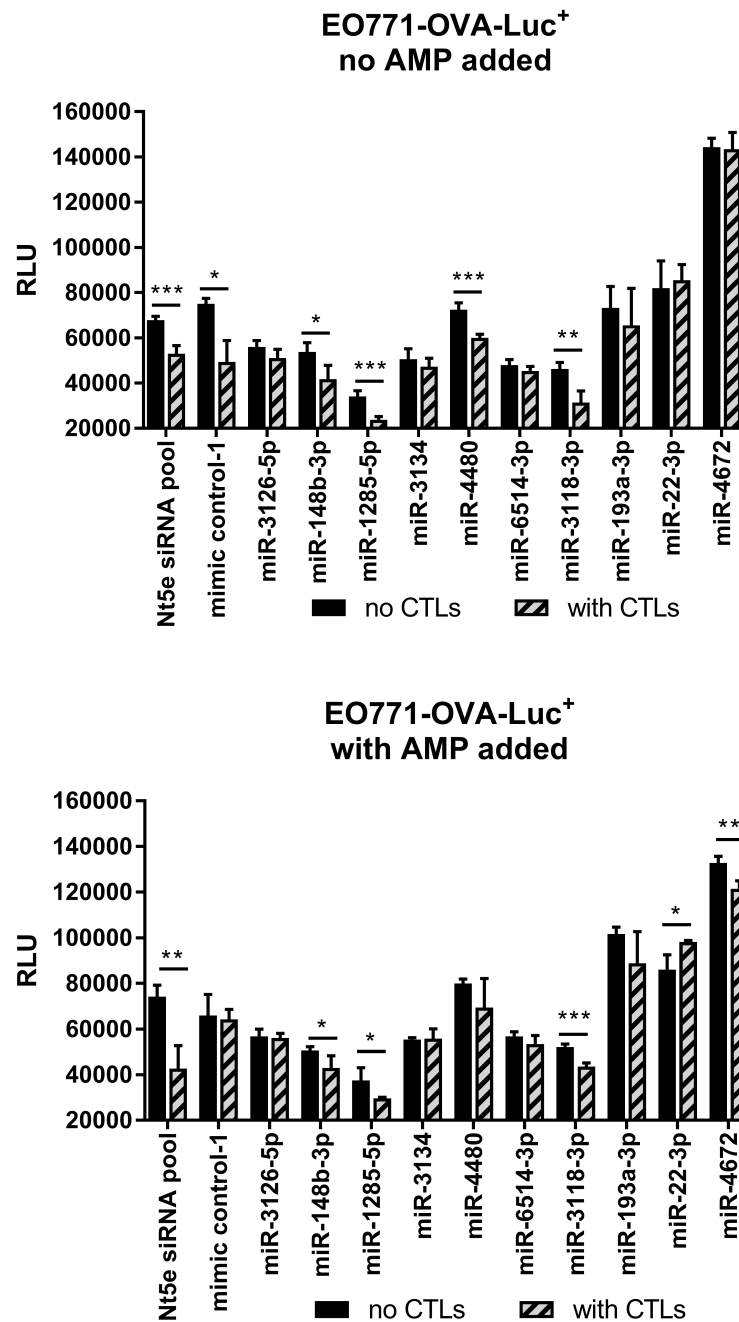


Figure 4.59: Effect of miRNAs on killing of transfected EO771-OVA-Luc⁺ cancer cells by CTLs 48 h post transfection. Cancer cells and CTLs were co-cultured for 24 h until luciferase signal was measured. All samples were compared to mimic control-1. Four replicates were performed per miRNA. *: p < 0.05; **: p < 0.01; ***: p < 0.001; ****: p < 0.0001.

4.12. miR-1285-5p and miR-3134 decreased AMP turn-over

Since the miRNA mediated effects in human cancer cells could not be comprehensively transferred to the murine system, possible changes in the enzymatic activity of NT5E after miRNA treatment was measured. It is expected that the change in adenosine production will make the cancer cells more or less susceptible to CTLs. That adenosine blocks effector T cell function is commonly known and for example described by Vigano *et al.* [242] or by Mastelic-Gavillet and co-workers [158]. The malachite green assay was used to detect free inorganic phosphate, which is released during the reaction from AMP to adenosine catalysed by the enzyme NT5E. This assay was described by Allard *et al.* [13] to be a suitable tool for measuring NT5E enzymatic activity. An exemplary performed malachite green assay with transfected MaMel-53a cells is shown in figure 4.60. Two days post transfection, 400 μ M AMP was added to the cells and the supernatant was collected 30 min later to measure the amount of generated free phosphate, which is proportional to the measured absorbance at 620 nm. Compared to mimic control-1, the amount of generated phosphate was significantly reduced for NT5E siRNA pool, miR-1285-5p, miR-3134 and miR-193a-3p. From the NT5E inhibiting agents only miR-22-3p had no effect. For the miRNAs, that enhance NT5E expression levels, the three miRNAs miR-134-3p, miR-6859-3p and miR-3126-5p caused a significant increase in AMP turn-over by NT5E resulting in higher free phosphate levels. miR-6514-3p, miR-224-3p and miR-4672 did not increase AMP turnover by NT5E and were comparable to mimic control-1 condition.

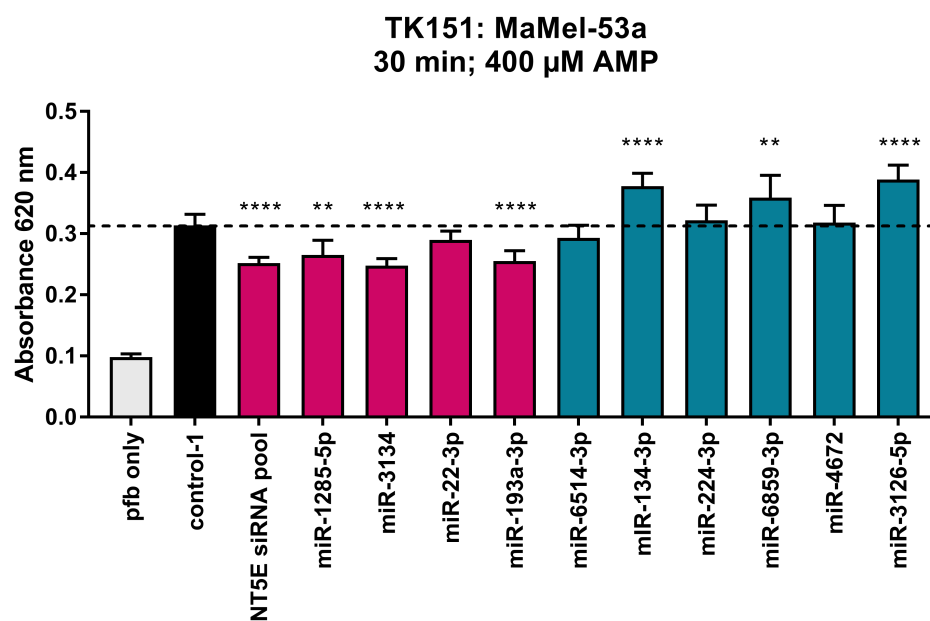


Figure 4.60: Malachite green assay in transfected MaMel-53a cells. Cancer cells were transfected with 50 nM miRNA/siRNA and cultured for 48 h. Then, 400 μ M AMP was added in phosphate-free buffer and supernatants were collected after 30 min incubation and the amount of produced free phosphate was measured. All samples were compared to mimic control-1. At least six replicates were performed per condition in malachite assay. Pink: NT5E decreasing miRNAs. Turquoise: NT5E enhancing miRNAs. *: $p < 0.05$; **: $p < 0.01$; ***: $p < 0.001$; ****: $p < 0.0001$.

The malachite green assay was performed for different cell lines and data was collected from up to six independent experiments. The compiled data from these experiments are shown in figure 4.61. Overall, different cell lines performed very different in the malachite green assay due to their different basal expression level of NT5E. For example the SK-Mel-28 cell line showing high NT5E expression quickly reached saturation whereas cell lines with intermediate expression levels like MDA-MB-231 or MaMel-05 exhibited an overall lower turn-over of AMP. As positive control, a NT5E siRNA pool was used. Regarding SK-Mel-28 and MDA-MB-231 cells, the NT5E siRNA could significantly reduce the AMP turn-over by NT5E. For the other cell lines only modest effects or no effects at all were observed. One of the strongest NT5E inhibiting miRNAs, miR-1285-5p, could also decrease AMP turn-over by NT5E.

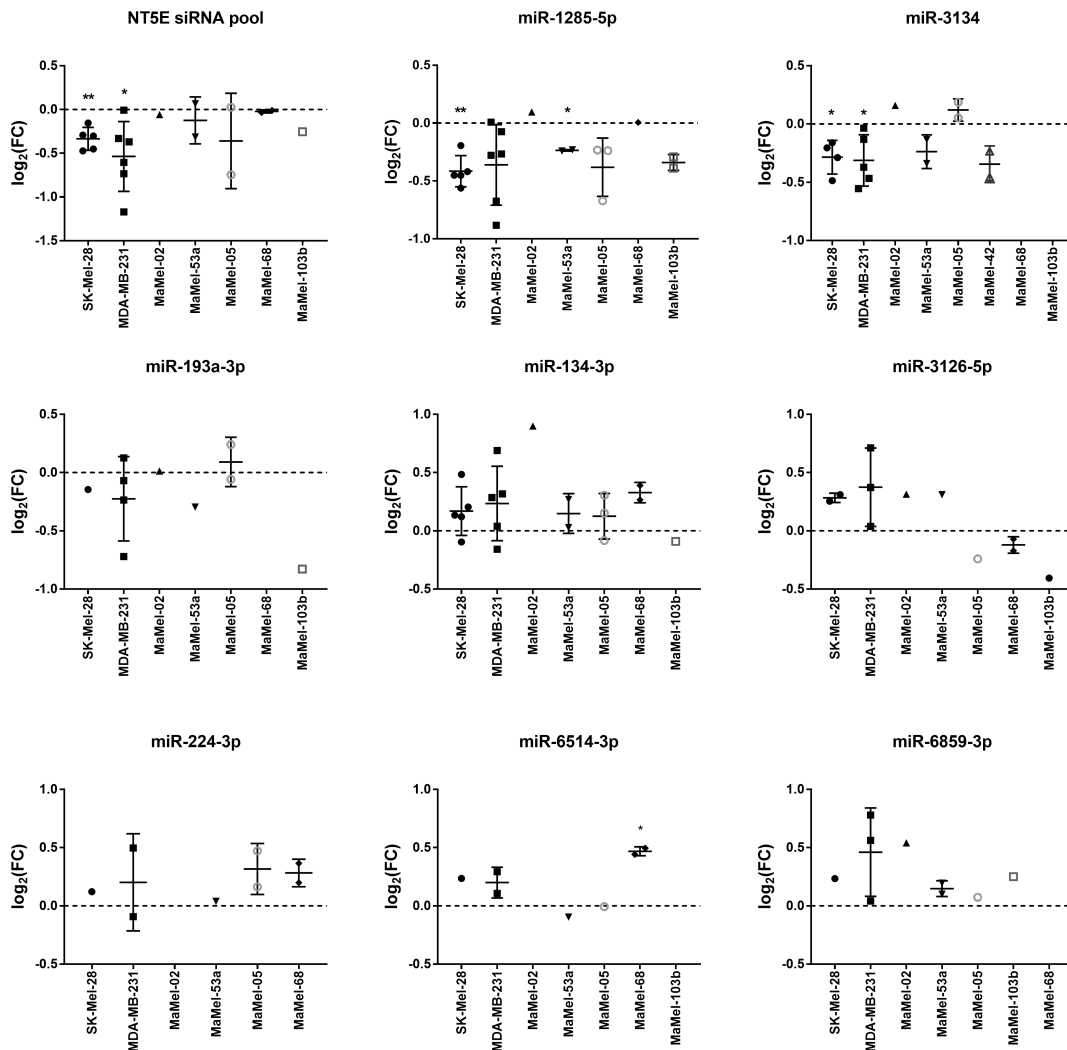


Figure 4.61: Effect of miRNAs on AMP turn-over mediated by NT5E. Cancer cells were transfected with 50 nM miRNA/siRNA and cultured for 48 h. Then, 400 μ M AMP was added in phosphate-free buffer and supernatants were collected after 30 min incubation and the amount of produced free phosphate was measured. Fold changes were calculated to mimic control-1 condition of the respective experiment. Each dot represents an independent experiment. *: $p < 0.05$; **: $p < 0.01$.

Regarding SK-Mel-28 and MaMel-53a cells, miR-1285-5p significantly decreased the amount of produced phosphate. Also in MDA-MB-231 cells miR-1285-5p showed the same tendency ($p = 0.052$) as well as in the case of MaMel-05 and MaMel-103b cells. miR-3134 significantly inhibited NT5E enzymatic activity for SK-Mel-28 and MDA-MB-231. Also for MaMel-53a and MaMel-42 miR-3134 caused a decrease in measured absorbance, but due to the low number of experiments performed, this effect is not statistically significant. For miR-193a-3p no significant reduction could be detected, but for most cell lines the effects trends towards a reduction of NT5E enzymatic activity, but more experiments are needed to draw a clear conclusion.

miR-134-3p was one of the top NT5E enhancing miRNAs from the library screen. Consistently, in the malachite assay miR-134-3p led to increased adenosine concentrations, but not to a significant extend. But in six of the seven tested cell lines a clear tendency towards enhanced phosphate production could be observed. miR-3126-5p showed higher turn-over of AMP by NT5E for SK-Mel-28, MDA-MB-231, MaMel-02 and MaMel-53a. But for MaMel-05, MaMel-68 and MaMel-103b a tendency towards reduction was observed. miR-6514-3p could significantly enhance NT5E-mediated AMP turn-over in MaMel-68 cells. Also for SK-Mel-28 and MDA-MB-231 cells the effect of miR-6514-3p points towards an activation of NT5E. But for MaMel-05 and MaMel-53a miR-6514-3p led to no change compared to mimic control-1 conditions. miR-6859-3p had in five tested cell lines the tendency of increasing phosphate concentration, but not to a significant degree.

In general, for the enhancing miRNAs the 48 h time point might be too early, since the indirect effects caused by these miRNAs might need more time to reach the peak in NT5E expression. Thus, the effect might be more pronounced at 72 h post transfection. Also for miR-224-3p, no significant changes could be measured, but also here the effect went into the expected direction. For the NT5E enhancing miRNAs the experiments should be repeated measuring at a later time point after transfection and maybe using a lower concentration of AMP to facilitate the measurement of decreased NT5E enzymatic activity.

CHAPTER 5.

DISCUSSION

The aim of this thesis was to gain more insights on miRNA mediated aberrant expression of immune checkpoint molecules. On the one hand the aim was to find miRNAs, that drive the expression of these genes in cancer cells in order to understand how cancer cells gain mechanisms for evading from the immune system. These miRNAs, that drive the expression of immune evasion relevant genes could be classified as oncogenic miRNAs (oncomiRs), since their expression helps cancer cells to survive and to lower their susceptibility to cytotoxic T cells. On the other hand, the aim was to find miRNAs, that inhibit the expression of immune checkpoint molecules. These miRNAs could be classified as potential tumor suppressive miRNAs (tsmiRs). The loss of expression of these tsmiRs could mark onset of cancer development or progression towards a more resistant and aggressive type. They also bear the potential of therapeutical interference.

Based on *in silico* predictions, we identified several miRNAs, that potentially target a set of immune checkpoint molecules. These miRNAs could be of special interest, since they bear the potential to simultaneously inhibit the expression of various genes, that would lead to an enhanced recognition and killing by immune cells. For example there was strong evidence, that miR-422a can inhibit NT5E, ENTDP1, CD274 and CTLA4. miR-442a was the top *in silico* hit predicted by six data bases to target NT5E. Indeed, the direct regulation of NT5E by miR-422a in head and neck squamous cell carcinoma was already described in literature. Bonnin and co-workers found that the expression levels of miR-422a were significantly reduced in patients which were categorized in the group of non-responders (NR). This finding was accordant with the observation that inhibition of miR-422a led to increased proliferation levels. Bonnin and co-workers could show that the expression of miR-422a and NT5E was inversely correlated [31]. To date, the direct regulation of ENTDP1, CD274 and CTLA4 by miR-422a is not experimentally validated. If the predicted capability of miR-422a to simultaneously target four immune checkpoint molecules holds true in experimental verification processes, miR-422a might be a very attractive compound to make cancers more susceptibility to killing by immune cells. Furthermore, miR-422a is described as tumor-suppressive miRNA by several studies. For example, miR-422a inhibits cell proliferation in colorectal cancer [252] and was found to act in a tumor-suppressive way by inhibiting the TGF β /SMAD pathway in non-small cell lung cancer[141]. Also miR-155 was among the miRNAs predicted to regulate all four selected immune evasion relevant genes. The direct targeting of CD274 by miR-155 was proven for lung adenocarcinoma cells [110] and also human primary cells [265]. There is also experimental evidence for the suppression of CTLA4 by miR-155 [221]. Additionally, also the direct regulation of ENTDP1 by miR-155 was already shown in murine cells [271]. miR-155 has been described as a tumor-suppressive miRNA in melanoma and gastric cancer and a current phase 2 study using miR-155 is running for the treatment of T-cell lymphoma [240]. Only the direct targeting of NT5E by miR-155 has not been reported, so far.

To get a more comprehensive understanding on miRNA mediated modulation of immune checkpoint molecule expression, a miRNA library screen was conducted in two cancer cell lines. The changes in surface expression of the selected immune checkpoint molecules NT5E, ENTPD1 and CD274 upon miRNA transfection were directly assessed. Using this approach numerous miRNAs could be successfully identified that inhibit as well as enhance the expression of the investigated immune checkpoint molecules. Compared to the pure *in silico* analysis, this approach also enables the discovery of potential oncomiRs that drive expression of immuno-suppressive genes. Furthermore, the screening allows to detect indirect interactions since not the binding to the respective 3'-UTR is analysed, but the net effect of a transfected miRNA on surface expression. That's the main advantage of the screen, since only changes in surface expression would also have an impact on susceptibility of cancer cells to killing by CTLs.

In total, 104 miRNAs were identified causing a significant reduction of CD274 surface expression level in the miRNA library screen. Out of these 104 miRNAs 55 were also predicted by the bioinformatic analysis to target CD274. Out of the 129 miRNAs that lead to a significant increase in CD274 surface levels, 42 miRNAs were predicted to actually target the CD274 3'-UTR. Using Fisher's Exact the association between inhibition of CD274 in the screen and predicted binding site from *in silico* analysis was found to be statistically highly significant ($p = 0.0021$). Furthermore, 61 miRNAs were identified that significantly enhanced ENTPD1 surface expression in the miRNA library screen. Of those, only four miRNAs were predicted to target the ENTPD1 3'-UTR. Overall, 43 miRNAs significantly inhibited ENTPD1 surface expression within the library screen and ten of these miRNAs were also predicted by computational analysis to regulate ENTPD1. Also for ENTPD1 the association between inhibition of ENTPD1 expression in the screen and predicted binding site from *in silico* analysis was statistically significant ($p = 0.0194$). Based on the miRNA library screen 84 miRNAs were identified in total that significantly lowered NT5E surface expression and 109 miRNAs that significantly enhanced NT5E surface levels. From the NT5E inhibiting miRNAs, 27 were also present among the *in silico* predictions. Only five of the NT5E enhancing miRNAs were predicted to bind NT5E 3'-UTR. In summary, the association between inhibition of NT5E in the library screen and predicted binding site from *in silico* analysis is considered to be extremely statistically significant ($p = 0.0001$). Considering only the bioinformatic analysis, far more miRNAs were predicted to target the studied immune checkpoint molecules than pronounced effects on surface expression were observed within the miRNA library screen. There were huge differences between the individual miRNA-target data bases and it was suspected that many of the predicted interactions were false positive predictions. Furthermore, even if a miRNA can theoretically bind to the 3'-UTR by calculation, the conditions within a cell can be also a reason why no regulation can be observed. For example the binding site of the miRNA could be blocked by other factors such as RNA-binding proteins or may not be accessible for the miRNA due to steric hindrance [223]. This is also reflected in the differences between the two screened cell lines. So, depending on the cell type, miRNAs can exert different functions since they have the potential to regulate hundreds of targets and each target in turn can be regulated by numerous miRNAs. What really matters in the end is the net effect of a miRNA on surface expression of the investigated immune checkpoint molecules.

For more in-depth analysis and validation of the library screen the focus was set on the miRNA mediated regulation of NT5E. Since the effects of miRNAs were tested in two distinct cell lines during the screen, only miRNAs were considered that had a consistent effect in both cell lines to avoid false positive hits. Ten miRNAs were selected, that enhanced NT5E surface expression and ten miRNAs, that decreased NT5E surface levels. During the validation process, it was narrowed down to the most promising miRNAs. First, measurements of surface NT5E expression upon individual miRNA transfection were repeated in the two cell lines also used for the screen. In addition, also other cancer cell lines were tested to assess whether the miRNA mediated effects are consistent or cell line specific. Up to 12 cell lines from three tumor entities were tested, but the majority of cell lines were derived from melanoma patients. For seven miRNAs from the ten selected NT5E inhibiting miRNAs their suppressive function on NT5E surface expression could be verified in independent experiments. For miR-1233-3p contrary results were observed and instead of the expected down-regulation an up-regulation in tested cell lines was measured. Also for miR-3118-3p no coherent results were obtained and depending on the cell line a significant inhibition or significant activation of NT5E surface expression was seen. In principle, for miR-143-5p the effect from the screen was confirmed, but the measured changes were only marginal. Thus, miR-1233-3p, miR-3118-3p and miR-143-5p were excluded from final experiments and functional assays. Among the top best performing miRNAs were miR-1285-5p and miR-3134, which considerably reduced NT5E levels in almost all tested cell lines. Only in cell lines with low NT5E expression, detection of significant changes failed, but for these cells also the NT5E siRNA pool was not capable of doing so. To note, for miR-1298-3p only experiments in a subset of cell lines could be performed, since the delivery of this miRNA mimic by the supplier was delayed. To draw final conclusions for this miRNA more experiments are mandatory. For the ten NT5E enhancing miRNAs obtained from the library screen, the effects of all ten miRNAs could be actually verified. Of note, the miRNA mediated up-regulation of NT5E surface expression was extremely consistent for the different cell lines tested. Such coherent results were not expected since it was speculated, that the NT5E enhancing miRNAs mediate their effect indirectly and that their effect might vary depending on the cell line. The best performing NT5E enhancing miRNA was miR-134-3p, for which increase of NT5E surface levels was measured in all tested cell lines. Also miR-224-3p and miR-6514-3p were among the top performing miRNAs. Overall, none of the selected NT5E enhancing miRNAs dropped out during the first validation step. To note, for miR-127-5p not all cell lines were tested since delivery of this miRNA mimic was delayed. As for miR-1298, more experiments are necessary to come to a final conclusion.

Having confirmed the results from miRNA library screen, the aim was to gain more understanding in the mode-of-action for each miRNA. It was hypothesized, that the NT5E inhibiting miRNAs exert their function via direct binding to NT5E 3'-UTR thereby blocking NT5E protein translation and eventually also causing degradation of NT5E mRNA. Indeed, all of the confirmed NT5E inhibiting miRNAs exhibit at least one binding site for NT5E 3'-UTR. Thus, luciferase reporter assays were used to measure the impact of miRNA-UTR interactions. In addition to the NT5E inhibiting miRNAs, also the NT5E enhancing miRNAs that also exhibited a potential binding site within the 3'-UTR were tested. In total, the reporter assay was performed in four cell lines to account for cell line specific effects that might falsify obtained results. Interestingly, for the NT5E enhancing miRNAs no or

only weak effects on luciferase signal was measured and for none of these miRNAs consistent results were obtained for all tested cell lines. For example, miR-224-3p and miR-3126-5p caused reduction of luciferase signal in two cell lines. Nevertheless, these miRNAs clearly induced NT5E surface expression. It can be not excluded, that these miRNAs can directly bind NT5E 3'-UTR, but even if they bind, their net-effect lead to increased NT5E levels. This also points out one of the drawbacks of exclusive *in silico* predictions. The information whether a miRNA can bind to a certain 3'-UTR does not necessarily implicate an inhibitory effect. Considering the massive amount of miRNAs predicted *in silico* to bind to NT5E 3'-UTR (584 miRNAs) on the one hand and the relatively small number of 43 miRNAs that significantly decreased NT5E expression with the library screen on the other hand, the discrepancy between *in silico* predictions and *in vitro* experimental observations becomes apparent. For the NT5E inhibiting miRNAs the strongest reduction in luciferase signal was observed for miR-1285-5p, followed by miR-3134. Interestingly, these two miRNAs have two distinct binding sites within the NT5E 3'-UTR, whereas the remaining miRNAs exhibit only one binding site. This could be one explanation why the strongest effects were observed for these two particular miRNAs. Also miR-22-3p, miR-193a/b-3p, miR-148b-3p and miR-3118-3p consistently led to reduced luciferase signals indicating their binding to NT5E 3'-UTR. To verify direct binding of miRNA to a given 3'-UTR, disruption of the respective binding site is inevitable. Therefore, one nucleotide within a binding site is deleted by site-directed mutagenesis. Since miR-3118-3p gave contrary results in the first validation step, this miRNA was excluded from the mutagenesis work-flow and mutated NT5E 3'-UTRs were generated for miR-1285-5p, miR-3134, miR-22-3p, miR-193a/b-3p and miR-148b-3p. By mutating the specific binding site it was possible to affirm the direct interaction of miR-22-3p, miR-193a/b-3p with NT5E 3'-UTR. For miR-148b-3p, miR-3134 and miR-1285-5p different constructs with mutated binding site were successfully generated, respectively. In future experiments these constructs will be utilized to verify the direct interaction of these three miRNAs with the NT5E 3'-UTR.

In contrast to the NT5E inhibiting miRNAs, the identification of mechanisms accountable for the observed increase upon miRNA transfection is more complex. It was suspected, that these miRNAs act indirectly e.g. by targeting a transcriptional inhibitor of NT5E or other regulators involved in NT5E protein life-cycle. In favour for this hypothesis is the observation, that the effect of NT5E enhancing miRNAs took longer to reach the maximal change in NT5E expression. For the NT5E inhibiting miRNAs strongest effects were observed already two days post transfection at cell surface level. For the enhancing miRNAs, the strongest effects were seen four days post transfection. It makes sense, that the inhibiting miRNAs can exert their effects faster, since the directly bind to NT5E 3'-UTR thereby blocking NT5E translation. The enhancing miRNAs might first bind to other targets, blocking the translation of the respective mRNA, which subsequently leads to changes in NT5E transcription or processing of the NT5E protein. To find this missing link between miRNA and NT5E activation several *in silico* approaches were applied. i) Enriched target genes across the miRNAs that enhanced NT5E surface levels were identified, ii) Correlation analysis was used to find potential NT5E inhibitory regulators and iii) Gene expression prediction was used to find most the important NT5E transcriptional regulators. Therefore, the NCI-60 data set as well as RNA-Seq data of melanoma and NHEM samples generated in this study were used, since the majority of used cell lines originated from melanoma patients. Based on the prediction

model ATF1, GFI1, SMAD4 and TCF7 were revealed as the regulators best explaining NT5E mRNA levels across the NCI-60 data set. SMAD2, SMAD4 and SMAD5 are proven to bind to rat NT5E promoter and to activate NT5E expression [74]. Rat and human transcripts share 89 % identity [281]. In contrast to NT5E activating SMAD transcription factors, GFI1 was found to inhibit Nt5e expression in murine Th17 cells [40]. Interestingly, Chalmin *et al.* also found GFI1 to inhibit Entpd1 expression. To date, there are no publications confirming the regulation of NT5E by ATF1 or TCF7. Both regulators are rather considered as transcriptional activators. Target enrichment analysis of miRNAs that enhanced NT5E as well as ENTPD1 within the miRNA library screen identified ZEB2 as an enriched transcription factor. Maybe ZEB2 is also involved in NT5E-ENTPD1 regulation, but to date there are no data to support this hypothesis. But also several other transcriptional regulators were predicted as targets of the NT5E and ENTPD1 enhancing miRNAs like Forkhead Box G1 (FOXG1), Zinc Finger And BTB Domain Containing 10 (ZBTB10) or Basonuclin 2 (BNC2). To find the most relevant amongst them, correlation analysis using NCI-60 data or melanoma expression data could help to select most relevant potential NT5E and ENTPD1 inhibitors.

Additionally, gene expression profiling upon transfection with selected NT5E enhancing miRNAs was performed and it was searched for consistently down-regulated genes showing negative association with NT5E expression. A list of potential candidates for the missing link was retrieved and the most promising genes amongst them were ARNT2, FURIN, MAZ and MYBL2. Further analysis and experiments of how the NT5E enhancing miRNAs impact the selected potential regulators and whether direct siRNA-mediated knock-down of these genes can mimic the effect of the miRNAs were performed in our lab by Tsu-Yang Chao in the scope of his master thesis. To date, there is no evidence in literature, that these genes might regulate NT5E expression. Until now, only few repressors of NT5E are known and in fact, only GFI1 and APC have been experimentally verified as transcriptional repressors of NT5E [128]. But for APC only three of the ten studied NT5E enhancing miRNAs exhibited a binding site and also there was no correlation between APC mRNA levels and NT5E expression. In contrast, for GFI1 seven miRNAs were predicted to bind this transcriptional repressor. Nevertheless, no impact of miRNAs on GFI1 levels could be measured and only a slight insignificant negative correlation of GFI1 with NT5E was observed in our expression data. The most promising candidate for the missing link was by far ARNT2. All ten NT5E activating miRNAs exhibited a binding site for this transcription factor. Furthermore, ARNT2 expression was significantly negatively associated with NT5E expression in our microarray data for transfected MaMel-02 and MDA-MB-231 cells. ARNT and ARNT2 are known to form hetero-dimers with HIF1A and AHR. The ARNT/HIF1A heterodimer binds hypoxia response elements and activates gene expression [97]. Interestingly, HIF1A is known to be an activator of NT5E expression [128]. Both, HIF1A and AHR are positively associated with NT5E expression within the NCI-60 panel. The NT5E promoter was checked for matching binding motifs for ARNT/HIF1A and ARNT/AHR. But there was no individual motif for ARNT or ARNT2 within NT5E promoter. Thus, the very speculative working theory is, that ARNT2 competes with ARNT for binding to HIF1A or AHR. Only the ARNT/HIF1A or ARNT/AHR complex is capable of activating NT5E transcription. By competing with ARNT, ARNT2 might lower the expression of NT5E. If our miRNAs reduced ARNT2 expression, more ARNT/HIF1A or ANRT/AHR complexes could be formed and lead to a subsequent higher NT5E expression. In line with this theory is the observation that only the

ARNT/AHR complex is able to activate the expression of CYP1A1 and that ARNT2 can bind with equal efficiency to AHR as ARNT, but the ARNT2/AHR complex is incapable of activating CYP1A1 transcription [97, 213]. Another potential mechanism of ARNT2 could be its inhibitory function on HIF1A expression itself, as it was shown by Qin and co-workers in the human breast cancer cell line MCF-7 [192]. Hence, it would be suspenseful to also include the connection of ARNT2-HIF1A-NT5E in future analysis and experiments. As shown in appendix figure 6.3 a decreasing effect on NT5E surface expression after transfection of SK-Mel-28 cells with HIF1A siRNA could be observed supporting the activating function of HIF1A on NT5E. Also interesting is the fact that high NT5E and HIF1A expression are significantly associated with a worse survival in breast cancer as shown in appendix figure 6.4 and 6.5. Whereas high ARNT2 expression is beneficial for patients' survival as shown in figure 6.6. ARNT2 seems to be a potential tumor suppressor protein. In deed, there are several publications describing its favourable role for patient survival. For example, down-regulation of ARNT2 expression in non-small cell lung cancer compared to normal tissue is described by Yang *et al.* and ARNT2 over-expression decreased cell viability and proliferation *in vitro* and in xenograft *in vivo* cancer model [261]. Similar observations were made in gastric cancer where ARNT2 over-expression also inhibited cell proliferation; furthermore, ARNT2 expression was reported to be reduced in gastric cancer tissues compared to adjacent normal tissues [117]. Also in oral squamous cell carcinoma, ARNT2 levels are significantly decreased compared to healthy counterpart tissues and up-regulated ARNT2 expression caused reduced cell viability and proliferation of cancer cells. Interestingly, Kimura *et al.* also identified the down-stream mechanism of ARNT2 over-expression. he authors also found decreased HIF1A levels upon ARNT2 activation mediated by the tumor suppressor gene VHL, which ubiquitinates HIF1A leading to enhanced degradation of HIF1A by proteosomal machinery [126].

In our future experiments, the effect of NT5E enhancing miRNAs on selected potential NT5E regulators will be verified in independent experiments on mRNA level by qPCR and on protein level by Western Blot. Additionally, it will be tested whether siRNA-mediated knock-down of these potential regulators can mimic the observed effect of the NT5E enhancing miRNAs. For successfully validated regulators the direct interaction and binding of miRNAs will be verified by luciferase reporter assays and mutagenesis of miRNA binding sites.

By using the malachite green assay the change in phosphate production was assessed thereby indirectly measuring changes in adenosine production by NT5E, which would interfere with cancer cell killing by CTLs. Surprisingly, huge differences between human and murine system were observed by testing the most promising miRNAs from the screen. Our initial intention to use the murine system to assess differences in CTL-mediated killing of breast cancer cell line EO771-OVA-Luc⁺ turned out to be not suitable, since the changes caused by miRNAs were often contrary to the results in human cell lines. Although most miRNAs were conserved and were also predicted to interact with murine Nt5e 3'-UTR huge differences were observed and the results were not comparable. This also highlights, that transferring findings from murine system to human setting and *vice versa* should be carefully verified. In future experiments the plan is to directly assess miRNA-mediated changes in T cell killing activity in human setting. Therefore, different options are practicable. The first one is killing of MaMel-05 by autologous TILs HD-M-269, which were generated in an extraordinary attempt at healing by our GMP facility from a melanoma patient. In first pilot experiments the IFN γ

secretion of TILs after co-culture with MaMel-05 was tested and a good stimulation of IFN γ secretion upon cultivation with the cancer cells was observed. An additional system which could be used would be MDA-MB-231 cells and a survivin specific CTL line, which is available in our laboratory. That MDA-MB-231 highly expresses survivin was shown by Li *et al.* [140]. Survivin is a small protein and a known inhibitor of apoptosis and is a well-studied tumor-associated antigen [20].

In the following the current knowledge and association with cancer of the miRNAs identified in this study to impact NT5E expression levels will be discussed.

miR-1285-5p

miR-1285-5p was the best performing miRNA for decreasing NT5E levels, which indicates a potential for miR-1285-5p to act as a tsmiRNA. Indeed, several publications underpin the tumor-suppressive role of miR-1285. For example, Hidaka and co-workers describe the tumor-suppressive function of miR-1285 in renal cell carcinoma (RCC). They found miR-1285 to be significantly down-regulated in RCC specimens compared to adjacent tissue. Furthermore, re-expression of miR-1285 RCC cell lines inhibited cell proliferation, migration and invasion. From all 20 miRNAs tested, miR-1285 exerted the strongest inhibitory effect. The authors also performed expression analysis of miR-1285 transfectants and found expression of 17 genes to be differentially decreased. Noteworthy, among those genes was also NT5E, which is in line with our findings. In this study the authors focused on TGM2 and validated direct binding of miR-1285 only for this target gene [102]. Also a study by Hironaka-Mitsubishi and colleges supports the tumor-suppressive role of miR-1285-5p. They previously showed, that low miR-1285-5p expression is correlated with poor prognosis in breast cancer. In their latest study they could show, that over-expression of miR-1285-5p leads to reduced cell proliferation in breast cancer cells through direct targeting of transmembrane protein 194A (TMEM194A) by miR-1285-5p. They also used MDA-MB-231 cells for their experiments. To note, the inhibiting effect on cell proliferation upon miR-1285-5p transfection became perceptible five days post transfection. Whereas three days post transfection no significant changes were measured [104]. This indicates that effects on cell proliferation caused by miR-1285-5p did not interfere with our observations from luciferase or malachite assays since these were measured latest three days post transfection.

Besides the supportive findings of miR-1285-5p as a tsmiRNA, there are also publications stating miR-1285-5p as an oncomiR. For instance, Zhou *et al.* identified miR-1285-5p to support cell proliferation and that blocking miR-1285-5p by antagomiR reduced proliferation and metastasis of non-small-cell lung carcinoma (NSCLC) cells. They showed, that miR-1285-5p acts by directly targeting the tumor-suppressor gene SMAD4 and CDHI. Also miR-1285-5p expression levels were higher in NSCLC tissue compared to normal colon tissue. They state, that miR-1285-5p is a key carcinogenic gene for the progression of NSCLC [285]. The comparison of NSCLC tissue and normal colon tissue might be not the best practice and comparison of healthy lung tissue might give more biological meaningful results. Nevertheless, the inhibition of cell proliferation by transfection of antagomiR-1285-5p seems to be valid. For renal cell carcinoma, breast cancer and melanoma miR-1285-5p seems to be a tsmiR, whereas it might act as an oncomiR in NSCLC. This again displays the poly-functional role

of miRNAs and the dependency of their net-effect on the specific cell type.

miR-3134

Until today, there are only two publications on miR-3134. A study of Sharma and co-workers from 2013 showed the interplay of miR-3134 and AU Rich elements (ARE)-mediated degradation. ARE are regulatory elements within the 3'-UTR that are normally bound by ARE-binding proteins leading to destabilization of the mRNA and its degradation or to stabilisation of the mRNA [181]. In the breast cancer cell line MCF7 Sharma *et al.* showed that over-expression of miR-3134 increased mRNA levels of the target genes SOX9, HLA-G, EGFR and VEGFA, which contain AREs. This indicates, that miR-3134 can increase transcript stability of target genes bearing AREs by binding to the ARE element itself. By deleting the ARE in the EGFR 3'-UTR, the effect of over-expressed miR-3134 was abolished. Interestingly, among genes that were significantly up-regulated in miR-3134 transduced MCF7 cells were also many genes encoding major histocompatibility complex (MHC) molecules, such as HLA-A, HLA-B, HLA-H, HLA-F, HLA-G, HLA-DRA and HLA-DPA1 [214]. This might be an important point to keep in mind also for our further studies, that will analyse the susceptibility of cancer cells to killing by CTLs. Despite the effect on NT5E surface levels and the resulting changes in adenosine production, altered MHC expression levels might also affect killing efficacy. For miR-3134 a strong decrease in NT5E surface expression was observed, which would ideally result in enhanced killing of cancer cells by CTLs, since less adenosine is produced that block effector T cell function. In addition, it might be that miR-3134 caused up-regulation of MHC molecule expression further facilitates CTL-mediate killing. Also of interest is the miR-3134 caused up-regulation of SOX9. SOX9 is a transcription factor, that can activate or inhibit target expression. The NT5E promoter actually contains a binding motif for SOX9 and we speculated, that SOX9 might act inhibitory on NT5E expression. So miR-3134 might decrease NT5E levels with two distinct mechanisms. First, miR-3134 directly targets NT5E 3'-UTR leading to block a in protein translation and enhanced mRNA degradation. Second. miR-3134 might enhance SOX9 expression, which in turn eventually inhibits NT5E expression.

miR-148b-3p

Also miR-148b-3p was among the NT5E inhibiting miRNAs and the inhibitory impact of miR-148b-3p on NT5E surface levels in transfected tumor cell lines was successfully proven. For this miRNA no significant effect on NT5E mRNA levels could be seen, but binding of miRNA to targets 3'-UTR does not necessarily lead to mRNA degradation and depending on the degree of complementary base pairing just a block of translation is possible as well. Based on the luciferase reporter assay, it was revealed that miR-148b-3p can bind to the NT5E 3'-UTR thereby mediating its NT5E inhibitory effect. Based on our findings, miR-148b-3p could be tsmiRNA. In gastric cancer tissue miR-148b-3p expression was found to be reduced compared to adjacent non-tumor tissue and high miR-148b-3p expression is associated with a better overall-survival of gastric cancer patients. Interestingly, miR-148b-3p inhibits gastric cancer cell proliferation and inhibits metastasis *in vivo* by directly targeting DOCK6 [142]. An opposite observation was made by Dai *et al.* in breast cancer. In their study they found miR-148b-3p to be enhanced in breast cancer tissues as well as breast cancer cell

lines compared to normal control samples and low miR-148b-3p levels were associated with a better survival probability. Transfection with miR-148b-3p mimics in breast cancer cell line T47D increased cancer cell proliferation, but for breast cancer cell line MDA-MB-468 the authors could not detect any significant effects upon miR-148b-3p transfection. However, migration of MDA-MB-468 cells was increased by treatment of the cells with miR-148b-3p mimics [52]. These findings would rather point towards an oncogenic function of miR-148b-3p. But on the other hand, previous studies in breast cancer showed that miR-148b-3p expression was lower in serum of breast cancer patients [155] and low miR-148b levels were also found to be correlated with relapse of breast cancer disease. In the study conducted by Cimino and co-workers, miR-148b inhibited tumor growth and metastasis formation in *in vivo* models. Additionally, the authors found that miR-148b can enhance the effect of chemotherapy-induced apoptosis [50]. Also in gastrointestinal stromal tumors miR-148b-3p has been reported to act as a tsmiRNA that inhibits cancer cell proliferation, migration and invasion by directly targeting the expression of the oncogene KIT [249]. Furthermore, miR-148b was also described as a tumor suppressor in renal carcinoma and inhibits cancer cell proliferation and migration *in vitro* as well as tumor growth *in vivo* [276]. In summary, miR-148b-3p seems to predominantly act a tsmiRNA, but it seems that it also has the potential to promote tumor progression.

miR-22-3p

miR-22-3p was among the *in silico* predicted miRNAs to target NT5E. In this study the bioinformatic predictions were confirmed and the NT5E inhibiting effect of miR-22-3p was proven in several cancer cell lines. Furthermore, the direct regulation of NT5E by miR-22-3p was sustained by luciferase reporter assays and through mutation of the respective binding site. In line with our observation are several reports allocating miR-22-3p as a miRNA with tumor-suppressive function. A recent study demonstrated down-regulated miR-22-3p expression levels in gastric cancer, and re-expression of miR-22-3p inhibited gastric cancer cell proliferation, migration and invasion. The authors identified one mechanism how cancer cells aberrantly regulate miR-22-3p levels. Enhanced lncRNA H19 levels and sponging of miR-22-3p by this lncRNA abrogates the inhibitory effects of miR-22-3p [82]. A similar mechanism was also observed in NSCLC where lncRNA NNT-AS1 promotes NSCLC progression by sponging miR-22-3p. Also for NSCLC, reduced miR-22-3p expression levels were observed and over-expression of miR-22-3p reduced NSCLC cell proliferation, migration, invasion and EMT transition [100]. Also in small-cell lung cancer (SCLC) miR-22-3p was found to inhibit cancer progression and treatment of SCLC cells with miR-22-3p even enhanced radiosensitivity [119].

miR-193a-3p

The regulation of NT5E by miR-193a/b-3p was already described by Ikeda *et al.* [112]. But in this study also the direct binding of miR-193a/b-3p to NT5E 3'-UTR could be successfully shown by site-specific mutagenesis of the respective binding site, which was not performed in the previous study mentioned. In this study the inhibitory effect of miR-193a-3p on NT5E surface level as well as mRNA levels was proven, which would designate miR-193a-3p as a tumor suppressive miRNA. Indeed, several publications describe miR-193a-3p as a tsmiRNA for various cancer types. It was discovered, that plasma and tissue miR-193a-3p levels are

strongly decreased in melanoma patients. miR-193a-3p reduced melanoma cell proliferation by targeting ERBB2, KRAS and mTOR and also enhanced apoptotic processes by inhibiting MCL1 [190]. In clinical HER-2 positive breast cancer samples as well as breast cancer cell lines miR-193a-3p expression was found to be reduced via hypermethylation of the miR-193a coding gene. Over-expression of miR-193a-3p led to a reduced cell proliferation, migration and invasion in breast cancer cell lines [230]. Also in ovarian cancer, miR-193a-3p was found to be inhibited by hypermethylation and transfection with miR-193a-3p suppressed ovarian cancer cell line proliferation and invasion [44]. Another mechanism how cancer cells inhibit miR-193a-3p levels to promote tumor progression was recently identified by Xie *et al.*. They found that sponging of miR-193a-3p by long non-coding RNA SNHG14 enhanced breast cancer cell line proliferation and invasion [259]. Also for colorectal cancer, miR-193a-3p levels were decreased and low miR-193a-3p are associated with a poor prognosis for colorectal cancer patients [144]. Furthermore, miR-193a-3p acts also as a tsmiRNA in lung cancer by directly targeting the oncogene KRAS [70].

miR-1298-3p

Also miR-1298-3p was among the top miRNAs that inhibited NT5E surface levels in both cell lines within the miRNA library screen. In the scope of this study miR-1298-3p could not be tested as extensively as the other miRNAs, since the delivery of the miRNA mimic was delayed. Thus, only the effect on surface NT5E expression upon miR-1298-3p could be validated and successfully verified. It is speculated, that this miRNAs also exerts its inhibitory effect by directly binding to NT5E 3'-UTR, since based on prediction algorithms, this miRNA has one binding site within the NT5E 3'-UTR. But additional luciferase reporter assays and mutations of the respective binding site are necessary to proof direct interaction. In line with our results is the described anti-tumoral activity of miR-1298. For example it was recently shown, that miR-1298 expression is reduced in breast cancer and experimental over-expression of miR-1298 inhibited cancer cell line proliferation and enhanced apoptotic processes. Furthermore, miR-1298 also led to reduced tumor growth and metastasis formation in a xenograft mice model [47]. Also for non-small cell lung cancer miR-1298 has been described as a tsmiRNA with decreased expression determined in cancer tissues compared to control samples, and low miR-1298 was associated with a worse prognosis. Furthermore, transfection with miR-1298 mimics inhibited proliferation, migration and invasion of NSCLC cells [62].

miR-134-3p

miR-134 and its association with cancer has been extensively studied. miR-134 is a prime example for miRNAs with opposed function depending on cancer type or even on the study. For several tumor types miR-134 was found to be down-regulated and acting as a tumor suppressive miRNA by inhibiting cell proliferation, apoptosis or metastasis [183]. For instance, miR-134 was found expressed to lower extent in tumor tissue of lung cancer [105], breast cancer [277, 136], hepatocellular carcinoma [272, 267] and glioblastoma [279, 176]. A common target of miR-134 in these studies underlining its tumor suppressive function was KRAS [183]. On the contrary, miR-134 was found as an oncomiR with elevated expression levels in uveal melanoma [241], lung cancer [165], colon cancer [9] and prostate cancer [138]. To note, most

of the studies were investigating the role of miR-134-5p. Furthermore, many investigations did not discriminate between miR-134-3p and miR-134-5p. Based on the findings made by this Thesis, miR-134-3p would be classified as a miRNA with oncogenic potential, since it strongly enhanced expression of immune checkpoint molecule NT5E in a broad panel of cancer cell lines. Furthermore, this miRNA also has the capability of increasing CD274 and ENTPD1 expression as it was observed within the miRNA library screen. More data and experiments are needed to verify the oncogenic potential of miR-134-3p. It might be, that this miRNA is a double-edged sword, on the one hand decreasing cancer cell proliferation and metastasis, but on the other hand also facilitating cancer cell immune evasion.

miR-6514-3p

To date, there are no publications about miR-6514-3p and its role in cancer development and progression. Overall, only one study mentioned this miRNA. In this study the authors investigated the effect of hypoxia-induced changes on miRNA expression in primary human umbilical vein endothelial cells (HUVECs) and miR-6514-3p was among the top 30 miRNAs, that were up-regulated (Fold-change > 4) 16 hours after exposure to hypoxic conditions of HUVECs to [115]. In this study miR-6514-3p was identified as miRNA with oncogenic potential since it increased expression of immune checkpoint molecule NT5E in a broad panel of human cancer cell lines. This study is the first to connect miR-6514-3p with cancer, but more experiments are needed to verify this miRNA as an oncomiR.

miR-224-3p

In this miR-224-3p was identified as a potential oncomiRNA by enhancing NT5E levels. The relationship of miR-224-3p and cancer progression has been intensively studied [46]. For example, miR-224-3p was found expressed to higher extent in NSCLC and to accelerate cancer cell proliferation while inhibiting apoptotic processes. Interestingly, sponging of miR-224-3p by lncRNA HCGII could prevent the oncogenic effects of miR-224-3p in NSCLC cells [244]. Also for colorectal cancer an oncogenic function of miR-224 was observed. miR-224 levels are significantly up-regulated in colorectal cancer tissue compared to normal tissues and miR-224 over-expression drives cancer cell migration and invasion [283]. Also in bladder cancer miR-224 expression is enhanced in cancer tissues compared to healthy control samples, and miR-224 promotes bladder cancer cell proliferation [262]. Furthermore, miR-224-3p expression levels were also enhanced in colon cancer, and miR-224-3p serum levels might be used for colon cancer diagnosis [250].

miR-6859-3p

Also miR-6859-3p was among the NT5E enhancing miRNAs and we could validate its effect in several melanoma cell lines as well as one breast cancer cell line. Our data suggest an oncogenic function of miR-6859-3p. But to date, there are no publications regarding miR-6859-3p and thus a cancer-related function of this miRNA is described within this Thesis for the first time. Future studies are necessary to confirm miR-6859-3p as a potential oncomiRNA and to gain more insights of its effects related to cancer progression.

miR-3126-5p

Regarding miR-3126-5p, there are not many information on its association with cancer. In hepatocellular carcinoma (HCC) patients, miR-3126-5p levels were found to be significantly reduced in serum compared to control samples showing that serum miR-3126-5p levels can be a prognostic biomarker for HCC diagnosis [280]. This would rather point towards a tumor-suppressive role of miR-3126-5p. In contrast, a study by Azuma and co-workers found miR-3126-5p to be significantly enhanced in cancer exosomes from gefitinib-resistant lung cancer cells [23]. As for the study of Azuma also in this work miR-3126-5p was found to rather be an oncomiR by driving NT5E expression, which would help cancer cells to evade from the immune system. But to classify miR-3126-5p as an oncomiR or tsmiR more data and experiments are necessary. This Thesis describes for the first time a role of miR-3126-5p in the regulation of immune checkpoint molecules.

miR-127-5p

miR-127-5p was identified in the miRNA library screen to consistently enhance surface NT5E expression in the two used cell lines for the screen. Due to delayed delivery of miR-127-5p mimic only the effect on NT5E surface expression could be validated for this miRNA within in the scope of this study. The NT5E enhancing effect of miR-127-5p was proven in four melanoma cell lines and one breast cancer cell line. miR-127-5p might be involved in generating an immuno-suppressive environment. But in literature miR-127 is rather described as a tsmiRNA. For instance, in hepatocellular carcinoma (HCC) miR-127-5p was found to inhibit growth and colony formation of HCC cells and to be commonly down-regulated in clinical HCC samples. The authors showed, that miR-127-5p suppresses the activity of Nuclear factor-B (NF- κ B) [109]. Also in cervical cancer, miR-127-5p is mentioned as a tumor suppressive miRNA by inhibiting FOXD1 expression. Sponging of miR-127-5p by lncRNA POU3F3, which is up-regulated in cervical cancer specimens, enhanced cancer cell proliferation, migration and invasion [42]. Also for breast cancer miR-127 levels were found to be decreased and low miR-127 expression is correlated with a worse overall- survival of breast cancer patients. Since miR-127 inhibits breast cancer cell proliferation, migration and invasion, Umeh-Garcia *et al.* tested a newly developed miR-127 pro-drug in a triple negative breast cancer model. The administration of the miR-127 pro-drug could successfully reduce primary tumor growth and metastasis formation of MDA-MB-231 and MDA-MB-468 cells in immunodeficient (NOD/SCID) mice [238]. Interestingly, in their study the authors also performed RNA-Seq analysis on MDA-MB-468 cells treated with the miR-127 pro-drug. According to their expression data, NT5E was significantly up-regulated upon treatment with miR-127 pro-drug. This is in line with our findings. It seems, that miR-127 is a double-edged sword. On the hand, it acts as a tsmiRNA by inhibiting cancer cell growth, but on the other hand, it might also enables cancer cells to evade from the immune system by enhancing the levels of the immune checkpoint molecule NT5E. Thus, treatment with miR-127 should be carefully considered and since Umeh-Garcia *et al.* used an immunodeficient animal model, there might be the change, that in real patient setting with normal immune system, the effect of miR-127 might not be beneficial, but rather even counter-active.

The results of this Thesis helps to shed more light in the process of immune evasion. The NT5E inhibiting miRNAs are promising tsmiRNA and based on literature, for most of our investigated NT5E inhibiting miRNAs there are substantial data that confirm their anti-tumoral activity. By reducing the expression level of these miRNAs, cancer cells can increase their NT5E expression, resulting in higher adenosine production within the tumor-microenvironment and thereby protecting themselves from CTL-mediated killing. One could speculate, that re-expression of these miRNAs would help to inhibit cancer progression and to counteract the inhibitory effects on immune cells by decreasing immune checkpoint expression. Extracellular adenosine mediates a variety of immunosuppressive effects e.g. reducing NK cell activity, enhancing immune suppression mediated by regulatory T cells and myeloid-derived suppressor cells, inhibiting cytotoxicity, cytokine production and proliferation of CTLs. Additionally, NT5E is not only involved in immune evasion, but also contributes to switch of melanoma cells to acquire invasive capacity and also mediates growth-stimulatory effects on cancer cells directly [185]. By blocking NT5E function or expression several cancer inhibiting mechanisms can be neutralized. In principle, also the miRNAs we identified could be used as therapeutic agents blocking NT5E expression or function. But due to the promiscuous nature of miRNAs their usage as drugs is connected with several challenges. Since miRNAs can exert different effects depending on the cell type, precise targeting and delivery to cancer cells is necessary. Finding suitable surface markers specific for cancer cells could help to specifically administer miRNAs, for example by nano-particles loaded with miRNA mimics. Intratumoral injection of miRNAs has been shown to increase efficacy and minimize side effects [98]. However, for already metastasised cancers this strategy is not applicable. Also several clinical trials using miRNA mimics were aborted because of severe adverse events. In addition to the use miRNAs, small-molecule inhibitors and monoclonal antibodies (mAb) directed against NT5E might be considered as alternative strategy. There are several on-going clinical trails testing the effect of NT5E blockage for treatment of advanced solid tumors as mono-therapy or in combination with other immune-checkpoint inhibitors [185]. The clinical relevance of the miRNAs identified in this Thesis might also be of relevance as potential biomarkers. Thus the miRNAs investigated here, could be of relevance for either diagnosis and prognosis of cancer disease and progression or as markers to choose the optimal treatment strategy.

The NT5E enhancing miRNAs identified in this Thesis might help to further understand how cancer cells can actively drive immune checkpoint molecule expression. Identification of the regulators between the miRNAs and NT5E might offer new opportunities for targeted treatment e.g. with small molecule inhibitors. Cancers with high expression levels of these miRNAs might be more suitable for anti-CD73 mAb therapy and miRNAs regulating CD73/NT5E expression and/or function might serve as biomarkers. However, future studies are needed to assess the correlation between the expression level of NT5E enhancing miRNAs and response to immune checkpoint blockade.

CHAPTER 6.

CONCLUSION

Within this Thesis for the first time a human miRNA library screen was conducted to assess the effects on multiple immune checkpoint molecules for two different cancer entities. Based on this comprehensive miRNA library screen novel miRNAs involved in the regulation of immune checkpoint molecules could be identified by this Thesis. Not only potential tumor suppressive miRNAs were found, but also putative oncogenic miRNAs that drive the expression of immune checkpoint molecules. Combining *in silico* prediction with *in vitro* analysis greater insights in the complex mechanisms of checkpoint inhibitor associated cancer cell immune evasion could be gained. Thus, miR-1285-5p and miR-3134 were identified as potential tumor suppressive miRNAs inhibiting NT5E expression at mRNA and protein level in melanoma and breast cancer cell lines. The results furthermore demonstrated that these miRNAs act by binding to the NT5E 3'-UTR. To verify the direct interaction of these miRNAs with the NT5E 3'-UTR several mutated binding sites were generated. Within the scope of this Thesis the direct binding of miR-22-3p and miR-193a/b-3p was verified. The reporter assays with mutated UTRs for miR-148b, miR-1285-5p and miR-3134 will be performed contemporary. Besides significantly decreasing NT5E levels, miR-1285-5p and miR-3134 miRNAs also alleviated NT5E's enzymatic activity resulting in a lower turn-over of AMP to adenosine and free inorganic phosphate. Application of these miRNAs might help, to reverse the immuno-suppressive tumor microenvironment into an immune cell stimulatory habitat to unleash T cell mediated killing of cancer cells. Furthermore, this Thesis was the first to describe miRNAs that cause an up-regulation of the immune checkpoint molecule NT5E. Astonishingly, the miRNA-mediated up-regulation of NT5E was found to be very consistent across a panel of numerous cancer cell lines. One of the strongest NT5E enhancers was miR-134-3p. Interestingly, this miRNA was also found to enhance ENTPD1 expression within the miRNA library screen. Thus, miR-134-3p bears the potential to drive expression of two enzymes acting in a cascade to produce adenosine from ATP and might be an important driver of immune evasion in cancer cells. Different approaches were used to unravel the mechanism of the miRNA-mediated up-regulation of NT5E and several promising "missing links" were identified. But future studies and individual knock-down experiments are needed to validate the effect of these regulators on NT5E expression levels. So far, it is not clear, whether the NT5E up-regulating miRNAs share similar mechanism and regulators responsible for the observed increase in NT5E expression, or whether each of this miRNAs act via a different pathway. Future studies are needed to answer these open questions.

Based on the miRNA library screen a massive amount of data was generated. Within this study the focus was set on one immune checkpoint molecule for additional validation. Future studies could also use the screen data generated in this work as groundwork for investigating the regulation of CD274, ENTPD1 and NT5E by miRNAs. The main findings of this thesis are summarized in figure 6.1. Of special interest might be miRNAs, that simultaneously

enhanced or inhibited several immune checkpoint molecules. For instance, miR-6804-3p and miR-134-3p increased NT5E, ENTPD1 and CD274 surface levels within the miRNA library screen. These two miRNAs might be attractive targets e.g. for antagomiR-treatment to block immuno-suppressive function of several immune checkpoint molecules at once.

In conclusion, this study helped to gain a better understanding in the regulation of immune evasion related genes by miRNAs. Several novel immuno-modulating oncogenic as well as tumor-suppressive miRNAs were identified. Especially miR-1285-5p was found as a very potent tumor-suppressive miRNA making cancer cells more susceptible to killing by cytotoxic T cells. In addition, our performed comprehensive miRNA library screen laid the ground-work for several future studies.

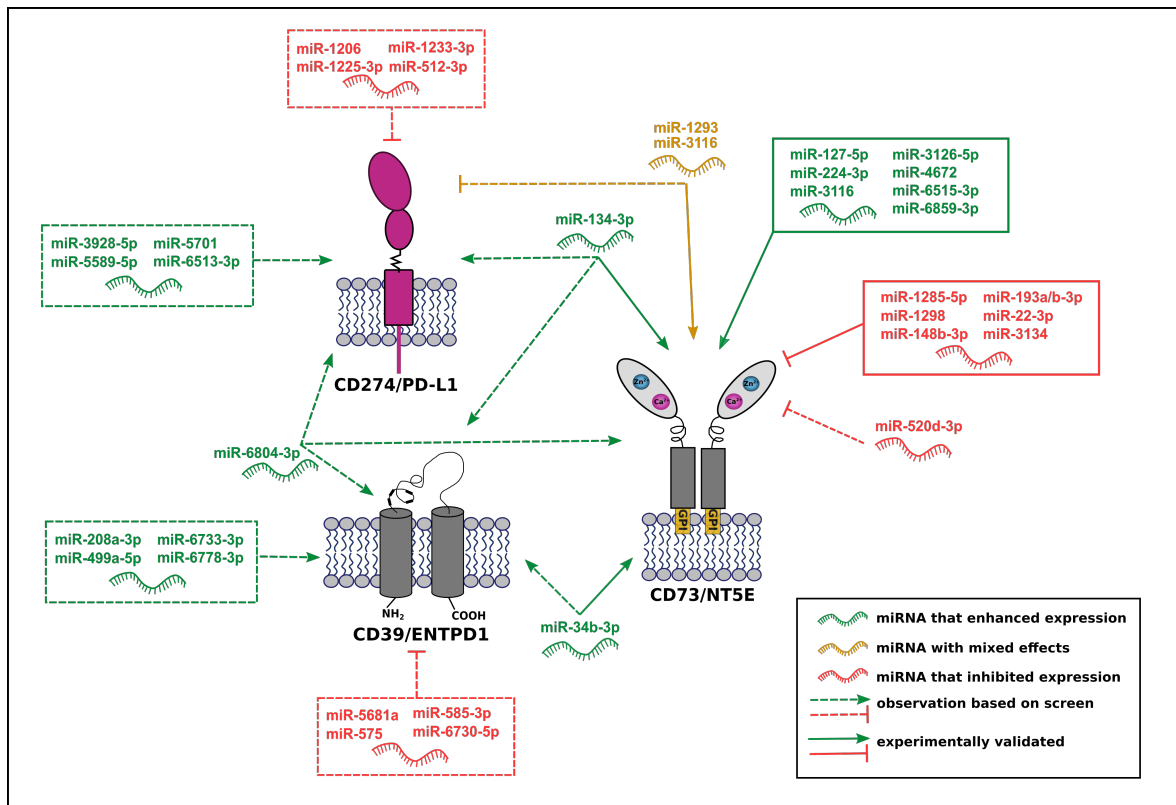


Figure 6.1: Graphical summary of this Thesis. The most important findings of this work were summarized in this figure. miRNAs that enhanced the expression of an immune checkpoint molecule are marked in green. miRNAs that inhibited the expression of an immune checkpoint molecule are marked in red. miRNAs that had mixed effects are shown in orange. Observations only based on the miRNA library screen are shown with dashed lines. Observations validated with independent experiments are shown with continuous lines.

APPENDIX

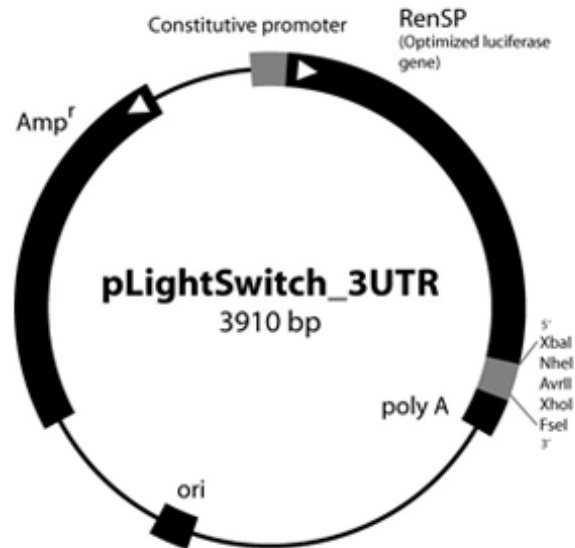


Figure 6.2: Vector map of pLS-3'-UTR plasmids used in this study. LightSwitch reporter vectors were used to assess binding of miRNAs to NT5E 3'-UTR in this study. Human NT5E 3'-UTR sequence was fused with gene encoding for Renilla firefly luciferase. Vectors contain Ampicillin cassette for selection.

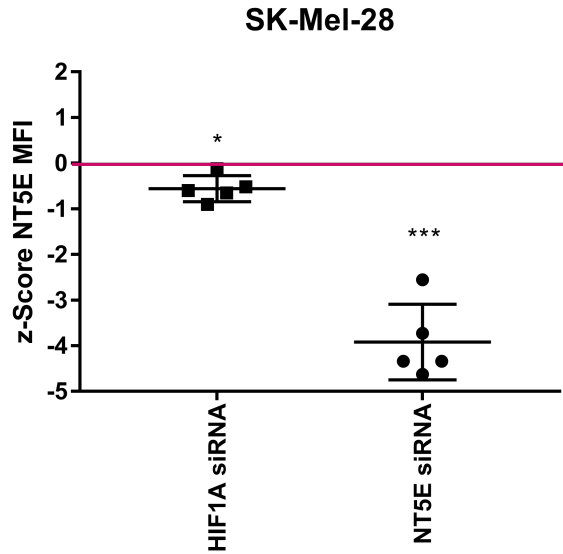


Figure 6.3: Effect of siRNAs on NT5E surface expression. SK-Mel-28 cells were transfected with 25 nM siRNA and 72 h post transfection changes in surface expression was assessed. Measured conditions were part of the miRNA library screen and NT5E MFI values were z-score normalized. NT5E siRNA pool clearly decreased NT5E expression. Also HIF1A siRNA significantly lowered the surface level of NT5E. Significance was assessed by one-sample t-test. *: $p < 0.05$; ***: $p < 0.001$.

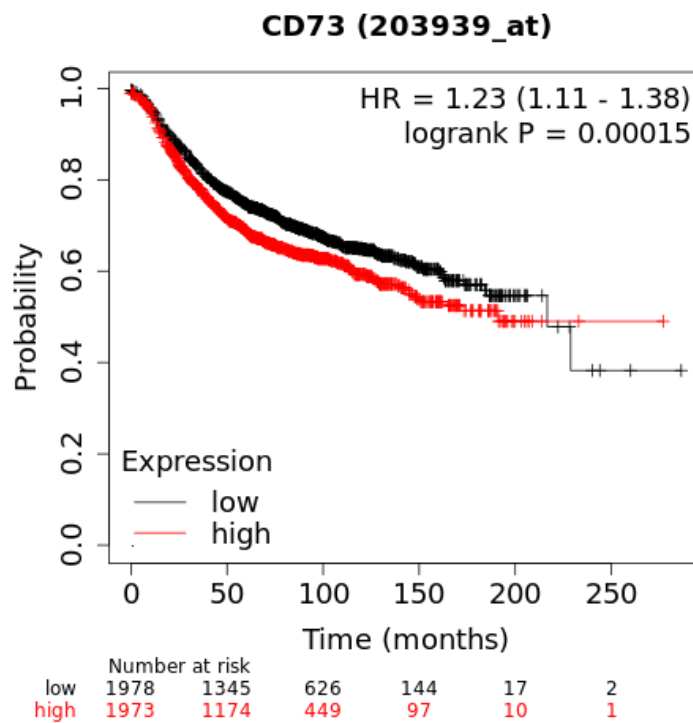


Figure 6.4: Kaplan-Meier curve based on NT5E expression in breast cancer. High NT5E expression is significantly associated with worse prognosis for breast cancer patients. Kaplan-Meier plots were generated with Kaplan-Meier Plotter [90].

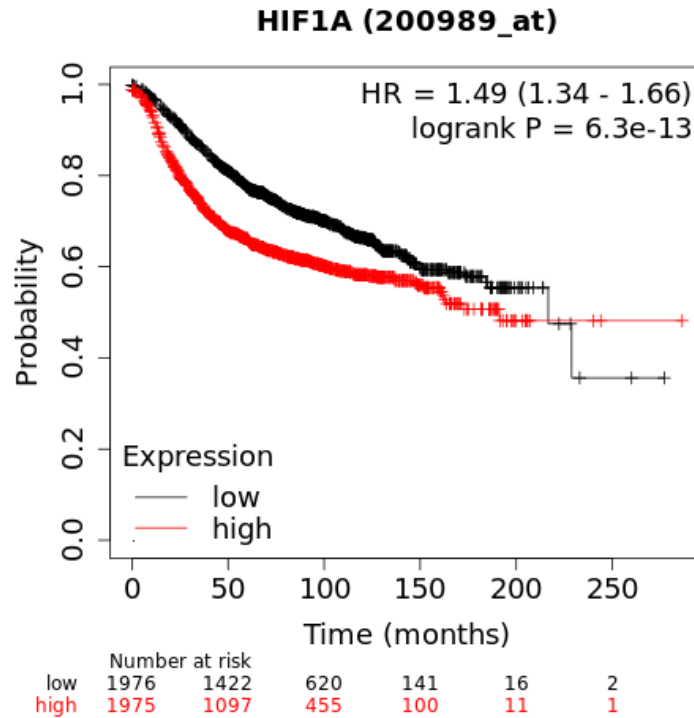


Figure 6.5: Kaplan-Meier curve based on HIF1A expression in breast cancer. High NT5E expression is significantly associated with worse prognosis for breast cancer patients. Kaplan-Meier plots were generated with Kaplan-Meier Plotter [90].

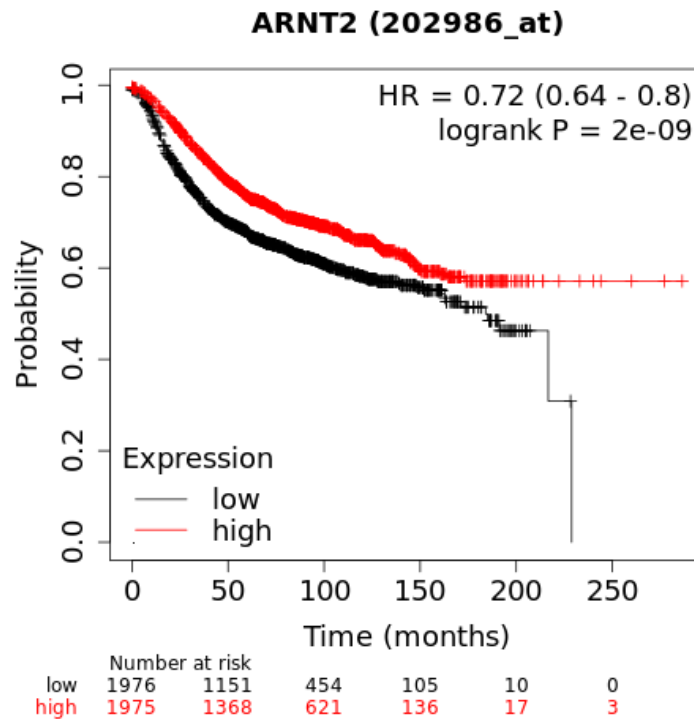


Figure 6.6: Kaplan-Meier curve based on ARNT2 expression in breast cancer. High NT5E expression is significantly associated with a better prognosis for breast cancer patients. Kaplan-Meier plots were generated with Kaplan-Meier Plotter [90].

OWN PUBLICATION LIST

- Alexandra Poos, **Theresa Kordaß**, Amol Kolte, Volker Ast, Marcus Oswald, Karsten Rippe, Rainer König:
Modelling TERT regulation across 19 different cancer types based on the MIPRIIP 2.0 gene regulatory network approach.
BMC Bioinformatics 20, Article number: 737 (2019).
- Volker Ast, **Theresa Kordaß**, Marcus Oswald¹, Amol Kolte¹, David Eisel, Wolfram Osen, Stefan Eichmüller, Alexander Berndt, Rainer König
MiR-192, miR-200c and miR-17 are fibroblast-mediated inhibitors of colorectal cancer invasion.
Oncotarget 2018;9:35559-35580.
- **Theresa Kordaß**, Claudia Weber, David Eisel, Antonino Pane, Wolfram Osen, Stefan B. Eichmüller:
MiR-193b and miR-30c-1 inhibit, whereas miR-576-5p enhances melanoma cell invasion in vitro.*
Oncotarget 2018; 9:32507-32522.
- **Theresa Kordaß**, Wolfram Osen, Stefan Eichmüller:
Controlling the Immune Suppressor: Transcription Factors and MicroRNAs Regulating CD73/NT5E.
Frontiers in Immunology 9/2018.
- Claudia E.M. Weber, Chonglin Luo, Agnes Hotz-Wagenblatt, Adriane Gardyan, **Theresa Kordaß**, Tim Holland-Letz, Wolfram Osen, Stefan B. Eichmüller:
miR-339-3p is a tumor suppressor in melanoma.
Cancer Res. 2016 Jun 15;76(12):3562-71.
- **Theresa Kordaß**, Claudia E. M. Weber, Marcus Oswald, Volker Ast, Mathias Bernhardt, Daniel Novak, Jochen Utikal, Stefan B. Eichmüller, Rainer König:
SOX5 is involved in balanced MTF regulation in human melanoma cells.
BMC Medical Genomics 12/2016; 9(1).
- **Theresa Schacht**, Marcus Oswald, Roland Eils, Stefan B. Eichmüller, Rainer König:
Estimating the activity of transcription factors by the effect on their target genes. Bioinformatics 08/2014; 30(17-17):i401-i407.

BIBLIOGRAPHY

- [1] Cancer. <https://www.who.int/news-room/fact-sheets/detail/cancer>. [Online; accessed 03-January-2021].
- [2] Cancer Statistics - National Cancer Institute. <https://www.cancer.gov/about-cancer/understanding/statistics>, Feb. 2015. [Online; accessed 03-January-2021].
- [3] Breast Cancer Staging | Jordan Breast Cancer Program. <http://www.jbcp.jo/understandingbreastcancer/33>, 2021. [Online; accessed 13-January-2021].
- [4] Draw Venn Diagram. <http://bioinformatics.psb.ugent.be/webtools/Venn/>, 2021. [Online; accessed 05-February-2021].
- [5] Gurobi - The fastest solver. <https://www.gurobi.com/>, 2021. [Online; accessed 24-January-2021].
- [6] Stages of Melanoma. <https://www.aimatmelanoma.org/stages-of-melanoma>, 2021. [Online; accessed 06-January-2021].
- [7] ACS. Survival rates for melanoma skin cancer. <http://www.cancer.org/cancer/skincancer-melanoma/>, 2016. [Online; accessed 17-January-2016].
- [8] V. Agarwal, G. W. Bell, J.-W. Nam, and D. P. Bartel. Predicting effective microRNA target sites in mammalian mRNAs. *eLife*, 4:e05005, Aug. 2015. Publisher: eLife Sciences Publications, Ltd.
- [9] F. E. Ahmed, N. C. Ahmed, P. W. Vos, C. Bonnerup, J. N. Atkins, M. Casey, G. J. Nuovo, W. Naziri, J. E. Wiley, H. Mota, and R. R. Allison. Diagnostic microRNA markers to screen for sporadic human colon cancer in stool: I. Proof of principle. *Cancer Genomics & Proteomics*, 10(3):93–113, June 2013.
- [10] L. Airas, J. Hellman, M. Salmi, P. Bono, T. Puurunen, D. J. Smith, and S. Jalkanen. CD73 is involved in lymphocyte binding to the endothelium: characterization of lymphocyte-vascular adhesion protein 2 identifies it as CD73. *The Journal of Experimental Medicine*, 182(5):1603–1608, Nov. 1995.
- [11] A. N. Al-Shura. 7 - Lymphocytes. In A. N. Al-Shura, editor, *Advanced Hematology in Integrated Cardiovascular Chinese Medicine*, pages 41–46. Academic Press, Jan. 2020.
- [12] B. Allard, P. A. Beavis, P. K. Darcy, and J. Stagg. Immunosuppressive activities of adenosine in cancer. *Current Opinion in Pharmacology*, 29:7–16, Aug. 2016.
- [13] B. Allard, I. Cousineau, K. Spring, and J. Stagg. Chapter fifteen - measurement of cd73 enzymatic activity using luminescence-based and colorimetric assays. In L. Galluzzi and N.-P. Rudqvist, editors, *Tumor Immunology and Immunotherapy – Molecular Methods*, volume 629 of *Methods in Enzymology*, pages 269 – 289. Academic Press, 2019.

- [14] B. Allard, M. S. Longhi, S. C. Robson, and J. Stagg. The ectonucleotidases CD39 and CD73: novel checkpoint inhibitor targets. *Immunological reviews*, 276(1):121–144, Mar. 2017.
- [15] B. Allard, M. Turcotte, and J. Stagg. Targeting CD73 and downstream adenosine receptor signaling in triple-negative breast cancer. *Expert Opinion on Therapeutic Targets*, 18(8):863–881, Aug. 2014.
- [16] D. Allard, B. Allard, and J. Stagg. On the mechanism of anti-CD39 immune checkpoint therapy. *Journal for Immunotherapy of Cancer*, 8(1), Feb. 2020.
- [17] K. N. Anderson, R. B. Schwab, and M. E. Martinez. Reproductive risk factors and breast cancer subtypes: a review of the literature. *Breast Cancer Research and Treatment*, 144(1):1–10, Feb. 2014.
- [18] C. M. B. Andrade, P. L. C. Lopez, B. T. Noronha, M. R. Wink, R. Borojevic, R. Margis, G. Lenz, A. M. O. Battastini, and F. C. R. Guma. Ecto-5-nucleotidase/CD73 knockdown increases cell migration and mRNA level of collagen I in a hepatic stellate cell line. *Cell and Tissue Research*, 344(2):279–286, May 2011.
- [19] L. Antonioli, P. Pacher, E. S. Vizi, and G. Haskó. CD39 and CD73 in immunity and inflammation. *Trends in Molecular Medicine*, 19(6):355–367, June 2013.
- [20] C. Arber, X. Feng, H. Abhyankar, E. Romero, M.-F. Wu, H. E. Heslop, P. Barth, G. Dotti, and B. Savoldo. Survivin-specific T cell receptor targets tumor but not T cells. *The Journal of Clinical Investigation*, 125(1):157–168, Jan. 2015.
- [21] N. Arts, S. Cané, M. Hennequart, J. Lamy, G. Bommer, B. V. d. Eynde, and E. D. Plaen. microRNA-155, Induced by Interleukin-1 β , Represses the Expression of Microphthalmia-Associated Transcription Factor (MITF-M) in Melanoma Cells. *PLOS ONE*, 10(4):e0122517, Apr. 2015. Publisher: Public Library of Science.
- [22] V. Ast, T. Kordaß, M. Oswald, A. Kolte, D. Eisel, W. Osen, S. B. Eichmüller, A. Berndt, and R. König. Mir-192, mir-200c and mir-17 are fibroblast-mediated inhibitors of colorectal cancer invasion. *Oncotarget*, 9(85):35559–35580, 2018.
- [23] Y. Azuma, T. Yokobori, A. Mogi, T. Yajima, T. Kosaka, M. Iijima, K. Shimizu, K. Shirabe, and H. Kuwano. Cancer exosomal microRNAs from gefitinib-resistant lung cancer cells cause therapeutic resistance in gefitinib-sensitive cells. *Surgery Today*, 50(9):1099–1106, Sept. 2020.
- [24] D. P. Bartel. MicroRNAs: target recognition and regulatory functions. *Cell*, 136(2):215–233, Jan. 2009.
- [25] R. Basu and M. Huse. Mechanical Communication at the Immunological Synapse. *Trends in Cell Biology*, 27(4):241–254, Apr. 2017.
- [26] O. Bensaude. Inhibiting eukaryotic transcription. which compound to choose? how to evaluate its activity? *Transcription*, 2(3):103–108, 2011. PMID: 21922053.

- [27] D. Betel, A. Koppal, P. Agius, C. Sander, and C. Leslie. Comprehensive modeling of microRNA targets predicts functional non-conserved and non-canonical sites. *Genome Biology*, 11(8):R90, Aug. 2010.
- [28] E. Bettelli, Y. Carrier, W. Gao, T. Korn, T. B. Strom, M. Oukka, H. L. Weiner, and V. K. Kuchroo. Reciprocal developmental pathways for the generation of pathogenic effector T H 17 and regulatory T cells. *Nature*, 441(7090):235–238, May 2006. Number: 7090 Publisher: Nature Publishing Group.
- [29] M. J. Bevan. Helping the CD8 + T-cell response. *Nature Reviews Immunology*, 4(8):595–602, Aug. 2004. Number: 8 Publisher: Nature Publishing Group.
- [30] M. Bhaskaran and M. Mohan. MicroRNAs: history, biogenesis, and their evolving role in animal development and disease. *Veterinary Pathology*, 51(4):759–774, July 2014.
- [31] N. Bonnin, E. Armandy, J. Carras, S. Ferrandon, P. Battiston-Montagne, M. Aubry, S. Guihard, D. Meyronet, J.-P. Foy, P. Saintigny, S. Ledrappier, A. Jung, R. Rimokh, C. Rodriguez-Lafrasse, and D. Poncet. MiR-422a promotes loco-regional recurrence by targeting NT5E/CD73 in head and neck squamous cell carcinoma. *Oncotarget*, 7(28):44023–44038, June 2016.
- [32] G. M. Borchert, W. Lanier, and B. L. Davidson. RNA polymerase III transcribes human microRNAs. *Nature Structural & Molecular Biology*, 13(12):1097–1101, Dec. 2006.
- [33] J. Braun, C. Hoang-Vu, H. Dralle, and S. Hüttelmaier. Downregulation of microRNAs directs the EMT and invasive potential of anaplastic thyroid carcinomas. *Oncogene*, 29(29):4237–4244, July 2010. Number: 29 Publisher: Nature Publishing Group.
- [34] C. J. Breitbach, B. D. Lichty, and J. C. Bell. Oncolytic Viruses: Therapeutics With an Identity Crisis. *EBioMedicine*, 9:31–36, July 2016.
- [35] C. Breunig, J. Pahl, M. Küblbeck, M. Miller, D. Antonelli, N. Erdem, C. Wirth, R. Will, A. Bott, A. Cerwenka, and S. Wiemann. MicroRNA-519a-3p mediates apoptosis resistance in breast cancer cells and their escape from recognition by natural killer cells. *Cell Death & Disease*, 8(8):e2973, Aug. 2017.
- [36] L. Buisseret, S. Pommey, B. Allard, S. Garaud, M. Bergeron, I. Cousineau, L. Ameye, Y. Bareche, M. Paesmans, J. P. A. Crown, A. Di Leo, S. Loi, M. Piccart-Gebhart, K. Willard-Gallo, C. Sotiriou, and J. Stagg. Clinical significance of CD73 in triple-negative breast cancer: multiplex analysis of a phase III clinical trial. *Annals of Oncology: Official Journal of the European Society for Medical Oncology*, 29(4):1056–1062, Apr. 2018.
- [37] F. Cardoso, S. Kyriakides, S. Ohno, F. Penault-Llorca, P. Poortmans, I. T. Rubio, S. Zackrisson, and E. Senkus. Early breast cancer: ESMO Clinical Practice Guidelines for diagnosis, treatment and follow-up†. *Annals of Oncology*, 30(8):1194–1220, Aug. 2019. Publisher: Elsevier.
- [38] T. M. Casey, J. Eneman, A. Crocker, J. White, J. Tessitore, M. Stanley, S. Harlow, J. Y. Bunn, D. Weaver, H. Muss, and K. Plaut. Cancer associated fibroblasts stimulated

- by transforming growth factor beta1 (TGF-1) increase invasion rate of tumor cells: a population study. *Breast Cancer Research and Treatment*, 110(1):39–49, July 2008.
- [39] C. Chakraborty, A. R. Sharma, G. Sharma, and S.-S. Lee. The Interplay among miRNAs, Major Cytokines, and Cancer-Related Inflammation. *Molecular Therapy. Nucleic Acids*, 20:606–620, Apr. 2020.
- [40] F. Chalmin, G. Mignot, M. Bruchard, A. Chevriaux, F. Végran, A. Hichami, S. Ladoire, V. Derangère, J. Vincent, D. Masson, S. C. Robson, G. Eberl, J. R. Pallandre, C. Borg, B. Ryffel, L. Apetoh, C. Rébé, and F. Ghiringhelli. Stat3 and Gfi-1 transcription factors control Th17 cell immunosuppressive activity via the regulation of ectonucleotidase expression. *Immunity*, 36(3):362–373, Mar. 2012.
- [41] S. Chanda, S. Nandi, and M. Chawla-Sarkar. Rotavirus-induced miR-142-5p elicits proviral milieu by targeting non-canonical transforming growth factor beta signalling and apoptosis in cells. *Cellular Microbiology*, 18(5):733–747, May 2016.
- [42] S. Chang, L. Sun, and G. Feng. SP1-mediated long noncoding RNA POU3F3 accelerates the cervical cancer through miR-127-5p/FOXD1. *Biomedicine & Pharmacotherapy*, 117:109133, Sept. 2019.
- [43] J. Chen, H. E. Feilotter, G. C. Paré, X. Zhang, J. G. W. Pemberton, C. Garady, D. Lai, X. Yang, and V. A. Tron. MicroRNA-193b represses cell proliferation and regulates cyclin D1 in melanoma. *The American Journal of Pathology*, 176(5):2520–2529, May 2010.
- [44] K. Chen, M. X. Liu, C. S.-L. Mak, M. M.-H. Yung, T. H.-Y. Leung, D. Xu, S.-F. Ngu, K. K.-L. Chan, H. Yang, H. Y.-S. Ngan, and D. W. Chan. Methylation-associated silencing of miR-193a-3p promotes ovarian cancer aggressiveness by targeting GRB7 and MAPK/ERK pathways. *Theranostics*, 8(2):423–436, Jan. 2018.
- [45] S. Chen, J. Fan, M. Zhang, L. Qin, D. Dominguez, A. Long, G. Wang, R. Ma, H. Li, Y. Zhang, D. Fang, J. Sosman, and B. Zhang. CD73 expression on effector T cells sustained by TGF- facilitates tumor resistance to anti-4-1BB/CD137 therapy. *Nature Communications*, 10(1):150, Jan. 2019. Number: 1 Publisher: Nature Publishing Group.
- [46] W. Chen, X.-m. Fan, L. Mao, J.-y. Zhang, J. LI, J.-z. Wu, and J.-h. Tang. MicroRNA-224: as a potential target for miR-based therapy of cancer. *Tumor Biology*, 36(9):6645–6652, Sept. 2015.
- [47] W. Chen, Q. Lu, S. Li, X. Zhang, and X. Xue. microRNA-1298 inhibits the malignant behaviors of breast cancer cells via targeting ADAM9. *Bioscience Reports*, 40(12), Dec. 2020.
- [48] Y. Chen and X. Wang. miRDB: an online database for prediction of functional microRNA targets. *Nucleic Acids Research*, 48(D1):D127–D131, Jan. 2020.
- [49] D. Cheng, S. Zhao, H. Tang, D. Zhang, H. Sun, F. Yu, W. Jiang, B. Yue, J. Wang, M. Zhang, Y. Yu, X. Liu, X. Sun, Z. Zhou, X. Qin, X. Zhang, D. Yan, Y. Wen, and

- Z. Peng. MicroRNA-20a-5p promotes colorectal cancer invasion and metastasis by downregulating Smad4. *Oncotarget*, 7(29):45199–45213, June 2016.
- [50] D. Cimino, C. D. Pittà, F. Orso, M. Zampini, S. Casara, E. Penna, E. Quaglino, M. Forni, C. Damasco, E. Pinatel, R. Ponzzone, C. Romualdi, C. Brisken, M. D. Bortoli, N. Biglia, P. Provero, G. Lanfranchi, and D. Taverna. miR148b is a major coordinator of breast cancer progression in a relapse-associated microRNA signature by targeting ITGA5, ROCK1, PIK3CA, NRAS, and CSF1. *The FASEB Journal*, 27(3):1223–1235, 2013. [_eprint: https://faseb.onlinelibrary.wiley.com/doi/pdf/10.1096/fj.12-214692](https://faseb.onlinelibrary.wiley.com/doi/pdf/10.1096/fj.12-214692).
- [51] S. P. Colgan, H. K. Eltzschig, T. Eckle, and L. F. Thompson. Physiological roles for ecto-5'-nucleotidase (CD73). *Purinergic Signalling*, 2(2):351–360, June 2006.
- [52] W. Dai, J. He, L. Zheng, M. Bi, F. Hu, M. Chen, H. Niu, J. Yang, Y. Luo, W. Tang, and M. Sheng. miR-148b-3p, miR-190b, and miR-429 Regulate Cell Progression and Act as Potential Biomarkers for Breast Cancer. *Journal of Breast Cancer*, 22(2):219–236, Apr. 2019.
- [53] J. Daniel Jensen and B. E. Elewski. The ABCDEF Rule: Combining the "ABCDE Rule" and the "Ugly Duckling Sign" in an Effort to Improve Patient Self-Screening Examinations. *The Journal of Clinical and Aesthetic Dermatology*, 8(2):15, Feb. 2015.
- [54] P. J. Darlington, M. G. Kirchhof, G. Criado, J. Sondhi, and J. Madrenas. Hierarchical Regulation of CTLA-4 Dimer-Based Lattice Formation and Its Biological Relevance for T Cell Inactivation. *The Journal of Immunology*, 175(2):996–1004, July 2005. Publisher: American Association of Immunologists Section: MOLECULAR AND STRUCTURAL IMMUNOLOGY.
- [55] E. Dassi, A. Re, S. Leo, T. Tebaldi, L. Pasini, D. Peroni, and A. Quattrone. AURA 2: Empowering discovery of post-transcriptional networks. *Translation (Austin, Tex.)*, 2(1):e27738, 2014.
- [56] D. Di Vizio, M. Morello, A. C. Dudley, P. W. Schow, R. M. Adam, S. Morley, D. Mulholland, M. Rotinen, M. H. Hager, L. Insabato, M. A. Moses, F. Demichelis, M. P. Lisanti, H. Wu, M. Klagsbrun, N. A. Bhowmick, M. A. Rubin, C. D'Souza-Schorey, and M. R. Freeman. Large oncosomes in human prostate cancer tissues and in the circulation of mice with metastatic disease. *The American Journal of Pathology*, 181(5):1573–1584, Nov. 2012.
- [57] R. Dinami, V. Buemi, R. Sestito, A. Zappone, Y. Ciani, M. Mano, E. Petti, A. Sacconi, G. Blandino, M. Giacca, S. Piazza, R. Benetti, and S. Schoeftner. Epigenetic silencing of miR-296 and miR-512 ensures hTERT dependent apoptosis protection and telomere maintenance in basal-type breast cancer cells. *Oncotarget*, 8(56):95674–95691, Nov. 2017.
- [58] R. Dinami, C. Ercolani, E. Petti, S. Piazza, Y. Ciani, R. Sestito, A. Sacconi, F. Biagioni, C. le Sage, R. Agami, R. Benetti, M. Mottolese, C. Schneider, G. Blandino, and S. Schoeftner. miR-155 drives telomere fragility in human breast cancer by targeting TRF1. *Cancer Research*, 74(15):4145–4156, Aug. 2014.

- [59] J. Dong, Y.-P. Zhao, L. Zhou, T.-P. Zhang, and G. Chen. Bcl-2 upregulation induced by miR-21 via a direct interaction is associated with apoptosis and chemoresistance in MIA PaCa-2 pancreatic cancer cells. *Archives of Medical Research*, 42(1):8–14, Jan. 2011.
- [60] G. Dotti, S. Gottschalk, B. Savoldo, and M. K. Brenner. Design and Development of Therapies using Chimeric Antigen Receptor-Expressing T cells. *Immunological reviews*, 257(1), Jan. 2014.
- [61] S. Dror, L. Sander, H. Schwartz, D. Sheinboim, A. Barzilai, Y. Dishon, S. Apcher, T. Golan, S. Greenberger, I. Barshack, H. Malcov, A. Zilberberg, L. Levin, M. Nessling, Y. Friedmann, V. Igras, O. Barzilai, H. Vaknine, R. Brenner, A. Zinger, A. Schroeder, P. Gonen, M. Khaled, N. Erez, J. D. Hoheisel, and C. Levy. Melanoma miRNA trafficking controls tumour primary niche formation. *Nature Cell Biology*, 18(9):1006–1017, Sept. 2016.
- [62] Z. Du, J. Wu, J. Wang, Y. Liang, S. Zhang, Z. Shang, and W. Zuo. MicroRNA-1298 is downregulated in non-small cell lung cancer and suppresses tumor progression in tumor cells. *Diagnostic Pathology*, 14, Dec. 2019.
- [63] M. E. Dudley, J. R. Wunderlich, T. E. Shelton, J. Even, and S. A. Rosenberg. Generation of Tumor-Infiltrating Lymphocyte Cultures for Use in Adoptive Transfer Therapy for Melanoma Patients. *Journal of immunotherapy (Hagerstown, Md. : 1997)*, 26(4):332–342, 2003.
- [64] G. P. Dunn, L. J. Old, and R. D. Schreiber. The three Es of cancer immunoediting. *Annual Review of Immunology*, 22:329–360, 2004.
- [65] M. L. Dustin. The immunological synapse. *Cancer immunology research*, 2(11):1023–1033, Nov. 2014.
- [66] K. L. Eales, K. E. R. Hollinshead, and D. A. Tennant. Hypoxia and metabolic adaptation of cancer cells. *Oncogenesis*, 5:e190, Jan. 2016.
- [67] S. B. Eichmüller, W. Osen, O. Mandelboim, and B. Seliger. Immune Modulatory microRNAs Involved in Tumor Attack and Tumor Immune Escape. *Journal of the National Cancer Institute*, 109(10), Oct. 2017.
- [68] D. Eisel. Reprogramming of M2-like macrophages by CD4+ T cells, transcription factor knockdown and miRNA transfection, 2019. ISSN: 0002-5755.
- [69] L. A. Emens. Breast Cancer Immunotherapy: Facts and Hopes. *Clinical Cancer Research: An Official Journal of the American Association for Cancer Research*, 24(3):511–520, Feb. 2018.
- [70] Q. Fan, X. Hu, H. Zhang, S. Wang, H. Zhang, C. You, C.-Y. Zhang, H. Liang, X. Chen, and Y. Ba. MiR-193a-3p is an Important Tumour Suppressor in Lung Cancer and Directly Targets KRAS. *Cellular Physiology and Biochemistry*, 44(4):1311–1324, 2017. Publisher: Karger Publishers.

- [71] S. Farber, G. D'Angio, A. Evans, and A. Mitus. Clinical studies of actinomycin d with special reference to wilms' tumor in children*. *Annals of the New York Academy of Sciences*, 89(2):421–424, 1960.
- [72] H. Farmer, N. McCabe, C. J. Lord, A. N. J. Tutt, D. A. Johnson, T. B. Richardson, M. Santarosa, K. J. Dillon, I. Hickson, C. Knights, N. M. B. Martin, S. P. Jackson, G. C. M. Smith, and A. Ashworth. Targeting the DNA repair defect in BRCA mutant cells as a therapeutic strategy. *Nature*, 434(7035):917–921, Apr. 2005. Number: 7035 Publisher: Nature Publishing Group.
- [73] L. Fattore, R. Mancini, M. Acunzo, G. Romano, A. Laganà, M. E. Pisanu, D. Malpicci, G. Madonna, D. Mallardo, M. Capone, F. Fulciniti, L. Mazzucchelli, G. Botti, C. M. Croce, P. A. Ascierto, and G. Ciliberto. miR-579-3p controls melanoma progression and resistance to target therapy. *Proceedings of the National Academy of Sciences*, 113(34):E5005–E5013, Aug. 2016. Publisher: National Academy of Sciences Section: PNAS Plus.
- [74] M. Fausther, N. Sheung, Y. Saiman, M. B. Bansal, and J. A. Dranoff. Activated hepatic stellate cells upregulate transcription of ecto-5-nucleotidase/CD73 via specific SP1 and SMAD promoter elements. *American Journal of Physiology - Gastrointestinal and Liver Physiology*, 303(8):G904–G914, Oct. 2012.
- [75] M. Fernandez-Gallardo, R. González-Ramírez, A. Sandoval, R. Felix, and E. Monjaraz. Adenosine Stimulate Proliferation and Migration in Triple Negative Breast Cancer Cells. *PLOS ONE*, 11(12):e0167445, Dec. 2016. Publisher: Public Library of Science.
- [76] M. Y. Fong, W. Zhou, L. Liu, A. Y. Alontaga, M. Chandra, J. Ashby, A. Chow, S. T. F. O'Connor, S. Li, A. R. Chin, G. Somlo, M. Palomares, Z. Li, J. R. Tremblay, A. Tsuyada, G. Sun, M. A. Reid, X. Wu, P. Swiderski, X. Ren, Y. Shi, M. Kong, W. Zhong, Y. Chen, and S. E. Wang. Breast-cancer-secreted miR-122 reprograms glucose metabolism in premetastatic niche to promote metastasis. *Nature Cell Biology*, 17(2):183–194, Feb. 2015. Number: 2 Publisher: Nature Publishing Group.
- [77] L. M. Francisco, P. T. Sage, and A. H. Sharpe. The PD-1 pathway in tolerance and autoimmunity. *Immunological Reviews*, 236(1):219–242, 2010. _eprint: <https://onlinelibrary.wiley.com/doi/pdf/10.1111/j.1600-065X.2010.00923.x>.
- [78] B. Friedenson. The BRCA1/2 pathway prevents hematologic cancers in addition to breast and ovarian cancers. *BMC Cancer*, 7(1):152, Aug. 2007.
- [79] F. Fuchs Wightman, L. E. Giono, J. P. Fededa, and M. de la Mata. Target RNAs Strike Back on MicroRNAs. *Frontiers in Genetics*, 9:435, 2018.
- [80] M. Fulciniti, N. Amodio, R. L. Bandi, A. Cagnetta, M. K. Samur, C. Acharya, R. Prabhala, P. D'Aquila, D. Bellizzi, G. Passarino, S. Adamia, A. Neri, Z. R. Hunter, S. P. Treon, K. C. Anderson, P. Tassone, and N. C. Munshi. miR-23b/SP1/c-myc forms a feed-forward loop supporting multiple myeloma cell growth. *Blood Cancer Journal*, 6:e380, Jan. 2016.

- [81] A. Gajos-Michniewicz and M. Czyz. Role of miRNAs in Melanoma Metastasis. *Cancers*, 11(3), Mar. 2019.
- [82] L. Gan, L. Lv, and S. Liao. Long non-coding RNA H19 regulates cell growth and metastasis via the miR-22-3p/Snail1 axis in gastric cancer. *International Journal of Oncology*, 54(6):2157–2168, June 2019. Publisher: Spandidos Publications.
- [83] M. Gato-Cañas, M. Zuazo, H. Arasanz, M. Ibañez-Vea, L. Lorenzo, G. Fernandez-Hinojal, R. Vera, C. Smerdou, E. Martisova, I. Arozarena, C. Wellbrock, D. Llopiz, M. Ruiz, P. Sarobe, K. Breckpot, G. Kochan, and D. Escors. PDL1 Signals through Conserved Sequence Motifs to Overcome Interferon-Mediated Cytotoxicity. *Cell Reports*, 20(8):1818–1829, Aug. 2017.
- [84] L. K. Gauen, Y. Zhu, F. Letourneur, Q. Hu, J. B. Bolen, L. A. Matis, R. D. Klausner, and A. S. Shaw. Interactions of p59fyn and ZAP-70 with T-cell receptor activation motifs: defining the nature of a signalling motif. *Molecular and Cellular Biology*, 14(6):3729–3741, June 1994.
- [85] D. Gerloff, J. Lützkendorf, R. K. Moritz, T. Wersig, K. Mäder, L. P. Müller, and C. Sunderkötter. Melanoma-Derived Exosomal miR-125b-5p Educates Tumor Associated Macrophages (TAMs) by Targeting Lysosomal Acid Lipase A (LIPA). *Cancers*, 12(2), Feb. 2020.
- [86] M. H. Geukes Foppen, M. Donia, I. M. Svane, and J. B. A. G. Haanen. Tumor-infiltrating lymphocytes for the treatment of metastatic cancer. *Molecular Oncology*, 9(10):1918–1935, Dec. 2015.
- [87] S. Grasedieck, A. Sorrentino, C. Langer, C. Buske, H. Döhner, D. Mertens, and F. Kuchenbauer. Circulating microRNAs in hematological diseases: principles, challenges, and perspectives. *Blood*, 121(25):4977–4984, June 2013.
- [88] V. Gray-Schopfer, C. Wellbrock, and R. Marais. Melanoma biology and new targeted therapy. *Nature*, 445(7130):851–857, Feb. 2007. Number: 7130 Publisher: Nature Publishing Group.
- [89] M. G. Guess, K. K. B. Barthel, B. C. Harrison, and L. A. Leinwand. miR-30 Family microRNAs Regulate Myogenic Differentiation and Provide Negative Feedback on the microRNA Pathway. *PLOS ONE*, 10(2):e0118229, Feb. 2015. Publisher: Public Library of Science.
- [90] B. Györffy, A. Lanczky, A. C. Eklund, C. Denkert, J. Budczies, Q. Li, and Z. Szallasi. An online survival analysis tool to rapidly assess the effect of 22,277 genes on breast cancer prognosis using microarray data of 1,809 patients. *Breast Cancer Research and Treatment*, 123(3):725–731, Oct. 2010.
- [91] S. Hadrup, M. Donia, and P. Thor Straten. Effector CD4 and CD8 T cells and their role in the tumor microenvironment. *Cancer Microenvironment: Official Journal of the International Cancer Microenvironment Society*, 6(2):123–133, Aug. 2013.

- [92] M. Hajjari, A. Salavaty, F. Crea, and Y. Kee Shin. The potential role of PHF6 as an oncogene: a genotranscriptomic/proteomic meta-analysis. *Tumor Biology*, 37(4):5317–5325, 2016.
- [93] R. Hamam, D. Hamam, K. A. Alsaleh, M. Kassem, W. Zaher, M. Alfayez, A. Aldahmash, and N. M. Alajez. Circulating microRNAs in breast cancer: novel diagnostic and prognostic biomarkers. *Cell Death & Disease*, 8(9):e3045–e3045, Sept. 2017. Number: 9 Publisher: Nature Publishing Group.
- [94] J. Han, Y. Lee, K.-H. Yeom, Y.-K. Kim, H. Jin, and V. N. Kim. The Drosha-DGCR8 complex in primary microRNA processing. *Genes & Development*, 18(24):3016–3027, Dec. 2004.
- [95] D. Hanahan and R. A. Weinberg. The Hallmarks of Cancer. *Cell*, 100(1):57–70, Jan. 2000. Publisher: Elsevier.
- [96] D. Hanahan and R. A. Weinberg. Hallmarks of Cancer: The Next Generation. *Cell*, 144(5):646–674, Mar. 2011. Publisher: Elsevier.
- [97] O. Hankinson. Why Does ARNT2 Behave Differently from ARNT? *Toxicological sciences : an official journal of the Society of Toxicology*, 103(1):1–3, May 2008.
- [98] J. Hanna, G. S. Hossain, and J. Kocerha. The Potential for microRNA Therapeutics and Clinical Research. *Frontiers in Genetics*, 10, 2019. Publisher: Frontiers.
- [99] K. R. Hansen, R. Resta, C. F. Webb, and L. F. Thompson. Isolation and characterization of the promoter of the human 5'-nucleotidase (CD73)-encoding gene. *Gene*, 167(1-2):307–312, Dec. 1995.
- [100] W. He, Y. Zhang, and S. Xia. LncRNA NNT-AS1 promotes non-small cell lung cancer progression through regulating miR-22-3p/YAP1 axis. *Thoracic Cancer*, 11(3):549–560, Mar. 2020.
- [101] A. Heinemann, F. Zhao, S. Pechlivanis, J. Eberle, A. Steinle, S. Diederichs, D. Schaden-dorf, and A. Paschen. Tumor suppressive microRNAs miR-34a/c control cancer cell expression of ULBP2, a stress-induced ligand of the natural killer cell receptor NKG2D. *Cancer Research*, 72(2):460–471, Jan. 2012.
- [102] H. Hidaka, N. Seki, H. Yoshino, T. Yamasaki, Y. Yamada, N. Nohata, M. Fuse, M. Nakagawa, and H. Enokida. Tumor suppressive microRNA-1285 regulates novel molecular targets: Aberrant expression and functional significance in renal cell carcinoma. *Oncotarget*, 3(1):44–57, Jan. 2012.
- [103] L. C. Hinske, G. S. França, H. A. M. Torres, D. T. Ohara, C. M. Lopes-Ramos, J. Heyn, L. F. L. Reis, L. Ohno-Machado, S. Kreth, and P. A. F. Galante. miRIAD-integrating microRNA inter- and intragenic data. *Database: The Journal of Biological Databases and Curation*, 2014, 2014.
- [104] A. Hironaka-Mitsuhashi, K. Otsuka, L. Gailhouste, A. S. Calle, M. Kumazaki, Y. Yamamoto, Y. Fujiwara, and T. Ochiya. MiR-1285-5p/TMEM194A axis affects cell proliferation in breast cancer. *Cancer Science*, 111(2):395–405, 2020. _eprint: <https://onlinelibrary.wiley.com/doi/pdf/10.1111/cas.14287>.

- [105] T. Hirota, Y. Date, Y. Nishibatake, H. Takane, Y. Fukuoka, Y. Taniguchi, N. Burioka, E. Shimizu, H. Nakamura, K. Otsubo, and I. Ieiri. Dihydropyrimidine dehydrogenase (DPD) expression is negatively regulated by certain microRNAs in human lung tissues. *Lung Cancer (Amsterdam, Netherlands)*, 77(1):16–23, July 2012.
- [106] D. Hockemeyer and K. Collins. Control of telomerase action at human telomeres. *Nature Structural & Molecular Biology*, 22(11):848–852, Nov. 2015.
- [107] S.-D. Hsu, C.-H. Chu, A.-P. Tsou, S.-J. Chen, H.-C. Chen, P. W.-C. Hsu, Y.-H. Wong, Y.-H. Chen, G.-H. Chen, and H.-D. Huang. miRNAMap 2.0: genomic maps of microRNAs in metazoan genomes. *Nucleic Acids Research*, 36(Database issue):D165–169, Jan. 2008.
- [108] J. Hu, Z. Shan, K. Hu, F. Ren, W. Zhang, M. Han, Y. Li, K. Feng, L. Lei, and Y. Feng. miRNA-223 inhibits epithelial-mesenchymal transition in gastric carcinoma cells via Sp1. *International Journal of Oncology*, 49(1):325–335, July 2016.
- [109] L. Huan, C. Bao, D. Chen, Y. Li, J. Lian, J. Ding, S. Huang, L. Liang, and X. He. MicroRNA-127-5p targets the biliverdin reductase B/nuclear factor-B pathway to suppress cell growth in hepatocellular carcinoma cells. *Cancer Science*, 107(3):258–266, Mar. 2016.
- [110] J. Huang, Q. Weng, Y. Shi, W. Mao, Z. Zhao, R. Wu, J. Ren, S. Fang, C. Lu, Y. Du, and J. Ji. MicroRNA-155-5p suppresses PD-L1 expression in lung adenocarcinoma. *FEBS open bio*, 10(6):1065–1071, June 2020.
- [111] E. Hui, J. Cheung, J. Zhu, X. Su, M. J. Taylor, H. A. Wallweber, D. K. Sasmal, J. Huang, J. M. Kim, I. Mellman, and R. D. Vale. T cell costimulatory receptor CD28 is a primary target for PD-1-mediated inhibition. *Science (New York, N.Y.)*, 355(6332):1428–1433, Mar. 2017.
- [112] Y. Ikeda, E. Tanji, N. Makino, S. Kawata, and T. Furukawa. MicroRNAs associated with mitogen-activated protein kinase in human pancreatic cancer. *Molecular cancer research: MCR*, 10(2):259–269, Feb. 2012.
- [113] Y. Inoue, K. Yoshimura, N. Kurabe, T. Kahyo, A. Kawase, M. Tanahashi, H. Ogawa, N. Inui, K. Funai, K. Shinmura, H. Niwa, T. Suda, and H. Sugimura. Prognostic impact of CD73 and A2A adenosine receptor expression in non-small-cell lung cancer. *Oncotarget*, 8(5):8738–8751, Jan. 2017.
- [114] M. A. Jafri, S. A. Ansari, M. H. Alqahtani, and J. W. Shay. Roles of telomeres and telomerase in cancer, and advances in telomerase-targeted therapies. *Genome Medicine*, 8(1):69, June 2016.
- [115] A. Janaszak-Jasiecka, A. Siekierzycka, S. Bartoszewska, M. Serocki, L. W. Dobrucki, J. F. Collawn, L. Kalinowski, and R. Bartoszewski. eNOS expression and NO release during hypoxia is inhibited by miR-200b in human endothelial cells. *Angiogenesis*, 21(4):711–724, Nov. 2018.

- [116] M. Jang, S. S. Kim, and J. Lee. Cancer cell metabolism: implications for therapeutic targets. *Experimental & Molecular Medicine*, 45(10):e45–e45, Oct. 2013. Number: 10 Publisher: Nature Publishing Group.
- [117] Y. Jia, S. Hao, G. Jin, H. Li, X. Ma, Y. Zheng, D. Xiao, and Y. Wang. Overexpression of ARNT2 is associated with decreased cell proliferation and better prognosis in gastric cancer. *Molecular and Cellular Biochemistry*, 450(1-2):97–103, Jan. 2019.
- [118] L. Jiang, X. Lv, J. Li, J. Li, X. Li, W. Li, and Y. Li. The status of microRNA-21 expression and its clinical significance in human cutaneous malignant melanoma. *Acta Histochemica*, 114(6):582–588, Oct. 2012.
- [119] W. Jiang, X. Han, J. Wang, L. Wang, Z. Xu, Q. Wei, W. Zhang, and H. Wang. miR-22 enhances the radiosensitivity of small-cell lung cancer by targeting the WRNIP1. *Journal of Cellular Biochemistry*, 120(10):17650–17661, Oct. 2019.
- [120] T. Jin, H. Suk Kim, S. Ki Choi, E. Hye Hwang, J. Woo, H. Suk Ryu, K. Kim, A. Moon, and W. Kyung Moon. microRNA-200c/141 upregulates SerpinB2 to promote breast cancer cell metastasis and reduce patient survival. *Oncotarget*, 8(20):32769–32782, May 2017.
- [121] K. B. Jones, Z. Salah, S. Del Mare, M. Galasso, E. Gaudio, G. J. Nuovo, F. Lovat, K. LeBlanc, J. Palatini, R. L. Randall, S. Volinia, G. S. Stein, C. M. Croce, J. B. Lian, and R. I. Aqeilan. miRNA signatures associate with pathogenesis and progression of osteosarcoma. *Cancer Research*, 72(7):1865–1877, Apr. 2012.
- [122] V. C. Jordan. A current view of tamoxifen for the treatment and prevention of breast cancer. *British Journal of Pharmacology*, 110(2):507–517, 1993. _eprint: <https://bppsups.onlinelibrary.wiley.com/doi/pdf/10.1111/j.1476-5381.1993.tb13840.x>.
- [123] L. A. Kalekar, S. E. Schmiel, S. L. Nandiwada, W. Y. Lam, L. O. Barsness, N. Zhang, G. L. Stritesky, D. Malhotra, K. E. Pauken, J. L. Linehan, M. G. O’Sullivan, B. T. Fife, K. A. Hogquist, M. K. Jenkins, and D. L. Mueller. CD4+ T cell anergy prevents autoimmunity and generates regulatory T cell precursors. *Nature immunology*, 17(3):304–314, Mar. 2016.
- [124] M. Kamińska, T. Ciszewski, K. Łopacka Szatan, P. Miotła, and E. Starosławska. Breast cancer risk factors. *Przegląd Menopauzalny = Menopause Review*, 14(3):196–202, Sept. 2015.
- [125] M. Kertesz, N. Iovino, U. Unnerstall, U. Gaul, and E. Segal. The role of site accessibility in microRNA target recognition. *Nature Genetics*, 39(10):1278–1284, Oct. 2007. Number: 10 Publisher: Nature Publishing Group.
- [126] Y. Kimura, A. Kasamatsu, D. Nakashima, M. Yamatoji, Y. Minakawa, K. Koike, K. Fushimi, M. Higo, Y. Endo-Sakamoto, M. Shiiba, H. Tanzawa, and K. Uzawa. ARNT2 Regulates Tumoral Growth in Oral Squamous Cell Carcinoma. *Journal of Cancer*, 7(6):702–710, Mar. 2016.

- [127] K. Knapp, M. Zebisch, J. Pippel, A. El-Tayeb, C. E. Müller, and N. Sträter. Crystal Structure of the Human Ecto-5-Nucleotidase (CD73): Insights into the Regulation of Purinergic Signaling. *Structure*, 20(12):2161–2173, Dec. 2012. Publisher: Elsevier.
- [128] T. Kordaß, W. Osen, and S. B. Eichmüller. Controlling the Immune Suppressor: Transcription Factors and MicroRNAs Regulating CD73/NT5E. *Frontiers in Immunology*, 9, 2018. Publisher: Frontiers.
- [129] A. Kozomara, M. Birgaoanu, and S. Griffiths-Jones. miRBase: from microRNA sequences to function. *Nucleic Acids Research*, 47(D1):D155–D162, Jan. 2019. Publisher: Oxford Academic.
- [130] L. Kreft, A. Soete, P. Hulpiau, A. Botzki, Y. Saeys, and P. De Bleser. ConTra v3: a tool to identify transcription factor binding sites across species, update 2017. *Nucleic Acids Research*, 45(W1):W490–W494, July 2017.
- [131] A. Krek, D. Grün, M. N. Poy, R. Wolf, L. Rosenberg, E. J. Epstein, P. MacMenamin, I. da Piedade, K. C. Gunsalus, M. Stoffel, and N. Rajewsky. Combinatorial microRNA target predictions. *Nature Genetics*, 37(5):495–500, May 2005. Number: 5 Publisher: Nature Publishing Group.
- [132] D.-A. Landau and F. J. Slack. MicroRNAs in Mutagenesis, Genomic Instability and DNA Repair. *Seminars in oncology*, 38(6):743–751, Dec. 2011.
- [133] C.-T. Lee, T. Risom, and W. M. Strauss. Evolutionary conservation of microRNA regulatory circuits: an examination of microRNA gene complexity and conserved microRNA-target interactions through metazoan phylogeny. *DNA and cell biology*, 26(4):209–218, Apr. 2007.
- [134] R. C. Lee, R. L. Feinbaum, and V. Ambros. The *C. elegans* heterochronic gene *lin-4* encodes small RNAs with antisense complementarity to *lin-14*. *Cell*, 75(5):843–854, Dec. 1993.
- [135] Y. Lee, M. Kim, J. Han, K.-H. Yeom, S. Lee, S. H. Baek, and V. N. Kim. MicroRNA genes are transcribed by RNA polymerase II. *The EMBO journal*, 23(20):4051–4060, Oct. 2004.
- [136] S.-K. Leivonen, K. K. Sahlberg, R. Mäkelä, E. U. Due, O. Kallioniemi, A.-L. Børresen-Dale, and M. Perälä. High-throughput screens identify microRNAs essential for HER2 positive breast cancer cell growth. *Molecular Oncology*, 8(1):93–104, Feb. 2014.
- [137] P. F. Lennon, C. T. Taylor, G. L. Stahl, and S. P. Colgan. Neutrophil-derived 5'-adenosine monophosphate promotes endothelial barrier function via CD73-mediated conversion to adenosine and endothelial A2B receptor activation. *The Journal of Experimental Medicine*, 188(8):1433–1443, Oct. 1998.
- [138] A. Li, J. Yu, H. Kim, C. L. Wolfgang, M. I. Canto, R. H. Hruban, and M. Goggins. MicroRNA array analysis finds elevated serum miR-1290 accurately distinguishes patients with low-stage pancreatic cancer from healthy and disease controls. *Clinical Cancer Research: An Official Journal of the American Association for Cancer Research*, 19(13):3600–3610, July 2013.

- [139] P. Li, Y. Guo, G. Bledsoe, Z. Yang, L. Chao, and J. Chao. Kallistatin induces breast cancer cell apoptosis and autophagy by modulating Wnt signaling and microRNA synthesis. *Experimental Cell Research*, 340(2):305–314, Jan. 2016.
- [140] S. Li, L. Wang, Y. Meng, Y. Chang, J. Xu, and Q. Zhang. Increased levels of LAPTM4B, VEGF and survivin are correlated with tumor progression and poor prognosis in breast cancer patients. *Oncotarget*, 8(25):41282–41293, Apr. 2017.
- [141] W.-Q. Li, J.-P. Zhang, Y.-Y. Wang, X.-Z. Li, and L. Sun. MicroRNA-422a functions as a tumor suppressor in non-small cell lung cancer through SULF2-mediated TGF- β /SMAD signaling pathway. *Cell Cycle*, 18(15):1727–1744, Aug. 2019. Publisher: Taylor & Francis _eprint: <https://doi.org/10.1080/15384101.2019.1632135>.
- [142] X. Li, M. Jiang, D. Chen, B. Xu, R. Wang, Y. Chu, W. Wang, L. Zhou, Z. Lei, Y. Nie, D. Fan, Y. Shang, K. Wu, and J. Liang. miR-148b-3p inhibits gastric cancer metastasis by inhibiting the Dock6/Rac1/Cdc42 axis. *Journal of Experimental & Clinical Cancer Research : CR*, 37, Mar. 2018.
- [143] D. Y.-w. Lin, Y. Tanaka, M. Iwasaki, A. G. Gittis, H.-P. Su, B. Mikami, T. Okazaki, T. Honjo, N. Minato, and D. N. Garboczi. The PD-1/PD-L1 complex resembles the antigen-binding Fv domains of antibodies and T cell receptors. *Proceedings of the National Academy of Sciences of the United States of America*, 105(8):3011–3016, Feb. 2008.
- [144] M. Lin, B. Duan, J. Hu, H. Yu, H. Sheng, H. Gao, and J. Huang. Decreased expression of miR-193a-3p is associated with poor prognosis in colorectal cancer. *Oncology Letters*, 14(1):1061–1067, July 2017.
- [145] H. Liu, P. D’Andrade, S. Fulmer-Smentek, P. Lorenzi, K. W. Kohn, J. N. Weinstein, Y. Pommier, and W. C. Reinhold. mRNA and microRNA expression profiles of the NCI-60 integrated with drug activities. *Molecular Cancer Therapeutics*, 9(5):1080–1091, May 2010.
- [146] N. Liu, X.-D. Fang, and Q. Vadis. CD73 as a novel prognostic biomarker for human colorectal cancer. *Journal of Surgical Oncology*, 106(7):918–919; author reply 920, Dec. 2012.
- [147] H.-Y. Loh, B. P. Norman, K.-S. Lai, N. M. A. N. A. Rahman, N. B. M. Alitheen, and M. A. Osman. The Regulatory Role of MicroRNAs in Breast Cancer. *International Journal of Molecular Sciences*, 20(19), Oct. 2019.
- [148] W. Lohcharoenkal, K. Das Mahapatra, L. Pasquali, C. Crudden, L. Kular, Y. Z. Akkaya Ulum, L. Zhang, N. Xu Landén, L. Girnita, M. Jagodic, M. Ståhle, E. Sonkoly, and A. Pivarcsi. Genome-Wide Screen for MicroRNAs Reveals a Role for miR-203 in Melanoma Metastasis. *The Journal of Investigative Dermatology*, 138(4):882–892, Apr. 2018.
- [149] L. Lu, J. Barbi, and F. Pan. The regulation of immune tolerance by FOXP3. *Nature Reviews. Immunology*, 17(11):703–717, Nov. 2017.

- [150] R. V. Luckheeram, R. Zhou, A. D. Verma, and B. Xia. CD4+T Cells: Differentiation and Functions. *Clinical and Developmental Immunology*, 2012, 2012.
- [151] A. T. Ludlow, A. L. Slusher, and M. E. Sayed. Insights into Telomerase/hTERT Alternative Splicing Regulation Using Bioinformatics and Network Analysis in Cancer. *Cancers*, 11(5), May 2019.
- [152] T. R. Lunavat, L. Cheng, B. O. Einarsson, R. Olofsson Bagge, S. Veppil Muralidharan, R. A. Sharples, C. Lässer, Y. S. Gho, A. F. Hill, J. A. Nilsson, and J. Lötval. BRAFV600 inhibition alters the microRNA cargo in the vesicular secretome of malignant melanoma cells. *Proceedings of the National Academy of Sciences of the United States of America*, 114(29):E5930–E5939, July 2017.
- [153] Z. Ma, T. Liu, W. Huang, H. Liu, H.-M. Zhang, Q. Li, Z. Chen, and A.-Y. Guo. MicroRNA regulatory pathway analysis identifies miR-142-5p as a negative regulator of TGF- pathway via targeting SMAD3. *Oncotarget*, 7(44):71504–71513, Sept. 2016.
- [154] S. K. Mallanna and A. Rizzino. Emerging roles of microRNAs in the control of embryonic stem cells and the generation of induced pluripotent stem cells. *Developmental Biology*, 344(1):16–25, Aug. 2010.
- [155] A. Mangolini, M. Ferracin, M. V. Zanzi, E. Saccenti, S. O. Ebnaof, V. V. Poma, J. M. Sanz, A. Passaro, M. Pedriali, A. Frassoldati, P. Querzoli, S. Sabbioni, P. Carcoforo, A. Hollingsworth, and M. Negrini. Diagnostic and prognostic microRNAs in the serum of breast cancer patients measured by droplet digital PCR. *Biomarker Research*, 3:12, 2015.
- [156] F. Mannavola, S. D’Oronzo, M. Cives, L. S. Stucci, G. Ranieri, F. Silvestris, and M. Tucci. Extracellular Vesicles and Epigenetic Modifications Are Hallmarks of Melanoma Progression. *International Journal of Molecular Sciences*, 21(1), Dec. 2019.
- [157] F. Marmé and A. Schneeweiss. Targeted Therapies in Triple-Negative Breast Cancer. *Breast Care*, 10(3):159–166, 2015. Publisher: Karger Publishers.
- [158] B. Mastelic-Gavillet, B. Navarro Rodrigo, L. Décombaz, H. Wang, G. Ercolano, R. Ahmed, L. E. Lozano, A. Ianaro, L. Derré, M. Valerio, T. Tawadros, P. Jichlinski, T. Nguyen-Ngoc, D. E. Speiser, G. Verdeil, N. Gestermann, O. Dormond, L. Kandalaf, G. Coukos, C. Jandus, C. Ménétrier-Caux, C. Caux, P.-C. Ho, P. Romero, A. Harari, and S. Vigano. Adenosine mediates functional and metabolic suppression of peripheral and tumor-infiltrating CD8+ T cells. *Journal for Immunotherapy of Cancer*, 7(1):257, Oct. 2019.
- [159] J. Mazar, D. Khaitan, D. DeBlasio, C. Zhong, S. S. Govindarajan, S. Kopanathi, S. Zhang, A. Ray, and R. J. Perera. Epigenetic Regulation of MicroRNA Genes and the Role of miR-34b in Cell Invasion and Motility in Human Melanoma. *PLOS ONE*, 6(9):e24922, Sept. 2011. Publisher: Public Library of Science.
- [160] B. Mazumder, V. Seshadri, and P. L. Fox. Translational control by the 3’-UTR: the ends specify the means. *Trends in Biochemical Sciences*, 28(2):91–98, Feb. 2003.

- [161] MedImmune LLC. A Phase 2 Open-label, Multicenter, Randomized, Multidrug Platform Study of Durvalumab (MEDI4736) Alone or in Combination With Novel Agents in Subjects With Locally Advanced, Unresectable (Stage III) Non-small Cell Lung Cancer (COAST). Clinical trial registration NCT03822351, clinicaltrials.gov, Nov. 2020. submitted: December 10, 2018.
- [162] S. A. Melo and M. Esteller. Dysregulation of microRNAs in cancer: playing with fire. *FEBS letters*, 585(13):2087–2099, July 2011.
- [163] F. Mignone, C. Gissi, S. Liuni, and G. Pesole. Untranslated regions of mRNAs. *Genome Biology*, 3(3):reviews0004.1–reviews0004.10, 2002.
- [164] V. R. Minciocchi, M. R. Freeman, and D. Di Vizio. Extracellular vesicles in cancer: exosomes, microvesicles and the emerging role of large oncosomes. *Seminars in Cell & Developmental Biology*, 40:41–51, Apr. 2015.
- [165] F. Mirzadeh Azad, P. Naeli, M. Malakootian, A. Baradaran, M. Tavallaei, M. Ghanei, and S. J. Mowla. Two lung development-related microRNAs, miR-134 and miR-187, are differentially expressed in lung tumors. *Gene*, 577(2):221–226, Feb. 2016.
- [166] D. Mittal, D. Sinha, D. Barkauskas, A. Young, M. Kalimutho, K. Stannard, F. Caramia, B. Haibe-Kains, J. Stagg, K. K. Khanna, S. Loi, and M. J. Smyth. Adenosine 2B Receptor Expression on Cancer Cells Promotes Metastasis. *Cancer Research*, 76(15):4372–4382, Aug. 2016.
- [167] X. Mo, H. Zhang, S. Preston, K. Martin, B. Zhou, N. Vadalía, A. M. Gamero, J. Soboloff, I. Tempera, and M. R. Zaidi. Interferon- Signaling in Melanocytes and Melanoma Cells Regulates Expression of CTLA-4. *Cancer Research*, 78(2):436–450, Jan. 2018.
- [168] R. Mohanty, C. R. Chowdhury, S. Arega, P. Sen, P. Ganguly, and N. Ganguly. CAR T cell therapy: A new era for cancer treatment (Review). *Oncology Reports*, 42(6):2183–2195, Dec. 2019. Publisher: Spandidos Publications.
- [169] A. M. Monteys, R. M. Spengler, J. Wan, L. Tecedor, K. A. Lennox, Y. Xing, and B. L. Davidson. Structure and activity of putative intronic miRNA promoters. *RNA (New York, N.Y.)*, 16(3):495–505, Mar. 2010.
- [170] W. Mu and W. Zhang. Bioinformatic Resources of microRNA Sequences, Gene Targets, and Genetic Variation. *Frontiers in Genetics*, 3, Mar. 2012.
- [171] R. Nahta, F. Al-Mulla, R. Al-Temaimi, A. Amedei, R. Andrade-Vieira, S. N. Bay, D. G. Brown, G. M. Calaf, R. C. Castellino, K. A. Cohen-Solal, A. Colacci, N. Cruickshanks, P. Dent, R. Di Fiore, S. Forte, G. S. Goldberg, R. A. Hamid, H. Krishnan, D. W. Laird, A. Lasfar, P. A. Marignani, L. Memeo, C. Mondello, C. C. Naus, R. Ponce-Cusi, J. Raju, D. Roy, R. Roy, E. P. Ryan, H. K. Salem, A. I. Scovassi, N. Singh, M. Vaccari, R. Vento, J. Vondráček, M. Wade, J. Woodrick, and W. H. Bisson. Mechanisms of environmental chemicals that enable the cancer hallmark of evasion of growth suppression. *Carcinogenesis*, 36 Suppl 1:S2–18, June 2015.

- [172] S. Nam, B. Kim, S. Shin, and S. Lee. miRGator: an integrated system for functional annotation of microRNAs. *Nucleic Acids Research*, 36(suppl_1):D159–D164, Jan. 2008.
- [173] N. Nanda and N. J. Roberts. ATM Serine/Threonine Kinase and its Role in Pancreatic Risk. *Genes*, 11(1):108, Jan. 2020. Number: 1 Publisher: Multidisciplinary Digital Publishing Institute.
- [174] A. Niezgoda, P. Niezgoda, and R. Czajkowski. Novel Approaches to Treatment of Advanced Melanoma: A Review on Targeted Therapy and Immunotherapy. *BioMed Research International*, 2015, 2015.
- [175] M. Nishio, T. Hida, K. Nakagawa, H. Sakai, N. Nogami, S. Atagi, T. Takahashi, H. Nokihara, H. Saka, M. Takenoyama, S. Fujita, H. Tanaka, K. Takeda, M. Satouchi, H. Isobe, M. Maemondo, K. Goto, T. Hirashima, K. Minato, and T. Tamura. Phase II studies of nivolumab (anti-PD-1, BMS-936558, ONO-4538) in patients with advanced squamous (sq) or nonsquamous (non-sq) non-small cell lung cancer (NSCLC). *Journal of Clinical Oncology*, 33(15_suppl):8027–8027, May 2015. Publisher: Wolters Kluwer.
- [176] C. S. Niu, Y. Yang, and C.-D. Cheng. MiR-134 regulates the proliferation and invasion of glioblastoma cells by reducing Nanog expression. *International Journal of Oncology*, 42(5):1533–1540, May 2013. Publisher: Spandidos Publications.
- [177] D.-Y. Oh and Y.-J. Bang. HER2-targeted therapies — a role beyond breast cancer. *Nature Reviews Clinical Oncology*, 17(1):33–48, Jan. 2020. Number: 1 Publisher: Nature Publishing Group.
- [178] A. Ohta. A Metabolic Immune Checkpoint: Adenosine in Tumor Microenvironment. *Frontiers in Immunology*, 7:109, 2016.
- [179] S. J. Oiseth and M. S. Aziz. Cancer immunotherapy: a brief review of the history, possibilities, and challenges ahead. *Journal of Cancer Metastasis and Treatment*, 3:250–261, Oct. 2017.
- [180] S. Oliveto, M. Mancino, N. Manfrini, and S. Biffo. Role of microRNAs in translation regulation and cancer. *World Journal of Biological Chemistry*, 8(1):45–56, Feb. 2017.
- [181] H. Otsuka, A. Fukao, Y. Funakami, K. E. Duncan, and T. Fujiwara. Emerging Evidence of Translational Control by AU-Rich Element-Binding Proteins. *Frontiers in Genetics*, 10, May 2019.
- [182] S. M. Pagnotta, C. Laudanna, M. Pancione, L. Sabatino, C. Votino, A. Remo, L. Cerulo, P. Zoppoli, E. Manfrin, V. Colantuoni, and M. Ceccarelli. Ensemble of gene signatures identifies novel biomarkers in colorectal cancer activated through PPAR and TNF signaling. *PloS One*, 8(8):e72638, 2013.
- [183] J.-Y. Pan, F. Zhang, C.-C. Sun, S.-J. Li, G. Li, F.-Y. Gong, T. Bo, J. He, R.-X. Hua, W.-D. Hu, Z.-P. Yuan, X. Wang, Q.-Q. He, and D.-J. Li. miR-134: A Human Cancer Suppressor? *Molecular Therapy. Nucleic Acids*, 6:140–149, Mar. 2017.
- [184] A. Passarelli, F. Mannavola, L. S. Stucci, M. Tucci, and F. Silvestris. Immune system and melanoma biology: a balance between immunosurveillance and immune escape. *Oncotarget*, 8(62):106132–106142, Dec. 2017.

- [185] A. Passarelli, M. Tucci, F. Mannavola, C. Felici, and F. Silvestris. The metabolic milieu in melanoma: Role of immune suppression by CD73/adenosine. *Tumour Biology: The Journal of the International Society for Oncodevelopmental Biology and Medicine*, 42(4):1010428319837138, Apr. 2019.
- [186] R. Paul, J. Lee, A. V. Donaldson, M. Connolly, M. Sharif, S. A. Natanek, U. Rosendahl, M. I. Polkey, M. Griffiths, and P. R. Kemp. miR-422a suppresses SMAD4 protein expression and promotes resistance to muscle loss. *Journal of Cachexia, Sarcopenia and Muscle*, 9(1):119–128, Feb. 2018.
- [187] N. Pencheva, H. Tran, C. Buss, D. Huh, M. Drobnjak, K. Busam, and S. F. Tavazoie. Convergent multi-miRNA targeting of ApoE drives LRP1/LRP8-dependent melanoma metastasis and angiogenesis. *Cell*, 151(5):1068–1082, Nov. 2012.
- [188] L. I. Plotkin, R. Pacheco-Costa, and H. M. Davis. microRNAs and connexins in bone: interaction and mechanisms of delivery. *Current Molecular Biology Reports*, 3(2):63–70, June 2017.
- [189] D. M. Poitz, A. Augstein, C. Gradehand, G. Ende, A. Schmeisser, and R. H. Strasser. Regulation of the Hif-system by micro-RNA 17 and 20a - role during monocyte-to-macrophage differentiation. *Molecular Immunology*, 56(4):442–451, Dec. 2013.
- [190] B. Polini, S. Carpi, S. Doccini, V. Citi, A. Martelli, S. Feola, F. M. Santorelli, V. Cerullo, A. Romanini, and P. Nieri. Tumor Suppressor Role of hsa-miR-193a-3p and -5p in Cutaneous Melanoma. *International Journal of Molecular Sciences*, 21(17), Aug. 2020.
- [191] S. K. Pong and M. Gullerova. Noncanonical functions of microRNA pathway enzymes - Drosha, DGCR8, Dicer and Ago proteins. *FEBS letters*, 592(17):2973–2986, 2018.
- [192] X.-Y. Qin, F. Wei, J. Yoshinaga, J. Yonemoto, M. Tanokura, and H. Sone. siRNA-mediated knockdown of aryl hydrocarbon receptor nuclear translocator 2 affects hypoxia-inducible factor-1 regulatory signaling and metabolism in human breast cancer cells. *FEBS Letters*, 585(20):3310–3315, Oct. 2011.
- [193] J. Reinhardt, J. Landsberg, J. L. Schmid-Burgk, B. B. Ramis, T. Bald, N. Glodde, D. Lopez-Ramos, A. Young, S. F. Ngiow, D. Nettersheim, H. Schorle, T. Quast, W. Kolanus, D. Schadendorf, G. V. Long, J. Madore, R. A. Scolyer, A. Ribas, M. J. Smyth, P. C. Tumei, T. Tüting, and M. Hölzel. Mapk signaling and inflammation link melanoma phenotype switching to induction of cd73 during immunotherapy. *Cancer Research*, 77(17):4697–4709, 2017.
- [194] W. C. Reinhold, M. Sunshine, H. Liu, S. Varma, K. W. Kohn, J. Morris, J. Doroshow, and Y. Pommier. Cellminer: A web-based suite of genomic and pharmacologic tools to explore transcript and drug patterns in the nci-60 cell line set. *Cancer Research*, 72(14):3499–3511, 2012.
- [195] Robert-Koch-Institut. Cancer in Germany 2015/2016. https://www.krebsdaten.de/Krebs/EN/Content/Publications/Cancer_in_Germany/cancer_chapters_2015_2016/, 2020. [Online; accessed 19-December-2020].

- [196] S. C. Robson, J. Sévigny, and H. Zimmermann. The E-NTPDase family of ectonucleotidases: Structure function relationships and pathophysiological significance. *Purinergic Signalling*, 2(2):409–430, June 2006.
- [197] T. J. Rogers, J. L. Christenson, L. I. Greene, K. I. O’Neill, M. M. Williams, M. A. Gordon, T. Nemkov, A. D’Alessandro, G. D. Degala, J. Shin, A.-C. Tan, D. M. Cittelly, J. R. Lambert, and J. K. Richer. Reversal of triple-negative breast cancer emt by mir-200c decreases tryptophan catabolism and a program of immunosuppression. *Molecular Cancer Research*, 17(1):30–41, 2019.
- [198] G. Romano and L. N. Kwong. miRNAs, Melanoma and Microenvironment: An Intricate Network. *International Journal of Molecular Sciences*, 18(11), Nov. 2017.
- [199] B. M. Roth, D. Ishimaru, and M. Hennig. The Core Microprocessor Component DiGeorge Syndrome Critical Region 8 (DGCR8) Is a Nonspecific RNA-binding Protein. *The Journal of Biological Chemistry*, 288(37):26785–26799, Sept. 2013.
- [200] B. Rowshanravan, N. Halliday, and D. M. Sansom. CTLA-4: a moving target in immunotherapy. *Blood*, 131(1):58–67, Jan. 2018.
- [201] J. A. Rudd-Schmidt, A. W. Hodel, T. Noori, J. A. Lopez, H.-J. Cho, S. Verschoor, A. Ciccone, J. A. Trapani, B. W. Hoogenboom, and I. Voskoboinik. Lipid order and charge protect killer T cells from accidental death. *Nature Communications*, 10, Nov. 2019.
- [202] N. Rusk. When microRNAs activate translation. *Nature Methods*, 5(2):122–123, Feb. 2008. Number: 2 Publisher: Nature Publishing Group.
- [203] R. Sadej and A. C. Skladanowski. Dual, enzymatic and non-enzymatic, function of ecto-5’-nucleotidase (eN, CD73) in migration and invasion of A375 melanoma cells. *Acta Biochimica Polonica*, 59(4):647–652, 2012.
- [204] R. Sadej, J. Sychala, and A. C. Skladanowski. Ecto-5’-nucleotidase (eN, CD73) is coexpressed with metastasis promoting antigens in human melanoma cells. *Nucleosides, Nucleotides & Nucleic Acids*, 25(9-11):1119–1123, 2006.
- [205] R. Sadej, J. Sychala, and A. C. Skladanowski. Expression of ecto-5’-nucleotidase (eN, CD73) in cell lines from various stages of human melanoma. *Melanoma Research*, 16(3):213–222, June 2006.
- [206] U. Sahin, P. Oehm, E. Derhovanessian, R. A. Jabulowsky, M. Vormehr, M. Gold, D. Maurus, D. Schwarck-Kokarakis, A. N. Kuhn, T. Omokoko, L. M. Kranz, M. Diken, S. Kreiter, H. Haas, S. Attig, R. Rae, K. Cuk, A. Kemmer-Brück, A. Breitkreuz, C. Tolliver, J. Caspar, J. Quinkhardt, L. Hebich, M. Stein, A. Hohberger, I. Vogler, I. Liebig, S. Renken, J. Sikorski, M. Leierer, V. Müller, H. Mitzel-Rink, M. Miederer, C. Huber, S. Grabbe, J. Utikal, A. Pinter, R. Kaufmann, J. C. Hassel, C. Loquai, and z. Türeci. An RNA vaccine drives immunity in checkpoint-inhibitor-treated melanoma. *Nature*, 585(7823):107–112, Sept. 2020. Number: 7823 Publisher: Nature Publishing Group.

- [207] D. Sarkar, E. Y. Leung, B. C. Baguley, G. J. Finlay, and M. E. Askarian-Amiri. Epigenetic regulation in human melanoma: past and future. *Epigenetics*, 10(2):103–121, 2015.
- [208] T. Schacht, M. Oswald, R. Eils, S. B. Eichmüller, and R. König. Estimating the activity of transcription factors by the effect on their target genes. *Bioinformatics*, 30(17):i401–i407, 2014. _eprint: <https://academic.oup.com/bioinformatics/article-pdf/30/17/i401/17149330/btu446.pdf>.
- [209] D. Schadendorf, D. E. Fisher, C. Garbe, J. E. Gershenwald, J.-J. Grob, A. Halpern, M. Herlyn, M. A. Marchetti, G. McArthur, A. Ribas, A. Roesch, and A. Hauschild. Melanoma. *Nature Reviews Disease Primers*, page 15003, Apr. 2015.
- [210] B. C. Schanen and X. Li. Transcriptional regulation of mammalian miRNA genes. *Genomics*, 97(1):1–6, Jan. 2011.
- [211] T. Schneider-Poetsch, J. Ju, D. E. Eyler, Y. Dang, S. Bhat, W. C. Merrick, R. Green, B. Shen, and J. O. Liu. Inhibition of eukaryotic translation elongation by cycloheximide and lactimidomycin. *Nature Chemical Biology*, 6(3):209–217, Mar. 2010.
- [212] P. Schröter, L. Hartmann, W. Osen, D. Baumann, R. Offringa, D. Eisel, J. Debus, S. B. Eichmüller, and S. Rieken. Radiation-induced alterations in immunogenicity of a murine pancreatic ductal adenocarcinoma cell line. *Scientific Reports*, 10(1):686, Jan. 2020. Number: 1 Publisher: Nature Publishing Group.
- [213] H. Sekine, J. Mimura, M. Yamamoto, and Y. Fujii-Kuriyama. Unique and overlapping transcriptional roles of arylhydrocarbon receptor nuclear translocator (Arnt) and Arnt2 in xenobiotic and hypoxic responses. *The Journal of Biological Chemistry*, 281(49):37507–37516, Dec. 2006.
- [214] S. Sharma, S. Verma, M. Vasudevan, S. Samanta, J. K. Thakur, and R. Kulshreshtha. The interplay of HuR and miR-3134 in regulation of AU rich transcriptome. *RNA Biology*, 10(8):1283–1290, Aug. 2013.
- [215] J. SHI and P.-K. WEI. Interleukin-8: A potent promoter of angiogenesis in gastric cancer. *Oncology Letters*, 11(2):1043–1050, Feb. 2016.
- [216] R. H. Shoemaker. The NCI60 human tumour cell line anticancer drug screen. *Nature Reviews. Cancer*, 6(10):813–823, Oct. 2006.
- [217] R. L. Siegel, K. D. Miller, and A. Jemal. Cancer statistics, 2016. *CA: A Cancer Journal for Clinicians*, 66(1):7–30, Jan. 2016.
- [218] A. H. Sims, A. Howell, S. J. Howell, and R. B. Clarke. Origins of breast cancer subtypes and therapeutic implications. *Nature Clinical Practice Oncology*, 4(9):516–525, Sept. 2007. Number: 9 Publisher: Nature Publishing Group.
- [219] M. V. Sitkovsky, D. Lukashev, S. Apasov, H. Kojima, M. Koshiba, C. Caldwell, A. Ohta, and M. Thiel. Physiological control of immune response and inflammatory tissue damage by hypoxia-inducible factors and adenosine A2A receptors. *Annual Review of Immunology*, 22:657–682, 2004.

- [220] N. T. Snider, P. J. Altshuler, S. Wan, T. H. Welling, J. Cavalcoli, and M. B. Omary. Alternative splicing of human NT5E in cirrhosis and hepatocellular carcinoma produces a negative regulator of ecto-5-nucleotidase (CD73). *Molecular Biology of the Cell*, 25(25):4024–4033, Dec. 2014.
- [221] E. Sonkoly, P. Janson, M.-L. Majuri, T. Savinko, N. Fyhrquist, L. Eidsmo, N. Xu, F. Meisgen, T. Wei, M. Bradley, J. Stenvang, S. Kauppinen, H. Alenius, A. Lauerma, B. Homey, O. Winqvist, M. Stähle, and A. Pivarcsi. MiR-155 is overexpressed in patients with atopic dermatitis and modulates T-cell proliferative responses by targeting cytotoxic T lymphocyte-associated antigen 4. *The Journal of Allergy and Clinical Immunology*, 126(3):581–589.e1–20, Sept. 2010.
- [222] J. Spychala and J. Kitajewski. Wnt and beta-catenin signaling target the expression of ecto-5'-nucleotidase and increase extracellular adenosine generation. *Experimental Cell Research*, 296(2):99–108, June 2004.
- [223] S. Srikantan, K. Tominaga, and M. Gorospe. Functional interplay between RNA-binding protein HuR and microRNAs. *Current protein & peptide science*, 13(4):372–379, June 2012.
- [224] J. Stagg. The double-edge sword effect of anti-CD73 cancer therapy. *Oncology*, 1(2):217–218, Mar. 2012. Publisher: Taylor & Francis _eprint: <https://doi.org/10.4161/onci.1.2.18101>.
- [225] G. R. Strohmeier, W. I. Lencer, T. W. Patapoff, L. F. Thompson, S. L. Carlson, S. J. Moe, D. K. Carnes, R. J. Mrsny, and J. L. Madara. Surface expression, polarization, and functional significance of CD73 in human intestinal epithelia. *Journal of Clinical Investigation*, 99(11):2588–2601, June 1997.
- [226] N. Sträter. Ecto-5'-nucleotidase: Structure function relationships. *Purinergic Signalling*, 2(2):343–350, June 2006.
- [227] C. Sun, R. Mezzadra, and T. N. Schumacher. Regulation and Function of the PD-L1 Checkpoint. *Immunity*, 48(3):434–452, Mar. 2018. Publisher: Elsevier.
- [228] K. Synnestvedt, G. T. Furuta, K. M. Comerford, N. Louis, J. Karhausen, H. K. Eltzschig, K. R. Hansen, L. F. Thompson, and S. P. Colgan. Ecto-5'-nucleotidase (CD73) regulation by hypoxia-inducible factor-1 mediates permeability changes in intestinal epithelia. *The Journal of Clinical Investigation*, 110(7):993–1002, Oct. 2002.
- [229] H. Tang, M. Deng, Y. Tang, X. Xie, J. Guo, Y. Kong, F. Ye, Q. Su, and X. Xie. miR-200b and miR-200c as prognostic factors and mediators of gastric cancer cell progression. *Clinical Cancer Research: An Official Journal of the American Association for Cancer Research*, 19(20):5602–5612, Oct. 2013.
- [230] Y. Tang, S. Yang, M. Wang, D. Liu, Y. Liu, Y. Zhang, and Q. Zhang. Epigenetically altered miR-193a-3p promotes HER2 positive breast cancer aggressiveness by targeting GRB7. *International Journal of Molecular Medicine*, 43(6):2352–2360, June 2019.
- [231] A. Thyagarajan, A. Shaban, and R. P. Sahu. MicroRNA-Directed Cancer Therapies: Implications in Melanoma Intervention. *Journal of Pharmacology and Experimental*

Therapeutics, 364(1):1–12, Jan. 2018. Publisher: American Society for Pharmacology and Experimental Therapeutics Section: Minireviews.

- [232] A. Tittarelli, M. Navarrete, M. A. Gleisner, P. Gebicke-Haerter, and F. Salazar-Onfray. Connexin-Mediated Signaling at the Immunological Synapse. *International Journal of Molecular Sciences*, 21(10), May 2020.
- [233] Z. Tong, Q. Cui, J. Wang, and Y. Zhou. TransmiR v2.0: an updated transcription factor-microRNA regulation database. *Nucleic Acids Research*, 47(D1):D253–D258, Jan. 2019.
- [234] S. S. Truesdell, R. D. Mortensen, M. Seo, J. C. Schroeder, J. H. Lee, O. LeTonqueze, and S. Vasudevan. MicroRNA-mediated mRNA Translation Activation in Quiescent Cells and Oocytes Involves Recruitment of a Nuclear microRNP. *Scientific Reports*, 2(1):842, Nov. 2012.
- [235] M. Tucci, A. Passarelli, F. Mannavola, L. S. Stucci, P. A. Ascierto, M. Capone, G. Madonna, P. Lopalco, and F. Silvestris. Serum exosomes as predictors of clinical response to ipilimumab in metastatic melanoma. *Oncoimmunology*, 7(2):e1387706, 2018.
- [236] S. Ugurel, R. K. Thirumaran, S. Bloethner, A. Gast, A. Sucker, J. Mueller-Berghaus, W. Rittgen, K. Hemminki, J. C. Becker, R. Kumar, and D. Schadendorf. B-RAF and N-RAS Mutations Are Preserved during Short Time In Vitro Propagation and Differentially Impact Prognosis. *PLOS ONE*, 2(2):e236, Feb. 2007. Publisher: Public Library of Science.
- [237] M. Šulc, R. M. Marín, H. S. Robins, and J. Vaníček. PACCMIT/PACCMIT-CDS: identifying microRNA targets in 3' UTRs and coding sequences. *Nucleic Acids Research*, 43(W1):W474–479, July 2015.
- [238] M. Umeh-Garcia, C. Simion, P.-Y. Ho, N. Batra, A. L. Berg, K. L. Carraway, A. Yu, and C. Sweeney. A Novel Bioengineered MicroRNA-127 Prodrug Suppresses The Growth And Metastatic Potential Of Triple Negative Breast Cancer Cells. *Cancer research*, 80(3):418–429, Feb. 2020.
- [239] N. Vandamme, G. Denecker, K. Bruneel, G. Blancke, z. Akay, J. Taminau, J. D. Coninck, E. D. Smedt, N. Skrypek, W. V. Loocke, J. Wouters, D. Nittner, C. Köhler, D. S. Darling, P. F. Cheng, M. I. G. Raaijmakers, M. P. Levesque, U. G. Mallya, M. Rafferty, B. Balint, W. M. Gallagher, L. Brochez, D. Huylebroeck, J. J. Haigh, V. Andries, F. Rambow, P. V. Vlierberghe, S. Goossens, J. J. v. d. Oord, J.-C. Marine, and G. Berx. The EMT Transcription Factor ZEB2 Promotes Proliferation of Primary and Metastatic Melanoma While Suppressing an Invasive, Mesenchymal-Like Phenotype. *Cancer Research*, 80(14):2983–2995, July 2020. Publisher: American Association for Cancer Research Section: Molecular Cell Biology.
- [240] F. Varrone and E. Caputo. The miRNAs Role in Melanoma and in Its Resistance to Therapy. *International Journal of Molecular Sciences*, 21(3), Jan. 2020.

- [241] N. Venkatesan, J. Kanwar, P. R. Deepa, V. Khetan, T. M. Crowley, R. Raguraman, G. Sugneswari, P. Rishi, V. Natarajan, J. Biswas, and S. Krishnakumar. Clinico-Pathological Association of Delineated miRNAs in Uveal Melanoma with Monosomy 3/Disomy 3 Chromosomal Aberrations. *PloS One*, 11(1):e0146128, 2016.
- [242] S. Vigano, D. Alatzoglou, M. Irving, C. Ménétrier-Caux, C. Caux, P. Romero, and G. Coukos. Targeting Adenosine in Cancer Immunotherapy to Enhance T-Cell Function. *Frontiers in Immunology*, 10, 2019. Publisher: Frontiers.
- [243] C. Wang, Z. Yun, T. Zhao, X. Liu, and X. Ma. MiR-495 is a Predictive Biomarker that Downregulates GFI1 Expression in Medulloblastoma. *Cellular Physiology and Biochemistry: International Journal of Experimental Cellular Physiology, Biochemistry, and Pharmacology*, 36(4):1430–1439, 2015.
- [244] G. Wang, L. Liu, J. Zhang, C. Huang, Y. Chen, W. Bai, Y. Wang, K. Zhao, and S. Li. LncRNA HCG11 Suppresses Cell Proliferation and Promotes Apoptosis via Sponging miR-224-3p in Non-Small-Cell Lung Cancer Cells. *Oncotargets and therapy*, 13:6553–6563, July 2020.
- [245] H. Wang, S. Lee, C. L. Nigro, L. Lattanzio, M. Merlano, M. Monteverde, R. Matin, K. Purdie, N. Mladkova, D. Bergamaschi, C. Harwood, N. Syed, P. Szlosarek, E. Brisoulis, A. McHugh, A. Thompson, A. Evans, I. Leigh, C. Fleming, G. J. Inman, E. Hatzimichael, C. Proby, and T. Crook. NT5E (CD73) is epigenetically regulated in malignant melanoma and associated with metastatic site specificity. *British Journal of Cancer*, 106(8):1446–1452, Apr. 2012.
- [246] L. Wang, S. Zhang, W. Zhang, G. Cheng, R. Khan, Z. Junjvlieke, S. Li, and L. Zan. mir-424 promotes bovine adipogenesis through an unconventional post-transcriptional regulation of stk11. *Frontiers in Genetics*, 11:145, 2020.
- [247] N. Wang, X. Xiang, K. Chen, P. Liu, and A. Zhu. Targeting of NT5E by miR-30b and miR-340 attenuates proliferation, invasion and migration of gallbladder carcinoma. *Biochimie*, 146:56–67, Mar. 2018.
- [248] Q. Wang, W. Lin, X. Tang, S. Li, L. Guo, Y. Lin, and H. F. Kwok. The Roles of microRNAs in Regulating the Expression of PD-1/PD-L1 Immune Checkpoint. *International Journal of Molecular Sciences*, 18(12), Nov. 2017.
- [249] Y. Wang, J. Li, D. Kuang, X. Wang, Y. Zhu, S. Xu, Y. Chen, H. Cheng, Q. Zhao, Y. Duan, and G. Wang. miR-148b-3p functions as a tumor suppressor in GISTs by directly targeting KIT. *Cell communication and signaling: CCS*, 16(1):16, Apr. 2018.
- [250] Y.-n. Wang, Z.-h. Chen, and W.-c. Chen. Novel circulating microRNAs expression profile in colon cancer: a pilot study. *European Journal of Medical Research*, 22, Nov. 2017.
- [251] C. E. M. Weber, C. Luo, A. Hotz-Wagenblatt, A. Gardyan, T. Kordaß, T. Holland-Letz, W. Osen, and S. B. Eichmüller. miR-339-3p Is a Tumor Suppressor in Melanoma. *Cancer Research*, 76(12):3562–3571, June 2016.

- [252] W.-T. Wei, X.-X. Nian, S.-Y. Wang, H.-L. Jiao, Y.-X. Wang, Z.-Y. Xiao, R.-W. Yang, Y.-Q. Ding, Y.-P. Ye, and W.-T. Liao. miR-422a inhibits cell proliferation in colorectal cancer by targeting AKT1 and MAPK1. *Cancer Cell International*, 17(1):91, Oct. 2017.
- [253] B. Weigelt, F. C. Geyer, and J. S. Reis-Filho. Histological types of breast cancer: How special are they? *Molecular Oncology*, 4(3):192–208, June 2010.
- [254] U. Wellner, J. Schubert, U. C. Burk, O. Schmalhofer, F. Zhu, A. Sonntag, B. Waldvogel, C. Vannier, D. Darling, A. zur Hausen, V. G. Brunton, J. Morton, O. Sansom, J. Schüler, M. P. Stemmler, C. Herzberger, U. Hopt, T. Keck, S. Brabletz, and T. Brabletz. The EMT-activator ZEB1 promotes tumorigenicity by repressing stemness-inhibiting microRNAs. *Nature Cell Biology*, 11(12):1487–1495, Dec. 2009.
- [255] D. Wolf, A. M. Wolf, H. Rumpold, H. Fiegl, A. G. Zeimet, E. Muller-Holzner, M. Deibl, G. Gastl, E. Gunsilius, and C. Marth. The expression of the regulatory T cell-specific forkhead box transcription factor FoxP3 is associated with poor prognosis in ovarian cancer. *Clinical Cancer Research: An Official Journal of the American Association for Cancer Research*, 11(23):8326–8331, Dec. 2005.
- [256] M. Wozniak, L. Peczek, L. Czernek, and M. Döchler. Analysis of the miRNA Profiles of Melanoma Exosomes Derived Under Normoxic and Hypoxic Culture Conditions. *Anticancer Research*, 37(12):6779–6789, Dec. 2017.
- [257] F. Xiao, Z. Zuo, G. Cai, S. Kang, X. Gao, and T. Li. miRecords: an integrated resource for microRNA–target interactions. *Nucleic Acids Research*, 37(Database issue):D105–D110, Jan. 2009.
- [258] M. Xie, H. Qin, Q. Luo, Q. Huang, X. He, Z. Yang, P. Lan, and L. Lian. MicroRNA-30a regulates cell proliferation and tumor growth of colorectal cancer by targeting CD73. *BMC cancer*, 17(1):305, May 2017.
- [259] S.-D. Xie, C. Qin, L.-D. Jin, Q.-C. Wang, J. Shen, J.-C. Zhou, Y.-X. Chen, A.-H. Huang, W.-H. Zhao, and L.-B. Wang. Long noncoding RNA SNHG14 promotes breast cancer cell proliferation and invasion via sponging miR-193a-3p. *European Review for Medical and Pharmacological Sciences*, 24(14):7543, July 2020.
- [260] C. Yan, Y. Chen, W. Kong, L. Fu, Y. Liu, Q. Yao, and Y. Yuan. PVT1-derived miR-1207-5p promotes breast cancer cell growth by targeting STAT6. *Cancer Science*, 108(5):868–876, May 2017.
- [261] B. Yang, E. Yang, H. Liao, Z. Wang, Z. Den, and H. Ren. ARNT2 is downregulated and serves as a potential tumor suppressor gene in non-small cell lung cancer. *Tumour Biology: The Journal of the International Society for Oncodevelopmental Biology and Medicine*, 36(3):2111–2119, Mar. 2015.
- [262] C. Yang, W. Yuan, X. Yang, P. Li, J. Wang, J. Han, J. Tao, P. Li, H. Yang, Q. Lv, and W. Zhang. Circular RNA circ-ITCH inhibits bladder cancer progression by sponging miR-17/miR-224 and regulating p21, PTEN expression. *Molecular Cancer*, 17, Jan. 2018.

- [263] L. Yang, Y. Cai, D. Zhang, J. Sun, C. Xu, W. Zhao, W. Jiang, and C. Pan. miR-195/miR-497 Regulate CD274 Expression of Immune Regulatory Ligands in Triple-Negative Breast Cancer. *Journal of Breast Cancer*, 21(4):371–381, Dec. 2018.
- [264] X. Yang, P. Vasudevan, V. Parekh, A. Penev, and J. M. Cunningham. Bridging Cancer Biology with the Clinic: Relative Expression of a GRHL2-Mediated Gene-Set Pair Predicts Breast Cancer Metastasis. *PLOS ONE*, 8(2):1–11, 2013. Publisher: Public Library of Science.
- [265] D. Yee, K. M. Shah, M. C. Coles, T. V. Sharp, and D. Lagos. MicroRNA-155 induction via TNF- and IFN- suppresses expression of programmed death ligand-1 (PD-L1) in human primary cells. *The Journal of Biological Chemistry*, 292(50):20683–20693, Dec. 2017.
- [266] R. Yi, Y. Qin, I. G. Macara, and B. R. Cullen. Exportin-5 mediates the nuclear export of pre-microRNAs and short hairpin RNAs. *Genes & Development*, 17(24):3011–3016, Dec. 2003.
- [267] C. Yin, P.-Q. Wang, W.-P. Xu, Y. Yang, Q. Zhang, B.-F. Ning, P.-P. Zhang, W.-P. Zhou, W.-F. Xie, W.-S. Chen, and X. Zhang. Hepatocyte nuclear factor-4 reverses malignancy of hepatocellular carcinoma through regulating miR-134 in the DLK1-DIO3 region. *Hepatology (Baltimore, Md.)*, 58(6):1964–1976, Dec. 2013.
- [268] A. Young, S. F. Ngiow, D. S. Barkauskas, E. Sult, C. Hay, S. J. Blake, Q. Huang, J. Liu, K. Takeda, M. W. L. Teng, K. Sachsenmeier, and M. J. Smyth. Co-inhibition of CD73 and A2AR Adenosine Signaling Improves Anti-tumor Immune Responses. *Cancer Cell*, 30(3):391–403, Sept. 2016.
- [269] M. Yu, G. Guo, L. Huang, L. Deng, C.-S. Chang, B. R. Achyut, M. Canning, N. Xu, A. S. Arbab, R. J. Bollag, P. C. Rodriguez, A. L. Mellor, H. Shi, D. H. Munn, and Y. Cui. CD73 on cancer-associated fibroblasts enhanced by the A2B-mediated feedforward circuit enforces an immune checkpoint. *Nature Communications*, 11(1):515, Jan. 2020.
- [270] K. M. Zak, R. Kitel, S. Przetocka, P. Golik, K. Guzik, B. Musielak, A. Dömling, G. Dubin, and T. A. Holak. Structure of the Complex of Human Programmed Death 1, PD-1, and Its Ligand PD-L1. *Structure (London, England: 1993)*, 23(12):2341–2348, Dec. 2015.
- [271] A. Zech, T. Müller, S. Cicko, K. Baudiss, K. Ayata, M. Braun, A. Meyer, and M. Idzko. A potential role of the proteoglycan biglycan in a murine model of allergic airway inflammation. *Pneumologie*, 67, Feb. 2013.
- [272] R. Zha, W. Guo, Z. Zhang, Z. Qiu, Q. Wang, J. Ding, S. Huang, T. Chen, J. Gu, M. Yao, and X. He. Genome-Wide Screening Identified That miR-134 Acts as a Metastasis Suppressor by Targeting Integrin 1 in Hepatocellular Carcinoma. *PLOS ONE*, 9(2):e87665, Feb. 2014. Publisher: Public Library of Science.
- [273] T. Zhan, N. Rindtorff, and M. Boutros. Wnt signaling in cancer. *Oncogene*, 36(11):1461–1473, Mar. 2017. Number: 11 Publisher: Nature Publishing Group.

- [274] F. Zhang, Y. Luo, Z. Shao, L. Xu, X. Liu, Y. Niu, J. Shi, X. Sun, Y. Liu, Y. Ding, and L. Zhao. MicroRNA-187, a downstream effector of TGF pathway, suppresses Smad-mediated epithelial–mesenchymal transition in colorectal cancer. *Cancer Letters*, 373(2):203–213, Apr. 2016.
- [275] G. Zhang, W. Zhang, B. Li, E. Stringer-Reasor, C. Chu, L. Sun, S. Bae, D. Chen, S. Wei, K. Jiao, W.-H. Yang, R. Cui, R. Liu, and L. Wang. MicroRNA-200c and microRNA-141 are regulated by a FOXP3-KAT2B axis and associated with tumor metastasis in breast cancer. *Breast cancer research: BCR*, 19(1):73, June 2017.
- [276] H. Zhang, Q. Ye, Z. Du, M. Huang, M. Zhang, and H. Tan. MiR-148b-3p inhibits renal carcinoma cell growth and pro-angiogenic phenotype of endothelial cell potentially by modulating FGF2. *Biomedicine & Pharmacotherapy*, 107:359–367, Nov. 2018.
- [277] J. Zhang, Y. Ma, S. Wang, F. Chen, and Y. Gu. C/EBP inhibits proliferation of breast cancer cells via a novel pathway of miR-134/CREB. *International Journal of Clinical and Experimental Pathology*, 8(11):14472–14478, 2015.
- [278] Y. Zhang, M. Fan, X. Zhang, F. Huang, K. Wu, J. Zhang, J. Liu, Z. Huang, H. Luo, L. Tao, and H. Zhang. Cellular microRNAs up-regulate transcription via interaction with promoter TATA-box motifs. *RNA*, 20(12):1878–1889, Dec. 2014.
- [279] Y. Zhang, J. Kim, A. C. Mueller, B. Dey, Y. Yang, D.-h. Lee, J. Hachmann, S. FINDERLE, D. M. Park, J. Christensen, D. Schiff, B. Purow, A. Dutta, and R. Abounader. Multiple receptor tyrosine kinases converge on microRNA-134 to control KRAS, STAT5B, and glioblastoma. *Cell Death and Differentiation*, 21(5):720–734, May 2014.
- [280] Y. Zhang, T. Li, Y. Qiu, T. Zhang, P. Guo, X. Ma, Q. Wei, and L. Han. Serum microRNA panel for early diagnosis of the onset of hepatocellular carcinoma. *Medicine*, 96(2):e5642, Jan. 2017.
- [281] Z. Zhang, S. Schwartz, L. Wagner, and W. Miller. A greedy algorithm for aligning DNA sequences. *Journal of Computational Biology: A Journal of Computational Molecular Cell Biology*, 7(1-2):203–214, Apr. 2000.
- [282] B. Zhao and Y.-G. Chen. Regulation of TGF- Signal Transduction. *Scientifica*, 2014:874065, Sept. 2014. Publisher: Hindawi Publishing Corporation.
- [283] Q. Zheng, J. J. Yu, C. Li, J. Li, J. Wang, and S. Wang. miR-224 targets BTRC and promotes cell migration and invasion in colorectal cancer. *3 Biotech*, 10(11), Nov. 2020.
- [284] Y. Zheng, S. Z. Josefowicz, A. Kas, T.-T. Chu, M. A. Gavin, and A. Y. Rudensky. Genome-wide analysis of Foxp3 target genes in developing and mature regulatory T cells. *Nature*, 445(7130):936–940, Feb. 2007.
- [285] S. Zhou, Z. Zhang, P. Zheng, W. Zhao, and N. Han. MicroRNA-1285-5p influences the proliferation and metastasis of non-small-cell lung carcinoma cells via downregulating CDH1 and Smad4. *Tumour Biology: The Journal of the International Society for Oncodevelopmental Biology and Medicine*, 39(6):1010428317705513, June 2017.

- [286] J. Zhu, Y. Zeng, W. Li, H. Qin, Z. Lei, D. Shen, D. Gu, J.-A. Huang, and Z. Liu. CD73/NT5E is a target of miR-30a-5p and plays an important role in the pathogenesis of non-small cell lung cancer. *Molecular Cancer*, 16(1):34, Feb. 2017.